Origin, diversity and transcriptional coding of periglomerular calretinin interneurons

Élodie Gaborieau

N°d'ordre NNT : 2017LYSE1307

THESE de DOCTORAT DE L'UNIVERSITE DE LYON

opérée au sein de
L'Université Claude Bernard Lyon 1

Ecole Doctorale N° ED 340
Biologie Moléculaire, Intégrative et Cellulaire (BMIC)

Spécialité de doctorat : Neurosciences

Soutenue publiquement le 20/12/2017, par :
Elodie GABORIEAU

Origine, diversité et contrôle transcriptionnel des interneurones périglomérulaires calrétinines du bulbe olfactif

---

Devant le jury composé de :

Anne DIDIER	Professeure des universités	Université Lyon 1	Présidente
Valérie CORONAS	Professeure des universités	Université Poitiers	Rapporteure
Marc-André MOUTHON	Chercheur	Université Paris XI	Rapporteur
Jean-Philippe HUGNOT	Maitre de conférence	Université Montpellier	Examinateur
Olivier RAINETEAU	Directeur de recherche	Université Lyon 1	Directeur de thèse

Origin, diversity and transcriptional control of calretinin periglomerular interneurons in the olfactory bulb

UNIVERSITE CLAUDE BERNARD - LYON 1

Président de l'Université	**M. le Professeur Frédéric FLEURY**
Président du Conseil Académique	M. le Professeur Hamda BEN HADID
Vice-président du Conseil d'Administration	M. le Professeur Didier REVEL
Vice-président du Conseil Formation et Vie Universitaire	M. le Professeur Philippe CHEVALIER
Vice-président de la Commission Recherche	M. Fabrice VALLÉE
Directrice Générale des Services	Mme Dominique MARCHAND

COMPOSANTES SANTE

Faculté de Médecine Lyon Est – Claude Bernard	Directeur : M. le Professeur G.RODE
Faculté de Médecine et de Maïeutique Lyon Sud – Charles Mérieux	Directeur : Mme la Professeure C. BURILLON
Faculté d'Odontologie	Directeur : M. le Professeur D. BOURGEOIS
Institut des Sciences Pharmaceutiques et Biologiques	Directeur : Mme la Professeure C. VINCIGUERRA
Institut des Sciences et Techniques de la Réadaptation	Directeur : M. X. PERROT
Département de formation et Centre de Recherche en Biologie Humaine	Directeur : Mme la Professeure A-M. SCHOTT

COMPOSANTES ET DEPARTEMENTS DE SCIENCES ET TECHNOLOGIE

Faculté des Sciences et Technologies	Directeur : M. F. DE MARCHI
Département Biologie	Directeur : M. le Professeur F. THEVENARD
Département Chimie Biochimie	Directeur : Mme C. FELIX
Département GEP	Directeur : M. Hassan HAMMOURI
Département Informatique	Directeur : M. le Professeur S. AKKOUCHE
Département Mathématiques	Directeur : M. le Professeur G. TOMANOV
Département Mécanique	Directeur : M. le Professeur H. BEN HADID
Département Physique	Directeur : M. le Professeur J-C PLENET
UFR Sciences et Techniques des Activités Physiques et Sportives	Directeur : M. Y.VANPOULLE
Observatoire des Sciences de l'Univers de Lyon	Directeur : M. B. GUIDERDONI
Polytech Lyon	Directeur : M. le Professeur E.PERRIN
Ecole Supérieure de Chimie Physique Electronique	Directeur : M. G. PIGNAULT
Institut Universitaire de Technologie de Lyon 1	Directeur : M. le Professeur C. VITON
Ecole Supérieure du Professorat et de l'Education	Directeur : M. le Professeur A. MOUGNIOTTE
Institut de Science Financière et d'Assurances	Directeur : M. N. LEBOISNE

Résumé de ce manuscrit de thèse en français

Ce travail de thèse a eu pour objectif de développer des outils afin d'étudier la neurogenèse postnatale dans le bulbe olfactif en s'adaptant à ses particularités spatiales et temporelles. Ces outils m'ont permis d'identifier deux sous populations d'interneurones calrétinines (CalR+) dans le bulbe olfactif aux propriétés particulièrement intéressantes et uniques. Les facteurs de transcription impliqués dans la genèse de ces interneurones CalR+ étant encore peu connus, les outils mis en place ont permis d'étudier le rôle du facteur de transcription Sp8 dans la spécification précoce mais aussi dans les étapes plus tardives de la différentiation de ces interneurones jusqu'à leur maturation dans le bulbe olfactif.

Les cellules souches neurales (CSNs) de la zone sous-ventriculaire (ZSV) présentent une activité germinale intense tout au long de la vie d'un individu. Cette zone germinative va subir un remaniement structurel important après la naissance associé à un changement d'identité des cellules souches neurales. Les CSNs postnatales de la ZSV sont finement régionalisées en microdomaines ayant des origines embryonnaires différentes et générant ainsi des sous-types neuronaux distincts dans le bulbe olfactif. Pour générer ces neurones, les cellules souches de la ZSV vont se différentier en neuroblastes puis s'engager dans la voie de migration rostrale afin d'atteindre les régions les plus antérieures du cerveau murin, le bulbe olfactif. Ainsi l'étude de la neurogenèse postnatale nécessite le développement de nouveaux outils finement adaptés aux particularités spatiales et temporelles de la neurogenèse postnatale. Ces nouveaux outils qui permettent d'étudier les différentes étapes de la différenciation de différents sous-types de neurones, sont décrits dans un premier chapitre technique. J'ai ainsi affiné les approches actuelles pour pouvoir manipuler l'expression génique dans les CSNs de la ZSV postnatale d'une manière contrôlée spatialement et temporellement. Ainsi, une approche d'électroporation postnatale classique a été affinée afin de pouvoir manipuler l'expression des gènes dans les CSNs à des étapes précises de leur différenciation tout en permettant d'étudier l'impact de ces manipulations sur le devenir à long terme de ces cellules.

Le développement du bulbe olfactif commence très tôt chez l'embryon avec l'arrivée des premières cellules olfactives jusqu'à l'établissement d'un réseau complet et fonctionnel autour de la naissance. Ainsi, les neurones nouveaux nés après la naissance vont s'intégrer dans un réseau déjà existant tout en maintenant le système

olfactif fonctionnel. Ce travail de thèse s'est focalisé sur les interneurones périglomérulaires (PG) générés dans la couche glomérulaire du bulbe olfactif. Des études antérieures ont mis en évidence que les interneurones calbindin (CalB+) et dopaminergiques (TH+) sont respectivement générés par les microdomaines latéral et dorsal de la ZSV. Les interneurones CalR + PG quant à eux sont générés à la fois par les microdomaines médial et dorsal de la ZSV. Alors que les interneurones CalB+ et TH+ sont générés principalement pendant les phases embryonnaire et périnatale, les interneurones CalR+ représentent la plus grande population d'interneurones périglomérulaires du bulbe olfactif produits après la naissance. Cependant, alors que les deux autres sous-types d'interneurones PG CalB+ et TH+ sont finement décrits dans la littérature, il existe peu d'informations concernant l'origine, la diversité et la fonction des interneurones CalR+ dans le bulbe olfactif, ainsi que les facteurs de transcription impliqués dans leur génération. Ces questions sont abordées dans le chapitre 2 de ce manuscrit. Le perfectionnement de l'approche d'électroporation a permis d'identifier deux sous-populations d'interneurones CalR + présentant des origines spatiales et temporelles différentes après la naissance, ainsi que d'explorer les implications fonctionnelles et morphologiques de cette diversité. Ainsi, une population précoce d'interneurones CalR+ est majoritairement originaire du mur médial de la ZSV alors qu'une deuxième population, originaire du mur dorsal, devient majoritaire au bout de 2 semaines de vie postnatale. Malgré une origine spatiale et temporelle qui évolue au cours du temps, les interneurones CalR+ ont des propriétés relativement semblables. Ainsi, une fraction importante et non décrite d'interneurones CalR + PG présente des propriétés de neurones immatures (c'est-à-dire qu'elle reçoit peu d'entrées synaptiques et est faiblement excitable), remettant en question leur rôle dans le traitement de l'information olfactive.

La différentiation d'un neurone est un processus qui se déroule par étapes successives grâce à des vagues transcriptionnelles. Les facteurs de transcription (FTs) impliqués dans la spécification des cellules souches en un sous-type particulier de neurones sont exprimés précocement dans la vie d'un neurone et sont aujourd'hui les plus largement décrits. Aujourd'hui, la communauté scientifique s'intéresse de plus en plus aux vagues transcriptionnelles plus tardives qui permettent la survie, la maturation et le maintien actif de l'identité des neurones matures dans le réseau

neuronale. Ces facteurs de transcription plus communément appelés gènes de sélection terminale sont encore peu décrits. Des études ont suggéré que le facteur de transcription Sp8, FT déjà connu pour ses rôles au cours du développement embryonnaire, serait ainsi impliqué dans la génération des interneurones CalR+ mais son rôle dans la neurogenèse postnatale et dans les étapes tardives de la différentiation d'un neurone reste à déterminer. Le rôle de ce FT dans la neurogenèse postnatale est décrit dans le chapitre 3. Après description du pattern d'expression de Sp8 dans le cerveau murin postnatal, des manipulations génétiques du facteur de transcription Sp8 ont été réalisées à divers stades de la différenciation des interneurones CalR+. Ces expériences ont mis en évidence son rôle précoce dans la prolifération et la différentiation précoce des cellules souches en neuroblastes, indépendamment de leur origine spatiale. De manière intéressante, les manipulations plus tardives ont mis en lumière un rôle inconnu jusqu'à présent dans la survie à long terme des interneurones CalR + PG matures, tout en excluant un rôle dans leur spécification précoce. Ces travaux décrivent le facteur de transcription Sp8 comme gène de sélection terminal indispensable à la survie et la maturation des interneurones CalR+ PG du bulbe olfactif.

L'ensemble de ces résultats amène ainsi un éclairage nouveau sur l'origine, la diversité et le codage transcriptionnel des interneurones CalR + PG et appellent à une caractérisation plus précise de leur rôle dans le traitement de l'information olfactive.

Ta persévérance vaincra toutes tes peurs et te permettra de réaliser tous tes rêves.

John Demartini

Le plus important n'est pas l'atteinte de tes objectifs mais de prendre conscience de la personne que tu es devenue pour atteindre ces objectifs. Car c'est cette personne qui te permettra de continuer à grandir afin de réaliser des choses encore plus extraordinaires.

Steve Legalle

REMERCIEMENTS

Cette page de remerciements s'adresse à toutes les personnes qui de près ou de loin ont contribué à l'avancée et la consécration de ces 4 ans de thèse, à mon épanouissement scientifique et à mon évolution personnelle.

Je tiens tout d'abord à remercier les membres du jury pour avoir accepté de venir discuter les résultats de mes travaux aujourd'hui, le Dr Anne Didier pour avoir accepté de présider mon jury, les Drs Valérie Coronas, et Marc-André Mouthon pour avoir consacrer de leur temps à l'évaluation de mon manuscrit de thèse et le Dr Jean-Philippe Hugnot pour avoir une nouvelle fois accepté d'évaluer et discuter mes travaux ainsi que pour son soutien et ses nombreux conseils lors mes comités de suivi de thèse.

Je tiens à adresser un merci particulier à Olivier, un faible mot pour t'exprimer toute ma gratitude. Pour reprendre les mots d'Amel, tu es « une personne passionnée ». Ma décision n'a pas été difficile à prendre au moment de quitter Strasbourg pour te rejoindre dans ton équipe, tu m'avais déjà convaincue de la pertinence de ta recherche. Tu m'as donné l'occasion d'investir une équipe nouvelle et de me construire avec elle. Tu m'as donné l'assurance que je n'avais pas en me confiant les rênes de manip importantes pour moi et pour les membres de l'équipe. Tu m'as fait confiance en me confiant des stagiaires pour les former et les accompagner dans leur cursus, un épanouissement total pour moi. Tu m'as appris à présenter et m'a embarqué dans cette aventure Pint of Science qui m'a ouvert au plaisir de la vulgarisation scientifique. Tu m'as fait évoluer autant sur le plan scientifique et professionnel que sur le plan personnel. J'ai beaucoup appris à tes côtés et malgré mes périodes de doutes, tu as su trouver les mots pour me soutenir jusqu'au bout afin de finaliser ces 4 années. Merci pour tout.

Je tiens également à remercier chaleureusement la directrice de l'école doctorale BMIC, Mme Françoise Monéger ainsi que le co-directeur, Mr Mathias Faure pour leur engagement auprès de nous étudiants, et surtout pour leur écoute, leur bienveillance et leur soutien qui m'ont aidé à parvenir à cette étape de ma vie d'étudiante aujourd'hui. Merci aussi à Fabienne Macro et Roxane Leclaire qui depuis leur bureau sont toujours disponibles pour nous renseigner et nous aider à accomplir ces tâches administratives complexes.

Merci Didier pour cette collaboration qui a donné une nouvelle impulsion à mon projet de thèse. Merci pour ta bonne humeur, les nombreux échanges autour de ce projet, et ton accueil chaleureux dans ton équipe à Strasbourg.

Merci à ceux qui m'ont mis le pied à l'étrier et m'ont donné le goût de la recherche, Olivier Lefebvre, Dominique Bagnard et à toute la Dream B team ainsi que Patricia, Caro, Annick. Merci pour tout ce que vous m'avez appris. Une pensée spéciale à Serge Potier aussi les nombreuses propositions de thèse que vous m'avez fait parvenir après mon master à Strasbourg. Merci pour votre investissement à tous.

Merci mes loulous, ma famille professionnelle depuis 4 ans. Merci Guillaume pour avoir passé nos commandes de dernière minute pendant 4 ans ;) et pour tes blagues toujours au top niveau qui apportent joie et bonne humeur dans ce bureau ! Merci Stefan pour ces moments passés à la paillasse à se former notamment aux électroporations, à mettre en place les protocoles dans le labo mais aussi et surtout pour les soirées bière ! Merci d'être juste toi et de nous avoir fait autant rire, ne change surtout pas ! Merci Vanessa pour tes rires, ta sagesse, et tes précieux conseils. Merci pour ton soutien inconditionnel et ta positive attitude en toutes circonstances ! Je vous souhaite à tous les trois de réussir dans tout ce que vous entreprendrez dans la vie. Comme dirai notre grand sage « Force et courage ! »

Merci Louis pour ton aide précieuse sur les dernières manips et pour les franches rigolades quand il s'agit de détendre l'atmosphère. Merci Quentin pour ta bonne humeur, tes petits mots post-it et pour avoir contribué à notre survie en préparant le café le matin ;). Merci à tous les stagiaires qui sont passés dans l'équipe (Marion, Aymeric, Charlotte, Louise, Linh, Julie).

Merci mes choupettes Claire et Amel ainsi que Yacine pour m'avoir autant apporté lors de vos stages. J'ai pris énormément de plaisir à travailler avec vous et à échanger avec vous sur les projets, les sciences, la fac et la recherche. Merci pour le travail que vous avez effectué pour ce manuscrit. Croyez en vous et continuez d'avancer sur le chemin que vous vous êtes tracé !

Merci à toute l'équipe de l'animalerie pour votre travail et votre bonne humeur. Merci Xavier pour tes précieux conseils sur l'élevage des souris. Merci Muriel et

Marco pour être toujours disponible et à notre écoute et toujours prêts à rendre service même le week-end.

Merci Chandara pour ton investissement permanent dans les tâches administratives, pour ta gentillesse et ta bonne humeur. Merci mon Nico d'avoir été là et d'être toi aussi toujours disponible pour donner un coup de main. Vous avez été tous les 2 de très belles rencontres.

Merci à tous mes amis/collègues de machine à café et de pauses goûter (Christine, Delphine, Charly, Loic, Lucas), les hard-workers du soir (Ana, Abi, Razvan), et les autres belles rencontres (Bianca, Sarah, Renaud, Clément), les anciens du labo (Fabrice, Vincent, Pierrot, Yann), pour votre aide lors de notre installation, pour tous vos conseils et pour les longues discussions scientifiques et moins scientifiques.

Merci à mes nouveaux copains de la Cordée Charpennes/République (et les autres aussi mais la Cordée Charpennes c'est la meilleure !). J'ai beaucoup appris à vos côté sur l'organisation professionnelle et sur moi-même. Votre bonne humeur, votre bienveillance et surtout les gouters de 16h tapantes ont été un atout majeur dans la finalisation de ce manuscrit.

Merci Mme Jamond pour nos nombreuses conversations sur la famille, les amis, les collègues. Je vois aujourd'hui le monde qui m'entoure avec un regard nouveau. Cette thèse je vous la dédie à vous aussi. Merci de m'avoir aidé à sortir la tête hors de l'eau.

Merci à mes soutiens quotidiens pour avoir été toujours présentes pour les bons comme pour les moins bons moments, Magali, pour nos soirées bar à vin et nos longues, très longues discussion sur le palier de la porte parce qu'il y a toujours quelque chose à raconter ; Mailys, tu es toujours à mes côtés pour me conseiller et chanter avec moi ;p même à l'autre bout de la planète ; Mathilde, ma tite sœur toujours la quand il faut pour discuter même 5 minutes entre 2 RDV et surtout pour rire et s'amuser ; Cindy, ma petite sœur de qui je me suis beaucoup rapprochée ces 4 dernières années et que j'ai su redécouvrir au cours de nombreux échanges sur notre façon de voir la vie à 700km l'une de l'autre; mes parents qui ont fait tout leur possible pour m'offrir l'opportunité de faire des études, mes grand parents, qui ont été et seront toujours là en Vendée ou bien ailleurs pour organiser nos petits café

Skype, et mes beaux-parents pour les week-end d'air pur sur la côte méditerranéenne qui m'ont permis de me ressourcer et de reprendre des forces (avec une mention particulière pour votre bonne cuisine méditerranéenne !).

Enfin, je n'ai pas de mots assez forts pour remercier celui qui me soutient et surtout me supporte depuis maintenant bientôt 9 ans. Des larmes de stress aux effusions de joie, tu as su m'accompagner dans ce panel d'émotions qu'ont été mes études supérieures. Il est temps maintenant d'ouvrir un nouveau livre pour écrire à 2 les lignes d'une nouvelle vie.

Abbreviation list

AEP: anterior entopeduncular area

ANR: anterior neural ridge

aNSC: active NSC

AOB: accessory olfactory bulb

AON: anterior olfactory nucleus

AP: action potential

bHLH: basic helix-loop-helix

BLBP: brain lipid binding protein

BMP: bone morphogenetic protein

Bp: base pairs

BP: basal progenitor

BrdU: bromodeoxyuridine

CalB: calbindin

CalR: calretinin

CNS: central nervous system

CSF: cerebrospinal fluid

DA: dopamine

Dcx: doublecortin

dpe: days post-electroporation

DPI: day post-injection

EdU: 5-ethynyl-2'-deoxyuridine

EGFP: enhanced GFP

EPL: external plexiform layer

EPO: electroporation

EPSC: excitatory post-synaptic current

GABA: γ-aminobutyric acid

GAD: glutamic acid decarboxylase

GCL: granular cell layer

GFAP: glial fibrillary acidic protein

GFP: green fluorescent protein

GLAST: glutamate aspartate transporter

IPC: intermediate progenitor cell

IPSC: inhibitory post-synaptic current
LGE: lateral ganglionic eminence
LOT: lateral olfactory tract
MCL: mitral cell layer
MGE: medial ganglionic eminence
NSC: neural stem cell
OB: olfactory bulb
OE: olfactory epithelium
ONL: olfactory nerve layer
OPC: oligodendrocyte precursor cell
OR: olfactory receptor
OSN: olfactory sensory neuron
PG: periglomerular
PGL: periglomerular layer
qNSC: quiescent NSC
RFP: red fluorescent protein
RGCs: radial glial cells
RMS: rostral migratory stream
RPC: rostral patterning center
SEZ: sub-ependymal zone
Shh: sonic hedgehog
Stim: stimulation
SVZ : subventricular zone
TAPs: transient amplifying progenitors
TF: transcription factor
TH: tyrosine hydroxylase
TNC: tenascin-C
TSG: terminal selector gene
VNO: vomero-nasal organ
VTA: ventral tegmental area
VZ: ventricular zone
YFP: yellow fluorescent protein

CONTENTS

I. INTRODUCTION PART 1:

THE PERIVENTRICULAR ZONE, A GERMINAL REGION THROUGHOUT BRAIN DEVELOPMENT

I.1. Appearance and patterning of neural stem cells (NSCs) during the embryonic development

During mammalian cerebral cortex development, three different cell types are generated in a complex spatial and temporal manner. The sequence of emergence of these three cell types is preserved throughout the neural axis. First neurons are produced, then macroglial cells: oligodendrocytes and astrocytes.

I.1.1. Formation of the primitive central nervous system (CNS)

Neurons and macroglia ultimately derive from a pseudostratified neuroepithelium of ectodermal origin that lines the cerebral ventricles early in embryonic development. Following formation of the three germ layers, bone morphogenetic protein-inhibiting signals from proteins such as noggin, chordin and follistatin, act to specify a region of the ectoderm in neurectoderm by three weeks of development in humans and around embryonic day E8.5 in mice (Rubenstein et al., 1994). A groove then forms along the long axis of the neural plate and, by week four of development in human and at E10.5 in mice, the neural plate wraps in on itself to give rise to the neural tube (**Figure 1A**), which is filled with cerebrospinal fluid (CSF). The CSF-filled central chamber is continuous from the telencephalon to the spinal cord and constitutes the developing ventricular system of the CNS. Neuroepithelial cells that line the lumen of this neural tube are the future NSCs that give rise to all cell subtypes of the CNS.

Upon closure of the neural tube, three vesicles form in the rostral most portion of the neural tube to form the prosencephalon, mesencephalon and rhombencephalon. These vesicles will further enlarge and subdivide to eventually form the different regions of the brain. For instance, the prosencephalon forms the telencephalon and diencephalon, the former developing into the cerebral cortex and basal ganglia. This early phase of brain growth is associated with the rapid proliferation of neuroepithelial cells. These cells constitute a single layer of cells called the ventricular zone (VZ), with their nuclei being positioned in a manner suggestive of a stratified epithelium. Therefore, they are defined as “pseudostratified neuroepithelial cells” (Miyata, 2008) (**Figure 1B**).

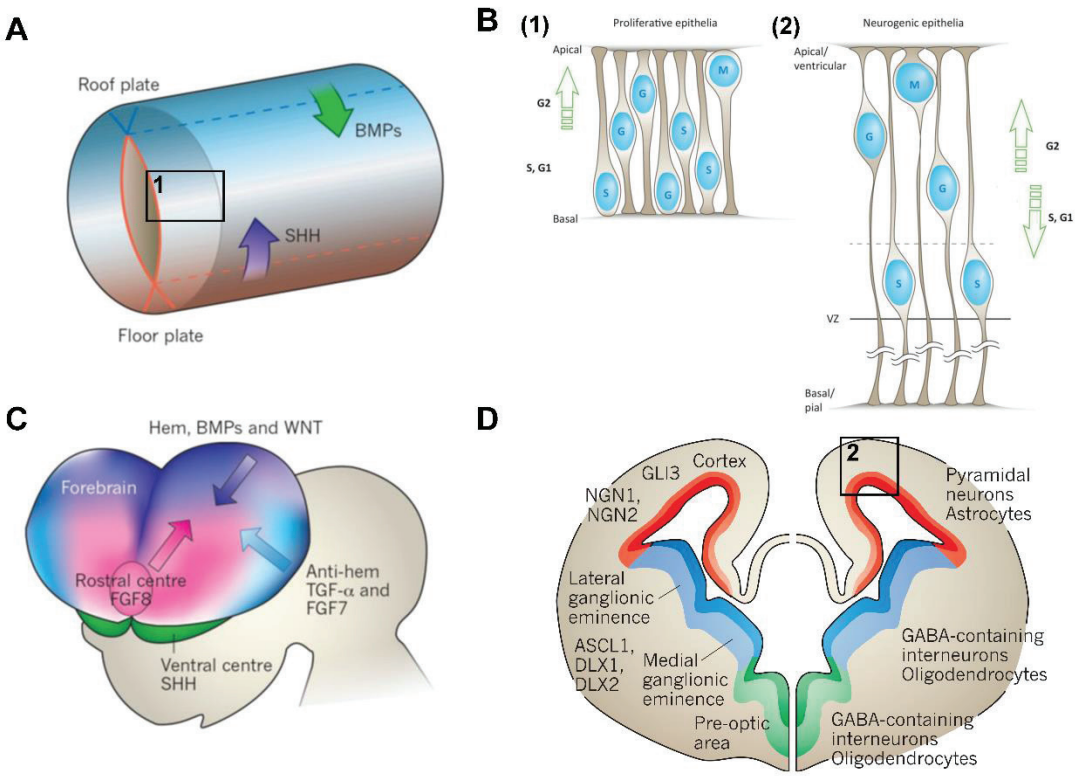

Figure 1: Patterning of embryonic NSCs

(A) The primitive neuroepithelium of the neural tube is patterned by organizing signals. Dorsalizing BMPs signal and ventralizing SHH signal emanate from the roof plate and the floor plate respectively. (B) Illustration of neuroepithelial cells organized in a pseudostratified neuroepithelium that transform into radial glial cells around E10. The interkinetic nuclear movement is characterized by a direct movement toward the apical surface during G2 phase, while cells in G1 and S phase are observed in the all length of pseudostratified epithelium. In the neocortex, the movement of radial glial cells nucleus correlates with cell-cycle phases. (S: S phase; G: G1 and G2 phase; M: mitosis) (C) Illustration of the signaling centers in the telencephalon. The anterior neural ridge (ANR, pink) expresses FGF8. The cortical hem is a source of Wnt and BMPs morphogens. The ventral organizer antagonizes the hem secreting SHH morphogen. The anti-hem opposes the ANR and the hem secreting TGFα and FGF7. (D) Coronal view of the embryonic forebrain (E14.5) showing the regionalization of the SVZ into microdomains expressing different transcription factors and generating specific cell lineages. (Illustrations from Lee & Norden 2013 (B); Rowitch & Kriegstein 2010 (A, C, D))
Abbreviations: VZ: ventricular zone

I.1.2. Emergence of radial glial cells (RGCs) from neuroepithelial cells

At mid-gestation around E9-10 in mouse, the first neurons in the CNS are born, heralding an important developmental transition in the development of the neural progenitor cells of the brain. Neuroepithelial cells begin to acquire features associated with glial cells and start to express astroglial markers such as the astrocyte-specific glutamate transporter (GLAST) (Malatesta et al., 2003), brain lipid-binding protein (BLBP), and Tenascin C (TN-C) (see for review Campbell & Götz 2002; Kriegstein & Götz 2003). They also express a variety of intermediate filament proteins including nestin and vimentin. Throughout brain development, these cells will remain in contact with both the pial and the ventricular surface (**Figure 1B**). This is achieved by the formation and the gradual lengthening of a basal process, in contact to the pial surface, while a shorter apical process remain in contact to the ventricular surface (Noctor et al., 2001, 2004). These processes allow them to integrate signals from both the CSF and meninges, such as retinoic acid, which play important roles in controlling their proliferative and differentiation behaviors (Siegenthaler et al., 2010). The presence of these processes that gives the cells a peculiar radial morphology, as well as their expression of glial markers define them as “radial glial cells” (RGCs) (**Figure 1B**).

RGCs present all the characteristics of NSCs: i.e. they have the capacity to self-renew and to produce all neural lineages (i.e. neurons, astrocytes and oligodendrocytes). Their self-renewal capacity is underlined by their complex mitotic behavior known as interkinetic nuclear migration. Several observations suggest that nuclear migration is linked to cell cycle progression (Miyata, 2008) (**Figure 1B**). This particular behavior allows the exposition of progenitor cell nuclei to neurogenic or proliferative signals regulating the differentiation process. The importance of cell polarity and the activation of signaling pathways like Notch are essential for the maintenance of RGCs identity and their self-renewal properties (Gaiano et al., 2000). For instance the disruption of Par complex, involved in the localization of cell polarity, leads to premature differentiation of RGCs (Costa et al., 2007; Bultje et al., 2009). Their multipotency is supported by fate mapping experiments, which reveal that RGCs serve as precursors of both neurons and macroglial cells in all brain regions (Anthony et al., 2004; Casper and McCarthy, 2006; Kriegstein and Alvarez-buylla,

2009). Thus, RGCs produce most, if not all of the neurons and glial cells that compose the CNS.

The CNS of mammals is a highly complex structure made up of a huge number of neurons, glial cells all derived from embryonic RGCs (Kriegstein and Alvarez-buylla, 2009). The primitive germinal layers consist of a primary proliferative zone called the ventricular zone (VZ) containing RGCs, the direct descendant of the primitive neuroepithelium. A secondary proliferative zone called the subventricular zone (SVZ) emerges later from the VZ (Farkas and Huttner, 2008). After an intense period of proliferation to create a pool of NSCs in the VZ, RGCs switch from proliferation to differentiation and undergo asymmetric divisions (Noctor et al., 2004). They give rise to rapidly proliferating cells called intermediate progenitors or basal progenitors (BPs). These progenitors are already lineage-restricted and will produce different subtypes of glutamatergic cortical neurons and GABAergic interneurons in a spatial and temporal specific manner.

I.1.3. Early regionalization of embryonic NSCs by morphogens and transcription factors

The production of neurons, including neuronal subtypes, and microglial cells follows a stereotyped spatial and temporal pattern. The regionalization of the telencephalon germinal activity starts with the emergence of four distinct signaling centers (also referred as “patterning centers”, (Hoch et al., 2009)) (**Figure 1C**). The expression of FGF8 at the rostral end of the neural plate, known as the anterior neural ridge (ANR) or commissural plate defines the rostral patterning center (RPC), a first signaling center important to establish regional patterning of the forebrain. A second dorso-medial center, the cortical hem, represents the main source of Wnt morphogens and is antagonistically regulated by the anterior mesendoderm expression of dickkopf 1 (Dkk1) as well as by the secretion of Hesx1 by the RPC. Similarly, bone morphogenic proteins (BMPs) are overexpressed in the cortical hem. Their activity is limited to nearby regions by the expression of BMPs antagonists by the RPC, including chordin and noggin. A ventral organizer, which is reciprocally regulated by RPC FGF8 expression, opposes the hem by secreting sonic hedgehog (Shh). Finally, a last signaling center, the anti-hem, is located between the hem and the ventral organizer. It secretes FGF7/15, TGFα and Wnt antagonists to oppose FGF8 and Wnt signaling activity and therefore participate in setting up the medio-

lateral and ventral patterning. Thus, at early developmental stages, reciprocal regulatory interactions are associated to the graded diffusion of morphogens to define the distinct rostro-caudal and dorso-ventral specificities of RGCs.

The coding of this patterning by morphogens is mediated by the expression of defined transcription factors (TFs). Here I will focus on two of these domains, the pallium and subpallium of the telencephalon (**Figure 1D**). Elevated levels of Wnts and BMPs lead to the expression of pallial markers such as Pax6 and Emx1. RGCs in this pallial (dorsal) region of the telencephalon generate glutamatergic neurons of the cerebral cortex as well as its most rostral region, the olfactory bulb (OB) (see part II.2 for a more detailed description of OB formation). During their differentiation, RGCs will sequentially express waves of TFs, which include Neurog2, Tbr2 and Tbr1 (Telley et al., 2016; Mihalas and Hevner, 2017). In contrast, Shh expression in the ventral most region of the developing forebrain results in the repression of these TFs and expression of subpallial markers such as TFs of the Gsh and Nkx family (Kriegstein and Götz, 2003). These two markers define progenitors of the medial and lateral ganglionic eminences (MGE: Nkx2.1 an LGE: Gsh2), as two independent subpallial regions. There, GABAergic interneurons are born that migrate to distinct regions of the forebrain (cortex, striatum, OB…) depending of their exact site of origin (Wichterle et al., 2001). Perturbation of this regionalization can be achieved by deletion of single TFs. For instance, the deletion of pallial genes Emx1/2, Pax6 and Neurog2, results in varying degrees of dorsal fate loss and in an enlargement of the ventral domain, as evidenced by the increased expression of subpallial markers (e.g. Gsh1/2; Nkx2.1 and Dlx1/2), and vice-versa.

I.2. Regionalized RGCs generate a high variability of cortical progenies

I.2.1. The precise timing of production of different neural cells is essential for generating the final complex cortical cytoarchitecture

The cerebral cortex is the most complex structure in the mammalian brain and displays a high diversity of neuronal subtypes. This complexity is established sequentially, as described above. The production of glutamatergic neurons occurs first from pallial progenitors. In the cerebral cortex, this specification follows a coordinated temporal pattern with preplate cells, which include Cajal-Retzius

neurons, produced first (**Figure 2A**). Then, the preplate is separated into marginal and subplate layers by immigrant cortical layer neurons that are born in an inside-out order: neurons destined for the deep layers VI and V are born first, followed by those destined for the more superficial layers IV, III and II (Miller and Nowakoski, 1988; Martynoga et al., 2012). Thus, a second level of complexity emerges through the specification of different subtypes of cortical neurons integrating specific cortical layers, where they exhibit specific patterns of gene expression and connectivity (Martynoga et al., 2012). While projection cortical neurons continue to be produced, GABAergic interneurons start to be generated from the MGE, the major source of cortical interneurons. Newborn interneurons migrate dorsally and invade the developing neocortex via the neocortical SVZ and differentiate into transient subpial granule neurons in the marginal zone and into a stable population of GABA-, parvalbumin-, or somatostatin- expressing interneurons throughout the cortical plate (Wichterle et al., 2001).

I.2.2. Migration pattern of cortical neurons and interneurons

During the elaboration of the different layers of the cortex, RGCs are essential for the migration of newborn neurons. They act as scaffold for glutamatergic neurons migration into the forming cortical plate (**Figure 2A**). This behavior appears crucial since the transplantation of neocortical progenitors in the adult brain does not allow the development of glutamatergic neurons in the cortex because of the absence of guiding RGCs (Wichterle et al., 1999). Time-lapse imaging of retroviral labeled RGCs reveals that newborn neurons migrate along the parental RGC and that migration continues while the guiding RGC is dividing (Noctor et al., 2001, 2008). Most, if not all, neuronal cells have to migrate from the sites where they are born to places where they terminally differentiate and integrate into the brain circuitry. However, not all neuronal precursors require RGCs for their translocation in the cortex. The LGE and MGE are two compartments of the subpallium that contain neuronal precursors capable of extensive migration in vivo and in vitro (Wichterle et al., 1999, 2001) (**Figure 2B**). While MGE precursors migrate through the cortical SVZ to reach cortical layers, LGE cells migrate ventrally and anteriorly and give rise to projection spiny neurons in the striatum, nucleus accumbens and olfactory tubercles as well as granule and periglomerular interneurons in the OB (see part II-2-2 for more details on OB neurogenesis).

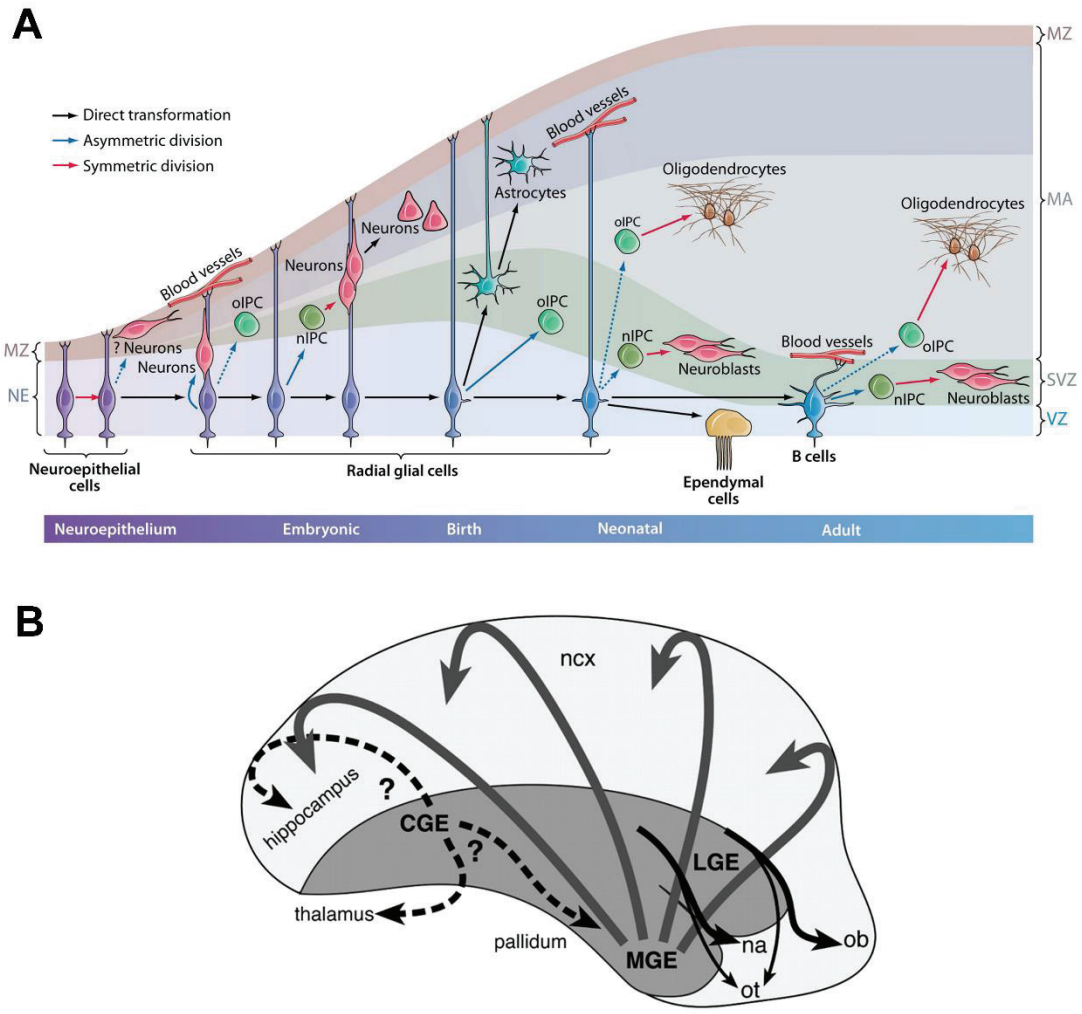

Figure 2: Formation of the neocortex

(A) Neuroepithelial cells in early development divide symmetrically to generate more neuroepithelial cells. Some neuroepithelial cells likely generate early neurons. As the developing brain epithelium thickens, neuroepithelial cells elongate and convert into radial glial cells (RGCs). RGCs divide asymmetrically to generate neurons directly or indirectly through intermediate progenitor cells (nIPCs). Oligodendrocytes are also derived from RGCs through intermediate progenitor cells that generate oligodendrocytes (oIPCs). As the progeny from RGCs and IPCs move into the mantel for differentiation, the brain thickness increases, further elongating RGCs. Radial glia have apical-basal polarity: apically (down), RGCs contact the ventricle, where they project a single primary cilium; basally (up), RGCs contact the meninges, basal lamina, and blood vessels. At the end of embryonic development, most RGCs begin to detach from the apical side and convert into astrocytes while oIPC production continues. Production of astrocytes may also include some intermediate progenitors not illustrated here. A subpopulation of RGCs retains apical contact and continues functioning as NSCs in the neonate. These neonatal RGCs continue to generate neurons and

oligodendrocytes through nIPCs and oIPCS; some convert into ependymal cells, whereas others convert into adult SVZ astrocytes (type B cells) that continue to function as NSCs in the adult. B cells maintain an epithelial organization with apical contact at the ventricle and basal endings in blood vessels. B cells continue to generate neurons and oligodendrocytes through (n and o) IPCs. This illustration depicts some of what is known for the developing and adult rodent brain. Timing and number of divisions likely vary from one species to another, but the general principles of NSC identity and lineages are likely to be preserved. Solid arrows are supported by experimental evidence; dashed arrows are hypothetical. Colors depict symmetric, asymmetric, or direct transformation. (Illustration from Kriegstein & Alvarez-buylla 2009). (B) A model of tangential neuronal migratory pathways in the developing mouse brain is illustrated on a longitudinal view of the developing telencephalic vesicle with the anterior end pointing to the right. Gray arrows depict the large scale migration of MGE cells into the developing neocortex (ncx). Black arrows depict the migratory pathways from different parts of the LGE. Cells from the dorso-anterior LGE migrate preferentially into the olfactory bulb (ob), while more posteriorly grafted LGE cells migrate preferentially into the nucleus accumbens (na). LGE cells disperse through the striatum and migrate ventrally to the olfactory tubercle (ot). Hypothetical migratory routes from the caudal ganglionic eminence (CGE) are depicted by broken arrows. (Illustrations from Wichterle et al. 2001).

Abbreviations: CGE: caudal ganglionic eminence; IPC: intermediate progenitor cell; LGE: lateral ganglionic eminence; MA: mantle; MGE: medial ganglionic eminence; MZ: marginal zone; na: nucleus accumbens; ncx: neocortex; NE, neuroepithelium; nIPC: neurogenic progenitor cell; oIPC: oligodendrocytic progenitor cell; ob: olfactory bulb; ot: olfactory tubercle; RG: radial glia; SVZ: subventricular zone; VZ: ventricular zone.

I.2.3. A high diversity of glial cells is generated in the developing brain

In the CNS, glial cells represent a heterogeneous population of cells that fulfill a number of complex functions in the brain. Glial cells represent 55.4% in the mouse cerebral cortex and 91.7% in humans (Herculano-Houzel, 2014).

Among all glial cells produced in the CNS, astrocytes represent the most abundant and heterogeneous glial population in the vertebrate brain and spinal cord. Cajal was the first who described distinct types of astrocytes in the human hippocampus. Astrocytes were generally classified in two main populations: (1) protoplasmic astrocytes that occupy the grey matter, (2) fibrous astrocytes, which reside in the white matter. However, the use of new genetic tools that specifically label astrocyte progeny and reveal their detailed morphology has revealed that astrocytes are much more heterogeneous than this classical and simple distinction (García-Marqués and López-Mascaraque, 2013).

Additionally to their morphological heterogeneity, astrocyte populations exhibit various functional properties. Astrocytes are essential in brain development and function. For instance, they serve as structural support, maintain the blood brain barrier, provide trophic and metabolic support to neurons and are involved in cell-cell signaling and regulate synaptogenesis and synaptic transmission through neurotransmitter recycling. Although certain astrocytes functions are common throughout the CNS, other functions influence the local neuronal circuitry and might be domain-specific. Recent studies have evidenced the clonal compartmentalization of astrocyte populations with clones of different sizes occupying different brain areas in accordance with their embryonic origin in the VZ-SVZ (Tsai et al., 2012). Regional differences in astrocytes have been recently shown to influence neuronal synaptogenesis and maturation through secretion of several extracellular matrix proteins (Eroglu and Barres, 2010). Thus, astrocytes organized in functional domains contribute to neuronal circuit formation and maturation by forming an astrocytic network (Houades et al., 2006). In the OB, astrocyte clones are observed, which are concentrated in a single or few adjacent glomeruli. Such compartmentalization would allow the formation of functional domains by promoting communication of astrocytes within a single glomerulus and could modulate sensorial information from the

olfactory epithelium (Roux et al., 2011; García-Marqués and López-Mascaraque, 2016).

This heterogeneity in astrocytes takes its origin early during development and could be influenced by extrinsic and intrinsic factors (García-Marqués and López-Mascaraque, 2013; Bribian et al., 2016). During embryonic development, astrocytes are produced after neurons and before oligodendrocytes all happening in partially overlapping waves (Rowitch and Kriegstein, 2010). In the cerebral cortex, glial cells are classified into astrocytes, oligodendrocytes, microglia, ependymal cells, tanycyte and NG2 cells (Tekki-Kessaris et al., 2001; Spassky et al., 2005; Nishiyama, 2007; Richardson et al., 2011; Khakh et al., 2015). As already described in the previous paragraphs, the differentiation of all cell types of the brain from their respective NSCs involves patterning of spatial genetic and environmental factors along the rostro-caudal and dorso-ventral axis of the CNS (Kohwi and Doe, 2013). RGCs from the embryonic VZ share neurogenic and gliogenic potencies (Rowitch and Kriegstein, 2010). Thus they generate first cortical neurons and later glial cells including ependymal cells, astrocytes and oligodendrocytes (Doetsch et al., 1999; Noctor et al., 2001; Kriegstein and Götz, 2003; Malatesta et al., 2003; Kriegstein and Alvarez-buylla, 2009). The switch from neurogenesis to gliogenesis is influenced by genetic and environmental factors affecting the differentiation programs of NSCs (Rowitch and Kriegstein, 2010). However, there are still controversies on the origin of macroglial cells from bipotential progenitors (Bribian et al., 2016). In the adult brain, NSCs also give rise to oligodendrocytes and mature astrocytes (Menn et al., 2006; Merkle et al., 2007; Gonzalez-Perez and Alvarez-buylla, 2011). Recent studies have revealed that different classes of astrocytes derive from single clones suggesting that astrocyte heterogeneity is specified early during CNS development (García-Marqués and López-Mascaraque, 2013). Glial lineage however presents characteristics that challenge their study. Indeed, embryonic RGCs give intermediate astroglial progenitors which migrate from the VZ-SVZ to their final destination where they start proliferating by symmetric divisions. New technics developed these last years allow the clonal study of this peculiar cell type and identified a high diversity of glial cells (García-Marqués and López-Mascaraque, 2013).

The second main type of macroglial cells in the brain are oligodendrocytes. Oligodendrocytes insulate axons to allow a rapid saltatory conduction and give

trophic support to axons (Nave, 2010). Myelination of axons by mature cortical oligodendrocytes begins during late embryonic development and persists into adulthood. Another type of glial cells, the NG2 glial cells behave as oligodendrocytes progenitors in white matter and are thus able to generate mature myelinating oligodendrocytes throughout life (Dimou et al., 2008). In grey matter however, they rarely give rise to astrocytes or oligodendrocytes. Oligodendrocytes like astrocytes derive from embryonic RGCs which give rise to oligodendrocytes precursors (OPCs) migrating to their final destination and proliferating intensively just before terminal differentiation. Neural progenitors that differentiate into cortical oligodendrocytes in the adult brain are derived from self-renewing NSCs during a period from E12 to P10. Three waves of OPCs generation have been described: (1) from the VZ-SVZ of the ventral region from the MGE to the anterior entopeduncular area (AEP), (2) then from the LGE and (3) finally from the Emx1 lineage (Naruse et al., 2017).

Several models have been described to explain the generation of glial lineages during development. Previous studies suggested that astrocytes and oligodendrocytes lineages might be related because of the existence of bipotential progenitors able to give rise to both cell type during the first stage of embryonic development (Levison and Goldman, 1993; McCarthy et al., 2001). Although this fact is clearly observable at early development stages, changes over development are more consistent with the model characterized by the progressive restriction of NSCs to generate distinct neural lineages during development (Mallamaci, 2013). The exact temporal and clonal origin of glial progeny has yet to be investigated.

I.3. Transformation of the periventricular zone after birth

I.3.1. The postnatal SVZ undergoes major cytoarchitectural changes early after birth

During the first postnatal weeks, relevant modifications in the maturing SVZ affect the glial cell population, in which the morphological changes do occur in parallel with changes in their identity attesting of the transition between embryonic RGCs and adult NSCs (**Figure 2A**). At birth, VZ RGCs exhibit an elongated soma orthogonal to the ventricular surface with a clear cytoplasm, a cilium extending to the ventricular lumen and a long radial process extended into the parenchyma thus being identifiable as radial glia (Tramontin et al., 2003). An actively proliferating VZ

characterized by interkinetic nuclear migration is still present in neonatal mice as evidenced by electron microscopy and birth dating experiments with 3H thymidine on newborn mice (Tramontin et al., 2003). Although proliferative VZ cells behave similarly in embryos and neonates (Tramontin et al., 2003), the anatomy of this region changes dramatically during the first postnatal weeks. Most of RGCs are progressively replaced by immature ependymal cells during the first 2-4 postnatal weeks (Spassky et al., 2005). Ependymal cells are generated from embryonic RGCs between E14 and E15 but differentiate and mature later as revealed by the appearance of cilia during the first postnatal week. Thus, at early postnatal stages, periventricular walls are covered of RGCs composed of a mix of at least 2 populations: 1) a first population of RGCs that gives rise to ependymal cells (Merkle et al., 2004; Spassky et al., 2005); 2) a second population of RGCs at the origin of adult NSCs (Tramontin et al., 2003; Merkle et al., 2004) (**Figure 2A**). The transition between embryonic RGCs and adult NSCs is also attested by a deep change in glial cell morphology characterized by the increase of the ramification of their cell body and the appearance of GFAP immunoreactivity during the second week in mice (Tramontin et al., 2003; Peretto et al., 2005). NSCs in the SVZ retract their processes and change the orientation of their process from radial to tangential on the external border, at the limit with the surrounding parenchyma (Alves et al., 2002; Peretto et al., 2005).

These changes in the morphology and the identity of VZ-SVZ glial cells lead to major changes in the cytoarchitecture of the postnatal germinal zone that evolves from an embryonic pseudostratified epithelium into the adult SVZ, separated from the ventricle by a layer of ependymal cells (and therefore also named sub-ependymal zone, SEZ, by some authors) (**Figure 3**). The SVZ expands greatly during the last third of prenatal development in parallel with progressive reduction of the VZ (Peretto et al., 1999, 2005; Tramontin et al., 2003). This trend continues during the first postnatal weeks folllowed by the disappearance of the VZ beyond P15 and the persistance of the SVZ exclusively. In most CNS regions, the germinal layers disappear soon after birth, leaving a non germinal epithelium composed of multiciliated ependymal cells. On the lateral and dorsal wall of the lateral ventricle, the SVZ is more prominent and persist throughout adulthood while the SVZ of the medial wall appear thinner. In rodents, because of the closure of the olfactory

ventricle, glial cells aggregate in the rostral part of the SVZ to form thick septa that will ultimately become the glial tubes during the third and fourth postnatal weeks and lead to the appearance of the rostral migratory stream (RMS) forming through the olfactory peduncles and bulb axes (Peretto et al., 1999). OB radial glia then progressively disappears during the first 3 weeks of postnatal life transforming into several subclasses of astrocytes (Chiu and Greer, 1996; Puche and Shipley, 2001). These first evolutions will further influence postnatal and adult neurogenesis with SVZ neuronal precursors undergoing long-distance migration to reach their final site of destination in the OB (Lois and Alvarez-Buylla, 1994).

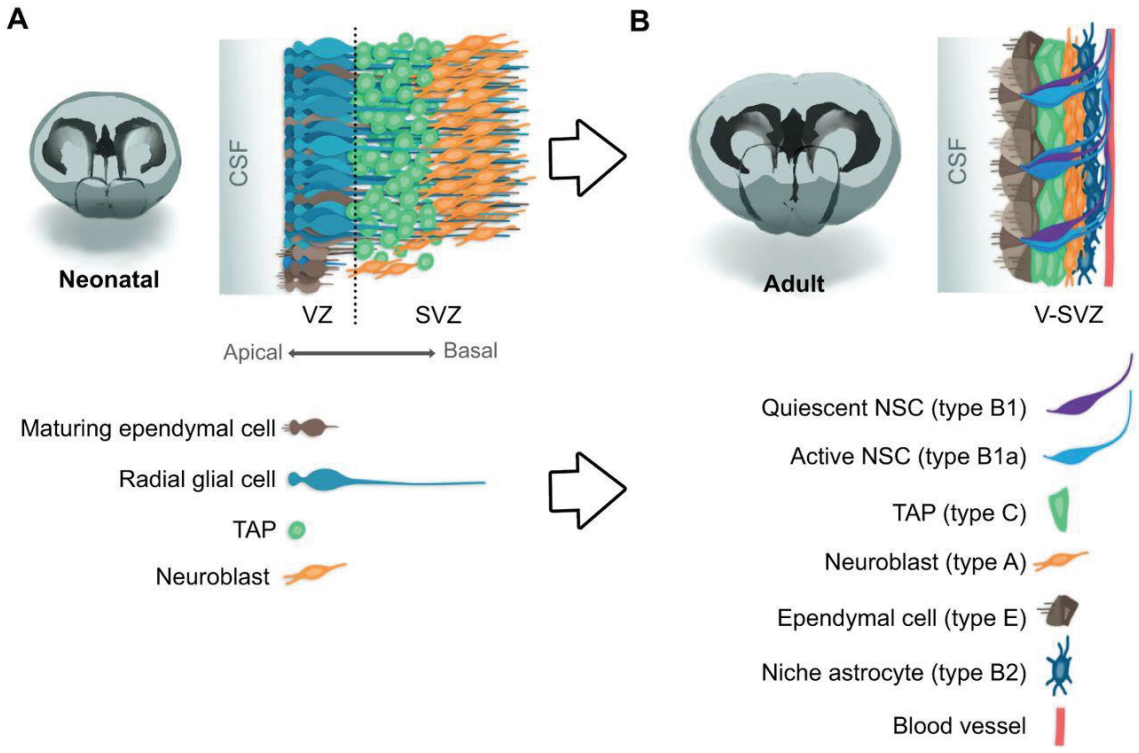

Figure 3: Cellular organization of the postnatal and adult V-SVZ

(A) In the first days after birth, the lateral wall is layered in a ventricular zone (VZ), which is composed of three layers of radial glial cells (RGCs), and a subventricular zone (SVZ), which is populated by proliferating transit amplifying progenitors (TAPs) and migrating neuroblasts. In the lateral wall, RGCs begin to retract their long basal processes following a ventro-dorsal gradient. Some RGCs begin to differentiate into ciliated ependymal cells. (B) Following postnatal maturation, the V-SVZ becomes considerably thinner and clearly structured (from ~300 µm at birth to <100 µm in the adult mouse). Adult quiescent and actively proliferating NSCs contact the CSF with an apical process that is surrounded by ciliated ependymal cells arranged in stereotypical pinwheel structures, although the density and organization of these pinwheels vary throughout walls and rostro-caudal coordinates. TAPs and neuroblasts are also more tightly organized compared with the neonatal V-SVZ – respectively in clusters (green) and dorsally migrating chains (orange) in close proximity to the NSCs. On the parenchymal side of the V-SVZ, the NSC basal end-feet contact the blood vessels. Note that the pattern of the pinwheel structures is shown as being very regular for simplification purposes; it is actually more complex and irregular *in vivo*. (Illustration from Fiorelli et al. 2015)

Abbreviations: SVZ : subventricular zone ; TAP: transient amplifying progenitor; VZ: ventricular zone; V-SVZ: ventricular-subventricular zone.

I.3.2. Adult NSCs confer a unique pinwheel structure to the ventricular surface

The adult SVZ continues to harbor NSCs, called type B cells, and described as a subpopulation of astrocytes because of their ramified morphology. Adult NSCs are slowly dividing and exhibit radial glia properties characterized by GFAP immunoreactivity (Lois et al., 1996; Doetsch et al., 1999; Peretto et al., 2005). These glial cells retain some cytological and molecular features of radial glia since they contain intermediate filament vimentin and nestin (Doetsch, 2003). Contrary to embryonic RGCs, adult NSCs are displaced from the VZ into the SVZ by ependymal cells (**Figure 3B**). Type B cells are thus isolated from the CSF in the lateral ventricle by a layer of two types of ependymal cells: multiciliated (E1) and a novel type (E2) of ependymal cells characterized by only two cilia and extraordinarily complex basal bodies. Ependymal cells thus confer a specific pinwheel organization to the adult ventricular surface. In the middle of these pinwheels, NSCs extend an apical ending protruding in the ventricle through the ependymal layer and a long basal process ending on blood vessels (Mirzadeh et al., 2008). SVZ NSCs are thus in intimate contact with all SVZ cell types and the cavity of the ventricle (Doetsch et al., 1997). Type B cells then give rise to transient amplifying progenitors (TAPs) called type C cells, with a high rate of proliferation. These immature progenitors give neuroblasts known as type A cells. Neuroblasts are bipolar cells with a large nucleus and a thin electrodense cytoplasm co-expressing β-tubulin, doublecortin (Dcx) and PSA-NCAM markers (Doetsch et al., 1997). These immature neuroblasts leave the SVZ and migrate a long distance throughout the RMS toward their final destination in the OB.

Thus, astrocytic NSCs keep their properties of multipotency from embryonic development to adulthood. Throughout adult life, cells born in the SVZ migrate a long distance along the RMS to the OB where they differentiate into mature interneurons (Lois and Alvarez-Buylla, 1994; Doetsch et al., 1999).

I.3.3. Active and quiescent NSCs persist in the postnatal and adult SVZ (or SEZ)

Since several years, we are used to think that postnatal NSCs only originate from embryonic RGCs (Tramontin et al., 2003). Interestingly, the labeling of neonatal RGCs highlight the evidences that they are able to produce all cell types of the adult

SVZ (Type B, C and A) but also migrating neuroblasts in the RMS and newborn neurons in the granular and glomerular layers of the OB (Merkle et al., 2004). In addition, the observations that adult B1 cells keep expression of RGCs markers and their epithelial baso-apical organization suggest a continuum in NSCs lineage from neuroepithelial cells of the neural tube to B1 cells in the adult SVZ. Recent studies however reveal that postnatal NSCs come from a subpopulation of embryonic RGCs emerging between E13.5 and E15.5 and slowly dividing until birth or becoming quiescent before their reactivation after birth (Calzolari et al., 2015; Fuentealba et al., 2015; Furutachi et al., 2015).

Quiescent (or slowly dividing) and actively dividing NSCs (aNSCs, activated NSCs) co-exist in the adult SVZ. aNSCs expressing the EGF receptor (EGFR) and nestin are actively proliferating and highly neurogenic in-vivo. In contrast, quiescent NSCs (qNSCs) are dormant or slowly dividing and are negative for Nestin and EGFR markers (Codega et al., 2015). While aNSCs of the SVZ are eliminated by antimitotic treatments, slowly dividing NSCs survive and are able to regenerate the SVZ in vivo (Pastrana et al., 2009). qNSCs dynamically integrate extrinsic and intrinsic signals to either actively maintain their dormant state or become activated to divide and give rise to differentiated progeny.

I.4. Conclusion

Thus, the periventricular region is a germinal zone which undergoes major architectural changes throughout development. The changes in NSCs identity, in their organization as well as their glial and neurogenic potential drastically challenge the study of postnatal neurogenesis. The development of specific tools is of prime importance to unravel the peculiarities of postnatal neurogenesis and better understand the mechanisms underlying the germinal capacities of postnatal NSCs.

II. INTRODUCTION PART 2:

THE OB IS AN INTERESTING MODEL SYSTEM TO STUDY POSTNATAL NEUROGENESIS AND CIRCUIT REMODELLING

II.1. Functional organization of the OB

II.1.1. The olfactory system

Olfaction is the most primitive sensory system. In humans, this sense is not the most developed, but for the rest of the animal world, detecting chemicals in the environment is critical for behavioral adaptation and survival. Therefore, the sense of smell as well as the gustative sense are also referred as the chemosensory system. They aim at giving information about the chemical environment to the brain through a complex but powerful mechanism of transduction. Therefore, it is not surprising that molecular mechanisms and signaling pathways underlying olfactory processing are highly conserved throughout evolution (Hildebrand and Shepherd, 1997).

Most mammals have developed two olfactory systems (**Figure 4**). The common or main olfactory system detects airborne substances, also called odorants. The wealth of odorants is important for animal survival by the initiation of complex behaviors like food localization, reproductive and maternal behaviors, recognition of co-species or emotional and social status. The sensitivity of the main olfactory system is remarkable and enables animals to discriminate thousands of odors molecules. The accessory system, also called vomero-nasal system, more likely detect fluid-phase stimuli. It aims at recognizing species-specific olfactory signals and contains information about location, reproductive state and availability of partners. Beside its role in controlling sexual behaviors, this second system also influences social behaviors such as territorially, aggression and suckling. In the following introduction, I will exclusively focus on the main olfactory system.

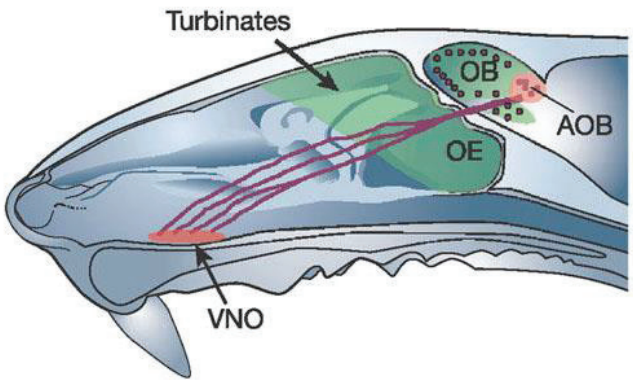

Figure 4: The sensory system in rodents

Sagittal view of the rat head. The main olfactory system (in green) is composed of the olfactory epithelium (OE) covering a set of cartilaginous flaps named turbinates, which serve to increase the surface area of the OE. The olfactory sensory neurons in the OE send their axons to the olfactory bulb (OB), the first relay for odor processing. The vomero-nasal organ (VNO) (in red) and the axons of vomero-nasal sensory neurons project into the accessory olfactory bulb (AOB). The structure of the nasal cavity is optimized for exposing the largest possible surface area of sensory neurons to a stimulus stream that is warmed, moistened and perhaps concentrated by sniffing. (Illustration from (Firestein, 2001))
Abbreviations: AOB: accessory olfactory bulb; OB: olfactory bulb; OE: olfactory epithelium; VNO: vomero-nasal organ.

II.1.2. OB anatomical organization allows discriminating between a large numbers of odorants

At birth, the main structures of the olfactory system (i.e. the OE and the OB) are already in place. The mammalian OB is a layered structure described as early as 1875 by famous anatomists like Camillo Golgi or Santiago Ramón y Cajal. Each layer is discernable on its cellular density, organization and subtypes of neurons composing them (**Figure 5**).

The most external layer of the OB, the olfactory nerve layer (ONL) contains the axons of the olfactory sensory neurons (OSNs) which convey the sensory information from the OE to the OB (**Figure 5 and 6B**). OSNs penetrate into the OB to reach the periglomerular layer (PGL), the first synaptic relay in the treatment of the olfactory information. There, OSNs axons project into specific glomeruli to synapse with the apical dendrite of excitatory projection neurons of the OB, the mitral and tufted cells. The olfactory signal is modulated by different subtypes of interneurons in the PGL and the granular cell layer (GCL). Then, mitral and tufted cells, which cell bodies are located in the external plexiform layer (EPL), and the mitral cell layer (MCL), respectively, project their axons directly to cortical olfactory areas via the lateral olfactory tract (LOT). Thus, olfactory cortex neurons are just separated from peripheral sensory neurons by two to three synapses.

Figure 5: Layered organization of the OB

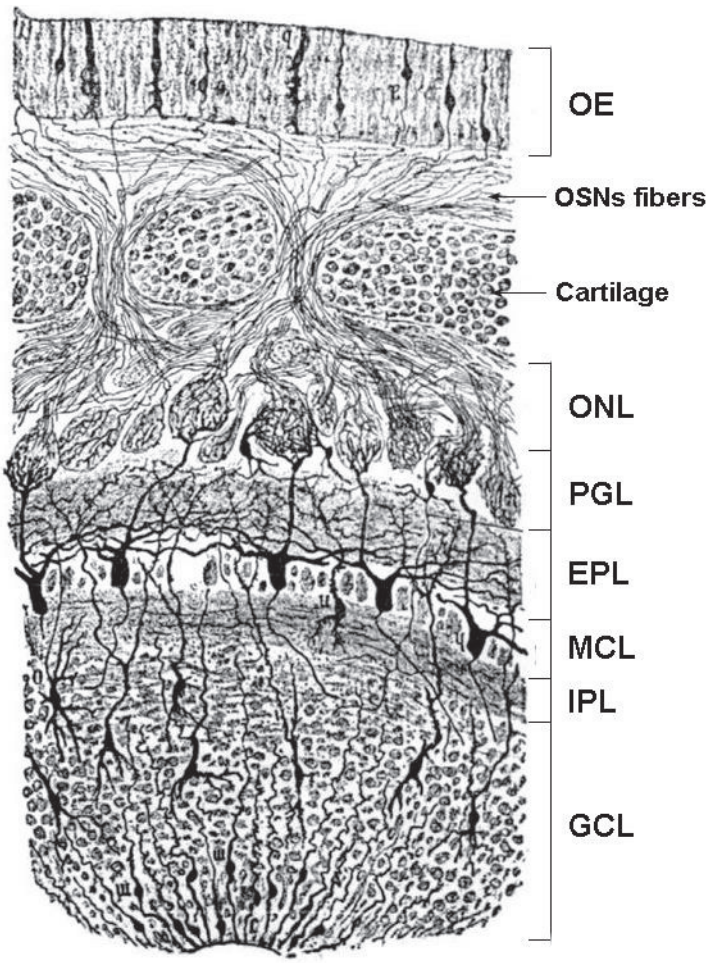

Illustration of one of the first representation of the distinct layers of the olfactory system by Cajal (1890-1891) “Antero-posterior section of the olfactory bulb and nasal mucosa of the newborn rat”. In the olfactory epithelium (OE), olfactory sensory neurons are represented as bipolar cells in between epithelial or supporting cells. Their axons form bundles of fibers that cross the ethmoidal cartilage to synapse in the periglomerular layer of the olfactory bulb. Mitral cells (big dark cells) in the mitral cell layer project their unique apical dendrite in one or few glomeruli and several lateral dendrites in the external plexiform layer. These dendrites are contacted by several subtypes of interneurons located in the periglomerular layer and the granular cell layer respectively. (Illustration adapted from Shepherd et al. 2011)
Abbreviations: EPL: external plexiform layer; GCL: granular cell layer; IPL: internal plexiform layer; MCL: mitral cell layer; OE: olfactory epithelium; ONL: olfactory nerve layer; OSNs: olfactory sensory neurons; PGL: periglomerular layer.

II.1.2.1. Odor information processing in the OB

The olfactory system of mammals detects a vast diversity of odorants via the expression of distinct olfactory receptors (ORs). A remarkable feature of the olfactory system is to stably integrate this information, despite of the continuous birth and replacement of several populations of OB interneurons throughout life. However, the olfactory system differs from classic sensory systems on the fact that it conveys olfactory information toward cortical areas with no thalamic relay. Thus, the information is first processed in the OB before being sent to the olfactory cortex.

Odor discrimination begins with the specific fixation of odorant molecules on ORs expressed by OSNs in the olfactory epithelium (**Figure 6A-B**). Each OSN expresses only one OR subtype among the ~1000 genes coding for ORs in the mammalian genome (Buck and Axel, 1991; Vassar et al., 1994; Malnic et al., 1999).

Odors consist in a panel of various odorant chemical compounds and are therefore attributed to the activation of select OSNs (**Figure 6B**). However, most ORs can be activated by multiple odors and most odors are able to activate more than one type of receptor (see for review Mori & Sakano 2011; Nishizumi & Sakano 2015). The integration of such variable sensory information implies the downstream treatment of specific odorant-mediated responses in a highly organized manner, by specific neuronal circuits.

Odor information detected by OSNs is first processed in the PGL of the OB. OSNs expressing a given OR specifically project their axons into a single or few anatomical structures called glomeruli (**Figure 6C**). OSNs synapse with the apical dendrite of mitral and tufted cells, which extend a single apical dendrite to a single glomerulus (Mombaerts, 2006), thereby integrating olfactory information from a specific subset of OSNs (Wachowiak and Shipley, 2006; Wilson and Mainen, 2006). In mice, a typical glomerulus receives ~1000 OSNs axons and is innervated by the primary dendrite of 20-50 mitral/tufted cells (Imai, 2014) among which 5-20 mitral cells (Sosulski et al., 2011; Ke et al., 2013). In the PGL, the olfactory information is already modulated by a large diversity of GABAergic PG interneurons, which shape the activity and therefore output of projection neurons (see part II.1.3 for further details on PG interneurons subtypes). This specific organization thus allows the segregation of the treatment of odorant molecules into defined glomerular functional units (Lledo et al., 2008; Dubacq et al., 2014).

Mitral and tufted cells associated with a common glomerulus are called “sister” cells and are electrically coupled, thus ensuring synchronous spiking (Schoppa and Westbrook, 2001). Mitral and tufted cells also extend lateral dendrites within the inner and external plexiform layers respectively, which contact the apical dendrites of GABAergic interneurons located in the GCL (Schoppa, 2006) (**Figure 6C**). These reciprocal dendro-dendritic synapses with granular interneurons elicit lateral inhibition of neighboring projection neurons (Yokoi et al., 1995). Granule cells represent a large population of interneurons in the OB and can be subdivided into several subtypes of interneurons, preferentially inhibiting tufted or mitral cells (Merkle et al., 2014; Geramita et al., 2016). Thus, the combination of mitral and tufted cells with lateral inhibition by granular interneurons further facilitates odor discrimination across a wide range of odor concentration.

Axons of mitral and tufted cells forming the lateral olfactory tract (LOT) then project toward olfactory cortex areas that integrate odor information originating from multiple ORs. Interestingly, a spatial regionalization is also observed in the LOT. While mitral cells preferentially project their axons through its dorsal part, tufted cells axons are mainly observed in its ventral part (Nagayama et al., 2010). Axons extend several collaterals targeting various olfactory areas including the anterior olfactory nucleus (AON), the olfactory tubercle, the pyriform cortex, the lateral entorhinal cortex, the cortical amygdala, etc.… (Imai, 2014). Although mitral and tufted cells convey olfactory information in parallel (Fukunaga et al., 2012; Igarashi et al., 2012), their projection pattern differs significantly in the cortex (Igarashi et al., 2012). While a single mitral cell innervates diverse cortical regions such as the AON, the piriform cortex, the olfactory tubercles, the amygdala and the lateral entorhinal cortex, tufted cells project mostly to a subregion of the anterior olfactory cortex (Sosulski et al., 2011; Igarashi et al., 2012). Thus, the convergence of the olfactory information toward a limited number of mitral cells is followed by a step of divergence, as mitral/tufted cells associated with a single glomerulus then diffusely project to almost all regions of the olfactory cortex (Nagayama et al., 2010; Sosulski et al., 2011). In turn, the olfactory cortex and especially the AON and the piriform cortex, send feedback projections toward the OB (Haberly and Price, 1978; Davis and Macrides, 1981). These cortico-bulbar projections mostly synapse with granular interneurons mediating feed-forward inhibition onto projection neurons (Balu et al., 2007; Mazo et al., 2016).

Thus, each glomerulus and its associated OSNs and projection neurons form a single OR module in the OB. This compartmental organization of ORs allows a precise representation of odor information in the OB as spatial maps. Distinct domains in the OB are discernable on OSNs location in the OE and expressed OR classes (see for review Mori & Sakano 2011). Therefore, odorants with similar molecule features tend to activate related areas in the OB.

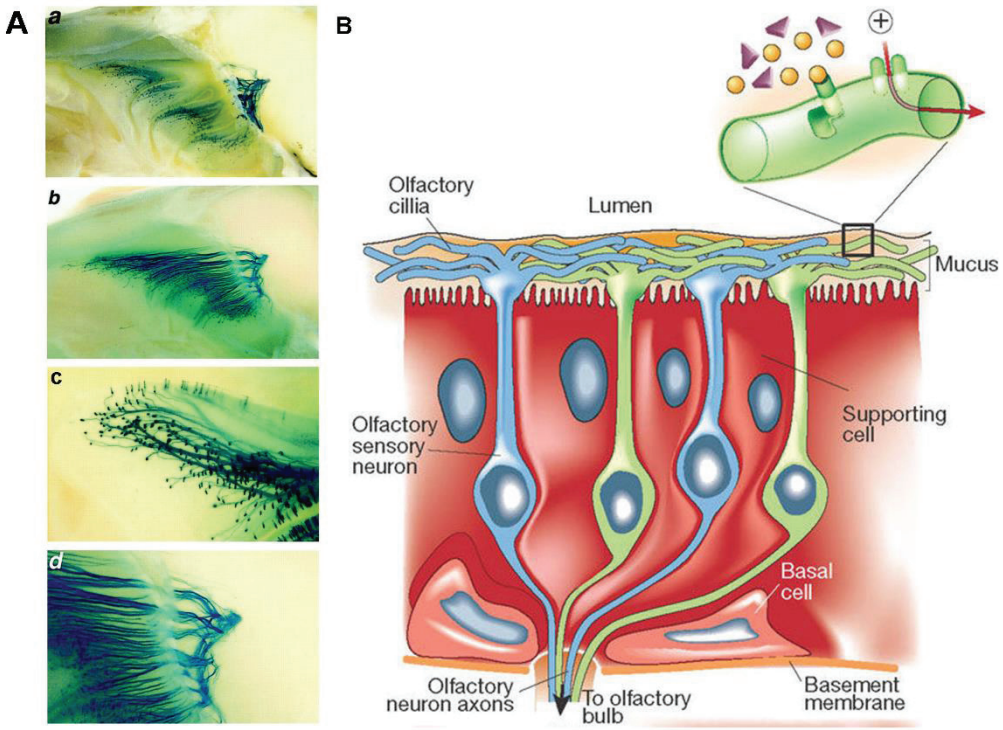
A
a
b
c
d
B
Olfactory cillia
Lumen
Mucus
Supporting cell
Olfactory sensory neuron
Basal cell
Olfactory neuron axons
To olfactory bulb
Basement membrane

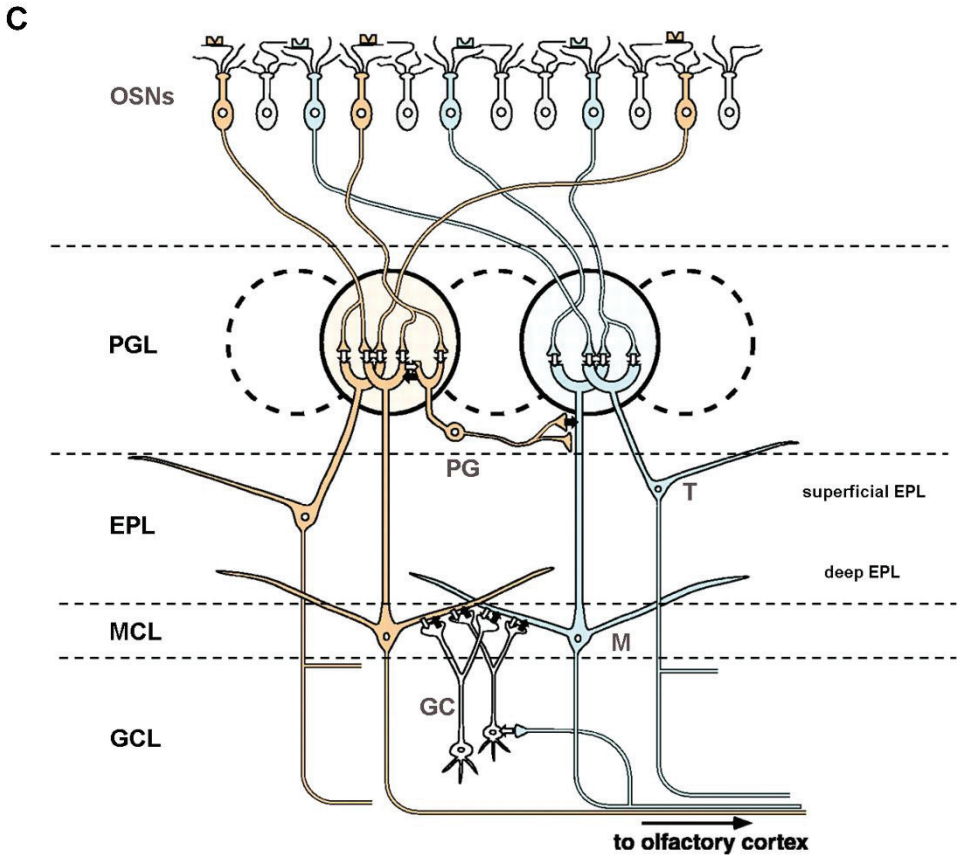
C
OSNs
PGL
PG
T
superficial EPL
EPL
deep EPL
MCL
M
GC
GCL
to olfactory cortex

Figure 6: Segregation of the olfactory information

(A) P2-IRES-tau-lacZ mice stained with X-Gal reveal the organization of olfactory sensory neurons (OSNs) expressing the same subtype of olfactory receptor (P2). While these P2 expressing OSNs are dispersed in the olfactory epithelium, they converge onto a single glomerulus in the OB. Overviews of the wall of the nasal cavity and the medial aspect of the bulb in a 4-weeks-old-mouse (a) and 4-months-old-mouse (b). High magnification on the olfactory epithelium (c). High magnification on a single glomerulus (d). (Figure adapted from Mombaerts et al. 1996). (B) The olfactory neuroepithelium is a relatively simple tissue consisting of three cell types: (1) OSNs are the primary sensing cells and the only neuronal cell type. OSNs are bipolar neurons with a single dendrite reaching the surface of the tissue and ending in a knock-like swelling from which project some 20-30 very fine cilia. These cilia lie in the thin layer of mucus covering the olfactory epithelium and are the site of the sensory olfactory transduction apparatus. They are covered by olfactory receptors (ORs) binding various odorant molecules. ORs are G-protein-coupled receptors (GPCRs) transducing the binding signal into an electrical event propagating into OSNs axons (see zoom picture). Like OB neurons, OSNs in the OE are also replaced over life. (2) Supporting cells, a kind of glial cell, which possess microvilli on their apical surface. In addition to their support role, they detoxify potentially toxic dangerous chemical. (3) A stem-cell population, known as basal cells, from which new OSNs are generated. (Illustration from Firestein 2001) (C) Circuit diagram summarizing the synaptic organization of the OB. Two glomeruli are represented in blue and orange. The axons from all OSNs expressing a given OR converge onto one or a few ‘glomeruli’ in the OB. The nearly 2,000 glomeruli in the rat OB are spherical structures, about 50–100 μm in diameter, which contain the incoming axons of OSNs and the apical dendrites of the projection neurons of the OB, the mitral cell and tufted cells. The olfactory information is first processed by GABAergic interneurons in the PGL and the GCL which contact respectively the apical dendrite and the lateral dendrites of mitral/tufted cells. Mitral and tufted cells axons leaving the OB project widely to higher brain structures of the olfactory cortex through the lateral olfactory tract (LOT). (Illustration adapted from Mori 1999)
Abbreviations: OSNs: olfactory sensory neurons; PGL: periglomerular layer; EPL: external plexiform layer; MCL: mitral cell layer; GCL: granular cell layer; PG: periglomerular cells; T: tufted cell; M: mitral cell; GC: granular cell.

II.1.3. The olfactory signal is modulated by several subtypes of interneurons in the PGL

At the level of each glomerulus, incoming signal onto mitral and tufted cells is shaped by PG interneurons that contribute to 50% of the inhibition received by those projection neurons (Dong et al., 2007). Inhibitory interneurons constitute the vast majority of all neurons in the OB but also the majority of newly generated neurons in postnatal life. In the OB, the ratio of local inhibitory interneurons to excitatory neurons (100:1) is much higher than in other parts of the brain, such as the neocortex (1:5). The balance between excitation and inhibition in the OB, is relatively conserved across mammalian species, suggesting that inhibitory interneurons play essential roles in the processing of olfactory information (Lledo et al., 2008).

In mice, most if not all PG interneurons can be identified by the expression of γ-aminobutyric acid (GABA) or the synthetic enzyme for GABA production, the glutamic acid decarboxylase (GAD) (Kohwi et al., 2007; Kosaka and Kosaka, 2007; Panzanelli P. et al., 2007; Parrish-Aungst et al., 2007) (**Figure 7C**). PG interneurons are subdivided into morphologically and immunohistochemically diverse subpopulations of interneurons (Batista-Brito et al., 2008; Kosaka and Kosaka, 2012). Three main, non-overlapping interneuron subtypes are described in the PGL of the OB (**Figure 7B**). Dopaminergic interneurons expressing the tyrosine hydroxylase (TH), the rate-limiting enzyme in dopamine production, possess the largest soma of the three main subtypes of PG interneurons. The two other subtypes express calcium-binding proteins, the calbindin (CalB) and the calretinin (CalR) (**Figure 7C**). CalR interneurons represent the largest population of PG interneurons subtypes (about 40 to 50 %) (Parrish-Aungst et al. 2007; Kohwi et al. 2007; Panzanelli P. et al. 2007). Although minor in the PGL, other subtypes of interneurons as well as glutamatergic neurons have been described even some of them remain to be fully characterized (Panzanelli P. et al., 2007; Parrish-Aungst et al., 2007; Brill et al., 2009; Merkle et al., 2014) (See part II.2.2 for further detail in PG interneurons generation).

PG interneurons are heterogeneous not only because of their chemical and morphological features, but also because of their synaptic connectivity in the olfactory glomeruli. Because OSNs do not spread into the entire glomerulus, two zones are

discernable into each glomerulus: a first zone where OSNs penetrate in the glomerulus called the olfactory nerve (ON)-zone and a non-ON zone. The dendrites of TH+ interneurons extend all over the glomerulus in ON and non-ON zone and penetrate into clusters of OSNs to make many contacts with their terminal arborization. They are considered as type I PG interneurons, activated by both OSNs and mitral and tufted cells (**Figure 7A**). In contrast, the dendritic arborization of CalB+ and CalR+ interneurons avoid the ON-zone and are thus considered as type II PG interneurons (Kosaka and Kosaka, 2005, 2007). They represent the majority of PG interneurons and receive synaptic inputs from the dendrites of mitral and tufted cells but rarely from OSNs (Toida et al., 1998; Panzanelli P. et al., 2007). Both type I and type II PG interneurons project their dendrites into a single glomerulus and only occasionally to multiple glomeruli. They are likely to mediate intra-glomerular inhibition, which tends to synchronize the output of a single glomerulus. Inter-glomerular inhibition is mediated by other subtypes of PG cells such as superficial short-axon cells (SA) which extend long axons over few to 10 glomeruli (Nagayama et al., 2014) (**Figure 7A**).

Thus, the high diversity of PG interneurons indicates they might mediate different functions within local circuits, which remains to be studied in future physiological studies. The relationship between the heterogeneity in chemospecific neurons and their connectivity and thus their role in the OB circuit remain to be elucidated.

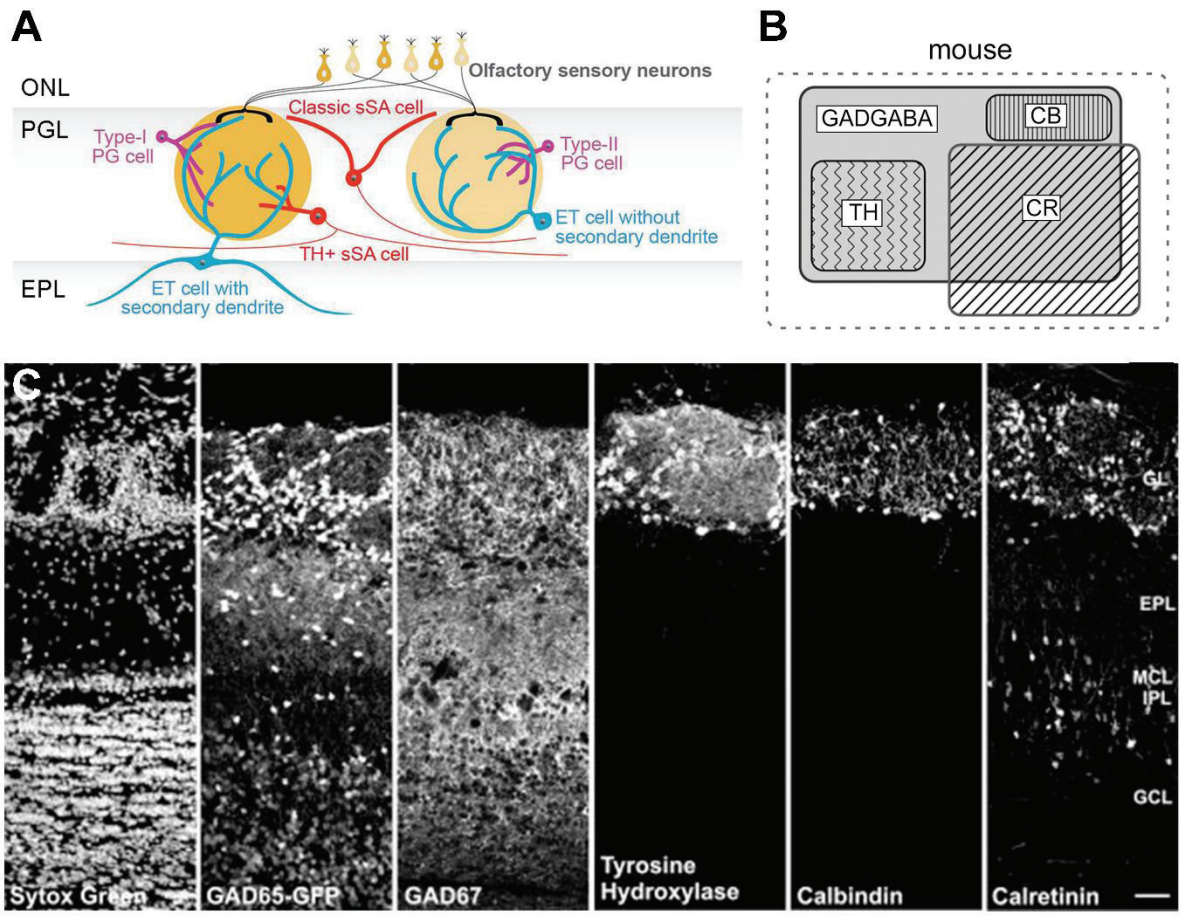

Figure 7: Expression of neurochemical markers in the mouse OB

(**A**) Schematic illustration of PG neuron subtypes: periglomerular interneurons (PG cells; purple), superficial short-axon cells (sSA cells; red), and external tufted cells (ET cells; blue). Two subtypes of PG interneurons can be defined based on their synaptic connections. Type I PG interneurons receive synaptic inputs onto their dendrites from both olfactory sensory neurons and projection neurons in the OB. Type II PG interneurons only receive inputs from mitral and tufted cells. Classically, sSA cells had an axon and dendrites which did not enter a glomerulus. More recently, reported types of sSA cells are positive for tyrosine hydroxylase (TH) and connected to a few to tens of glomeruli. Different subtypes of ET cells are determined by their morphology: those without and those with secondary dendrites. The ET cells with secondary dendrites are more frequently found around the border, between the PGL and the superficial external plexiform layer (s-EPL). ET cells have a larger soma than the other PG cell types. (Illustration from Nagayama et al. 2014). (**B**) Schematic representation of the proportion of the main PG interneurons in the mouse OB. The outer rectangles (broken line) indicate the approximate total cells in the PGL detected by DAPI staining. The area ratios of the rectangles of individual chemically defined cell groups approximately correspond to the proportions of their population sizes. In the mouse OB, all of the TH+ and CalB+ interneurons and the majority of CalR+ interneurons are GAD/GABA expressing cells. TH, CalB and CalR characterize distinct and non-overlapping subpopulations of PG interneurons. (Illustration from Kosaka & Kosaka 2007). (**C**) Immunodetection of the main subtypes of PG interneurons in GAD65-GFP transgenic mice.

The nuclear dye Sytox Green stains all cells. GAD65-GFP is expressed by a subpopulation of cells in all layers. GAD67 immunoreactivity in cell bodies and processes is present in all layers except the ONL. Tyrosine hydroxylase is expressed in neurons restricted to the PGL and only rarely in other layers. Calbindin-expressing interneurons are present in the PGL while Calretinin is expressed by a subpopulation of cells in most OB layers. Scale bar: 50µm. (Illustrations from Parrish-Aungst et al. 2007).
Abbreviations: ONL: olfactory nerve layer; PGL: periglomerular layer; EPL: external plexiform layer; sSA: superficial short-axon cells; PG: periglomerular cells; ET: external tufted cells; TH: tyrosine hydroxylase; CalB: calbindin; CalR: calretinin; GAD: glutamic acid decarboxylase; GABA: γ-aminobutyric acid

II.2. Development of the primitive olfactory bulb

The complex organization of the olfactory system originates from the spatial and temporal regulation of its development during embryogenesis. Despite a common ectodermal origin, the OE (the peripheral component of the olfactory system) derives from the olfactory placode, while the OB emerges from the anterior most germinal regions of the neural tube, similarly to other central nervous system (CNS) structures.

The OB develops from the ventral pallium of the rostral telencephalon (López-Mascaraque et al., 1996). In mouse, the development of the OB starts at E9-E10.5, although it only appears as a distinctive enlargement of the rostral telencephalon after E12.5 (Hinds, 1968a; Inaki et al., 2004). From E12.5, two regions are discernable in the OB. (1) A ventricular zone (VZ) formed by neuroepithelial cells transforming into radial glial cells. In young rodents, this radial glia extends from the VZ lining the olfactory ventricle, to the outer pial surface (Valverde et al., 1992) and is at the origin of the future projection neurons (Bailey et al., 1999) before transforming into several subclasses of astrocytes during the first postnatal weeks (Chiu and Greer, 1996; Puche and Shipley, 2001). (2) A thin mantle zone extending into a superficial mantle zone in which newborn projection neurons accumulate (Bailey et al., 1999).

The exact nature of the signals that induce the initial formation of the OB is not yet fully understood. Studies have first suggested that the arrival of pioneer OSNs axons into the VZ was responsible for the specification of the OB. For instance, the cell-cycle length of cells that give rise to the future OB is significantly prolonged compared to adjacent cortical cells twenty-four hours after the arrival of OSNs axons. The concomitant increase in differentiation in the presumptive OB is believed to trigger the evagination of the OB (Gong and Shipley, 1995). In line with these findings, focal denervation experiments or ablation of the olfactory epithelium lead to abnormality in OB development (Pinching and Powell, 1971a, 1971b; Couper Leo et al., 2000). However, other studies suggest that initial OB formation occurs even in the absence of OSNs axons, and support a role for FGF signaling, also involved in the patterning of the rostral telencephalon. For instance, a normal development of the OB is observed in Dlx-5 mutants in which OSNs failed to reach and innervate the OB

(Levi et al., 2003; Long et al., 2003) as well as in Pax6 mutant mice that lack an olfactory epithelium (Jiménez et al., 2000). Further, the OB does not form in *Foxg1-Cre; FGFr1*$^{fl/fl}$ mice until E16.5 and a small protrusion develops prenatally but does not exhibit the characteristic lamination of normal OB (Hebert, 2003). Further supporting the hypothesis that OB formation is dictated by intrinsic mechanisms, the pioneer populations of OB cells (i.e. the first projection neurons and the first interneurons) differentiate between E10.5 and E12.5 respectively (Hinds, 1968a; Tucker et al., 2006), i.e. before the arrival of the first OSN axons which occurs around E13-15 in mice (Blanchart et al., 2006). Together, these observations suggest that the OB develops in two steps: a first step independent from the OE and OSNs at early embryonic stages and mostly regulated by intrinsic mechanisms, and a second step following arrival of the first OSNs from the OE that refines the OB primordium.

II.2.1. Establishment of OB layers and connectivity

In rodents, the initial stages of OB development present many similarities with the development of the cerebral cortex. The first cells to be born are the glutamatergic projection neurons of the OB, mitral cells and tufted cells, which are generated by RGCs from E11 to E18 (Hinds, 1968a; Bayer, 1983). Granular and periglomerular interneurons are generated from distant sources, predominantly postnatally and, moreover, throughout life (Hinds, 1968a).

II.2.1.1. Development of projection neurons and of their connection to cortical areas

Similarly to cortical neurons, OB projection neurons (i.e. mitral and tufted cells) are produced in an inside out sequence: deep mitral cells are produced first between E11 and E13 in mouse. Their birthdate determines their spatial location in OB neuronal circuits. While early born mitral cells integrate preferentially dorso-medially in the rostral OB, later-born integrate ventro-laterally in the caudal region of the OB (Imamura et al., 2011). Then superficial tufted cells located in the EPL appear around E13 and E18 with a peak of production around E15 (Hinds, 1968b; Imamura et al., 2011). Mitral and tufted cells start to extend their axons to the olfactory cortex around E11.5 initiating the future lateral olfactory tract (LOT) around E15 (López-Mascaraque et al., 1996; Walz et al., 2006). At E16, the first axons collaterals of the LOT reach the anterior olfactory nucleus (AON) and the piriform cortex. This is

followed by the addition of new axons innervating the entorhinal cortex and the olfactory tubercle during the first postnatal week (López-Mascaraque et al., 1996; Blanchart et al., 2006; Walz et al., 2006).

After they have started to extend axons, mitral cells adopt a radial orientation and develop multiple and widespread primary apical dendrites, shaped by the arrival of OSNs (López-Mascaraque et al., 1996). OSNs penetrate into the OB and make synapses with the apical dendrite of mitral cells to form proto-glomeruli (Blanchart et al., 2006). The selection of a single apical dendrite is achieved by pruning and mitral cells acquire their final morphology with one apical dendrite and several lateral dendrites developing in the deeper external plexiform layer (EPL). During this refinement process, the somas of mitral cells align and form the mitral cell layer while tufted cells are restricted to the EPL.

II.2.1.2. Development of the periglomerular layer

The development of the periglomerular layer (PGL) coincides with the arrival of OSNs around E15 (Blanchart et al., 2006). OSNs axons enter the rodent CNS where they remain restricted to the marginal zone, forming a presumptive nerve fiber layer (Treloar et al., 1999). From E16, the disorganized OSNs axons separate to progressively target distinct glomeruli. Each glomerulus is innervated by OSNs expressing the same ORs and constitutes a unique functional unit. The mechanisms that contribute to the formation of glomeruli and the highly specific pattern of innervation are not yet completely understood (Mombaerts, 1996, 2006; Mombaerts et al., 1996). OB radial glial cells are also believed to participate to PGL development by stabilizing the glomeruli during the last phases of OB development (Puche and Shipley, 2001).

II.2.1.3. Connection of OSNs to the OB

During embryonic development, OSNs expressing the same receptor converge their axons in a specific pair of glomeruli at stereotypic location generating an olfactory map observed at the level of the glomeruli. Mammalian ORs play an instructive role in targeting of OSNs axons to form this glomerular map (Mombaerts et al., 1996). Interestingly, mice expressing a foreign olfactory receptor (rat OR) can establish specific intrabulbar circuits for that OR (Belluscio et al., 2002). Recent studies suggest that guidance molecules such as semaphorins, ephrins and

teneurins may also mediate the precise connection between OSNs and targeted glomerulus in mammals as already described in drosophila (Kobayakawa et al., 2007).

II.2.2. Generation of OB inhibitory interneurons

II.2.2.1. Arrival of the first populations of OB interneurons

In contrast to projection neurons originating from OB radial glial cells, OB interneurons arise from extra-bulbar sources, i.e. the embryonic LGE and the postnatal SVZ. Although the majority of OB interneurons are produced between E18 and P5 (Hinds, 1968a), genetic loss-of-function and fate mapping studies (Corbin et al., 2000; Wichterle et al., 2001; Yun et al., 2001, 2003) demonstrated that a pioneer population of interneurons is generated from LGE progenitors between E12.5 and E14.5 (Hinds, 1968a). These progenitors migrate along a pathway that presages the future rostral migratory stream (RMS) (Toresson and Campbell, 2001; Tucker et al., 2006). This population remains detectable in the OB until P60 (Hinds, 1968a; Tucker et al., 2006) and is thought to act as a framework for postnatal and adult neurogenesis. Studies have also strongly suggested that, in addition to receiving interneurons from the LGE, intrabulbar precursor cells produce interneurons within the OB (Lemasson, 2005; Vergaño-Vera et al., 2006). For instance, both GABAergic and dopaminergic interneurons are generated from E13.5 OB precursor cells (Vergaño-Vera et al., 2006).

II.2.2.2. Different subtypes of OB interneurons continue to be generated after birth

At postnatal and adult stages, OB interneurons mainly originate from the most anterior part of the SVZ (Doetsch et al., 1999) (**Figure 8A**), although other studies revealed that the RMS itself is a source of multipotent NSCs able to generate OB neurons (Gritti et al., 2002). In contrast to cortical neurons and the first population of OB neurons that migrate radially along VZ RGCs, postnatal NSCs give rise to neuroblasts that migrate a long way through the RMS toward the OB (Luskin, 1993; Lois and Alvarez-Buylla, 1994) (**Figure 8A**). These studies gave rise to the current view that the SVZ originating from the embryonic LGE constitutes a reservoir of

NSCs and that the RMS is the highway for their neuronal progeny to target the more rostral regions of the brain.

II.2.2.3. Migration of OB precursors

NSCs from the SVZ produce continuously tens of thousands new neurons in the OB per day in the young adult mouse. They engage into the RMS through tangential migration by forming elongated chains, a process that involves expression of PSA-NCAM (Menezes et al., 1995; Lois et al., 1996; Wichterle et al., 2001; Murase and Horwitz, 2004). Neuroblasts migration is regulated by repulsive and attractive cues such as slits (Nguyen-Ba-Charvet, 2004), ephrins (Conover et al., 2000), GABA neurotransmitter (Bolteus and Bordey, 2004) and growth factor such as BDNF (Snapyan et al., 2009), while blood vessels serve as a physical substrate for migrating neuroblasts (Snapyan et al., 2009).

After reaching the core of the OB, neuroblasts initiate radial migration towards the different layers of the OB where they mature and functionally integrate. This reorientation in migration implies that neuroblasts separate from each other to disperse into the OB. Several factors such as reelin, tenascin R, or IGF1 have been implicated in these processes (Hack et al., 2002; Saghatelyan et al., 2004; Hurtado-Chong et al., 2009).

Apparently, this unique ability of LGE neuroblasts to migrate toward the OB is acquired between E12.5 and E14.5 (Wichterle et al., 1999, 2001; Tucker et al., 2006). At this stage, transplantation of progenitors from the MGE or the OB in the LGE fail to give rise to neuroblasts that efficiently migrate to the OB (Tucker et al., 2006).

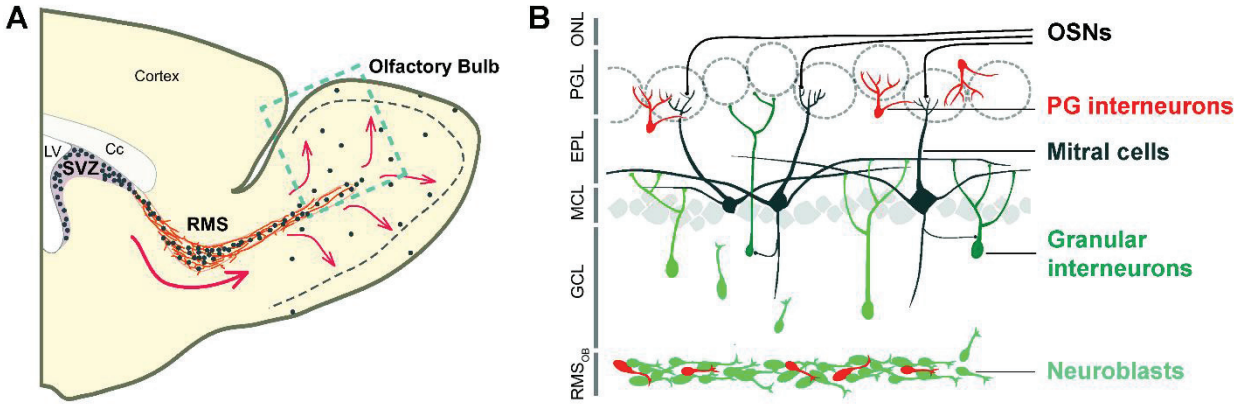

Figure 8: Cohorts of adult-generated neurons are constantly arriving into the olfactory bulb (OB)

(A) Illustration of the postnatal and adult OB neurogenesis process on a sagital view of the adult mouse brain. Newborn cells migrate tangentially, using blood vessels, from their site of generation (the subventricular zone: SVZ) to the OB via the rostral migratory stream (RMS). In the OB, they migrate radially and integrate into the pre-existing neuronal network. (B) View of boxed area in A representing the laminar organization of the OB. Newborn cells differentiate into different subtypes of OB interneurons, mostly granule and PG interneurons. Mitral cells are also replaced in the postnatal brain as well as olfactory sensory neurons (OSNs) in the olfactory epithelium. (Illustration adapted from Breton-Provencher & Saghatelyan 2012).
Abbreviations: LV: lateral ventricle; CC: corpus callosum; SVZ: Subventricular zone; RMS: rostral migratory stream; RMS$_{OB}$: RMS of the OB; GCL: granule cell layer; MCL: mitral cell layer; EPL: external plexiform layer; PG interneurons: periglomerular interneurons; ONL: olfactory nerve layer; OSNs: olfactory sensory neurons.

II.2.2.4. Regionalization and diversity of postnatal NSCs

It has long been thought that NSCs of the SVZ were a homogeneous population of multipotent progenitors capable of generating the high diversity of neuronal subtypes produced after birth. This original view was however challenged by the demonstration of a regionalization of this germinal region. Currently, SVZ NSCs are considered as diverse and restricted populations of progenitors (reviewed in Fiorelli et al. 2015) (**Figure 9A-E**)

Original fate mapping studies following in-utero electroporation support that most OB interneurons arise from the dorsal part of the embryonic LGE (Marín and Rubenstein, 2001; Wichterle et al., 2001; Yun et al., 2001; Stenman et al., 2003). More recent observations however suggest a broader origin of OB interneurons (**Figure 9A-B**). Indeed, fate mapping of Dlx1/2-expressing progenitors (i.e. markers of the LGE and MGE) revealed that at least seven subtypes of OB interneurons are

derived from these subpallial domains (Batista-Brito et al., 2008). Subsequent fate mapping experiments took advantage of domain-restricted markers to drive Cre expression in given subpopulation of progenitors (i.e. Nkx2.1-, Gsh2-, Dlx5-6-, Emx1-, Dbx1-Cre) (Kohwi et al., 2007; Young et al., 2007). Combining this approach with BrdU and subtypes specific markers to identify adult-born neurons, they evidenced that the lateral and dorsal microdomains of the postnatal and adult SVZ originated from the embryonic LGE and pallium, respectively. They also revealed that both domains were able to contribute to OB neurogenesis throughout life. However, these two populations of NSCs were shown to be restricted in generating specific subtypes of OB neurons. While Emx1+ (pallium-derived) NSCs generate mostly CalR+ and TH+ interneurons in the PGL, they are not able to generate CalB+ PG interneurons. In contrast, Gsh2+ (LGE-derived) NSCs generate all CalB+ PG interneurons (Kohwi et al., 2007; Young et al., 2007) (**Figure 9D-E**). Together, these observations underline a first level of SVZ regionalization.

Other studies revealed further regional heterogeneity along both the dorso-ventral and rostro-caudal SVZ axis. To date, fifteen different subpopulations of NSCs were identified in the SVZ at different rostro-caudal and dorso-ventral levels, including the RMS and the lateral, dorsal and medial microdomains of the SVZ (Merkle et al., 2007, 2014). Further, experiments based on viral transduction of discrete spatial microdomains of the P0 mouse SVZ, confirmed that dorsal NSCs are more likely to give rise to TH+ PG interneurons, antero-medial NSCs to generate CalR+ interneurons, and ventral NSCs to give rise to CalB+ interneurons (Merkle et al., 2007) (**Figure 9C-E**). An identical regionalization is observed in the production of granular cells by specific microdomains of the SVZ (**Figure 9E**). While dorsal SVZ regions produce superficial granule cells, ventral regions mostly give rise to deep granule cells. CalR+ interneurons are found in both granular and PG layers and originate from the medial SVZ and the RMS. Finally, targeted electroporation of postnatal SVZ microdomains (Fernández et al., 2011; de Chevigny et al., 2012) confirmed these findings and revealed that NSCs from the medial SVZ are biased to generate PG interneurons (>85%), whereas those from the lateral wall primarily adopt a granular cell (GC) fate (>90%). In an intermediate fashion, NSCs located in the dorsal SVZ generate both PG and granular interneurons in a 1 to 2 proportion (Fernández et al., 2011).

These experiments highlight that the site of origin in the SVZ determines the molecular identity of newborn neurons, their final position in the OB, as well as their pattern of connectivity (Kelsch et al., 2007) (see part 3 for further information in transcription factors regulating the identity of postmitotic neurons). This regionalization suggests that postnatal and adult NSCs keep some characteristics of embryonic patterning throughout life. It is still debated to which extent this regionalization is regulated by intrinsic or extrinsic factors, or both (Sequerra, 2014).

II.2.2.5. Temporal regulation of OB neurogenesis

Each of these discrete niches produces specific interneuron populations with a unique temporal profile. Fate mapping studies of Dlx1/2-expressing NSCs, which give rise to the vast majority of OB interneurons, described a unique temporal signature for each subtype (Batista-Brito et al., 2008). Within the PGL, the production of TH+ interneurons is maximal during early embryogenesis (E12.5) and decreases thereafter. In contrast, the generation of CalB+ interneurons is maximal during late embryogenesis (E15.5) and declines postnatally, whereas CalR+ interneurons production is low during embryogenesis and increases postnatally. At birth, the three interneurons subtypes are produced in equal proportion, making this early postnatal timepoint particularly interesting to study factors controlling their specification (**Figure 9G**). Other subtypes of OB neurons are generated only perinataly such as parvalbumin neurons in the EPL.

Thus, in contrast to most structures of the mammalian CNS like cortical neurons, in which neurons are generated during a discrete window of time, the OB acquires new neurons over an extended period (i.e. both prenatal and postnatal) of time (**Figure 9G**). It is clear that the timing by which these populations are produced is tightly orchestrated. Interestingly, the distribution and the proportion of the main subtypes PG interneurons populations remain constant in postnatal brain (Kohwi et al., 2007; Batista-Brito et al., 2008). Given that each subtype of interneuron will integrate and differentially affect OB circuits, the temporal pattern of their production is likely to shape the functional maturation of the OB

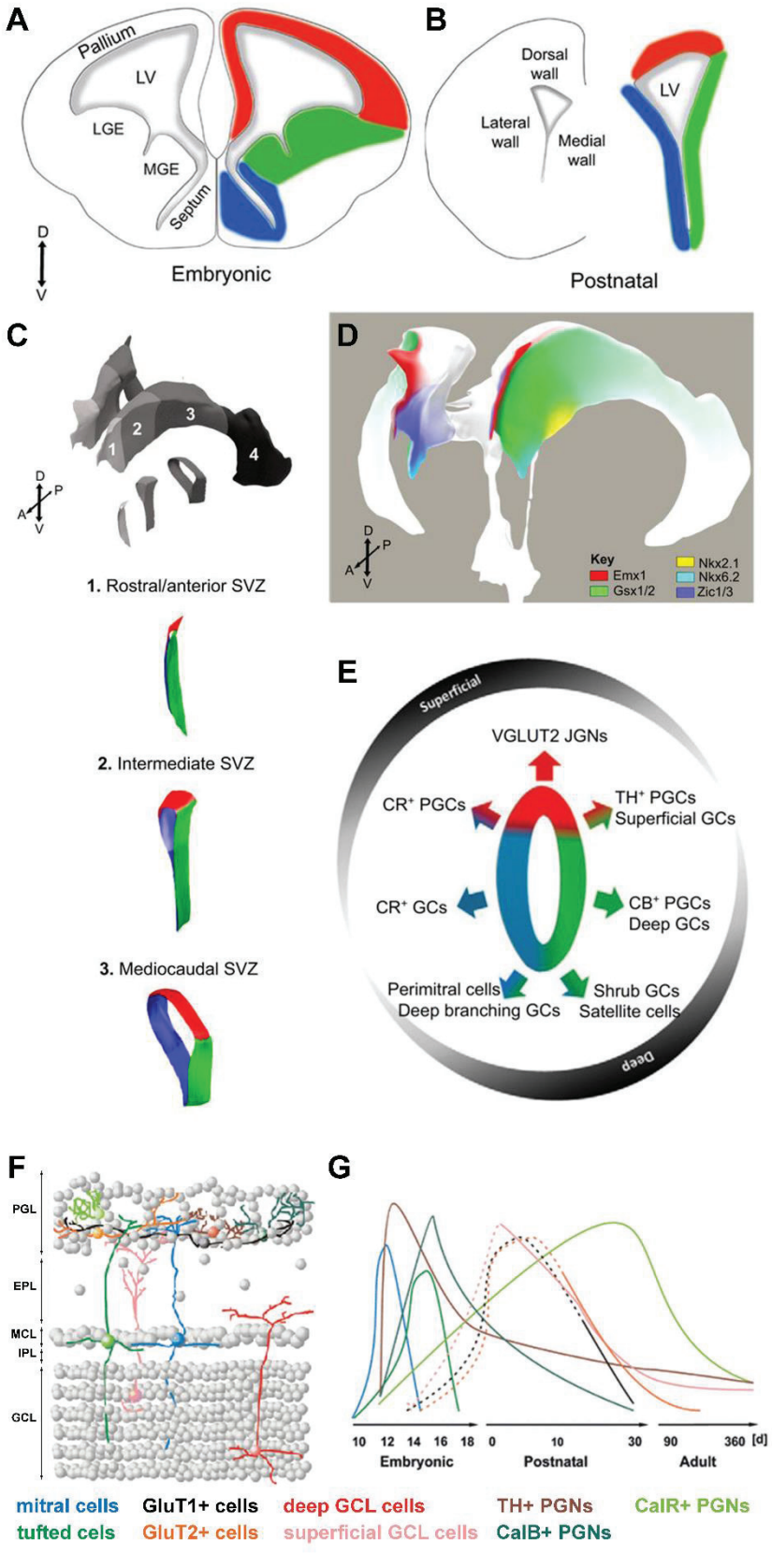
A
Pallium
LV
LGE
MGE
Septum
D
V
Embryonic
B
Dorsal wall
Lateral wall
Medial wall
LV
Postnatal
C
1
2
3
4
D
P
A
V
1. Rostral/anterior SVZ
2. Intermediate SVZ
3. Mediocaudal SVZ
D
Key
Emx1
Gsx1/2
Nkx2.1
Nkx6.2
Zic1/3
E
Superficial
VGLUT2 JGNs
CR+ PGCs
TH+ PGCs
Superficial GCs
CR+ GCs
CB+ PGCs
Deep GCs
Perimitral cells
Deep branching GCs
Shrub GCs
Satellite cells
Deep
F
PGL
EPL
MCL
IPL
GCL
G
10 12 14 16 18 0 10 30 90 360 [d]
Embryonic
Postnatal
Adult
mitral cells
tufted cels
GluT1+ cells
GluT2+ cells
deep GCL cells
superficial GCL cells
TH+ PGNs
CalB+ PGNs
CalR+ PGNs

Figure 9: V-SVZ heterogeneity stems from its embryonic origin.

(A-B) The V-SVZ walls (right) derive from their embryonic counterparts (left): the pallium, lateral and medial ganglionic eminences (LGE and MGE) and septum. Color-coding: red, pallium/dorsal wall; blue, medial/medial wall; green, ganglionic eminences/lateral wall. (C) A volumetric 3D reconstruction of the LVs is shown (top). Four anteroposterior subdivisions are illustrated by different shades of gray. Transverse sections of subdivisions 1, 2 and 3 with color-coded walls (red, dorsal; green, lateral; blue, medial) are shown beneath. Overall, these three regions are the source of the vast majority of OB neurons produced after birth. (D) Fate-mapping studies have shown that fate specification programs are conserved from development to adulthood in the NSCs of the different walls. Dorsal NSCs derive from $Pax6^+$, $Emx1/2^+$ pallial progenitors (red domain). Medial wall NSCs derive from ventral medial progenitors expressing Zic1/3 and Nkx6.2 (blue and cyan domains). Lateral wall NSCs, the most abundant population in the adult, derive from ventral subpallial $Gsh2^+$, $Nkx2.1^+$ progenitors (green and yellow domains). (E) The color-coding in A-D is conserved here to illustrate the SVZ microdomains of origin of specific OB neuron subtypes. The spatial location of NSCs dictates neuronal subtype production, as summarized in a schematic representation of a coronal section of the SVZ. In general, a dorsal or medial localization results in newly born neurons acquiring a more superficial fate in the OB, whereas those neurons originating from the lateral wall (where neurogenic activity is also observed in considerably more caudal areas) adopt a deeper location. (Illustration from Fiorelli et al. 2015). (F-G) Spatio-temporal generation of the major neuronal subtypes in the OB. (F) Scheme depicting the laminar organization of the OB and the color-coded neuronal subtypes. (G) Specific neuronal subtypes are generated within defined time-windows. Note that the projection neurons are made exclusively during development, while the production of different classes of interneurons proceeds to the neonatal stages and even adulthood (y-axis is not to the scale). Dashed lines indicate hypothetical timing as sufficient experimental data are lacking. (Illustration from Weinandy et al. 2011)

Abbreviations: LV: lateral ventricle; LGE: lateral ganglionic eminence; MGE: medial ganglionic eminence; SVZ: subventricular zone; CR, calretinin; CB, calbindin; TH, tyrosine hydroxylase; VGLUT2, vesicular glutamate transporter 2 (Slc17a6); GCs, granule cells; PGCs, periglomerular cells; JGNs, juxtaglomerular neurons.

II.3. Maturation and integration of neurons in preexisting circuits

The OB is a good model to study the making and remodeling of neuronal circuits. The persistent neurogenesis observed in the postnatal and adult OB represents a unique mechanism by which pre-existing neuronal circuits may adapt to a changing environment. This plasticity must however occur without affecting the established olfactory functions, which are vital to the animal.

II.3.1. Continuous replacement of OB neurons throughout life

Throughout life, adult-born neurons integrate into the preexisting neural circuitry of the mammalian OB. Thousands of cells reach the OB every day, from 10 000 to 80 000 (Kaplan, 1985; Lois and Alvarez-Buylla, 1994). This implies that up to 1% of the seven million granule interneurons in the OB could be replaced in a day. In contrast, neurogenesis in the subgranular zone of the hippocampus occurs at a considerably lower rate (about 9000 newborn neurons per day in young adults rats (Alvarez-Buylla et al., 2001) which correspond to 0.03% of the total population of the dentate gyrus). In contrast to the dentate gyrus where neurogenesis contributes to the increase in neuronal number of granule cells, the size of the OB (Petreanu and Alvarez-Buylla, 2002) as well as the size of PG interneurons populations remain constant in postnatal and adult OB (Kohwi et al., 2007; Batista-Brito et al., 2008), suggesting that OB neurons are replaced throughout life. Accordingly, expression of the diphtheria toxin (DTA) in nestin+ progenitors results in a significant depletion of the GC population as soon as three weeks after DTA expression, which become more pronounced over extended periods of time (Imayoshi et al., 2008).

The majority of newborn neurons differentiate into GCs and only 10% become PG interneurons. The proportion of newborn PG interneurons in the adult OB increases with age while, in contrast, GCs are constantly replaced throughout life and remain constant (Lagace et al., 2007; Ninkovic et al., 2007). GABAergic interneurons integrating the PGL and GCL represent 95% of adult-born neurons while only 5% are glutamatergic short axon cells (Brill et al., 2009). Thus, the addition of adult-born neurons mostly suggests that OB postnatal neurogenesis acts as increasing the inhibition within the neural network of the OB, thus allowing a better discrimination of olfactory information.

II.3.2. Distinct OB neuronal subtypes are replaced at different rates

The observation of a continuous addition of new neurons together with the stable number of OB cells throughout life imply that neurogenesis is counterbalanced by a concomitant cell death. Such programmed cell death has been demonstrated in the OB and may have an important regulatory function by eliminating supernumerary neurons (Biebl et al., 2000). Indeed, a single injection of BrdU in adult animals shows that the population of newborn neurons reach a pick one month after injection while a massive cell death (representing ~50% of the population of labeled cells) is observed during the following two months (Winner et al., 2002). This elimination is prominent in the OB compared to the SVZ and the RMS (Biebl et al., 2000; Petreanu and Alvarez-Buylla, 2002). The use of retroviral approaches confirmed the death of half of the newborn neurons between 15 and 45 days after their birth. It also revealed that most of them were mature neurons, harboring dendritic arborization and receiving connections (Petreanu and Alvarez-Buylla, 2002). Thus, only 50% of the GCs and the PGCs added to the OB during adulthood survive over prolonged periods of time (Petreanu and Alvarez-Buylla, 2002; Whitman and Greer, 2007a). Interestingly, once neurons survived this first wave of cell death, they remain visible in the OB for at least 19 months in the GCL (Winner et al., 2002), and mainly rely on sensory inputs (Petreanu and Alvarez-Buylla, 2002).

Further investigations revealed that the whole population of deep GCs was replaced by new neurons over a 12-months period, while only half of superficial GCs were replaced (Imayoshi et al., 2008). It is tempting to speculate that subpopulations of GCs persist to maintain lifelong olfactory functions, while others present a more sustain turnover to integrate novelty aspects. Other BrdU experiments suggest that PG interneuron subtypes are also replaced at different rates (Kohwi et al., 2007). Thus, while TH+ interneurons have a higher turnover rate compared with CalR+ interneurons, CalB+ interneurons mature slowly and harbor a lower turnover rate. The effects of this differential turnover onto olfactory information integration and processing remain to be explored.

II.3.3. Maturation and refinement of OB circuitry

New neurons are continuously recruited throughout adulthood in the OB. In contrast to the function of neurons born during development, new neurons born in the

adult brain continually replace older neurons within mature circuits in the OB. This plasticity highlights the capacity of the OB to change its structure and function during maturation, learning or environmental challenges. In many neuronal systems, activity-dependent refinement and remodeling of initially coarse patterns of synaptic connections is required for the development of fully functional networks. However, the function of neuronal replacement remains poorly understood especially in the PGL. Our current knowledge about the maturation of adult-born cells in the OB is dominated by the data obtained in GCs. GCs reach their final maturation 4 weeks after birth, sequentially passing through five distinct maturation stages, from neuroblasts migrating in the RMS to mature GCs with a complex dendritic arborization (Carleton et al., 2003; Kelsch et al., 2008).

RMS neuroblasts already express functional metabotropic and ionotropic AMPA/kainate-type glutamate receptors. These receptors are tonically activated and have been shown to regulate neuroblasts proliferation and migration, respectively (Giorgi-gerevini et al., 2005; Platel et al., 2008a, 2008b). In contrast to previous studies (Carleton et al., 2003), it has been demonstrated that migrating neuroblasts also acquire functional NMDA receptors during their tangential migration (Platel et al., 2011). The earliest functional GABAergic and glutamatergic synaptic inputs were found at day post injection (DPI) 3 (Panzanelli et al., 2009). GABAergic synaptic inputs seemed to mature by DPI 7, whereas the maturation of glutamatergic synaptic inputs was not completed before DPI 21 (Carleton et al., 2003; Panzanelli et al., 2009). During the third week after birth, newborn GCs develop input synapses in their proximal dendritic domain (Kelsch et al., 2008). Most of their dendro-dendritic output synapses develop only during the fourth week after birth. These data together with the ability to fire action potentials, developing at four weeks after virus injection in the SVZ (Carleton et al., 2003) suggest that newborn GCs have to listen to the neural network they integrate into for several weeks before they can send any output signals and thus influence the ongoing neuronal activity.

Although we cannot exclude the influence of important environmental cues (i.e. attractive/repulsive signals for neuroblasts migration; role of PGCs in OB formation and refinement), the sequential acquisition of the characteristics of neuronal subtypes requires the expression of waves of TFs (see Introduction part III).

The long-term survival and the integration of adult newborn neurons has been extensively studied in the GCL of the OB and evidence that adult neurogenesis contributes to odor learning. A recent study using multiphoton imaging in awake and anesthetized mice supports for rapid integration of adult-born neurons into existing circuits, followed by experience-dependent refinement of their functional connectivity (Wallace et al., 2017). For instance, adult-born GCs become responsive to odorants soon after they arrive in the OB, before gradually becoming more selective over a period of ~3 weeks. Interestingly, this period of strong responsiveness is further prolonged by environment enrichment.

In the adult brain, the survival of newly generated granular neurons is critically regulated by the degree of sensory inputs occurring during a precise time window. Accordingly, a sensitive period has been determined between 14 and 28 days after the generation of a GC during which sensory experience strongly influence the survival of newborn neurons (Yamaguchi and Mori, 2005). This is during this period that newborn GCs receive glutamatergic contacts suggesting that sensorial experience and synapse formation are two part of the same process determining the survival of new granule cells.

Additionally, synaptogenesis is not homogeneous in the OB during prenatal development. In vivo time lapse studies have shown that newborn interneurons are structurally dynamics not only during their maturation and integration phases but also during their synaptic integration (Mizrahi, 2007; Livneh and Mizrahi, 2011; Kovalchuk et al., 2015). Synapse formation is more frequent in the PGL than in the EPL and is the less important in the GCL. By birth, the number of synapses continues to increase. The density of synapses reach a peak around P15-P20 in the PGL after which it slowly declines while the synaptic density continues to increase in the EPL and internal GCL up to P44. This increase in synaptogenesis is likely to reflect the addition of new neurons in the GCL (Whitman and Greer, 2007a, 2007b). This synaptogenesis continues throughout adulthood in parallel to changes in the olfactory environment. A recent study reveals that mature spines of adult-born but not early-born neurons relocate in an activity-dependent manner. A three-dimensional model suggests that spine relocation allows fast reorganization of OB network with functional consequences for odor information processing (Livneh and Mizrahi, 2011; Livneh et al., 2014; Breton-Provencher et al., 2016).

II.4. Role of adult born neurons in the constantly changing brain

The olfactory system is essential for the survival of many animal species providing vital information on food location and influencing social and reproductive behaviors. OB interneurons play an important role in the rhythmic activity of the OB. While PG interneurons coordinate theta activity by regulating baseline and odor evoked inhibition, GCs are involved in the synchronization of mitral cells activity and the generation of gamma rhythms (Arevian et al., 2008; Fukunaga et al., 2014)

Most of the data concerning the functional role of adult born neurons and their implication in olfactory behaviors has been obtained from GCs population, maybe because the vast majority of adult born neurons, around 95%, differentiate into GCs, while only 5% become PG interneurons (Winner et al., 2002). In general, studies aimed at understanding the role of adult born neurons in odor information processing and olfactory behavior considering OB interneurons as a homogeneous population of neurons. Indeed, less is known about the neurochemical heterogeneity of GCs and renewal in the adult OB has been evidenced only for CalR+, mGluR2+ and small number of 5T4+ GC populations (Parrish-Aungst et al., 2007; Batista-Brito et al., 2008; Merkle et al., 2014). This constant neuronal turnover in the postnatal and adult OB imposes the challenge of preserving normal odor information processing despite persistent morphological and functional changes in the number of interneurons subpopulation and their synaptic connections with principal cells. The mechanisms involved in the maintenance of this functional system are driven by intrinsic cues specific to each neuronal subtype but also in an activity dependent manner. Sensory stimulation plays an important role in the maturation, survival and integration of newborn neurons in the OB (Petreanu and Alvarez-Buylla, 2002; Rochefort and Lledo, 2005; Saghatelyan et al., 2005; Alonso et al., 2006; Mandairon et al., 2006; Moreno et al., 2009; Sultan et al., 2010).

II.5. Conclusion

Although interneurons are continuously replaced in the OB throughout life, the processing of odors remains remarkably efficient. Evidences suggest that adult neurogenesis and the refinement of olfactory circuitries are essential for odor memory, learning and adaptive behaviors. However, the functional implication of the diversity of OB periglomerular interneurons subtypes and of their temporal generation

remains to be fully elucidated. It is likely that each PG interneurons population form circuits playing distinct functions in olfaction. Answering this question requires systematic analysis of each interneuron subtype to link the embryonic origin and molecular identity of these neurons to their physiologic properties in the OB and their function in odor processing.

III. INTRODUCTION PART 3:

LIFE OF A NEURON: FROM BIRTH TO INTEGRATION IN A FUNCTIONAL NEURONAL CIRCUIT

III.1. How to become a neuron?

As described in the previous part, postnatal and adult OB neurogenesis generate a high diversity of neurons in the PGL and GCL that are likely to play an important role in the refinement of olfaction. However, questions remain regarding the transcriptional coding of this diversity, i.e. the transcriptional mechanisms controlling the specification of NSCs to produce neurons with defined neurotransmitter phenotype, positions and connectivity. While the transcription factors (TFs) involved in corticogenesis have been extensively explored, those underlying postnatal OB neurogenesis are not fully understood.

The identity of a neuron is defined by its morphology, its functional properties, the neurotransmitter it secretes but also its connectivity within neuronal networks. This identity is gradually acquired during differentiation, a process that can take several weeks (**Figure 10**). Differentiation of NSCs and their specification in defined neuronal subtypes is initiated by the expression of specific TFs, which trigger transcriptional waves that gradually shape neuronal cell fate (Telley et al., 2016). Some of these TFs are then maintained in post-mitotic neuroblasts and are likely to play important roles in their migration and survival until their complete integration into functional circuits. Whether neuronal identity is determined early in NSCs or later in TAPs and migrating neuroblasts is not yet clear.

The specification of NSCs in the postnatal SVZ is determined by the early expression of specific TFs (Kohwi et al., 2007; Young et al., 2007). Thus, regional differences exist regarding the transcriptional profile of NSCs and TAPs of the different micro-domains of the SVZ (Giachino et al., 2014; Azim et al., 2015). Recent work indicates that this regionalization of the postnatal SVZ is already predetermined in the embryonic VZ starting at E11.5, when a subpopulation of embryonic progenitor's in the developing cortex, striatum, and septum segregates by entering quiescence to become reactivated after birth (Fuentealba et al., 2015). These observations suggest that developmental mechanisms used to generate defined types of neurons in the embryo still operate in the postnatal OB (see also introduction part II.2.2).

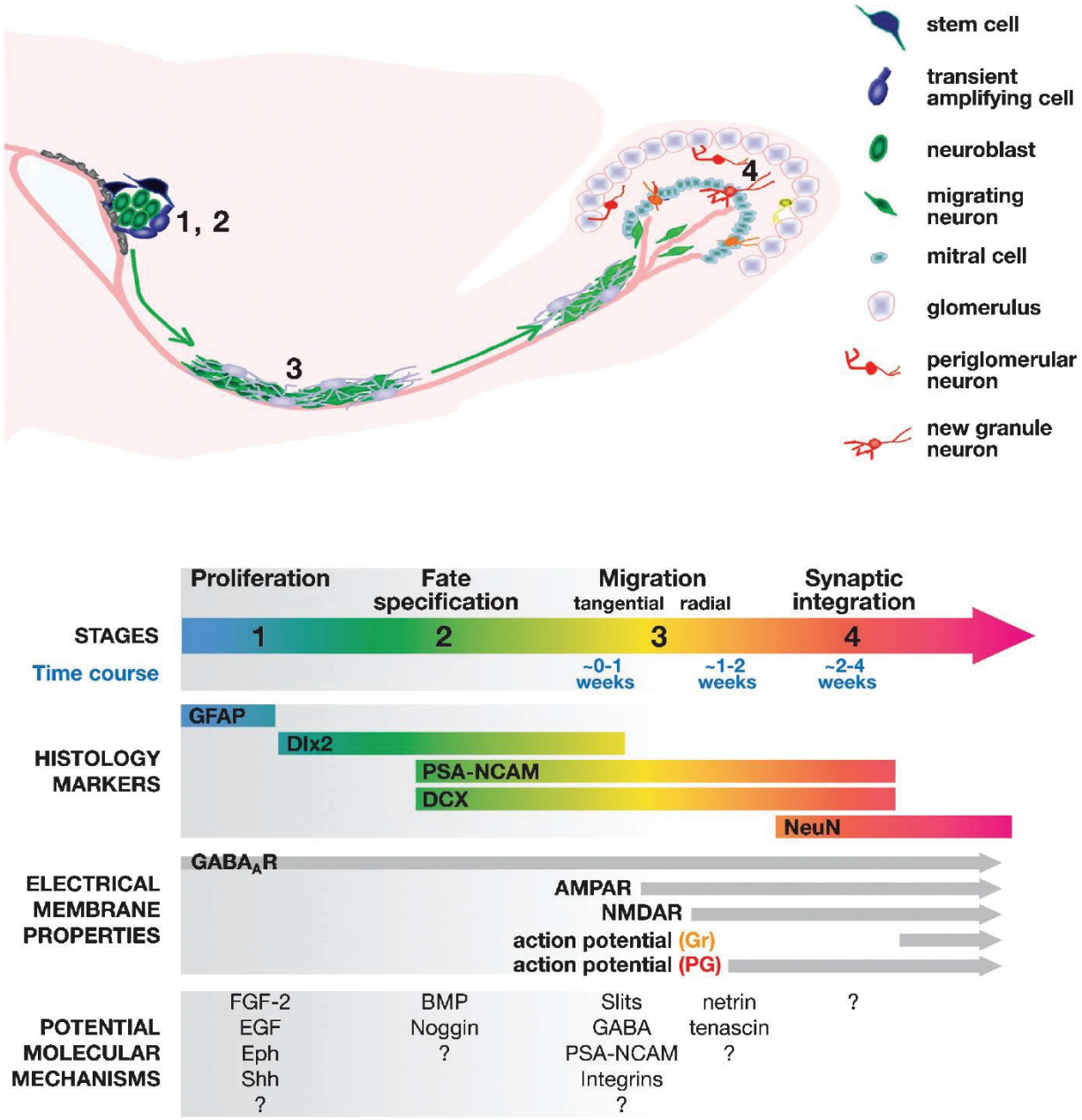

Figure 10: Adult neurogenesis in the SVZ of the lateral ventricle and OB

Adult neurogenesis in the SVZ/olfactory systems undergoes four developmental stages. Stage 1. Proliferation: stem cells (blue) in the SVZ of the lateral ventricles give rise to transient amplifying cells (light blue). Stage 2. Fate specification: transient amplifying cells differentiate into immature neurons (green). Adjacent ependymal cells (gray) of the lateral ventricle are essential for neuronal fate specification by providing inhibitors of gliogenesis. Stage 3. Migration: Immature neurons (green) migrate with each other in chains through the rostral migratory stream (RMS) to the olfactory bulb. The migrating neurons are unsheathed by astrocytes. Once reaching the bulb, new neurons then migrate radially to the outer cell layers. Stage 4. Synaptic integration: Immature neurons differentiate into either granule neurons (Gr, orange) or periglomerular neurons (PG, red). These unusual interneurons lack an axon and instead release their neurotransmitter from the dendritic spines at specialized

reciprocal synapses to dendrites of mitral or tufted cells. The specific properties of each stage are summarized below, mainly on the basis of studies in adult mice. Summary of five developmental stages during adult SVZ neurogenesis: (1) activation of radial glia-like cells in the subventricular zone in the lateral ventricle (LV); (2) proliferation of transient amplifying cells; (3) generation of neuroblasts; (4) chain migration of neuroblasts within the rostral migratory stream (RMS) and radial migration of immature neurons in the olfactory bulb (OB); and (5) synaptic integration and maturation of granule cells (GC) and periglomerular neurons (PG) in the olfactory bulb. Also shown are expression of stage-specific markers, sequential process of synaptic integration, and critical periods regulating survival and plasticity of newborn neurons. (Illustration from Ming & Song 2005)
Abbreviations: GFAP: glial fibrillary acidic protein; DCX: doublecortin; NeuN: neuronal nuclei; LTP: long-term potentiation.

III.2. Knowledges coming from corticogenesis

Early neuronal differentiation is directed by series of early transcriptional waves that instruct the sequence of events whose proper sequence is critical for normal progression through development. These waves provide discrete time windows during which specific transcriptional complexes are present simultaneously and can interact.

III.2.1. Early specification of cortical progenitors

How neuronal identity is dynamically specified in cortical progenitors has been described in a recent paper (Telley et al., 2016). During corticogenesis, excitatory neurons are born from VZ-progenitors and migrate radially to assemble into circuits. Combining a high temporal-resolution technology allowing fluorescent tagging of isochronic cohorts of newborn VZ cells with single-cell transcriptomics in mouse, they identified and functionally characterized neuron-specific primordial transcriptional programs as they dynamically unfold. Thus, newborn cells committed to layer IV of the neocortex sequentially expressed Pax6 when progenitors in the VZ, Tbr2/Eomes when progenitors in the SVZ, and the early neuronal TF Tbr1 within the first 48 hours following mitosis. Temporal expression of these TFs correlates with transcriptional waves that involves hundreds of genes, revealing a highly dynamic process characterized by overlapping signature shifts in protein expression. Thus, the expression of proliferative and neurogenic transcripts reveals that exit from the cell cycle and initial postmitotic specification are partially overlapping rather than strictly sequential processes.

Segregation of type-specific transcripts between newborn neurons and their progenitors can be detected in proliferating progenitors. This suggests an early priming of progenitors that already express postmitotic transcripts, as well as neural subtype specific transcripts (Llorens-Bobadilla et al., 2015; Telley et al., 2016). Together, these data identify progenitor and neuron-specific transcripts activated following cell division and reveal rapid cell-type specific segregation and regulation of transcripts following mitosis. This early priming continues at later stage with expression of transcripts involved in synaptogenesis, as early as in the first 12 hours post mitosis.

The precise timing of early differentiation programs is critical for the successful organization of the cortical networks it belongs to (premature expression of a wave-late transcript Nrn1 lead to premature differentiation and early loss of migration capacity, leading to neuronal mispositioning at birth) (Telley et al., 2016). Precise and dynamic temporal control over the expression of even single genes thus controls the proper sequence and pace of neuronal differentiation, which is essential for circuit assembly.

III.2.2. Generic TFs involved in glutamatergic neurons generation

As describe above, pallial progenitors generate predominantly glutamatergic neurons during embryogenesis, including those of the OB. Pallial progenitors express the TF Pax6 that regulates the expression of a cascade of TFs important to specify cortical neurons towards a glutamatergic fate. Thus, Pax6 regulates the expression of the basic helix-loop-helix (bHLH) TFs Neurogenin1 (Neurog1) and Neurogenin2 (Neurog2). In the developing cortex, Neurog2 has been proposed to be directly responsible for the activation of a cortical glutamatergic transcriptional pathway and the concomitant repression of GABAergic TFs such as Dlx2 (Fode et al., 2000). At later stages, Neurog2 is believed to act in sequence with Mash1 to regulate the transition of neuronal precursors from the VZ to the SVZ (Britz et al., 2006). In addition, Neurog2 induces expression of Tbr2 (also known as Eomes) and Tbr1 which are expressed in progenitors and early post-mitotic glutamatergic neurons, respectively (Hevner et al., 2006).

In the OB, all subtypes of glutamatergic neurons derive from Neurog2+ progenitors. Projection neurons, that is, mitral and tufted cells, are produced at early

embryonic stages, while a heterogeneous population of glutamatergic PG neurons is generated at later embryonic as well as at perinatal stages. These glutamatergic neurons are specified from Pax6 progenitors and express the same waves of TFs has previously described in the development of cortical progenitors (**Figure 11**). While most PG neurons express Tbr2, those generated later also express Tbr1. Based on morphological features, these PG neurons have been identified as tufted interneurons and short axon cells, respectively, with dendritic arborizations that project into adjacent glomeruli (Brill et al., 2009; Winpenny et al., 2011).

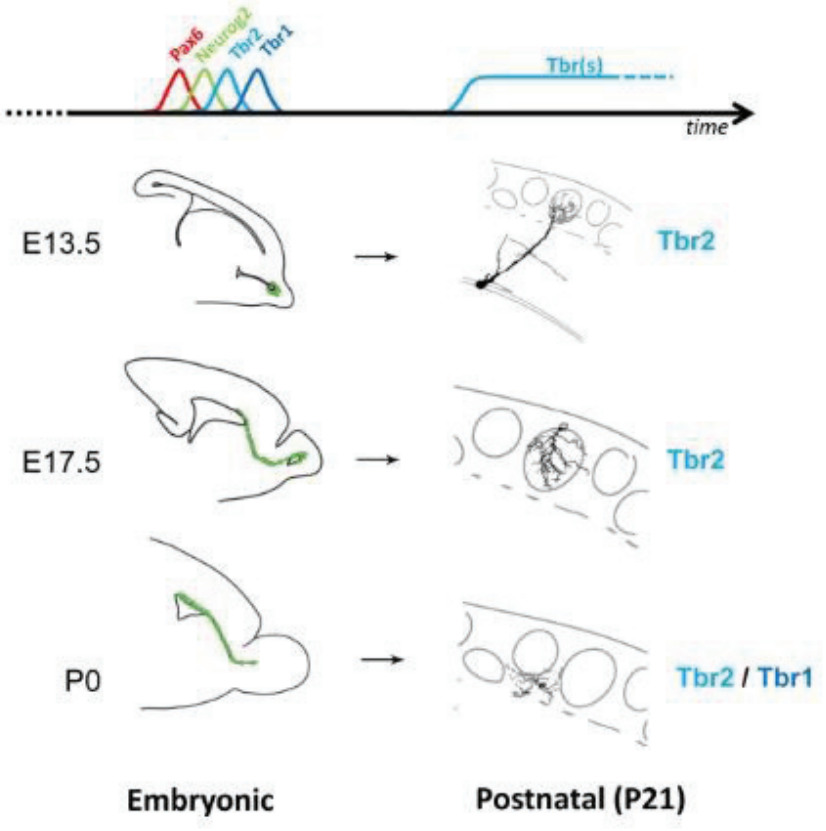

Figure 11: Specification of glutamatergic neurons in the OB

The drawings on the left represent the pattern of Neurog2 expression in the mouse OB, RMS and dorsal wall of the lateral ventricle at the developmental stages analyzed in this study (E13.5, E17.5 and P0). Note that at all stages progenitors sequentially and transiently express Pax6, Neurog2, Tbr2 and Tbr1. The drawings on the right are neurolucida reconstructions of mature neurons produced at these different developmental stages. Note the different morphologies. All neurons express Tbr2 independently of their date of birth, but only neurons generated at late developmental stages also express Tbr1. (Illustration from Winpenny et al. 2011).

III.3. TFs governing the early specification of OB interneurons

The postnatal and adult SVZ is a germinal region regionalized in several microdomains generating different subtypes of interneurons as describe in introduction part II. In addition, distinct TF expression profiles have been defined in the developing telencephalon (see introduction part I.1.3). The early regionalization of the embryonic VZ of the LGE persists in the walls of the SVZ after birth in the form of the differential expression of defined TFs (reviewed in Fiorelli et al., 2015).

III.3.1. Gsh and Dlx family TFs are involved in early OB interneurons specification

Key molecular determinants of GABAergic neuron specification during embryonic development are Gsh1/2 (Genomic screened homeobox) genes and Dlx1/2 (Distalless) genes. Indeed, mice lacking both Gsh or Dlx genes lose virtually all GABAergic telencephalic interneurons before birth (Eisenstat et al., 1999; Toresson et al., 2000; Toresson and Campbell, 2001). In the embryonic telencephalon, Gsh2 is expressed in the LGE and represses the expression of more dorsally expressed genes such as Pax6 (see introduction part I) (Toresson et al., 2000; Yun et al., 2001; Waclaw et al., 2009). Furthermore, Gsh1 and Gsh2 function together in generating most of the striatal and OB interneurons (Corbin et al., 2000; Toresson and Campbell, 2001). All OB interneuron subtypes require Gsh1/2 to regulate their appropriate differentiation (Yun et al., 2003; Wang et al., 2009). Overexpression experiments have shown that Gsh2 promotes OB neuronal differentiation toward a GABAergic interneurons in detriment to Tbr1 projection neurons (Corbin et al., 2000; Toresson et al., 2000; Toresson and Campbell, 2001; Yun et al., 2001, 2003; Waclaw et al., 2009).

In the embryonic forebrain and in particular in the LGE, the expression of Dlx1/2 precedes those of Dlx5/6 (Eisenstat et al., 1999). Dlx5/6 expression is observed in migrating neuroblasts of the RMS and remains in the different OB neuronal subtypes in the PGL, the GCL, the MCL (Allen et al., 2007) (Brill et al., 2008). Accordingly, Dlx5/6 progenitors from the embryonic LGE are known to give rise to at least a part of TH+, CalB+ and CalR+ PG interneurons (Kohwi et al., 2007). The absence of Dlx5 leads to defects in the differentiation of OB interneurons and selective depletion of TH+ and GAD67+ PG interneurons. The effect of Dlx5 as well

as Dlx2 could be mediated by a direct activation of Wnt5a that promotes GABAergic differentiation (Paina et al., 2011).

In contrast, Dlx1/2 expression appears early in TAPs and persists in the RMS and OB. The combined deletion of Dlx1 and Dlx2 results in the loss of GABAergic interneurons and TH+ interneurons due to defects in neuronal migration and maturation. Thus, Dlx1 and Dlx2 seem to cooperate at early steps of OB neuronal differentiation (Anderson et al., 1997; Long et al., 2007). Dlx2 expressing progenitors give rise to TH+, CalB+ and CalR+ PG interneurons, as well as PV+ cells in the EPL (Batista-Brito et al., 2008). Cell-autonomous manipulations by viral vectors demonstrate that Dlx2 promotes neuroblasts differentiation and regulates neuronal subtype specification by promoting acquisition of a TH+ PG fate. Indeed, overexpression of Dlx2 induces a dopaminergic phenotype in the OB during both development and adulthood (Brill et al., 2008). Notably, this effect occurs by a cooperation of Dlx2 and Pax6 at the expense of the CalR+ PG fate (Brill et al., 2008) (see part III-3-2 for role of Pax6 in OB neurogenesis). Furthermore, the effect of Dlx2 could be regulated by the miR-124 during cell differentiation (Cheng et al., 2009).

III.3.2. The Emx gene family contributes to pallium development and postnatal neurogenesis

As already discussed, the larger part of the postnatal SVZ derives from the embryonic LGE. However, more recent work reveals that other domains of the developing telencephalon, including the pallium and the septum, are also a source of OB interneurons. Indeed, the TF Emx1, a pallial marker during embryogenesis remains expressed in the postnatal OB. Lineage tracing of Emx1 indicates that progenitors derived from Emx1 lineage are located in the dorsal wall of the adult SVZ, continue to proliferate and generate OB interneurons (Willaime-Morawek et al., 2006; Kohwi et al., 2007; Young et al., 2007). Among PG interneurons, a significant proportion of CalR+ interneurons is derived from Emx1 progenitors accordingly to their origin from both the medial and dorsal most regions of the SVZ (Kohwi et al., 2007; Fernández et al., 2011). In contrast, progenitors from the Gsh2 lineage give rise to very few CalR+ interneurons (Young et al., 2007). These observations have been confirmed by graft experiments, showing that CalR+ interneurons are generated when progenitors from the embryonic pallium, but not the embryonic LGE,

were grafted into the adult SVZ (Kohwi et al., 2007).

Altogether, these observations suggest that the pallium contributes to the formation of the postnatal SVZ, thereby increasing the heterogeneity of the postnatal germinal niche and the diversity of OB neurons generated after birth.

III.3.3. The TF Pax6 is involved in the early specification of TH+ interneurons as well as their survival.

During brain development, the activity of the TF Pax6 has been highlighted by original studies in the Pax6 mutant Sey/Sey mouse. Pax6 is involved in the development of the olfactory system including the OB and the olfactory cortex (see for review Nomura, Haba, and Osumi 2007) (see also part II-2). During embryogenesis, Pax6 is expressed in the pallium and in a ventral gradient in the ventral pallium until the dLGE and governs the generation of glutamatergic neurons. Accordingly to its role in cortical NSCs during embryogenesis, Pax6 also influences the self-renewal and proliferation of adult NSCs and neural differentiation in the OB (Curto et al., 2014). In the postnatal brain, the expression of Pax6 is detected in subpopulations of GABAergic PG interneurons of the OB as well as in parvalbumin+ and CalR+ neurons of the EPL (Dellovade et al., 1998). Most proliferating adult SVZ progenitors express the TF Pax6, but only a small subpopulation of migrating neuroblasts and new OB interneurons derived from these progenitors retain Pax6 expression (Kohwi et al., 2005). The transplantation of GFP+ embryonic forebrain progenitors of the dLGE from Pax6 mutant Small Eye (Pax6 Sey/Sey) mice into the SVZ of adult wild-type mice allowed the analysis of its cell-autonomous effects without the confounding effects that this mutation has on the olfactory epithelium and OB. The results reveal that Pax6 Sey/Sey progenitors produce neuroblasts capable of migrating into the OB but that fail to generate TH+ PG interneurons and superficial granule cells (Kohwi et al., 2005). Accordingly, Pax6 plays a role for GABA and TH+ PG interneuron specification (Hack et al., 2005; Kohwi et al., 2005).

III.3.4. Sp8 and Zic TF may be involved in CalR interneurons specification

In the postnatal brain, Zic1 and Zic2 are TFs expressed in progenitors from the dorsal SVZ (Tiveron et al., 2017), while Zic3 is expressed in the medial wall of the SVZ (Merkle et al., 2014; Fiorelli et al., 2015). Recent observations highlight a role of

Zic TFs in PG interneurons specificiation. The majority of Zic+ interneurons are CalR+ PG interneurons, while Zic is not expressed in TH+ interneurons. Further, Zic1 and Zic2 are able to repress the dopaminergic fate and induce the second major population derived from the dorsal SVZ, the CalR+ PG interneurons (Tiveron et al., 2017).

Another TF, the zinc finger TF Sp8, has been suggested to play a role in CalR+ fate specification (Waclaw et al., 2006). Sp8 is expressed in neurogenic regions, which give rise to OB interneurons during embryonic and postnatal life. Its expression has been described to persist in mature CalR+ PG interneurons while it is largely excluded from TH+ PG interneurons. Deletion of Sp8 during embryogenesis revealed its requirement for the normal generation of OB interneuron subtypes, in particular CalR+ PG interneurons. Sp8 knock out results in an increase in cell death within the MGE and RMS, as well as an abnormal neuroblasts migration in the OB. These observations suggest that Sp8 would contribute to OB interneuron diversity by regulating the survival, migration, and specification of neuroblasts and maturing interneurons (Waclaw et al., 2006).

III.4. The identity and survival of mature neurons is actively maintained throughout life

After their generation and specification in periventricular regions, neuronal precursors maintain an immature and migratory state until their arrival in the respective target structures. This maturation resumes with the occurrence of terminal differentiation and synaptic integration. Little is known about the factors that control these late maturation steps. Once their maturation and integration are complete, it was generally accepted that the transcriptional activity in mature neurons was minimal and mainly localized at synapses in order to modify their efficiency. However, recent studies (summarized in Deneris and Hobert 2015) have shown that some TFs involved in neuronal subtype specification continue to be expressed in fully mature neurons. These TFs called "terminal selector genes" (TSGs) have been proposed to actively maintain a transcriptional program essential for the survival and maintenance of mature neurons identity. Therefore, the identity and integrity of post-mitotic neurons appear to be maintained by the same TFs that initiated the specification and which regulate the expression of a whole battery of terminal differentiation genes

(receptors to neurotransmitters, ion channels, genes for the synthesis pathways of neurotransmitters, structural proteins, etc.).

III.4.1. Genes involved in the maturation, survival and identity of mature neurons

The first TF identified as a “terminal selector gene” was Nurr1 which play essential role in the differentiation, maturation, and maintenance of midbrain dopaminergic neurons. Nurr1 determines dopaminergic identity through the activation of a gene battery and maintain the expression of dopamine neurotransmitter identity gene. For instance, Nurr1 is important in fetal and neonatal mesencephalic dopaminergic neurons since its deletion leads to a severe and progressive loss of dopaminergic identity and tissue dopamine transmitter levels in the substantia nigra and the VTA (Kadkhodaei et al., 2009, 2013). For instance, the deletion of Nurr1 in early adult dopaminergic neurons leads to a severe decrease in DA neurons gene battery. Further, loss of adult Nurr1 leads to dystrophic dopaminergic dendrites, which is a pathological feature reported in early stages of Parkinson disease. Nurr1 has also been implicated in the regulation of genes involved in neuroprotection against oxidative and excitotoxic stress (Volakakis et al., 2010).

In the OB, the analysis of gene expression in neuroblasts and maturing neurons from the PGL revealed that the expression of the bHLH TF NeuroD1 strikingly coincides with terminal differentiation (Boutin et al., 2010). The overexpression of NeuroD1 in progenitors of the SVZ leads to the rapid appearance of cells with morphological and molecular characteristics of mature neurons in the SVZ and RMS. Conversely, shRNA-induced knockdown of NeuroD1 inhibits terminal neuronal differentiation.

Other TFs have been identified in the regulation of neuronal survival in a highly subtype-specific manner. In addition to its role in the specification of TH+ PG interneurons, the TF Pax6 also regulates the survival of these neurons by directly controlling the expression of crystallin aA (CryaA), which blocks apoptosis by inhibition of procaspase-3 activation (Ninkovic et al., 2015). Indeed, while the knockdown of CryαA by shRNA reduces the number of TH+ OB interneurons, the re-expression of CryαA fully rescues the survival of Pax6-deficient TH+ interneurons in vivo.

III.5. The transcription factor Sp8

A large part of my PhD work has focused on the role of the TF Sp8 in OB neurogenesis. Here, I described in more details current knowledges on this TF and its role during embryonic development and OB neurogenesis.

III.5.1. Sp transcription factor family / Structure

Sp8 is a zinc finger TF that belongs to the zinc finger protein super family. These TFs are known to bind RNA, DNA, as well as other proteins and lipids. As a consequence, they are involved in a diversity of cellular processes such as transcriptional regulation, mRNA stability and processing, or protein turnover. Zinc finger domains are abundant and highly conserved in evolution due to the high structural stability and redox stability of the zinc ion, which allows the formation of stable complexes.

A functional classification of mammalian zinc finger proteins has been proposed at the beginning of the 2000's, based on the presence and the composition of zinc finger domains (Bouwman and Philipsen, 2002; Ravasi et al., 2003). At least five different zinc finger domains have been described. The most common, the Cys2His2 (C2H2) zinc finger, binds to GC-boxes and CACCC-elements which are recurrent motifs found in regulatory sequences of the promoter region and involved in DNA/RNA binding (Bouwman and Philipsen, 2002). The number of sequential zinc finger domains determines specific binding sites to different DNA regions and the substitution in amino acids regulates the affinity of these TFs to their targeted sequences. Thus, splice variants that can modify the number of zinc finger domains, can lead to different function or cellular localization of a same gene.

The best characterized members of the zinc finger protein family are the Sp/KLF TFs (specificity protein/Krüppel-like factor). These TFs are all transcriptional regulators expressing a highly conserved DNA-binding domain composed of three C2H2 zinc fingers at their C-terminal end. Sp/KLF members recognize the same GC and GT boxes commonly found within the promoter regions of their target genes albeit with different affinities due to the substitutions of amino acids in the zinc fingers. Their N-terminal end is composed by transcriptional activator or repressor.

Thus, this family of TFs is involved in various developmental processes, such as cell growth and differentiation.

Despite the common expression of three C2H2 finger domains, Sp TFs differ from KLF TFs by the expression of a Sp box by their N-terminal end (Harrison et al., 2000). Furthermore, a buttonhead (btd) box is found in a domain, rich in charged amino acid. The btd-box may contribute with the Sp box to the transactivation potential of these TFs (Bouwman and Philipsen, 2002). Indeed, a deletion of the btd-box leads to a reduced activity of the TF. Nine members (i.e. Sp1 to Sp9) have been identified so far. The Sp family is divided into a Sp1-like family (Sp1-4) and a Sp8-like family (Sp5–9) based on the domain structures of their N-terminal ends. While Sp1-like TFs present transcriptional activator glutamine-rich domain A and B, members of the Sp8 family lack similar sequences replaced by smaller domain of unknown function. The last member Sp9 has been identified in 2004 (Kawakami, 2004).

Sp8 is one of the last members discovered in 2002 by Bouwman and Philipsen and described later by Ravasi and collaborators in 2003 (Bouwman and Philipsen, 2002; Ravasi et al., 2003). It has been suggested that Sp8 which shares domain with the KLF factors and Sp factors could be at the origin of the segregation between the Sp and KLF families (Ravasi et al., 2003). The Sp8 gene is composed of three exons. The two first exons are composed by 5'UTR sequences and the third one contains all the coding sequence and 3'UTR sequences. Mice mutants have been created to investigate the role of this TF by targeting the entire Sp8 gene or just its coding sequences. Their phenotypes will be described in the next paragraphs.

III.5.2. Functions of Sp transcription factors

Most mutations of Sp TFs in transgenic animal models are lethal at embryonic stages or at birth. Indeed, in accordance with their expression pattern, the absence of Sp TFs leads to severe alterations in fundamental biological processes during embryonic development, such as cardiac malformation (Sp4) or defect in bone formation (Sp7 and Sp3). Sp1, Sp2, and Sp3 are expressed in many, if not all, mammalian tissues and have been shown to regulate the expression of genes involved in cell cycle control, differentiation, development, and oncogenesis. On the opposite, the expression of Sp4–9 is considerably more restricted. Sp4 is expressed in the conductive system of the heart and its deletion leads to cardiac malformation

and decrease in viability and growth. The deletion of Sp7, also called osterix, is responsible for the inability to form bones, due to a defect in osteoblasts differentiation. On the contrary, Sp5 knock-out does not present any overt phenotype (Harrison et al., 2000).

Sp-related proteins have been identified in many species such as drosophila, invertebrates, zebrafish, mice and human. Thus, mammalian Sp TFs are evolutionary conserved and can partially supplant the function of invertebrate homologues. Because Sp8 can rescue the defects in head development in Drosophila btd mutants, Sp8 and its family are considered as functional homologue of the Drosophila btd gene (Liang et al., 2013).

III.5.3. Role of Sp8 during embryonic development

Different Sp TFs are expressed in the developing nervous system such as Sp4, Sp5, Sp8 and Sp9 (Supp et al., 1996; Treichel et al., 2001; Bell et al., 2003). The role of Sp8 in murine embryonic development has been described by Bell and collaborators in 2003 and then completed by other teams. The complete deletion of Sp8 gene leads to a striking phenotype, with severe truncation of both forelimbs and hind limbs, absent tail, as well as defects in anterior and posterior neuropore closure leading to exencephaly and spina bifida. As a consequence, Sp8 null embryos do not survive at birth and are characterized by a lack of tail, hindlimb and forelimb structures as well as exencephaly and spina bifida (Bell et al., 2003). However, conditional ablation of Sp8 is necessary to study the most tardive stages of embryonic and postnatal development.

III.5.3.1. The transcription factor Sp8 is essential for the efficient closure of the neural tube

Sp8 expression appears very early during mouse embryonic development as soon as E7.5 during gastrulation. In the developing nervous system, its expression appears around E8.5 in the neuroepithelium of the forming neural tube and the anterior neural ridge (ANR) (Bell et al., 2003; Treichel et al., 2003; Zembrzycki et al., 2007). The exencephaly observed in Sp8 mutants at E13 is due to the absence of normal anterior neuropore closure at E9. In Sp8 mutants, the anterior neuropore stays open due to a continuous expression of FGF8 in a ring of cells surrounding the open anterior neuropore after E9 and this effect is Sp8 gene dosage dependent.

Furthermore, in accordance with the high expression of Sp8 in the posterior neuropore, Sp8 null mice also exhibit a defect in posterior neuropore closure at E9.5 leading to spina bifida with a complete absence of tail.

III.5.3.2. Sp8 is required for the proper function of key signaling centers.

Formation and maintenance of signaling centers need to be tightly spatially and temporally regulated, in order to control tissue development properly. Sp8 is known to maintain the expression of early genetic markers expression and allows the development of signaling centers in various tissues, including the CNS.

Outside the CNS, Sp8 expression is restricted to limbs and tail. Sp8 mutants exhibit severe phenotypes including truncations of both fore- and hind-limbs and a complete absence of tail (Bell et al., 2003; Treichel et al., 2003; Kawakami, 2004). This phenotype is due to a malformation of the apical ectodermal ridge (AER) a pivotal signaling center for limb outgrowth. This specialized epithelial structure is source of FGF8 and is regulated by the expression of both Sp8 and Sp9 (Treichel et al., 2003). Limb outgrowth induction is based on cross-talk between epidermal and mesenchymal tissue and is mediated by FGF and Wnt-β-catenin signaling. Both Sp8 and Sp9 are expressed in the AER, regulating and maintaining the expression of keys signaling molecules essential for the maturation and the maintenance of the AER. Loss- and gain-of-function approaches revealed that both Sp8 and Sp9 positively regulate FGF8 expression in the AER and contribute to limb outgrowth in vertebrate embryos (Kawakami, 2004).

In the CNS, expression of Sp5, Sp8 and Sp9 closely relates to the three main telencephalic patterning centers during embryonic development (Sahara et al., 2007). As described in the first chapter of this introduction, these signaling centers are defined by the expression of related morphogens regulating their correct patterning and the correct formation of the brain. For instance, Sp8 is expressed in ectodermal signaling centers that drive craniofacial development, and is not detectable in the neural crest and paraxial mesoderm cells that directly contribute to the face. Furthermore, elevated levels of Sp8 expression have been shown in the ANR, olfactory placodes and epidermal ectoderm during craniofacial development (Kasberg et al., 2013). Altogether, these observations reveal that during embryonic

development, Sp8 has an important role in maintaining the expression of key genes and interacts with morphogens expressed by signaling centers to regulate their proper patterning.

III.5.4. Sp8 in OB neurogenesis

Using a conditional mutagenesis strategy, Waclaw and collaborators have uncovered a crucial requirement for Sp8 in the regulation of OB interneurons development. Indeed, Sp8 is expressed in most neuroblasts of the RMS and remains expressed in each of the calretinin and GABAergic but non-dopaminergic interneuron subtypes suggesting that these populations are most dependent on Sp8 function for their normal development and/or survival. Moreover, at least the neuroblasts which generate CalR+ interneurons require Sp8 for their correct specification. In its absence, these cells misexpress Pax6 and display abnormal migratory behaviors (Waclaw et al., 2006).

In addition, the TF Sp8 has been identified as an important factor in the specification of other OB neuron subtypes. For instance, PV+ interneurons in the EPL express Sp8 (Li et al., 2011). The ablation of Sp8 by Cre/loxP recombination (see also chapter 1 and 3) severely reduces the number of PV+ interneurons in the EPL of the OB suggesting that Sp8 is required for the normal production of PV+ interneurons. Furthermore, somatostatin+ interneurons in the EPL in mice and in the PGL in rats also express Sp8. In mice, the generation of somatostatin+ interneurons is maximal during late embryogenesis and decreases after birth. The ablation of Sp8 by Cre/loxP recombination severely reduces the number of somatostatin+ interneurons in the EPL highlighting the importance of Sp8 for the normal production of this subtype of OB interneurons (Jiang et al., 2013).

III.6. Conclusion

Altogether, these observations indicate that TFs are involved in both early and late stages of neuron's life. While their expression in progenitors defines their specification in defined neuronal subtypes, their (re)expression at later stage is often observed, which appears to be important for the intergrity of mature neurons. While the transcriptional coding of postnatal OB neurogenesis starts to be unravelled, the role of Sp8 has not been thoughfully explored due to its pleiotropic roles in CNS

development. During my PhD, I aimed at developing conditional and temporally controlled transgenic approaches to investigate the role of this TF in specification and/or as a terminal selector gene.

IV. CHAPTER 1:

REFINING ELECTROPORATION AS A TOOL TO STUDY THE SPATIAL AND TEMPORAL SPECIFICITIES OF POSTNATAL SUBVENTRICULAR ZONE GERMINAL ACTIVITY

In this chapter, I performed all animal maintenance, experiments and analysis with the grateful help of Claire Santamaria during her master 2 internship. The transposon and ER^{T2}-CRE-ER^{T2} experiments were performed with the help of Stefan Zweifel and Julie Corcia.

IV.1. Introduction

After birth, proliferation and neurogenesis continue in the subventricular zone (SVZ) of the brain until adulthood (Luskin, 1993; Lois and Alvarez-Buylla, 1994). However, the anatomy of this region changes dramatically during the first postnatal weeks. At early postnatal stages, periventricular walls are covered of radial glial cells (RGCs, referred as NSCs thereafter for clarity reasons) composed of a mix of at least two populations: 1) a first population of RGCs that gives rise to ependymal cells (Merkle et al., 2004; Spassky et al., 2005); 2) a second population of RGCs at the origin of adult NSCs (Tramontin et al., 2003; Merkle et al., 2004). During the first postnatal weeks, the organization of the postnatal VZ-SVZ evolves from an embryonic pseudostratified epithelium into the adult SVZ, separated from the ventricle by a layer of ependymal cells (and therefore also named sub-ependymal zone, SEZ, by some authors). Thus, a narrow window of postnatal opportunity exists during which NSCs of the postnatal SVZ remain directly accessible to electroporation, thereby facilitating mechanistic studies exploring the factors controlling their proliferation and differentiation.

NSCs of the postnatal SVZ generate both glial cells and neurons throughout life. Generation of these two cell lineages shows clear spatial and temporal specificities, which represent constrains in designing experimental approaches to study them. Glial cells disperse at proximity of the ventricles, then amplify by local proliferation in the parenchyma (García-Marqués and López-Mascaraque, 2013; García-Marqués et al., 2014; Figueres-Oñate et al., 2015). Neurons are generated by progenitors that proliferate three to four times in the SVZ before differentiating into neuroblasts, which engage into tangential migration through the rostral migratory stream (RMS). Upon reaching the olfactory bulb (OB), neuroblasts migrate to specific cell layers and gradually mature and differentiate into functional neurons. Thus, the proliferation, migration, maturation and integration of newborn neurons occur in a timely controlled manner into defined forebrain compartments. Because of these specificities, postnatal SVZ neurogenesis represents an attractive model system for studying these processes separately: i.e. 1) proliferation in the SVZ, 2) migration in the RMS, 3) maturation/integration in the OB.

The differentiation process of both glial and neuronal cells takes several weeks to complete. For neurons, it is estimated that full differentiation of their dendritic/axonal processes and acquisition of functional properties take up to 8 weeks (Luskin, 1993; Winner et al., 2002; Carleton et al., 2003) and involves the expression of specific sets of genes controlled by subtype-specific transcription factors (TFs). These TFs are expressed at both early and late steps of differentiation, with some such as Pax6 and Tbr2/Eomes remaining expressed in fully mature neurons (Kohwi et al., 2005; Brill et al., 2008; Roybon et al., 2009; Winpenny et al., 2011; Ninkovic et al., 2015). Understanding the functions of such TFs over time (i.e. at specific steps of the differentiation process) necessitates their manipulation on the short and/or the long term and in specific targeted regions. In addition, the generation of specific neuronal/glial subtypes by defined regions of the SVZ (reviewed in Fiorelli et al. 2015), necessitate developing new flexible approaches that can integrate spatial constrains to temporal genetic manipulation.

In-vivo electroporation is a convenient technique for performing spatial and temporal genetic manipulation of postnatal SVZ neural stem cells and of their progenies. Indeed, the accessibility of postnatal NSCs bordering the lateral ventricles and their proliferation capacities allow an efficient electroporation in neonatal mice (Boutin et al., 2008). *In-vivo* electroporation also presents the advantage to efficiently target specific regions of the postnatal SVZ (Fernández et al., 2011), and is therefore superior to other gene transfer methods, such as viral vectors, to perform genetic manipulation in a spatially controlled manner. This approach however suffers from several drawbacks, which complicate the temporal control of transgene expression. Indeed, the high proliferative behavior of NSCs as well as their glial progeny results in a rapid dilution of the electroporated plasmids. This, combined with gradual plasmid degradation and silencing, makes a tight temporal control of genetic manipulation particularly challenging. Recent advances in plasmid design may allow overcoming these limitations to develop innovative ways to integrate temporal and/or conditional control of transgene expression following electroporation.

During the course of my PhD, I explored new ways to refine the electroporation approach in order to achieve temporal control of transgene expression. Targeting defined NSCs of SVZ microdomains, I aimed at developing new tools for:

1) transient or permanent genetic manipulations for short versus long term studies of postnatal SVZ germinal activity
2) immediate or delayed genetic manipulations to dissociate the early versus late effects of a given transcription factor in OB neurogenesis (see also in chapter 3

IV.2. Material and Methods

IV.2.1. Animals

Non-integrative approach and gene manipulation were performed in C57BL/6J mice OF1 mice were used for the development and the validation of the transposon approach. Rosa-YFP mice (Jackson Laboratory: B6.129X1-*Gt(ROSA)26Sor*$^{tm1(YFP)Cos}$/J) were used for the conditional gene expression approach. These mice have a *loxP*-flanked STOP sequence followed by the Enhanced Yellow Fluorescent Protein gene (YFP) inserted into the *Gt(ROSA)26Sor* locus, i.e. an ubiquitously expressed locus. Following Cre recombination, this sequence was removed and permanent expression of YFP occurs.

All animal experiments were approved by the relevant French ethical authorities.

IV.2.2. Plasmids

Different plasmids were used to perform these experiments. Plasmids expressing a reporter protein, pCX-GFP (given by C. Boutin); pCAG-RFP; pUb-tdTomato (given by D. Jabaudon) were used to label and follow electroporated cells. They were combined with pCAG-Cre (Addgene; #13775) or pCAG-ER^{T2}-Cre-ER^{T2} (Addgene; #13777) in transgenic mice to permanently label NSCs and their progeny or for conditionally and temporally-controlled manipulation of gene expression in these NSCs respectively. For co-electroporations, the plasmid of interest (Cre or ER^{T2}-Cre-ER^{T2}) was always used at a ratio of 2:1, to be sure that all GFP labeled cells were recombined. All plasmids were Ampicillin resistant except the pCAG-RFP plasmid, Kanamycin resistant.

For the transposon approach, a fluorescent protein EmGFP (Emerald Green Fluorescent Protein), was inserted into the pPB(Exp)-CAGG>3xNLS/EmGFP plasmid (pPB-EmGFP plasmid). Three nuclear localization sequences (3xNLS) were inserted

at the N-terminus of the EmGFP reporter gene to force nuclear localization of the translated protein. The transposon genomic integration was achieved by co-electroporation of a transposase containing plasmid pRP[Exp]-Puro-CAGG>Pbase (pRP-pbase). An ampicillin sequence was added to the two plasmids as selection gene. In both constructs, transcription of the transgenes was controlled by a strong CAGG promoter.

IV.2.2.1. Bacterial transformation and amplification

For the pUb-tdTomato and transposon plasmid, a bacterial transformation was performed with 50µl of HB101 bacterial cell suspension + 1ul of 5µg/µl plasmid solution. After 20min incubation on ice, bacterial suspension was subjected to heat shock for 30sec at 42°C and cool down for 2min on ice. To allow a better recovery of bacteria, 50µL of bacterial suspension were incubated into 450µL of SOC outgrowth medium (Biolabs, #B90205) on a shaker at 37°C for 1h. Bacterial suspension (20µL) was spread on autoclaved Ampicillin (100µg/mL) or Kanamycin (50µg/mL) Agar plate and placed in an incubator at 37°C overnight. A single colony was incubated into 3mL LB-Broth (Invitrogen, #12795) + ampicillin (100µg/mL) over day and transferred overnight at 37°C in 250mL or 500mL LB-Broth maxiculture. Maxicultures were then centrifuge 15min at 4000rpm, 4°C and kept at -20°C. 1mL of maxiculture was conserved as bacterial stock after dilution in 30% glycerol and placed at -80°C. For the other plasmids, a sample of the bacterial stock was directly spread on Ampicillin-Agar plates and incubated at 37°C overnight.

IV.2.2.2. Plasmid extraction

The bacterial pellet was resuspended in Glucose-Tris-EDTA + lysozyme for 20min at RT. Bacterial lysis was performed in NaOH/SDS for 4min, then mix with a solution of Potassium Acetate and formic acid 1.8M to inhibit the reaction. After centrifugation, the solution was filtered through gauze tissue and incubated with Polyethylene-Glycol (PEG) 40% on ice for 40min to create a gradient that precipitate dsDNA. After 15min centrifugation at 4000rpm, the pellet was resuspended in Tris-EDTA 5:1 pH8 + NH4Ac 7.5M 15min on ice to precipitate RNA and centrifuge 10 min at 14000 rpm, 4°C. To avoid a contamination by proteins, the supernatant was first incubated with RNAseA (70µg/mL) 30min at 37°C and with proteinase K (70µg/mL) 1h at 56°C. Two extractions with phenol chlorophorm eliminate the last traces of

proteins. DNA was precipitated with cold isopropanol, centrifuged 15min at 14000rpm, 4°C and resuspended in sterile water and placed at 4°C overnight for a complete dilution. Supercoiled DNA was precipitated with PEG-LiCl for at least 40min at RT, centrifuge. The pellet was washed three times in 70% Ethanol. Plasmids were dissolved in sterile PBS at a concentration of 5 µg/µl and conserved at -20°C for several months. The final concentration was measured with a nanodrop (Nanodrop 2000/2000C, ThermoScientific). For electroporation, plasmids solutions were combined with a contrast solution of fast green (0.2% final) in sterile PBS.

IV.2.3. Electroporations

Electroporations were performed on mice between 1 and 2 days after birth as previously described (Boutin et al., 2008). First, pups were first anesthetized for 2 min in the ice and then placed and fixed on a support so that the skin of the head was tense. A landmark was placed in the middle of a line drawn between the lambda and the eye of the animal. The injection of the plasmid solution (1.5 µL) into the lateral ventricle was carried out using a Hamilton 34G syringe at 2.5 mm depth. The accuracy of the injection into the lateral ventricle was controlled by transparency thanks to a cold light source and the contrast solution integrated into the plasmid solution. Correctly injected animals were then subjected to 5 pulses at 95 V of 50 ms separated by 950ms with an Electroporator NEPA21 type II (Nepa Gene Co., Ltd) and tweezer electrodes coated with a conductive gel (Signa gel, Parker Laboratories, Fairfield, New Jersey, USA). Animals were then warmed up on a hot plate at 36.4 ° C and then returned into the cage with their mother. The animals were not put back directly into the nest but in a corner of the cage in order to promote the maternal behavior of the mother.

IV.2.4. BrdU and EdU administration

BrdU was added in drinking water at a concentration of 1mg/mL with sucrose at 10mg/mL for 15 days. Bottles were protected from light with aluminium and changed every 2 days following this protocol. EdU solution in sterile PBS (10mg/mL) was injected i.p. at a final concentration of 50mg/kg.

IV.2.5. Tissue processing

After deep anesthesia with intraperitoneal injection of pentobarbital (60mg/kg), mice were transcardially perfused with a Ringer solution followed by a 4% paraformaldehyde solution and brains removed, post-fixed for 24h and cut with a vibratome (Leica VT1000 S). 50µm sections were collected from the olfactory bulb to the lateral ventricle in series of 6 and kept at -20° C in antifreeze solution (glucose 15%, sodium azide 0,02%, ethylene glycol 30%, PB 0,1M).

IV.2.6. Immunostaining

Free floating sections were blocked in TNB-Tx buffer (BSA 0.25%, Casein, 0.05%, Top block 0.25% + triton X100 0.4%). For BrdU staining, section were subjected to an antigen retrieval by incubating them at 37°C° in HCl 2N for 30 minutes followed by 30minutes in Borate Buffer 0.1M at room temperature. For c-fos staining, sections were incubated at 80°C in Citrate Buffer (10 mM, pH 6) for 20 minutes. Sections were then incubated with the primary antibody overnight (see table 1). Then, sections were incubated with the corresponding secondary antibody 2h at RT (see table 1). To amplify YFP signal, sections were incubated with a biotinylated secondary antibody followed by streptavidin-DTAF for 30min. Finally, sections were counterstained with DAPI and mounted with Fluoromount mounting medium.

Table 1:

1ary antibodies	**Specie**	**Concentration**	**Source (catalog number)**
Anti-BrdU	Rat	1:500	ABD Serotech (ABD0030)
Anti-GFP	Chicken	1:1000	JAVES (GFP-1020)
Anti-Doublecortin	Goat	1:500	Santa Cruz (Sc-8066)
Anti-RFP	Rabbit	1:1500	MBL (PM005)
Secondary Antibodies	**Specie**	**Concentration**	**Source (catalog number)**
Anti-mouse AlexaFluor 555	Donkey	1:1000	TermoFisher (A-31570)
Anti-mouse AlexaFluor 647	Donkey	1:1000	ThermoFisher (A-31571)
Anti-rabbit Alexa Fluor 555	Donkey	1:1000	ThermoFisher (A-31572)
Anti-rabbit AlexaFluor 647	Donkey	1:1000	ThermoFisher (A-31573)
Anti-goat Alexa Fluor 555	Donkey	1:1000	ThermoFisher (A21446)
Anti-chicken biotinylated	Donkey	1:1000	Jackson Lab (703-065-155)
Streptavidin-DTAF	-	1:250	Jackson Lab (016-010-084)

IV.2.7. Acquisitions, quantifications and statistics

Overviews were acquired with an epifluorescent microscope (Leica DM5500, objective HCX PL APO 40x). Confocal pictures were acquired with a Leica SP5 using

a 20X or 40x objective (HCX PL APO 40x 1.25 oil) and Leica SPE with 1NX, 20X and 40X objective.

For spatial and temporal origin of OB interneurons, quantifications were done on live images using an epifluorescent microscope (Leica DM5500, objective HCX PL APO 40x 1,25 oil). YFP-positive cells and co-localization with BrdU and or Dcx markers were analyzed in the glomerular layer (>180 YFP-positive cells per EPO; ≥3 animals per EPO).

Graphs were performed on GraphPad prism and statistical significance was determined by unpaired *t* test at the $p < 0.05$ level or a Mann-Whitney test when data do not assume a normal distribution.

IV.3. Results

IV.3.1. Non-integrative plasmids as convenient tools for transient transgene expression in postnatal forebrain NSCs

IV.3.1.1. Postnatal electroporation efficiently targets postnatal NSCs

The efficiency of the electroporation in the postnatal brain has been demonstrated some years ago (Boutin et al., 2008). A brief anesthesia by hypothermia allows performing the procedure while ensuring fast recovery of pups. The plasmid solution is injected in the right lateral ventricle of 2 postnatal days (P2) pups and the accuracy of the injection directly controlled by addition of fast green, a contrast agent, into plasmid solution (**Figure 1A**). The position of the electrodes precisely determines the targeted microdomain of the SVZ, here the medial wall (**Figure 1B-C**) (Fernández et al., 2011). The fast expression of the reporter protein in targeted cells is detectable as soon as 8h following electroporation (data not shown). The rapid dilution of the plasmid in proliferating cells of the SVZ restricts reporter gene expression to only few cohorts of newborn neurons (**Figure 1D**). These labeled neurons can be followed until their complete differentiation process and integration into the OB (**Figure 1F-G**). Transgene expression however declines over time due to plasmid degradation and silencing (**Figure 1E**). Thus, the introduction of non-integrative transgenes in postnatal NSCs via electroporation allows a precise but transient spatial manipulation of gene expression.

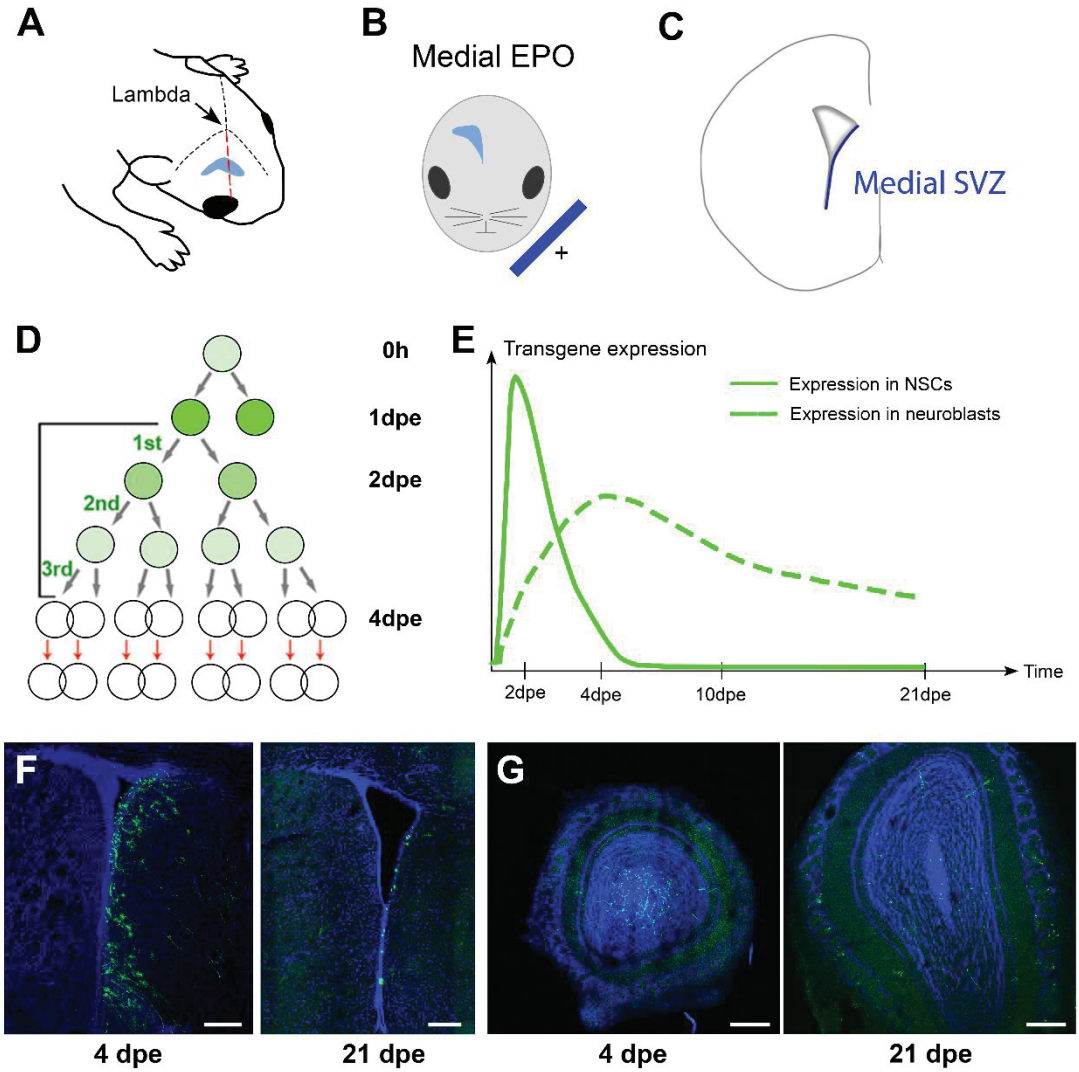

Figure 1: The electroporation approach allows a fast and precise labeling of postnatal NSCs

(A) The site of injection of the transgene is determined in the middle of a line (red dashed line) drawn between the lambda (dark dashed lines represent cranial sutures) and the eye of the animal and visualized through the skull thanks to fast green solution (illustrated in blue in the lateral ventricle). (B-C) The position of the positive electrode (+) determines the targeted microdomain of the SVZ, here the medial wall. (D-E) The expression of the reporter gene is established rapidly in targeted NSCs, persists in post-mitotic neuroblasts and decreases overtime with cell divisions in proliferating NSCs or by plasmid degradation and silencing. (F-G) Electroporation of the pCX-GFP plasmid in NSCs of the medial wall of the SVZ. (F) Expression of the GFP reporter protein in the SVZ at 4 and 21 dpe. The few GFP+ cells in the SVZ at 21 dpe compared to the high number of cells at 4 dpe demonstrate the rapid dilution of the non-integrative plasmid in proliferative cells. Scale bar: 200µm. (G) Expression of the GFP reporter protein in newborn neurons in the OB at 4 and 21 dpe. The high number of GFP+ neuroblasts reaching the OB at 4 dpe compared to neurons migrating in the cortical layers of the OB suggests a potential degradation or silencing of the plasmid in post-mitotic cells. Scale bar: 200µm. (Illustration (D) adapted from (Ponti et al., 2013)

Abbreviations: EPO: electroporation; SVZ: subventricular zone; NSCs: neural stem cells; dpe: days post-electroporation

IV.3.1.2. Plasmids testing for long-term fate mapping experiments in fixed and live tissues

A sustained and ubiquitous expression of the reporter protein is essential to investigate the differentiation of NSCs, which takes up to several weeks. The level of transgene expression originally relies on several parameters: (1) the number of copies, (2) the activity of the promoter and (3) the stability and brightness of the reporter fluorescent protein.

The number of copies is directly dependent on the size of the plasmid, with larger constructs being less efficiently electroporated. In this chapter, all plasmids used have a size of 5800bp to 7000bp.

The differentiation of postnatal NSCs in both glial and neuronal cells, combined with the length of this process, requires the use of strong and ubiquitous promotors to drive transgene expression. Several promoters fulfill these requirements and have been interchangeably used in previous studies: the CAG, the pCX and the pUb promoters (Matsuda and Cepko, 2004; Boutin et al., 2008). The CAG promoter is composed by the cytomegalovirus (CMV) early enhancer element, the promoter of chicken beta-actin gene (the first exon and the first intron) and the splice acceptor of the rabbit beta-globin gene. The pCX promoter is a shorter variant of this promoter containing only the CMV enhancer and the chicken beta actin promoter. Finally, the pUb promoter corresponds to the human ubiquitin C promoter. All of these promoters ensure a strong and ubiquitous expression of the selected reporter gene in all electroporated cells. The ubiquitous nature of these promoters ensures the labeling of both glial cells and neurons.

Finally, the brightness and stability of the reporter gene add to the first two parameters to ensure optimal long-term fate mapping of the reporter cells. Here, I have compared the following plasmids, i.e. pCX-GFP, pCAG-RFP and pUb-tdTomato, for their capacity to label newborn neurons for up to 3 weeks. The presence of numerous GFP positive cells at 21 dpe in the OB confirmed the usability of the pCX-GFP plasmid for *in-vivo* postnatal electroporation (**Figure 2A-C**). In contrast, the electroporation of a pCAG-RFP plasmid led to only few labeled cells in the SVZ (**Figure 2D**) and in the OB (**Figure 2E-F**) and the brightness of this fluorescent protein *in-vivo* without staining was weak. The intensity of the GFP

fluorescent protein was also weak in the OB at 21 dpe, when compared to earlier timepoints, and required to be amplified by immunostaining. Thus, the GFP transgene is a convenient tool for a fine analysis of postnatal neurogenesis on histological sections but is not adapted for studies in living tissue.

Electrophysiological experiments presented in chapter 2 required direct visualization of the reporter proteins under the microscope. Testing of the pUb-tdTomato plasmid revealed a strong expression of tdTomato in neurons of the granular cell layer as well as of the glomerular layer, up to two months, without the need to perform immunostaining. At 17 dpe, intensely labeled electroporated NSCs can be observed in the SVZ (**Figure 2G**), as well as in the OB (**Figure 2H-I**). In addition, the tdTomato fluorescent protein diffuses extensively into the dendritic arborization of newborn neurons (**Figure 2I-J**). Compared to GFP expression, the tdTomato allows a net detection of the finest arborization of CalR+ periglomerular interneurons, as described in chapter 2. Indeed, unlike other neuronal subtypes such as CalB+ interneurons that present a well-defined dendritic arborization (easily distinguishable with GFP), CalR+ neurons present a finer arborization with bulges and thus heterogeneous branches in terms of diameter.

Altogether, these observations suggest that while the pCX-GFP plasmid is convenient for long-term experiments involving histology (see all experimental chapters), the pUb-tdTomato plasmid has to be preferred for long-term experiments involving the use of living tissues (see chapter 2).

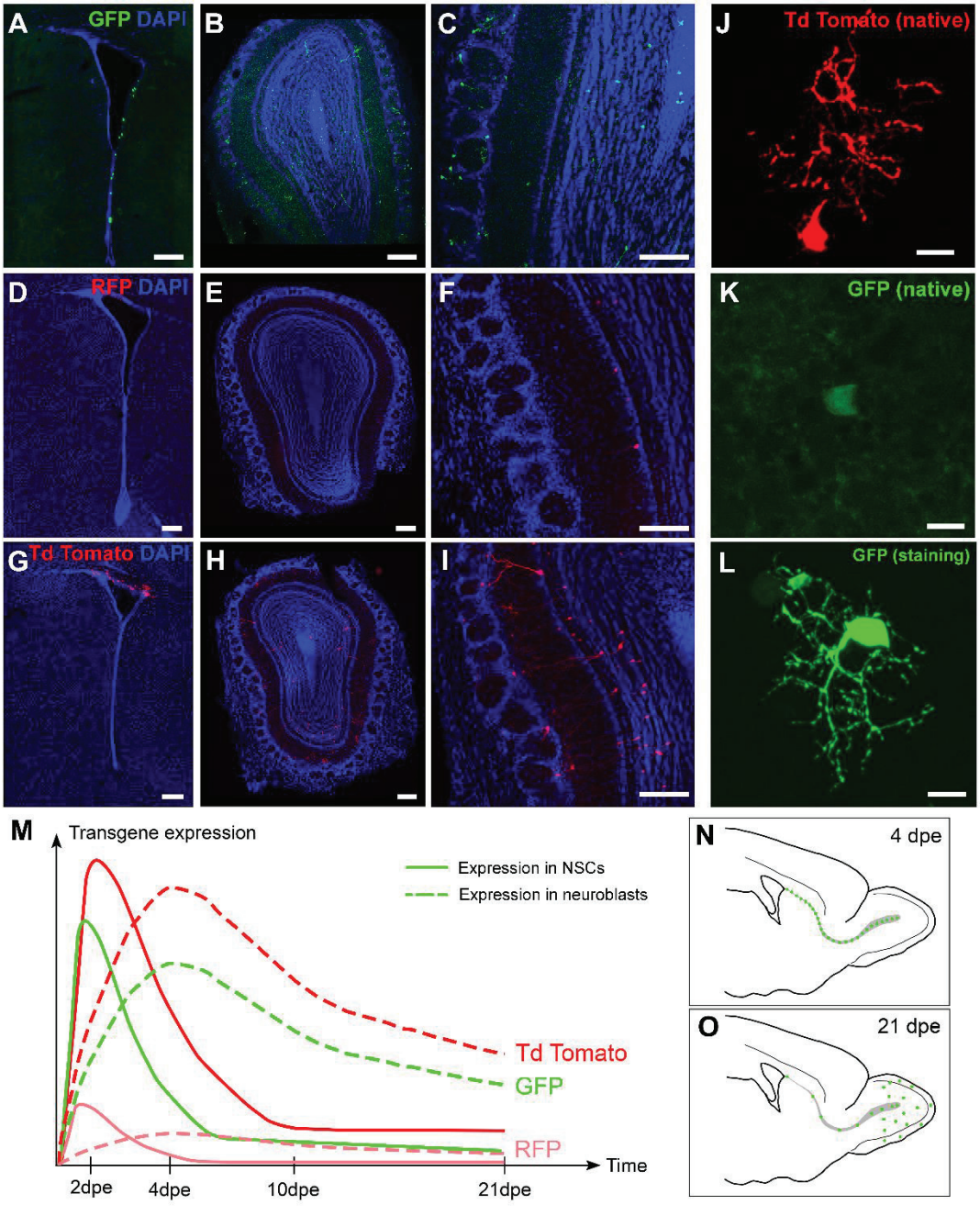
A
GFP DAPI
B
C
J
Td Tomato (native)
D
RFP DAPI
E
F
K
GFP (native)
G
Td Tomato DAPI
H
I
L
GFP (staining)
M
Transgene expression
Expression in NSCs
Expression in neuroblasts
Td Tomato
GFP
RFP
Time
2dpe
4dpe
10dpe
21dpe
N
4 dpe
O
21 dpe

Figure 2: td-Tomato and GFP reporter proteins are efficient to investigate neuronal differentiation process during the first 3 weeks of postnatal life

(A-C) Electroporation of the pCX-GFP plasmid in NSCs of the medial wall of the SVZ. The native GFP signal has been amplified with immunostaining. GFP+ cells are observed in the SVZ as well as in the different layers of the OB at 21 dpe. Scale bars: 200µm. (D-I) Comparison between medial electroporation of the pCAG-RFP plasmid (D-F) and the pUb-tdTomato plasmid (G-I). Sections were just counterstained with DAPI and mounted for microscopy at 17 dpe. Very few RFP+ cells can be observed in the SVZ and the OB while the expression of the td-Tomato in SVZ cells and many newborn neurons of the OB is brighter. Scale bars: 200µm (J-L) High magnification confocal pictures of the arborization of periglomerular neurons in the OB. The expression of the native td-Tomato is strong enough to distinguish the fine dendrites of the arborization (G) while the native GFP (K) need to be reveal by immunostaining (L). (M) Illustration of the transient expression of non-integrative transgenes (pCX-GFP, pUb-tdTomato and pCAG-RFP) in SVZ-NSCs and neuroblasts. (N-O) Schematic representation of the position of electroporated cells during their differentiation from the SVZ to the OB. At 4 dpe, labeled cells are proliferating and start migrating in the RMS (N). When reaching the OB, they complete their maturation and integration in the different layers of the OB at 21 dpe (O).
Abbreviations: dpe: days post electroporation, NSCs: neural stem cells

IV.3.1.3. The medial SVZ contributes to postnatal OB neurogenesis

After birth, NSCs of the SVZ generate neuroblasts migrating along the RMS toward the OB. While germinal activity and neurogenesis of the dorsal and lateral most regions of the SVZ have been extensively described, less is known about the medial SVZ. Four days following electroporation (4 dpe) of the pCX-GFP plasmid, an important population of cells is labeled in the medial SVZ (**Figure 3A**). These GFP+ cells can be observed throughout the entire medial wall of the SVZ highlighting the efficiency of the electroporation in this wall. The majority of these cells have morphology of RGCs with long processes extending into the septum (**Figure 3B-B'**). A single pulse of EdU 24h before sacrifice reveals the presence of proliferating cells in the medial SVZ (**Figures 3C and D**). Note that high EdU+ cells express low level of GFP (**Figure 3C-C'**), highlighting the dilution of the non-integrated transgene with cell divisions (**Figure 1D**). Altogether, these results support that a germinal activity persists in the medial most regions of the SVZ, which can be efficiently studied by targeted electroporation.

At 4 dpe, post-mitotic neuroblasts have initiated their migration in the RMS. A significant number of migrating neuroblasts (about twenty per section) were observed from the most caudal regions of the RMS to its most rostral part in the OB (**Figure 4A-A''**). At this stage, the first newborn neurons reach the end of their tangential migration toward the OB, but they have not yet initiated their radial migration within this region. This radial migration occurs in the following days, as indicated by the presence of GFP+ neurons in the granular and glomerular layers of the OB by 10 dpe (**Figure 4C-4C'**). By 21 dpe, all newborn neurons have reached their final position and display dendritic arborizations suggesting their full integration in OB neuronal circuitries (**Figure 4D**). The expression level of GFP however drops over time (compare **Figure 4D' and 4C'**) preventing the full visualization of dendritic arbors in some of the more weakly GFP+ cells. At this longer timepoint, a larger number of GFP+ cells can be seen in the glomerular layer than in the granule cell layer, indicating that the postnatal medial SVZ mainly generates periglomerular interneurons.

Altogether, these results demonstrate that electroporation of non-integrative transgenes is a rapid technique to label and easily follow newborn neurons for few

weeks until their complete integration into the OB. Making use of this approach, we show that NSCs of the medial wall of the SVZ are still able to generate newborn neurons that migrate and integrate into the OB after birth.

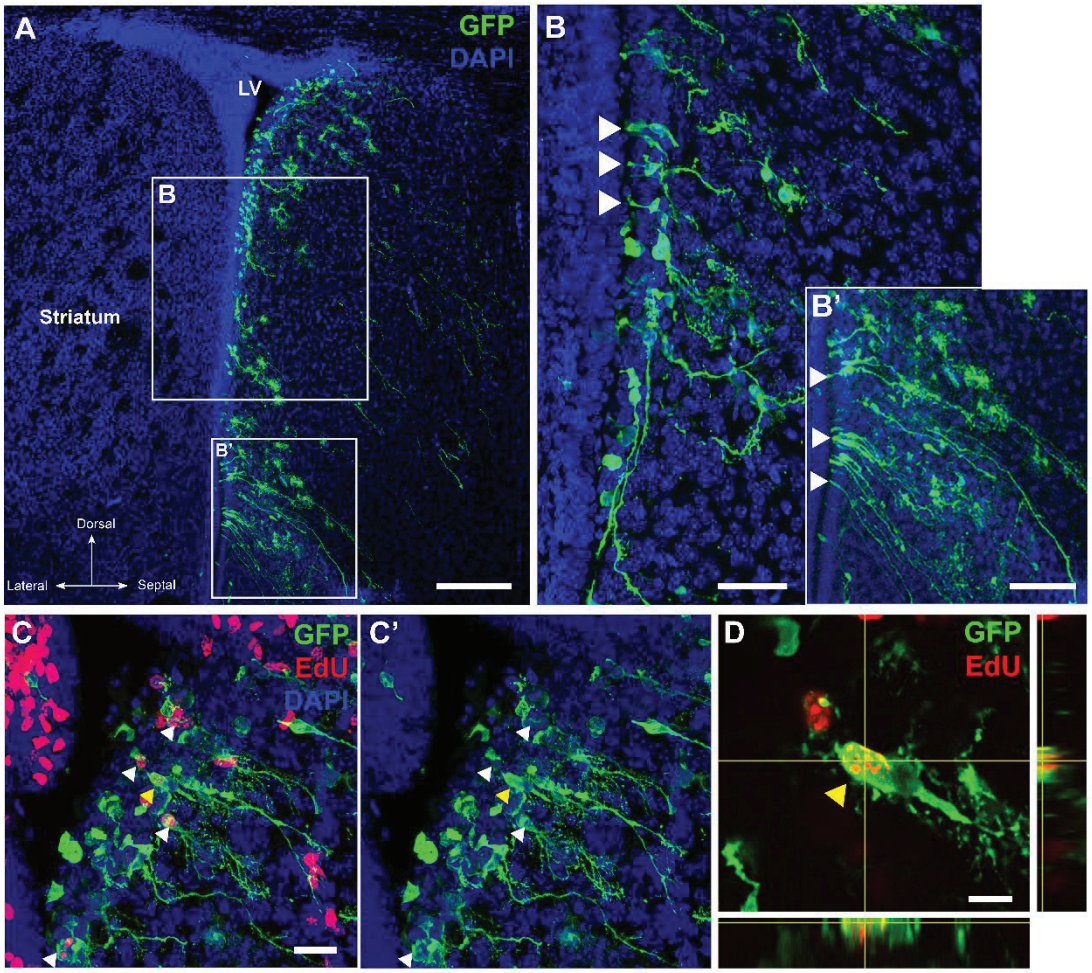

Figure 3: NSCs and actively proliferating progenitors of the postnatal SVZ are efficiently targeted by electroporation

Electroporation of the pCX-GFP plasmid in NSCs of the medial wall of the SVZ. (A-B) At 4 dpe, many electroporated GFP+ cells with a radial glial morphology (white arrows) are observed in the SVZ. Scale bars: 200µm (A) 40µm (B); 50µm (B'). (C-C') A single pulse of EdU 24h before sacrifice reveals the presence of proliferative cells in the medial SVZ. Because of their divisions, these cells start to dilute the non-integrative plasmid (EdU high, GFP low; white arrows). Scale bar: 20µm. (D) High magnification on a proliferative progenitors (yellow arrow). Scale bar: 10µm.
Abbreviation: LV: lateral ventricle

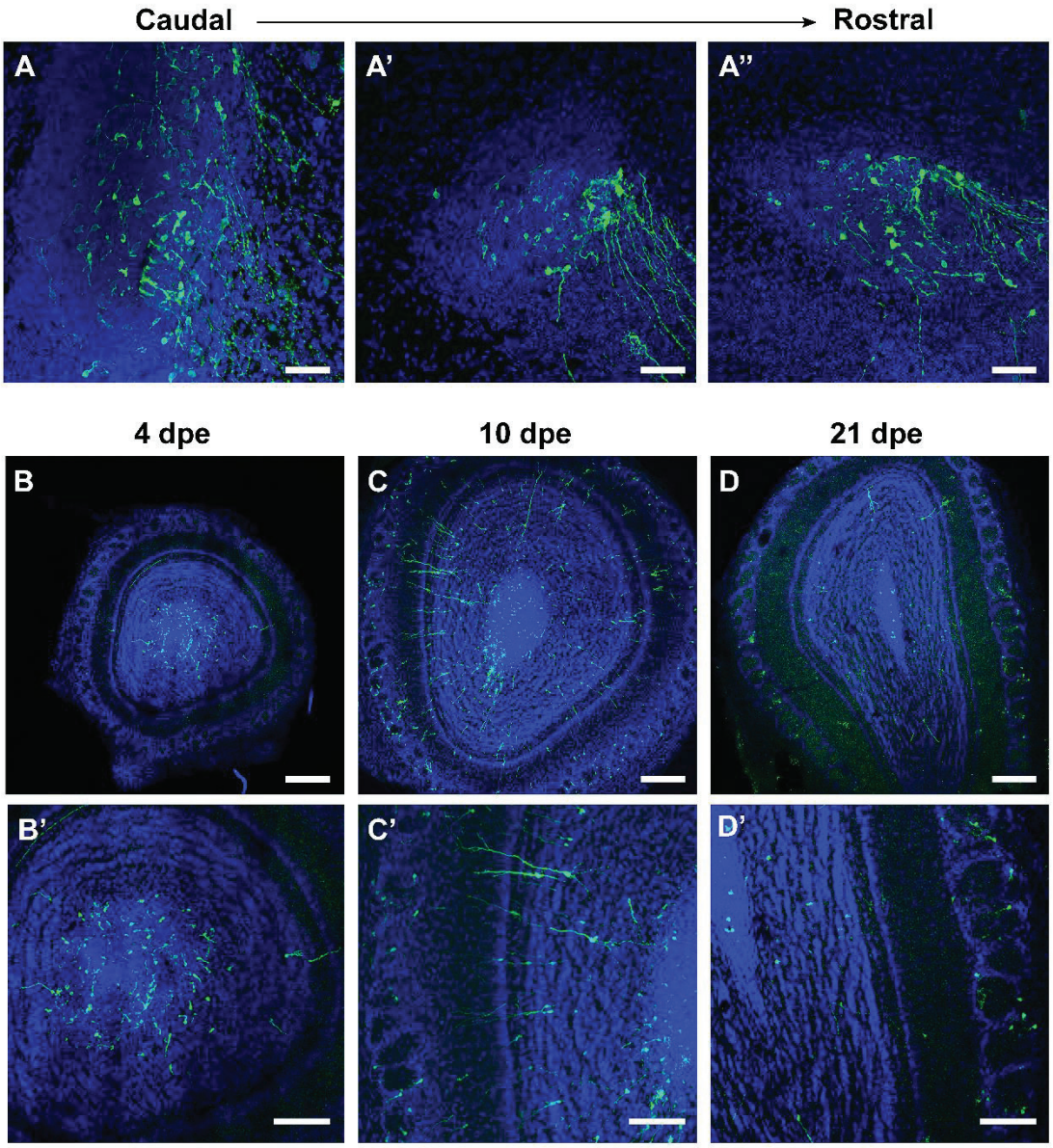

Figure 4: Sequential tangential and radial migration by electroporated cells from the medial SVZ

(A) Neuroblasts migrating thought the RMS at 4 dpe following medial electroporation. Note the presence of numerous GFP+ cells from its more caudal region (A) to its more rostral one in the OB (A''). (B-D) Distribution of GFP+ cells at defined timepoints post-electroporation. While neuroblasts have reached the most rostral part of the RMS by 4 dpe (B), they only start their radial migration at later timepoints to distribute in specific OB layers (C). By 21 dpe many electroporated cells have downregulated GFP due to plasmid dilution, degradation and/or silencing (compare C and D). Scale bars: 50µm (A); 200µm (B, C, D); 100µm (B', C', D')

IV.3.2. Cre-lox approach allows a permanent labeling of postnatal NSCs and their progeny

The results presented above demonstrate that non-integrative plasmids are convenient tools to follow and investigate the differentiation and the integration of newborn neurons in the OB during the first few weeks after birth. These results however also highlight some limitations of this approach: 1) the dilution of the plasmid in proliferating NSCs prevents the long-term fate mapping of this cell population; 2) the labeling of just few neurons born during the first days after birth limits the study of the neurogenic capacities of NSCs in postnatal life. We tried to resolve these limitations by testing a Cre-lox approach. I electroporated a Cre plasmid in the Cre-reporter Rosa-YFP transgenic mice (Novak et al., 2000; Geoffroy and Raineteau, 2007). The transient expression of a Cre recombinase in electroporated cells allows the recombination of a STOP cassette placed behind the promoter and thus, the permanent expression of the YFP reporter protein in targeted cells. Thus, the expression of YFP is only influenced by the activity of the Rosa locus. In this part, I investigated the potential of this approach for long-term fate mapping of SVZ NSCs.

IV.3.2.1. The permanent labeling of postnatal SVZ-NSCs allows their study over extended periods of time

After birth, RGCs segregate into two distinct populations, ependymal cells and NSCs. While ependymal cells do not proliferate and keep transgene expression for some weeks, NSCs rapidly dilute the electroporated plasmids. In order to combine the flexibility of electroporation to target specific SVZ regions with long term visualization and fate mapping of NSCs, we electroporated Cre-reporter Rosa-YFP transgenic mice with a non-integrative Cre plasmid. YFP was efficiently and rapidly induced in electroporated cells (as soon as 24 hours following electroporation, (Geoffroy and Raineteau, 2007). YFP+ cells are observed until 90 days following electroporation in the SVZ (the longer investigated time point) demonstrating permanent and stable YFP expression in electroporated cells (**Figure 5**).

The cytoplasmic YFP expression allows the distinction of two main cell morphologies in the SVZ. Elongated morphologies, characteristic of ependymal cells were found in all electroporated walls of the SVZ at both P45 and P90 (**Figure 5A', F, G** and data not shown). In addition, morphologies typical of postnatal NSCs, i.e.

showing a little thin apical process, residual of the long apical process that extent until the pial surface of embryonic RGCs, were observed in all SVZ walls. Their density was higher in the anterior most part of the SVZ (**Figure 5D**), where most germinal activity is located (Mirzadeh et al., 2008; Fiorelli et al., 2015). In more caudal regions, the SVZ become thinner and is composed of a majority of ependymal cells, (especially in the dorsal SVZ (**Figure 5E**)) with rarer radial cells, observed only in the lateral wall. Thus, the presence of NSCs-like morphologies suggests that postnatal NSCs keep a residual germinal potential even 3 months following electroporation. The localization of these NSCs in the anterior part of the SVZ correlates with the gradual spatial restriction of germinal activity to the anterior most SVZ region after birth.

To confirm a persistent germinal activity by at least a fraction of labeled NSCs, we administrated BrdU in drinking water for 15 days (from P60 to P75) to label both rapidly and slow proliferating cells and sacrificed the animals at P90. Some YFP+ BrdU+ cells were observed in the SVZ at P90 (**Figure 5B-C**). These cells were however rare indicating that NSCs continue either to proliferate and dilute the BrdU or eventually vanish from the SVZ to undergo final differentiation after producing few cohorts of neuroblasts.

Altogether, these data validate the approach in Rosa-YFP mice to permanently label postnatal NSCs for at least 3 months following electroporation. Furthermore, the expression of the reporter protein YFP is strong enough to identify SVZ cell-types by their morphology.

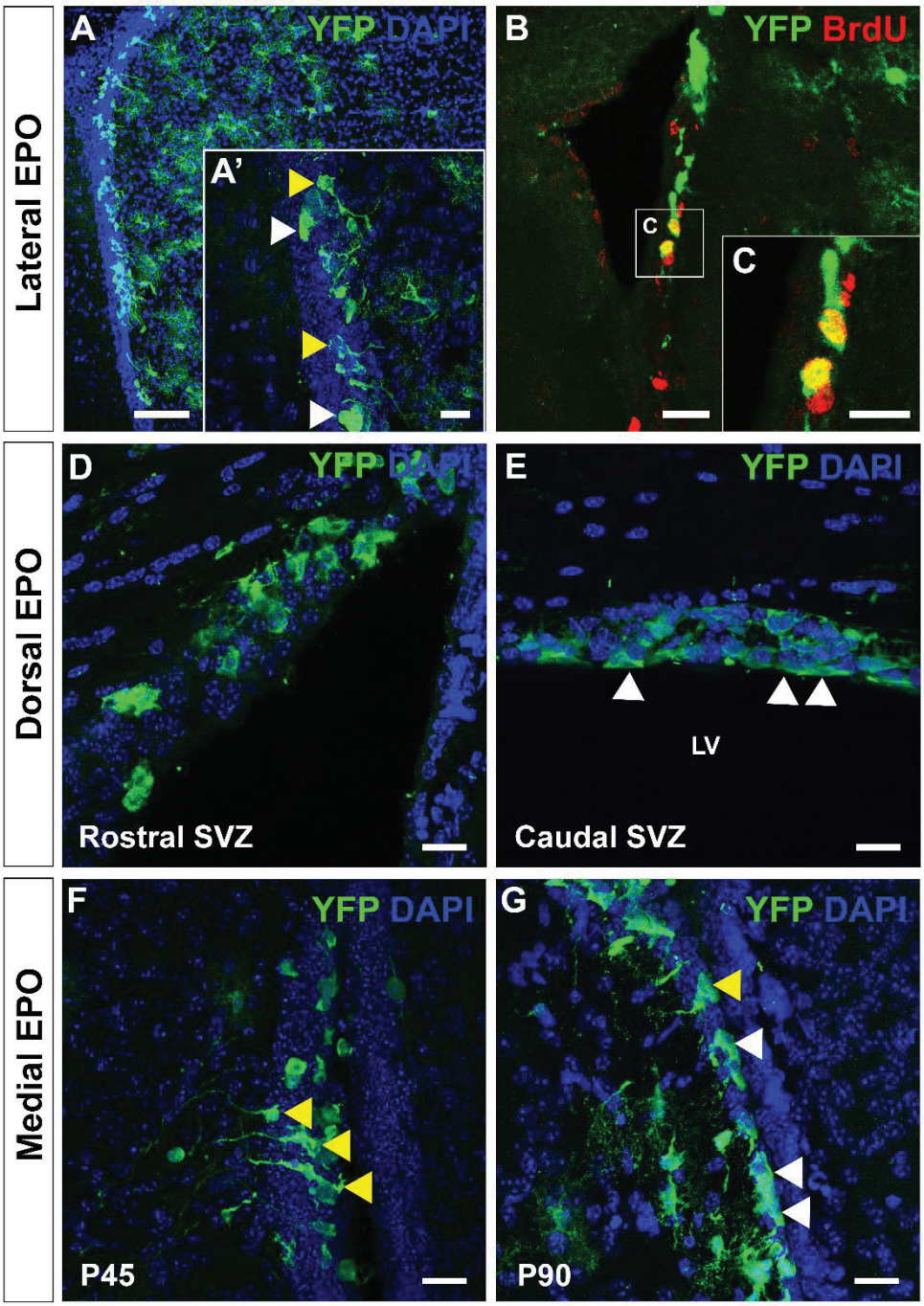

Figure 5: NSCs persist in the postnatal SVZ until three months after birth

(A-B) At P90, ependymal cells and NSCs are found in all the lateral SVZ. Only few BrdU+ cells are observed exclusively in the lateral SVZ of 3 months brain. Scale bar: 100µm (A), 20µm (B), 10µm (C). (D-E) The presence of YFP+ cells in the dorsal SVZ at P90. In the most caudal part, the SVZ becomes thinner and is composed by ependymal cells. Scale bars: 20µM. (F-G) NSCs with a residual process are still observed in the ventral part of the medial wall of the SVZ at P45 but disappear at P90. Scale bars: 20µm.
EPO: electroporation; SVZ: subventricular zone

IV.3.2.2. All SVZ walls continue producing neurons in the OB for several months after birth

The observation of YFP+ cells with stem cell morphologies in the SVZ 3 months after electroporation suggests a persistent germinal activity of electroporated NSCs over postnatal life. This is further supported by the observation of migrating YFP+ Dcx+ neuroblasts in the most caudal (not shown) and rostral regions of the RMS at both P45 and P90 (**Figure 6A-C**). In order to study the time course of neuronal production in the OB, we combined our approach with chronic BrdU administration between P12 and P27 days or between P60 and P75 (**Figure 6D**). By combining this approach with immunodetection of the immature neuronal marker Dcx, we could discriminate three populations of neurons: i.e. a first population generated before BrdU treatment (YFP+/BrdU-/Dcx-), a second generated during the period of BrdU treatment (YFP+/BrdU+/Dcx-), and a third generated during the last two weeks before perfusion (YFP+/Dcx+). This protocol therefore allowed us to investigate temporal changes in the germinal activity of the distinct SVZ microdomains targeted by the electroporation procedure.

Analysis of animals perfused at P45 revealed that OB neurons produced by the lateral and dorsal SVZ during the first 2 weeks (from P2 to P12) period represented 50% of all neurons generated during the first 1.5 months of postnatal life (**Figure 6E**). These values dropped to 25% for the following 2 weeks period (from P12 to P27) to remain stable until P45. Interestingly, the decline in the germinal activity of the medial SVZ appears more pronounced. Thus, more than 80% of the neurons generated by this wall were produced during the first two postnatal weeks, to fall to less than 10% thereafter. Altogether, these results indicate that a rapid decline of germinal activity occurs in all SVZ walls after birth. But while this decline is similar between the dorsal and lateral SVZ walls, it is more pronounced in the medial wall, which loses most of his germinal activity by 2 weeks after birth. This drop in neurogenic capacities of SVZ walls is similar in the granular and periglomerular layers of the OB, although the lateral wall seems to produce less neurons in the periglomerular layer at P90.

We next analyzed animals perfused at P90. In these animals, BrdU was administered between P60 and P75. Immunodetection of BrdU and Dcx revealed a drop in the proportion of neurons generated during the third postnatal month

(YFP+/BrdU+/Dcx- produced between P60 and P75 and YFP+/Dcx+ between P75-P90, respectively) that was comparable for all SVZ walls (**Figure 6F**). Thus, while the original drop in germinal activity occurs faster in the medial SVZ, it stabilizes and becomes comparable between walls by 3 months.

Altogether, these data highlight different dynamics in the decline of germinal activity of distinct SVZ walls during the first 1.5 months of postnatal life. They however show that a residual germinal activity persists in all walls of the SVZ at longer timepoints (3 months), including in the medial wall.

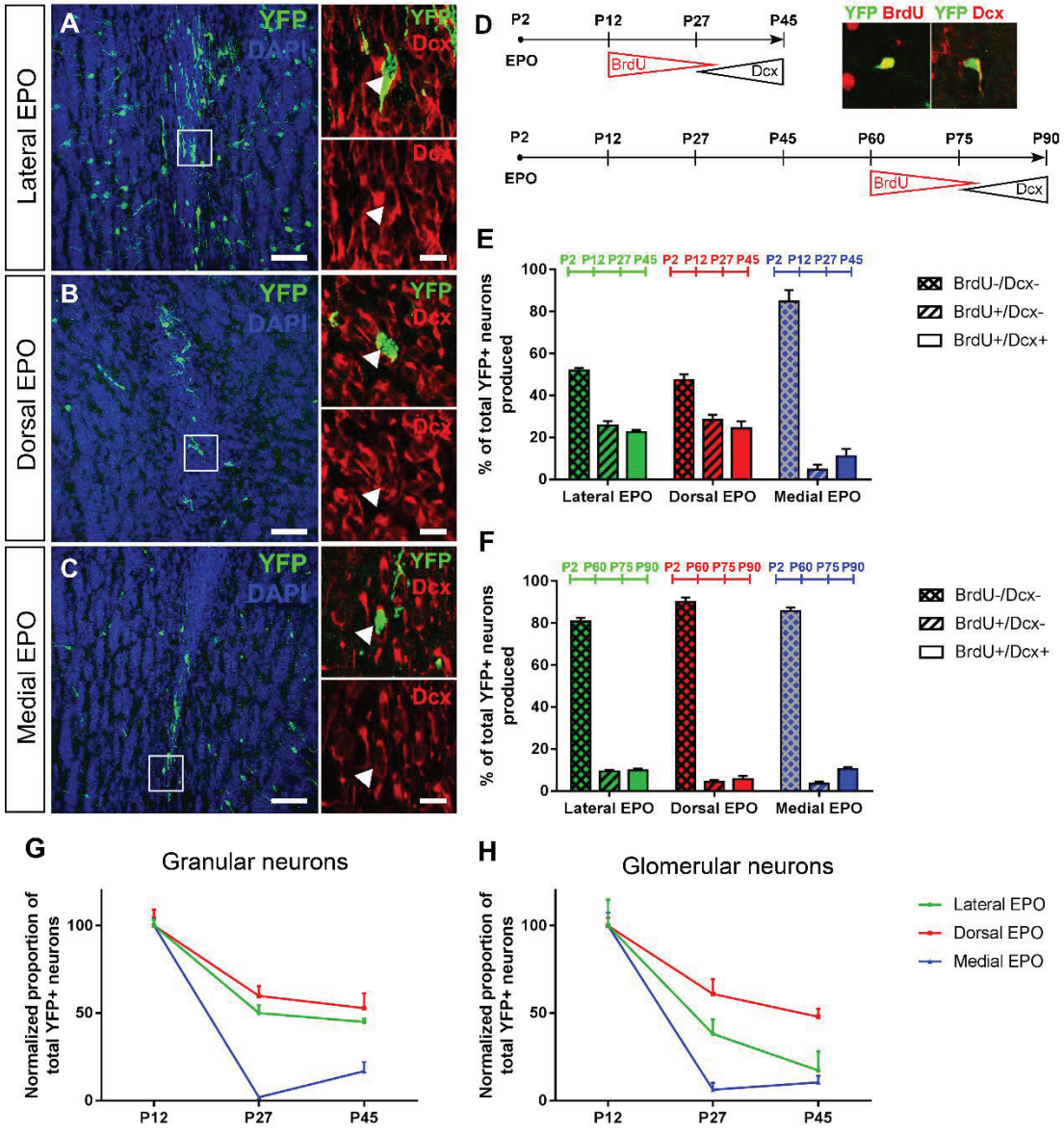
Lateral EPO
Dorsal EPO
Medial EPO
A
B
C
YFP
DAPI
Dcx
D
P2
P12
P27
P45
P60
P75
P90
EPO
BrdU
Dcx
YFP BrdU
YFP Dcx
E
F
P2 P12 P27 P45
P2 P60 P75 P90
% of total YFP+ neurons produced
BrdU-/Dcx-
BrdU+/Dcx-
BrdU+/Dcx+
Lateral EPO
Dorsal EPO
Medial EPO
G
Granular neurons
H
Glomerular neurons
Normalized proportion of total YFP+ neurons

Figure 6: All SVZ walls continue producing neurons after birth but with different dynamics

(A-C) Migrating neuroblasts originating from the lateral (A), dorsal (B) and medial (C) SVZ are observed in the most rostral part of the RMS at P90 indicating continuous neurogenesis for several months after electroporation. High magnifications revealed Dcx expression by migrating neuroblasts. Scale bars: 50µm; 10µm (high magnifications). (D) Schematic representation of the protocols used in this study to birthdate cohorts of neurons born at distinct postnatal times. Illustrations of BrdU (red) and Dcx (black) immunodetection in recombined YFP+ neurons. (E-F) Proportions of YFP+ newborn neurons generated by the lateral, dorsal and medial walls of the SVZ during the first 1.5 months (E) and 3 months (F) of postnatal life. These 1.5 and 3 months are divided into 3 distinct periods following the described protocol. A first period corresponding to oldest YFP+ cells (born between P2 and P12 or P2 and P60 respectively), a second period when BrdU+ cells are generated (between P12 and P27 or P60 and P75 respectively) and the last 15 days before sacrifice when Dcx+ cells are produced (between P27 and P45 or P75 and P90 respectively). (G-H) Normalized proportion of granular (G) and periglomerular neurons (H) originating from the three SVZ microdomains at 45dpe

IV.3.2.3. Permanent labeling of NSCs progeny allows the study of postnatal gliogenesis over extended periods of time

Gliogenesis begins during embryogenesis and peaks during the first weeks after birth. However, the contribution of the different walls of the SVZ to gliogenesis has not been intensively studied because of the intense proliferation of glial progenitors and the resulting dilution of reporter plasmids (Figueres-Oñate et al., 2015). We took advantage of the permanent labeling of NSCs and of their progeny to investigate the spatial contribution of SVZ NSCs to gliogenesis in details.

Mapping of YFP+ glial cell subtypes on coronal sections of the forebrain revealed that the vast majority of these cells were observed at short distance of the lateral ventricle (**Figures 7-9**), while they were virtually absent from the OB. Moreover, a clear regionalization in the distribution of glial cells produced by the medial, dorsal and lateral SVZ was evidenced (compare cell distribution in **Figures 7-9**). Thus, glial YFP+ cells were exclusively observed in the cortex and corpus callosum following dorsal electroporation (**Figure 8**), in the striatum, nucleus accumbens and caudate nucleus following lateral electroporation (**Figure 7**) and in the medial nucleus, preoptic nucleus, and ventral pallidum following medial electroporation (**Figure 9**). Thus, the glial progeny of postnatal NSCs is highly compartmentalized regarding their spatial origin in the SVZ.

Depending on their spatial origin in the SVZ, different subtypes of glial cells are generated by NSCs. Three main types of glial cells were identified based on their localization, distinctive morphologies and markers expression: 1) astrocytes characterized by their dense tufted processes and GFAP expression; 2) oligodendrocytes based on their simpler / larger processes and Olig2 expression; 3) oligodendrocytes in the corpus callosum defined by their elongated/paralleled processes and Olig2 expression. While all walls of the SVZ gave rise to both astrocytes and oligodendrocytes, the proportion of these cell types greatly varied. The dorsal wall produced essentially oligodendrocytes in the corpus callosum and overlying cortex, while a minority of astrocytes could also be observed (**Figure 10C-D**). These astrocytes migrate further in the cortex in the anterior brain and stay close to the SVZ in the most caudal brain. The originality of the medial SVZ is its capability to produce both astrocytes and oligodendrocytes in the hippocampus (**Figure 10G-I**).

Thus, the glial progeny of postnatal NSCs have specific fates depending on its spatial origin in the SVZ.

In order to investigate the continuous production of glial cell subtypes, I next investigated the presence of YFP+/BrdU+ glial cells at P90 following BrdU administration between P60 and P75. BrdU+ oligodendrocytes were found in the septum or the striatum (**Figure 10K**) as well as in the corpus callosum (**Figure 10J**). Interestingly, no BrdU+ astrocytes were observed, suggesting a rapid dilution of the BrdU or an absence of BrdU integration due to a reduced proliferation in this cell lineage.

Altogether, our results demonstrate that the Cre-lox approach enables the permanent labeling of postnatal NSCs and of their progeny. Our results confirm the stable activity of the Rosa locus in cells of all neural lineages, thereby allowing one to investigate the spatial and temporal dynamics of both postnatal neurogenesis and gliogenesis. This approach however relies on the use of transgenic animals, which could be circumvented by the use of integrating plasmids, as described in the next paragraph.

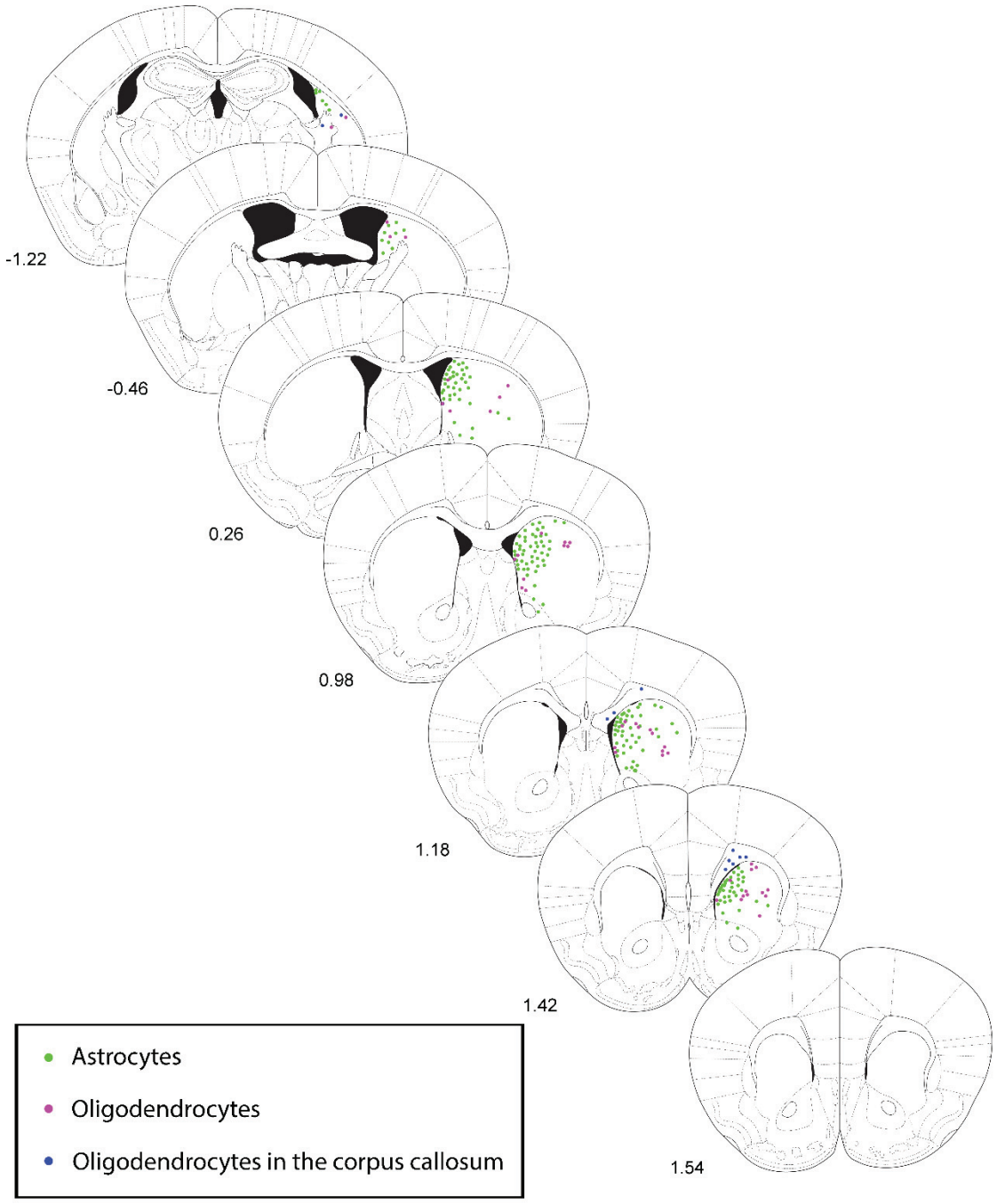

Figure 7: Glial progeny from NSCs of the lateral wall of the SVZ

The glial progeny of NSCs from the lateral SVZ was mapped at P90 onto serial coronal section along the rostro-caudal axis. The coordinates are indicated for each coronal section. The lateral SVZ generates a major part of astrocytes in the striatum that migrate close to the lateral ventricles but also oligodendrocytes that disperse further in the striatum.

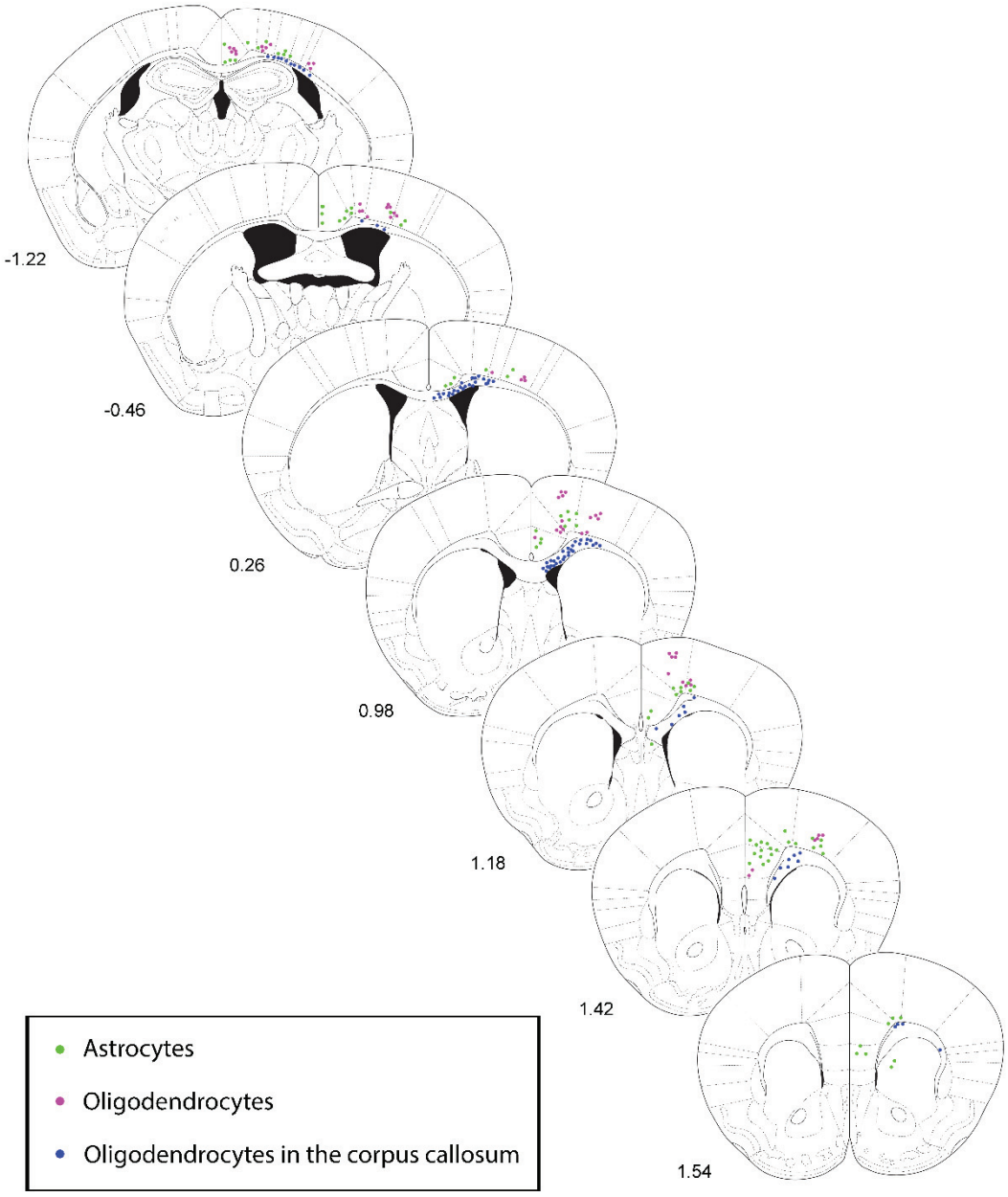

Figure 8: Glial progeny from NSCs of the dorsal wall of the SVZ

The glial progeny of NSCs from the dorsal SVZ was mapped at P90 onto serial coronal section along the rostro-caudal axis. The coordinates are indicated for each coronal section. Gliogenesis from the dorsal SVZ is focused on oligodendrocytes in the corpus callosum. Astrocytes are also found in the cortex close to the corpus callosum while oligodendrocytes migrate further in cortical layers.

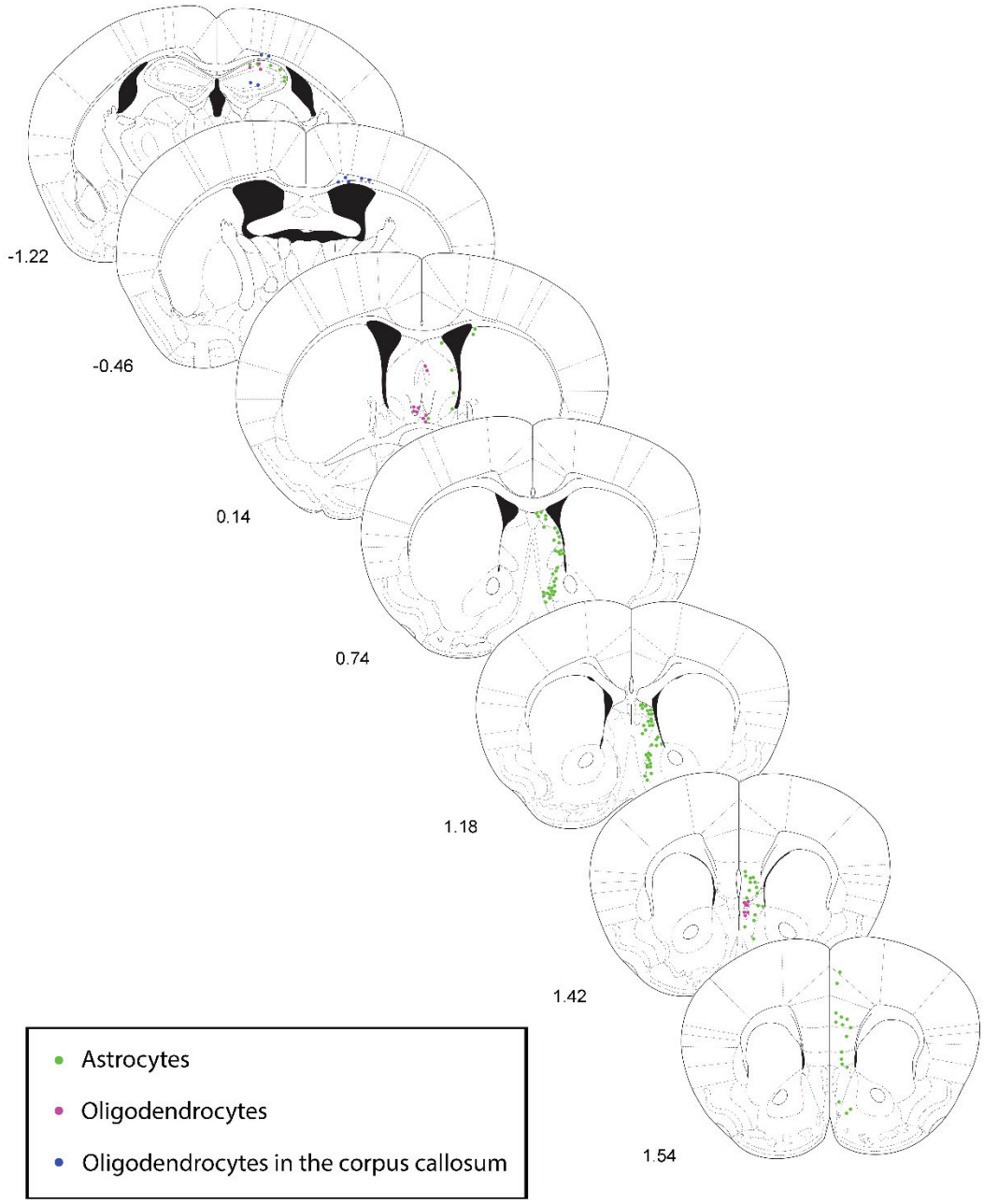

Figure 9: Glial progeny from NSCs of the medial wall of the SVZ

The glial progeny of NSCs from the medial SVZ was mapped at P90 onto serial coronal section along the rostro-caudal axis. The coordinates are indicated for each coronal section. NSCs from the medial SVZ generate both astrocytes and oligodendrocytes in the septum. Interestingly, a considerable number of astrocytes and oligodendrocytes are also migrating into the hippocampus.

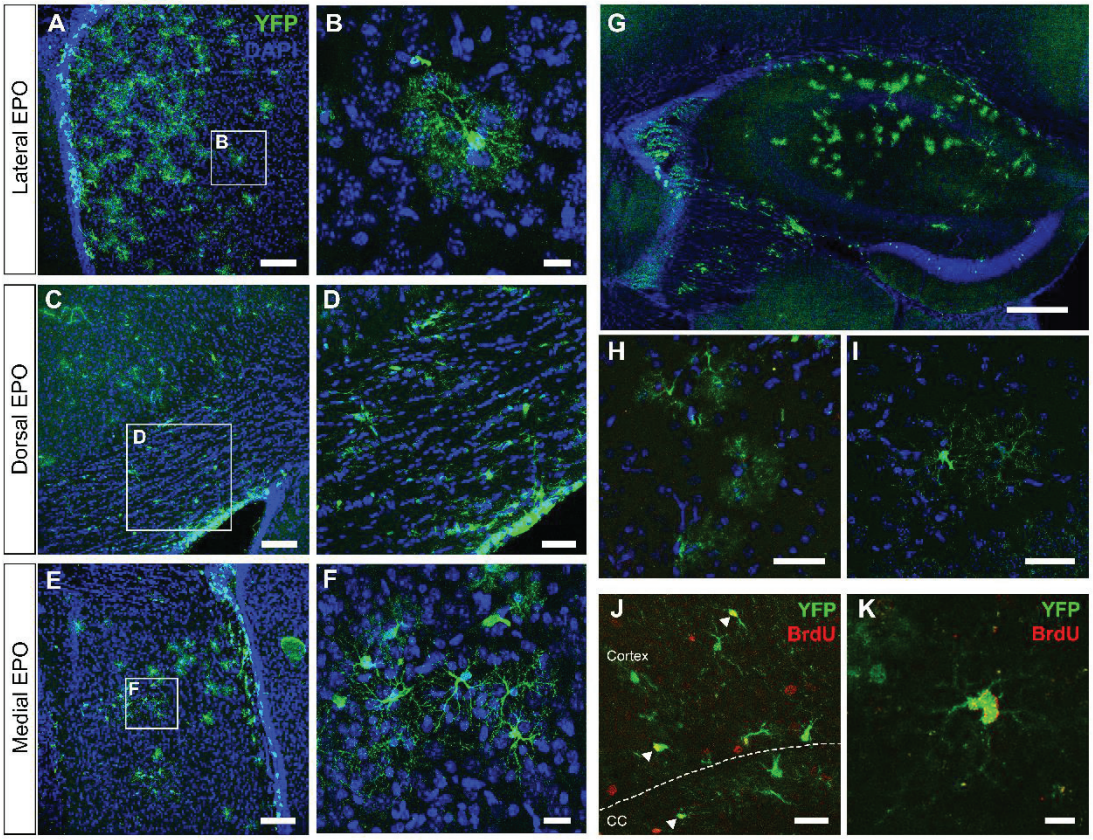

Figure 10: All SVZ walls produce glial cells although with different fate and in distinct forebrain compartments

Glial progeny of NSCs from the lateral, dorsal and medial SVZ at P90. (A-B) NSCs of the lateral wall of the SVZ generate a majority of astrocytes shown in high magnification in (B). Scale bars: 100µm, 10µm. (C-D) NSCs of the dorsal SVZ generate oligodendrocytes in the corpus callosum (D) and both astrocytes and oligodendrocytes in the close parenchyma. Scale bars: 100µm, 50µm. (E-F) NSCs of the medial SVZ generate both astrocytes and oligodendrocytes shown in high magnification picture (F). Scale bars: 100µm, 20µm. (G-I). The medial SVZ also give rise to glial cell in the hippocampus. Scale bar: 200µm. High magnifications show astrocytes (H) and oligodendrocytes (I). Scale bars: 40µm. (J-I) Administration of BrdU between P60 and P75 birthdates glial cells. The dorsal SVZ produces oligodendrocytes and astrocytes in the close parenchyma 2 months after birth (J). BrdU+ oligodendrocytes originating from the lateral SVZ are also observed in the striatum (K). Scale bars: 50µm, 20µm.

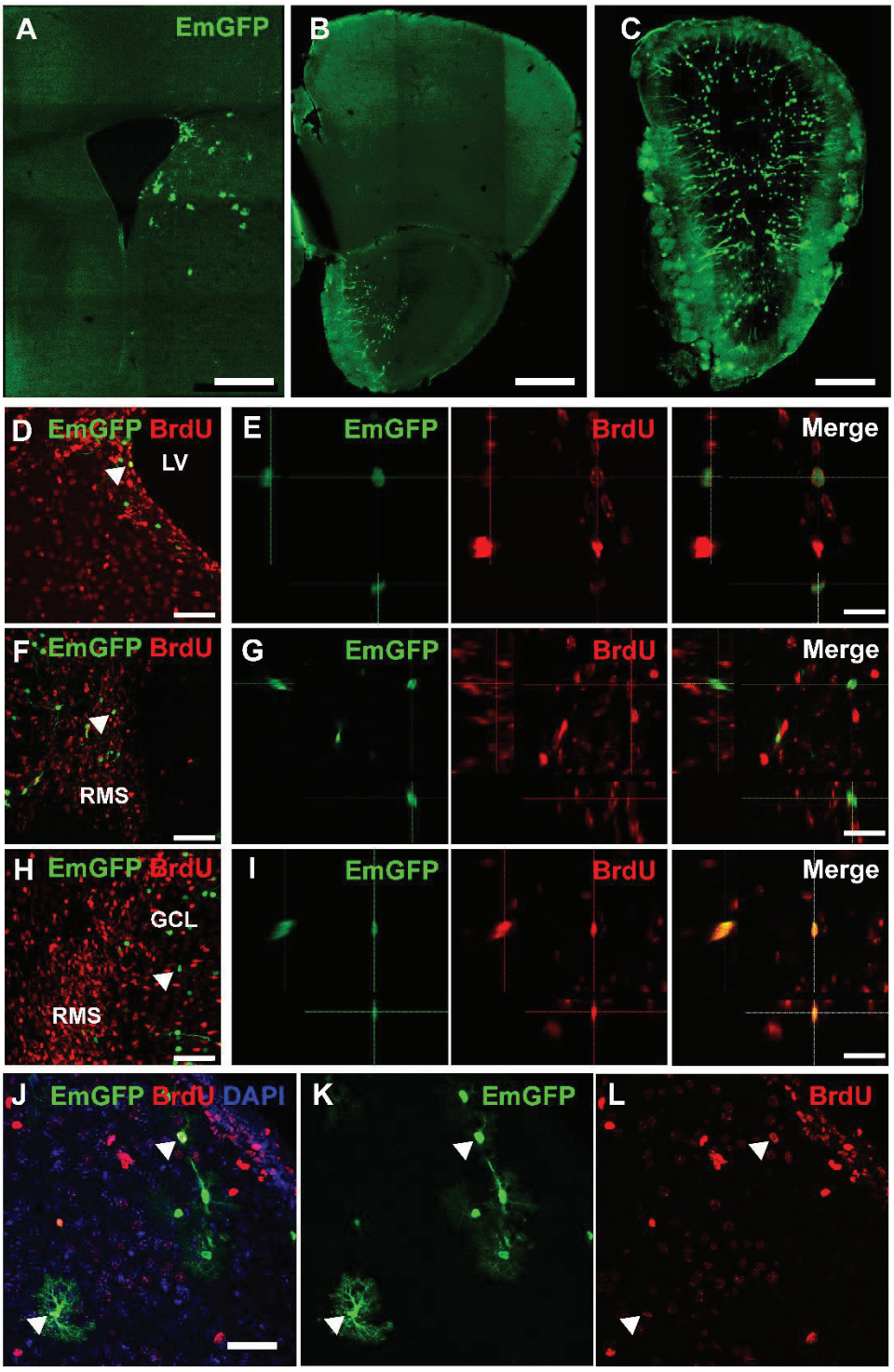

Figure 11: Glial and neuronal progeny of NSCs are followed until three months after genomic integration of transposon construct

(A-C) Overview of EmGFP+ cells 21 days after integration of the transposon construct in NSCs in the SVZ (A) and their progeny in the RMS (B) and the OB (C). Scale bars: 500µm. (D-I) BrdU administration one week before sacrifice at P45 reveals newborn EmGFP+ BrdU+ cells in the SVZ (D-E), the RMS (F-G) and the OB (H-I). Scale bars: 50µm (D, F, H); 20µm (E, G, I). (J-L) The presence of BrdU+ EmGFP+ astrocytes a 21 dpe evidences the permanent labeling of glial cells. Scale bar: 40µm.

IV.3.4. The genomic integration of a transposon prevents the loss of the transgene expression over extensive periods of time

In this part, we aimed at testing the potential of transposons for *in-vivo* electroporation of SVZ-NSCs and long term transgene expression in newborn neurons in the OB. A plasmid expressing a reporter protein, EmGFP flanked by 2 TR sequences was co-electroporated with a plasmid encoding a transposase. The co-expression of these two vectors allowed the integration of the EmGFP vector into the genome. The observation of EmGFP+ cells in the SVZ, the RMS and the OB at 21 dpe and until P45 (**Figure 11A-C** and data not shown) supports both the sustained expression of the reporter gene in early born neurons but also the temporal accumulation of later born neurons in the OB. To further confirm the correct integration and long-term expression of the transgene in SVZ-NSCs and their progeny, the mitotic marker BrdU was injected one week before sacrificing the animals to identify EmGFP+ cells born at late time-points. BrdU+ cells were found in the EmGFP+ population of the SVZ (**Figure 11D-E**), the RMS (**Figure 11F-G**) and the OB (**Figure 11H-I**) at 45 dpe meaning that some EmGFP+ cells were still actively proliferating 5 weeks following electroporation. Interestingly, BrdU+ glial astrocytes were also observed in the striatum at 21 dpe (**Figure 11J-L**) indicating that transgene expression remains stable even in highly proliferative cells like astrocytes.

Altogether, these results confirm the efficient integration of the transposon constructs into SVZ-NSCs genome, and their continuous expression in progenitors, glial cells and newborn neurons generated by postnatal NSCs.

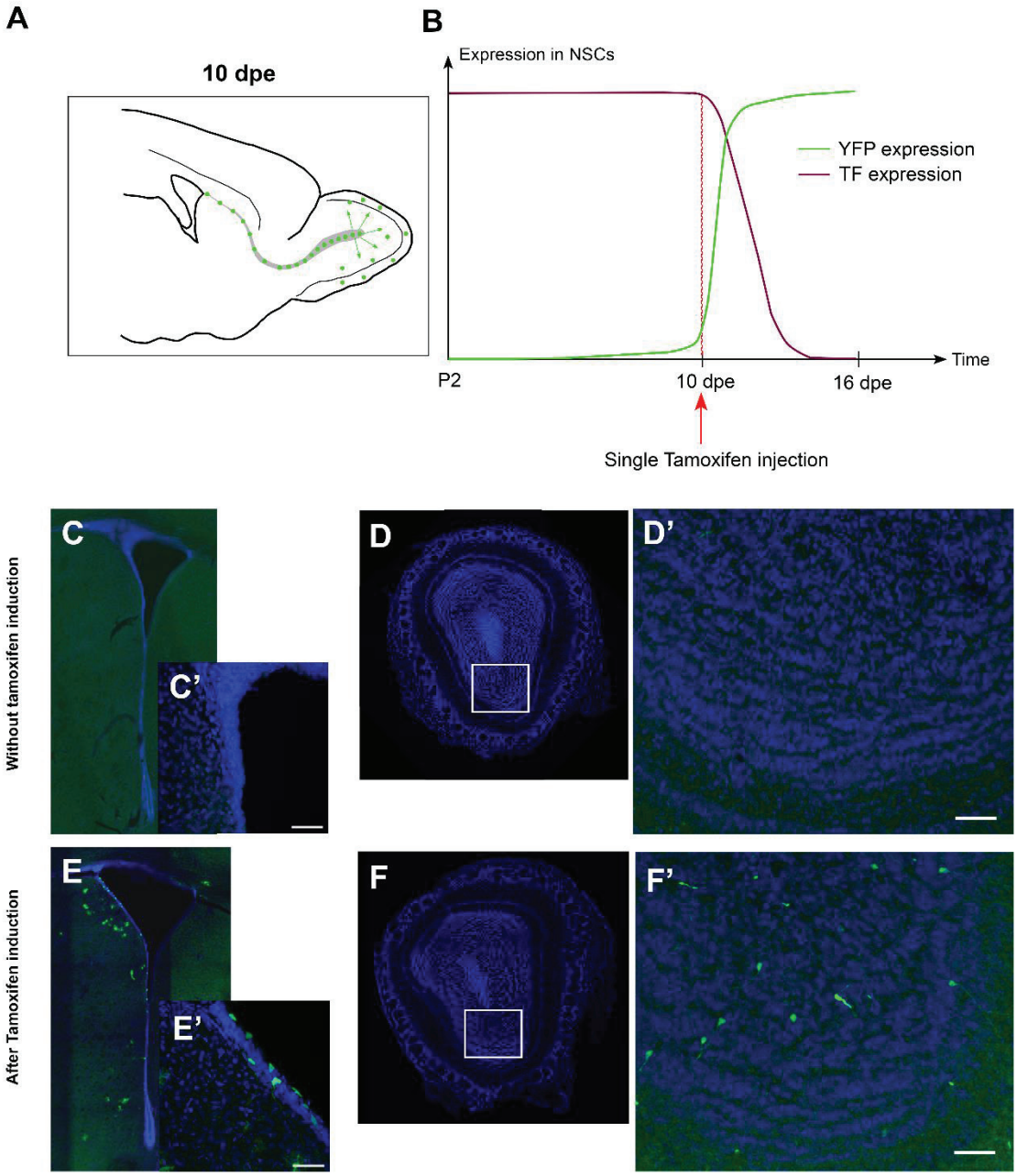

Figure 12: ER^{T2}-Cre-ER^{T2} plasmid allows timely-controlled manipulation of gene expression

(A) Schematic representation of the position of electroporated cells during their differentiation from the SVZ to the OB at 10 dpe. (B) Illustration of the permanent expression of YFP after Cre-recombination and the simultaneous and potential ablation of a target gene in transgenic mice after single tamoxifen injection at 10 dpe. (C-F) Lateral electroporation of an ER^{T2}-Cre-ER^{T2} plasmid in Rosa-YFP mice. The absence of recombination and therefore YFP expression before tamoxifen injection at 10 dpe in the SVZ (C-C') and the OB (D'). The specific expression of YFP is revealed after tamoxifen injection in recombined cells in the SVZ (E-E') and the OB (F'). Scale bars: 20µm.

IV.3.6. Timely-controlled manipulation of gene expression

The results described above highlight a complex spatial and temporal dynamic of NSCs differentiation in the postnatal brain, which occurs on extended periods of time in distinct forebrain compartments. Addressing the transcriptional coding of this process may require a conditional and timely controlled manipulation of gene expression (see for example chapter 3). Although previous approaches are sufficient for early manipulation of transgene expression, it does not allow the timely-controlled expression of transgene and therefore its restriction to the late phases of the differentiation process.

To induce a permanent and delayed expression of a Cre transgene and therefore manipulate gene expression at late steps of neuronal differentiation, we tested a pCAG-ER^{T2}-CRE-ER^{T2} non-integrative plasmid in Cre-reporter Rosa-YFP mice. ER^{T2} sequences should allow the specific nuclear translocation and activation of the Cre recombinase following tamoxifen injection. A single tamoxifen injection (20mg/mL) at 10 dpe when electroporated cells are maturing in the OB (**Figure 12A-B**) induces the permanent expression of YFP in recombined cells. Although few in number, YFP+ cells were observed in the SVZ and the OB (**Figure 12E-F'**) meaning that a single injection of tamoxifen is sufficient to induce an efficient recombination in electroporated cells. However, ER^{T2}-CRE-ER^{T2} transgene could induce background recombination. To assess if the presence of ER^{T2} sequences is sufficient to prevent the Cre activity in basal conditions, three animals were sacrificed at 10 dpe before tamoxifen injection. No YFP+ cells were found in control brains in the SVZ or in the OB (**Figure 12C-D**) showing that ER^{T2} sequences prevent efficiently the random nuclear translocation of the Cre recombinase.

Altogether, these results show that the ER^{T2}-CRE-ER^{T2} system allows a timely-controlled expression of transgene in maturing neurons and highlights the high specificity of this inducible system for delayed expression. Thus, this system is applicable in transgenic animals for timely controlled manipulation of gene expression during the differentiation process (i.e. Sp8, described in chapter 3).

IV.4. Discussion

This chapter is an overview of the electroporation approaches used in the lab that I developed and refined during the first year of my PhD. After birth, both neurogenesis and gliogenesis persist in the forebrain, with newborn neurons migrating through the RMS toward the OB and glial cells dispersing at proximity of the lateral ventricles. Many subtleties exist regarding the spatial and temporal identity of SVZ neural stem cells and of the progenies they produce. The regionalization and high dynamic nature of this postnatal germinal region offers unique opportunities to study the mechanisms that guide NSCs differentiation and specification, but also represent unique methodological challenges. Here I have embraced these challenges by refining postnatal electroporation approach and by developing a “tool box” to study the biology of postnatal neurogenesis and gliogenesis.

Postnatal neurogenesis has first been studied in a global manner by targeting proliferating progenitors with viral constructs or thymidine analogues such as BrdU. In the 2000s, the description of a regionalization of the SVZ has required the development of new techniques to distinguish NSCs and their respective progenies depending of the spatial location in the SVZ. Several approaches have been used to fate-map specific spatial populations of embryonic and postnatal NSCs. Most embryonic studies make use of transgenic approaches allowing Cre recombinase expression under the regulation of promoters of pallial and sub-pallial transcription factors (TFs). These experiments have shown that NSCs from the postnatal SVZ originate from distinct embryonic regions and generate specific progenies, including specific neuronal subtypes in the different layers of the OB (Willaime-Morawek et al., 2006; Kohwi et al., 2007; Ventura and Goldman, 2007; Young et al., 2007; Fiorelli et al., 2015). Other approaches have been developed to target postnatal NSCs in a spatially restricted manner. Cortical injections of adeno-associated virus have been shown to infect RGCs through their basal process, early after birth (Merkle et al., 2007). This approach allows transgene expression, such as Cre, in discrete population of RGCs and therefore their long term labeling and fate mapping in Cre-reporter mice. More recently, electroporation have been shown to efficiently target postnatal NSCs (Boutin et al., 2008). Refinement of this approach allowed the specific targeting of spatial subpopulations of NSCs in various regions of the SVZ (Fernández et al., 2011). The approach I have established in this chapter is a mix of

these two last approaches, as it combines the simplicity of the postnatal electroporation with the long-term transgene expression of the viral approach. Obtained results confirmed previous work on the preferential generation of specific OB neuronal subtype by the dorsal, lateral and medial NSCs of the SVZ (Fernández et al. 2011; also reviewed in Fiorelli et al. 2015). In addition, the permanent labeling of NSCs adds temporal information to this previous study. Indeed, a fundamental feature of the SVZ is the gradual decrease in the germinal capacity of NSCs during postnatal life. This decrease has been well characterized at late postnatal timepoints, i.e. during aging. Thus, a dramatic decrease in neurogenesis has been described and occurs by ~6-12 months of age in rodents (Enwere, 2004; Molofsky et al., 2006; Shook et al., 2012). Accordingly, the total number of proliferating cells in the niche is reduced by 50-75% at 24 months of age (Tropepe et al., 1997; Maslov et al., 2004; Luo et al., 2006; Capilla-Gonzalez et al., 2014). Our long-term fate mapping study demonstrates that this decline initiates very rapidly after birth. Birth dating of consecutive cohorts of recombined cells indeed shows a drastic reduction of OB neurogenesis during the first month of postnatal life. Although this rapid decline was observed in all SVZ walls, our results indicate that it is more pronounced for the medial wall. These data suggest that the maintenance and germinal activity of NSCs differs depending on their spatial origin in the SVZ and therefore their embryonic origin. Thus, regions of the postnatal SVZ become rapidly “silent” after birth, affecting the balance in neuronal subtypes being produced. It should however be noted that the ratio of newly formed periglomerular interneuron subtypes (TH+, CalB+ or CalR+) does not change further between 3 months and 2 years (Kohwi et al., 2007), suggesting that the loss of NSC activity at later timepoint is more homogeneous and largely lineage independent (Shook et al., 2012).

One of the main challenges in studying postnatal NSCs is their ability to produce both neuronal and glial cells, which present striking differences in their proliferative and properties distribution. Our results show that only permanent fate mapping approaches allowed to fully appreciate the regionalization in the production of glial cells by the different walls of the SVZ. This prevents the rapid dilution of non-integrating reporter plasmids through multiple rounds of divisions, as exemplified by the rapid dilution of BrdU in astrocytes observed in this study. Our results indicate that SVZ microdomains produce glial cells that migrate to defined brain

compartments, i.e. brain regions directly facing the corresponding SVZ wall. The regional generation of glial cell subtypes has been illustrated in a number of studies. Fate mapping studies revealed that astrocytes are allocated to spatial domains in accordance with their embryonic sites of origin in the ventricular zone (Tsai et al., 2012). Similarly, oligodendrocytes of the cortex and subcortical regions have defined dorso-ventral origin (Tekki-Kessaris et al., 2001; Costa et al., 2007). This regional distribution is likely to underline functional specificities of glial cells residing in distinct brain regions. For instance, transcriptomic analysis of astrocytes isolated from various brain regions reveals heterogeneous expression of several astrocytic markers (Morel et al., 2017). Regional differences in astrocytes have been recently shown to influence neuronal synaptogenesis and maturation through secretion of several extracellular matrix proteins (Eroglu and Barres, 2010). Our results also show a bias in the subtype of glial cells being produced by distinct glial wall. For instance, while dorsal NSCs produce mainly oligodendrocytes, those from the medial and lateral wall produce a majority of astrocytes. These differences are likely to reflect differences in glial subtypes that exist in various brain regions. Thus, while differences in oligodendrocytes density and their association with the white matter tract overlying the dorsal SVZ are well known, differences also exist for astrocytes which density greatly varies between brain regions (Azevedo et al., 2009). Altogether, this emerging field of study could benefit from approaches such as those developed in this chapter to better understand regional differences in forebrain astrogenesis.

Although several advances have been achieved, the molecular mechanisms underlying the differentiation and specification of NSCs remain to be fully explored (Agoston et al., 2014; Beclin et al., 2016; Figueres-Oñate and López-Mascaraque, 2016; Naser et al., 2016). A puzzling observation is the expression of select TFs at both early and late stages of NSCs differentiation. For instance, Pax6 is a TF expressed early in embryonic progenitors of the pallium and progenitors of the dorsal postnatal SVZ and remains express in mature dopaminergic OB interneurons originating from these progenitors (Brill et al., 2008; Ninkovic et al., 2010). The TF Sp8 is another TF expressed early in migrating neuroblasts and that remains expressed in only defined subtypes of mature interneurons in the OB (Waclaw et al., 2006). This pattern of expression suggests that TFs may play distinct roles in progenitors and maturing neurons. The study of their role in the more advanced

stages of differentiation requires the development of new techniques for conditional manipulation of gene expression. The use of an ER^{T2}-CRE-ER^{T2} transgene allowed the delayed expression of YFP reporter protein and thus would allow a delayed manipulation of gene expression in transgenic animals (see chapter 3 for Sp8 gene manipulation). This approach is limited to a few days post electroporation due to the use of a non-integrative plasmid which is diluted or possibly lost during the differentiation process. This limitation could be circumvented by the use of an ER^{T2}-CRE-ER^{T2} transposon, which would extend the usability of this approach to later stages while avoiding the costly and time-consuming establishment of transgenic lines.

Altogether, our results demonstrate that electroporation is an adaptable approach to study postnatal neurogenesis and gliogenesis. A future refinement of this approach would be to develop tools to perform long-term clonal analysis of SVZ NSCs. A recent attempt towards this direction is illustrated by the StarTrack method (García-Marqués and López-Mascaraque, 2013; García-Marqués et al., 2014). This approach allows the stable expression of six fluorescent reporter proteins under the regulation of human glial fibrillary acidic protein (hGFAP) promoter expressed either in the cytoplasm or in the nucleus. Using these tools will allow the investigation of the potency of postnatal NSCs in great details, i.e. their capacity to produce cells of distinct neural lineages. Our data suggest that at least some NSCs become exhausted shortly after birth and stop producing new neurons, as previously reported (Calzolari et al., 2015). Is this exhaustion preceded by the generation of cohorts of glial cells, or are distinct NSCs populations producing neuronal vs glial progenies? Long-term clonal analysis would allow addressing these remaining questions.

Agoston Z, Heine P, Brill MS, Grebbin BM, Hau A-C, Kallenborn-Gerhardt W, Schramm J, Götz M, Schulte D (2014) Meis2 is a Pax6 co-factor in neurogenesis and dopaminergic periglomerular fate specification in the adult olfactory bulb. Development 141:28–38

Azevedo FAC, Carvalho LRB, Grinberg LT, Farfel JM, Ferretti REL, Leite REP, Filho WJ, Lent R, Herculano-Houzel S (2009) Equal numbers of neuronal and nonneuronal cells make the human brain an isometrically scaled-up primate brain. J Comp Neurol 513:532–541.

Beclin C, Follert P, Stappers E, Barral S, Coré N, de Chevigny A, Magnone V, Lebrigand K, Bissels U, Huylebroeck D, Bosio A, Barbry P, Seuntjens E, Cremer H (2016) miR-200 family controls late steps of postnatal forebrain neurogenesis via Zeb2 inhibition. Sci Rep 6:35729

Boutin C, Diestel S, Desoeuvre A, Tiveron M-C, Cremer H, Camille Boutin Angelique Desoeuvre, Marie-Catherine Tiveron, Harold Cremer SD (2008) Efficient in vivo electroporation of the postnatal rodent forebrain. PLoS One 3:e1883

Brill MS, Snapyan M, Wohlfrom H, Ninkovic J, Jawerka M, Mastick GS, Ashery-Padan R, Saghatelyan A, Berninger B, Götz M (2008) A dlx2- and pax6-dependent transcriptional code for periglomerular neuron specification in the adult olfactory bulb. J Neurosci 28:6439–6452

Calzolari F, Michel J, Baumgart EV, Theis F, Götz M, Ninkovic J (2015) Fast clonal expansion and limited neural stem cell self-renewal in the adult subependymal zone. Nat Neurosci 18:90-92

Capilla-Gonzalez V, Cebrian-Silla A, Guerrero-Cazares H, Garcia-Verdugo JM, Quiñones-Hinojosa A (2014) Age-Related Changes in Astrocytic and Ependymal Cells of the Subventricular Zone Vivian. Glia 62:790–803.

Carleton A, Petreanu LT, Lansford R, Alvarez-Buylla A, Lledo P-M (2003) Becoming a new neuron in the adult olfactory bulb. Nat Neurosci 6:507–518.

Costa MR, Kessaris N, Richardson WD, Gotz M, Hedin-Pereira C (2007) The Marginal Zone/Layer I as a Novel Niche for Neurogenesis and Gliogenesis in Developing Cerebral Cortex. J Neurosci 27:11376–11388

Enwere E (2004) Aging Results in Reduced Epidermal Growth Factor Receptor Signaling, Diminished Olfactory Neurogenesis, and Deficits in Fine Olfactory Discrimination. J Neurosci 24:8354–8365

Eroglu C, Barres BA (2010) Regulation of synaptic connectivity by glia. Nature 468:223–231.

Fernández ME, Croce S, Boutin C, Cremer H, Raineteau O (2011) Targeted electroporation of defined lateral ventricular walls: a novel and rapid method to study fate specification during postnatal forebrain neurogenesis. Neural Dev 6:13.

Figueres-Oñate M, García-Marqués J, Pedraza M, De Carlos JA, López-Mascaraque L (2015) Spatiotemporal analyses of neural lineages after embryonic and postnatal progenitor targeting combining different reporters. Front Neurosci 9:87.

Figueres-Oñate M, López-Mascaraque L (2016) Adult olfactory bulb interneuron phenotypes identified by targeting embryonic and postnatal neural progenitors. Front Neurosci 10:194.

Fiorelli R, Azim K, Fischer B, Raineteau O (2015) Adding a spatial dimension to postnatal ventricular-subventricular zone neurogenesis. Development 142:2109–2120.

García-Marqués J, López-Mascaraque L (2013) Clonal identity determines astrocyte cortical heterogeneity. Cereb Cortex 23:1463–1472.

García-Marqués J, Nuñez-Llaves R, López-Mascaraque L (2014) NG2-Glia from Pallial Progenitors Produce the Largest Clonal Clusters of the Brain: Time Frame of Clonal Generation in Cortex and Olfactory Bulb. J Neurosci 34:2305–2313.

Geoffroy CG, Raineteau O (2007) A Cre-lox approach for transient transgene expression in neural precursor cells and long-term tracking of their progeny in vitro and in vivo. BMC Dev Biol 7:45

Kohwi M, Osumi N, Rubenstein JLR, Alvarez-Buylla A (2005) Pax6 is required for making specific subpopulations of granule and periglomerular neurons in the olfactory bulb. J Neurosci 25:6997–7003.

Kohwi M, Petryniak MA, Long JE, Ekker M, Obata K, Yanagawa Y, Rubenstein JL, Alvarez-Buylla A (2007) A subpopulation of olfactory bulb GABAergic interneurons is derived from Emx1- and Dlx5/6-expressing progenitors. J Neurosci 27:6878–6891.

Lois C, Alvarez-Buylla A (1994) Long-distance neuronal migration in the adult mammalian brain. Science 264:1145–1148.

Luo J, Daniels SB, Lennington JB, Notti RQ, Conover JC (2006) The aging neurogenic subventricular zone. Aging Cell 5:139–152.

Luskin MB (1993) Restricted proliferation and migration of postnatally generated neurons derived from the forebrain subventricular zone. Neuron 11:173–189.

Maslov AY, Barone TA, Plunkett RJ, Pruitt SC (2004) Neural Stem Cell Detection, Characterization, and Age-Related Changes in the Subventricular Zone of Mice. J Neurosci 24:1726–1733.

Matsuda T, Cepko CL (2004) Electroporation and RNA interference in the rodent retina in vivo and in vitro. Proc Natl Acad Sci U S A 101:16–22

Merkle FT, Mirzadeh Z, Alvarez-buylla A (2007) Mosaic organization of neural stem cells in the adult brain. Science 317:381–384

Merkle FT, Tramontin AD, García-Verdugo JM, Alvarez-Buylla A (2004) Radial glia give rise to adult neural stem cells in the subventricular zone. Proc Natl Acad Sci 101:17528–17532.

Mirzadeh Z, Merkle FT, Soriano-Navarro M, García-Verdugo JM, Alvarez-Buylla A (2008) Neural stem cells confer unique pinwheel architecture to the ventricular surface in neurogenic regions of the adult brain. Cell Stem Cell 11:265–278.

Molofsky A V, Slutsky SG, Joseph NM, He S, Krishnamurthy J, Sharpless NE, Morrison SJ (2006) Increasing p16INK4a expression decreases forebrain progenitors and neurogenesis during ageing. Nature 443:448–452.

Morel L, Chiang MSR, Higashimori H, Shoneye T, Iyer LK, Yelick J, Tai A, Yang Y (2017) Molecular and Functional Properties of Regional Astrocytes in the Adult Brain. J Neurosci 37:3956–16

Naser R, Vandenbosch R, Omais S, Hayek D, Jaafar C, Al Lafi S, Saliba A, Baghdadi M, Skaf L, Ghanem N (2016) Role of the Retinoblastoma protein, Rb, during adult neurogenesis in the olfactory bulb. Sci Rep 6:20230

Ninkovic J, Pinto L, Petricca S, Lepier A, Sun J, Rieger MA (2010) The Transcription Factor Pax6 Regulates Survival of Dopaminergic Olfactory Bulb Neurons via Crystallin a A.

Ninkovic J, Pinto L, Petricca S, Lepier A, Sun J, Rieger M a, Schroeder T, Cvekl A, Favor J, Sciences V (2015) The transcription factor Pax6 regulates survival of dopaminergic olfactory bulb neurons via crystallin αA. Neuron 68:682–694.

Novak A, Guo C, Yang W, Nagy A, Lobe CG (2000) Z/EG, a double reporter mouse line that expresses enhanced green fluorescent protein upon Cre-mediated excision. Genesis 28:147–155.

Ponti G, Obernier K, Guinto C, Jose L, Bonfanti L, Alvarez-Buylla A (2013) Cell cycle and lineage progression of neural progenitors in the ventricular-subventricular zones of adult mice. Proc Natl Acad Sci U S A 110:E1045-54

Roybon L, Deierborg T, Brundin P, Li J-Y (2009) Involvement of Ngn2, Tbr and NeuroD proteins during postnatal olfactory bulb neurogenesis. Eur J Neurosci 29:232–243

Shook BA, David H. Manz, Peters JJ, Kang S, C. J, Conover (2012) Spatio-Temporal Changes to the SVZ Stem Cell Pool Through Aging. J Neurosci 32:6947–6956.

Spassky N, Merkle FT, Flames N, Tramontin AD, Garcıa-Verdugo J-M, Alvarez-Buylla A (2005) Adult Ependymal Cells Are Postmitotic and Are Derived from Radial Glial Cells during Embryogenesis. J Neurosci 25:10–18.

Tekki-Kessaris N, Woodruff R, Hall a C, Gaffield W, Kimura S, Stiles CD, Rowitch DH, Richardson WD (2001) Hedgehog-dependent oligodendrocyte lineage specification in the telencephalon. Development 128:2545–2554.

Tramontin AD, García-Verdugo JM, Lim DA, Alvarez-Buylla A (2003) Postnatal development of radial glia and the ventricular zone (VZ): A continuum of the neural stem cell compartment. Cereb Cortex 13:580–587.

Tropepe V, Craig CG, Morshead CM, van der Kooy D (1997) Transforming growth factor-alpha null and senescent mice show decreased neural progenitor cell proliferation in the forebrain subependyma. J Neurosci 17:7850–7859.

Tsai H, Li H, Fuentealba LC, Molofsky A V, Zhuang H, Tenney A, Murnen AT, Stephen PJ, Merkle F, Kessaris N, Alvarez-buylla A, William D, Rowitch DH (2012) Regional Astrocyte Allocation Regulates CNS Synaptogenesis and Repair. Science (80-) 337:358–362.

Ventura RE, Goldman JE (2007) Dorsal Radial Glia Generate Olfactory Bulb Interneurons in the Postnatal Murine Brain. J Neurosci 27:4297–4302

Waclaw RR, Allen ZJ, Bell SM, Erdélyi F, Szabó G, Potter SS, Campbell K (2006) The zinc finger transcription factor Sp8 regulates the generation and diversity of olfactory bulb interneurons. Neuron 49:503–516.

Willaime-Morawek S, Seaberg RM, Batista C, Labbé E, Attisano L, Gorski JA, Jones KR, Kam A, Morshead CM, Van Der Kooy D (2006) Embryonic cortical neural stem

cells migrate ventrally and persist as postnatal striatal stem cells. J Cell Biol 175:159–168.

Winner B, Cooper-Kuhn CM, Aigner R, Winkler J, Kuhn HG (2002) Long-term survival and cell death of newly generated neurons in the adult rat olfactory bulb. Eur J Neurosci 16:1681–1689.

Winpenny E, Lebel-Potter M, Fernandez ME, Brill MS, Götz M, Guillemot F, Raineteau O (2011) Sequential generation of olfactory bulb glutamatergic neurons by Neurog2-expressing precursor cells. Neural Dev 6:12.

Young KM, Fogarty M, Kessaris N, Richardson WD (2007) Subventricular Zone Stem Cells Are Heterogeneous with Respect to Their Embryonic Origins and Neurogenic Fates in the Adult Olfactory Bulb. J Neurosci 27:8286–8296

V. CHAPTER 2:

ORIGIN AND PROPERTIES OF CALRETININ-EXPRESSING PERIGLOMERULAR NEURONS IN THE OLFACTORY BULB

In this chapter, I performed all electroporation experiments, immunostaining and quantifications. BrdU quantifications in the CalR::EGFP model and all electrophysiological experiments were performed by Nuria Benito, Alvaro Sanz Diez and Didier De Saint Jan

Origin and properties of calretinin-expressing periglomerular interneurons

Nuria Benito[1], Elodie Gaborieau[2], Alvaro Sanz Diez[1], Seher Kosar[1], Olivier Raineteau[2] and Didier De Saint Jan[1]

[1]*Institut des Neurosciences Cellulaires et Intégratives, Centre National de la Recherche Scientifique, Unité Propre de Recherche 3212, Université de Strasbourg, 67084 Strasbourg, France*

[2]*Univ Lyon, Université Claude Bernard Lyon 1, Inserm, Stem Cell and Brain Research Institute U1208, 69500 Bron, France*

ABSTRACT

Calretinin-expressing periglomerular (PG) cells are by far the most abundant interneuron subtype in the glomerular layer of the olfactory bulb. They are also the main PG cell subtype generated postnatally. Yet, little is known about their temporal and spatial origin as well as their properties and functions. Here, we show that these cells present a dual spatial origin, i.e. the medial and dorsal SVZ that continue producing them well into adulthood. Cells from both origins have similar electrophysiological properties despite presenting small morphological differences. Remarkably, they show a reduced activity when compared to other PG cells. In olfactory bulb slices, patch clamp recordings reveal that their membrane and synaptic properties resemble those of immature neurons and persist as so over time. *In-vivo*, they are less activated by odorants than other PG cell as measured by an analysis of c-fos expression. Thus, despite of their abundance, calretinin-expressing cells present properties distinct from other PG interneurons subtypes, which question their role in olfactory processing.

V.1. Introduction

GABAergic interneurons constitute the vast majority of all neurons in the olfactory bulb (OB), the first relay for odor processing in the brain. Thus, inhibition likely plays crucial roles in transforming a spatially organized olfactory sensory input into a temporal output code in mitral and tufted cells, the principal neurons. However, as elsewhere in the brain, OB interneurons are diverse and the functional implications of this diversity are still partially understood. Answering this question requires a systematic analysis of each interneuron subtype, linking developmental origin and physiology to molecular identity. Many studies have focused on reciprocal dendro-dendritic synapses made on mitral and tufted cells lateral dendrites by the most abundant interneurons in the OB, the granule cells. Much less is known about the role played by periglomerular (PG) interneurons that exclusively interact with the apical dendrites of mitral and tufted cells.

PG cells form a diverse population of interneurons that surround each glomerulus where mitral and tufted apical dendrites receive synaptic inputs from olfactory sensory neurons (OSNs). They produce a strong intraglomerular inhibition of principal neurons (Najac et al., 2011, 2015, Shao et al., 2012, 2013; Geramita and Urban, 2017). Current models suggest that PG cells mediated intraglomerular inhibition serves as gatekeepers that shunt weak OSN inputs (Gire and Schoppa, 2009) and differently modulates the slow respiration-locked membrane potential oscillations of tufted and mitral cells thereby separating the firing phase of these two output channels along the respiration cycle (Fukunaga et al., 2012; Fukunaga et al., 2014). Perhaps surprisingly, these models incorporate classical feedforward inhibitory circuits and rely on so-called type I PG cells that are synaptically contacted by OSN terminals. However, type I PG cells are a minority (Shao et al., 2009; Najac et al., 2015) and there is still no evidence that they inhibit mitral or tufted cells. Most PG cells are type II PG cells that only receive synaptic inputs from the dendrites of mitral and tufted cells. Calbindin (CalB)-expressing interneurons are the prototypical type II PG cells (Kosaka and Kosaka, 2007). Together, these CalB-like PG cells produce a potent feedback inhibition that competes with the OSN-evoked excitatory input and modulates the spike output of principal neurons (Najac et al., 2015).

Calretinin (CalR)-expressing PG cells are the most abundant PG cell subtype (40-50% of the whole population) (Kosaka and Kosaka, 2007; Panzanelli P. et al., 2007; Parrish-Aungst et al., 2007; Whitman and Greer, 2007) and also the main subtype generated during the postnatal period, including adulthood, from neural stem cells (NSCs) located in the walls of the subventricular zone (SVZ) (Batista-Brito et al., 2008). Similarly to CalB(+) PG cells, dendrites of CalR(+) PG cells, avoid compartments of the glomerulus that are enriched of OSN terminals (Kosaka and Kosaka, 2007) and express typical molecular markers of GABAergic neurons (Panzanelli P. et al., 2007). Based onto these anatomical characteristics, CalR(+) PG cells have therefore been classified as type II PG cells. Consistent with this classification, we recently confirmed that CalR(+) PG cells do not receive synaptic inputs from OSNs. Several observations however suggest unique properties of CalR(+) PG cells. For instance, they have different embryonic origins than CalB(+) PG cells (Kohwi et al., 2007) and present distinctive membrane properties (Fogli Iseppe et al., 2016).

We combined fate mapping approaches and patch-clamp recordings to characterize the origin and functional properties of this so far overlooked interneuron subtype. We found that CalR(+) PG cells show a dual spatial origin, i.e. the medial and dorsal SVZ that continue producing them well into adulthood, although at different pace. Despite of these distinct origins, we show that CalR(+) PG cells are homogeneous in term of electrophysiological properties despite presenting small morphological differences. Interestingly, CalR(+) PG cells show immature traits, i.e. little synaptic input and spiking activity, which persist over extended periods of time. Together, these observations reveal unexpected heterogeneity of type 2 PG cell populations and call for future studies aimed at deciphering their role in shaping olfactory information processing.

V.2. Material and Methods

All experiments were performed in accordance with European requirements 2010/63/UE and have been approved by the Animal Care and Use Committee CELYNE (APAFIS#187 & 188) and CREMEAS.

V.2.1. Animals

The Rosa^{YFP} mice express YFP upon Cre recombination (Jackson Laboratory: B6.129X1-*Gt(ROSA)26Sor*$^{tm1(EYFP)Cos}$/J, lice 006148; Jackson laboratory; (Srinivas et al., 2001). These mice have a *loxP*-flanked STOP sequence followed by the Enhanced Yellow Fluorescent Protein gene (EYFP) inserted into the *Gt(ROSA)26Sor* locus, i.e. an ubiquitously expressed locus. Following Cre recombination, this sequence was removed and permanent expression of YFP occurs. The CalR::EGFP mice express EGFP under the control of the CalR promoter (Caputti et al., 2009). The Kv3.1::EYFP mice express EYFP under the control of the Kv3.1 K^+ channel promoter (Metzger et al., 2002).

V.2.2. Electrophysiology

V.2.2.1. Slice preparation

Transgenic mice of different ages were decapitated and the olfactory bulbs removed and immersed in ice-cold solution containing (in mM) 83 NaCl, 26.2 $NaHCO_3$, 1 NaH_2PO_4, 2.5 KCl, 3.3 $MgSO_4$, 0.5 $CaCl_2$, 70 sucrose, and 22 D-glucose, pH 7.3 (300 mOsm/l), bubbled with 95% O_2/5% CO_2. Horizontal olfactory bulb slices (300 µm) were cut using a Microm HM 650V vibratome (Microm, Germany) in the same solution. The slices were incubated for 30 min at 34˚C and then stored until use at room temperature in artificial cerebrospinal fluid (ACSF) containing (in mM) 125 NaCl, 25 $NaHCO_3$, 2.5 KCl, 1.25 NaH_2PO_4, 1 $MgCl_2$, 2 $CaCl_2$, and 25 D-glucose, continuously oxygenated with 95% O_2/5% CO_2.

V.2.2.2. Electrophysiology

Experiments were conducted at 32-34°C under an upright microscope (SliceScope, Scientifica, Uckfield, UK) with differential interference contrast (DIC) optics. Loose cell-attached recordings (15-100 MΩ seal resistance) were made with pipettes filled with ACSF and used several times on different neurons. OSN axons

bundles projecting inside a given glomerulus were stimulated using a theta pipette filled with ACSF as previously described [Najac, 2015 #49]. The electrical stimulus (100 µs) was delivered using a Digitimer DS3 (Digitimer, Welwyn Garden City, UK). Most of the whole-cell recordings were made with pipettes (3-6 MOhm) filled with (in mM): 135 K-gluconate, 2 MgCl2, 0.025 CaCl2, 1 EGTA, 4 Na-ATP, 0.5 Na-GTP, and 10 HEPES, pH 7.3 (280 Osm/L). Voltages indicated in the paper were corrected for the junction potential (-15 mV). The tip of the recording pipette was systematically coated with wax and we used the capacitance neutralization of the amplifier in order to reduce the capacitance of the pipette. Sodium currents were recorded using a Cs-based internal solution, containing (in mM): 120 Cs-MeSO3, 20 tetraethylammonium-Cl, 5 4-aminopyridine, 2 MgCl2, 0.025 CaCl2, 1 EGTA, 4 Na-ATP, 0.5 Na-GTP, and 10 HEPES, pH 7.3 (280 Osm/L, 10 mV junction potential), and in the presence of CdCl (100 µM), Tetraethylammonium (20 mM) and 4-aminopyridine (5 mM) in the bath. Atto 594 fluorescent dye (5 mM) was routinely added to the internal solution to confirm the glomerular projection of the recorded cell. In current-clamp recordings, a constant hyperpolarizing current was injected in order to maintain the cell at a potential of -60/-70 mV. With a null current injected, the membrane potential remained at positive potentials. In voltage-clamp recordings, the access resistance was compensated from 50 to 80%.

Recordings were acquired with a multiclamp 700B amplifier (Molecular Devices, Sunnyvale, CA), low-passed filtered at 2-4 kHz and digitized at 10 kHz using the AxoGraph X software (Axograph Scientific).

V.2.3. Plasmids

Plasmids pUb-TdTomato plasmid (gift from Prof D. Jabaudon) and pCAG-CRE (#13775, Addgene, Cambridge, MA, USA) were prepared with a PEG-LiCl protocol (Ausubel et al, 1987) and used at a concentration of 5µg/µL. For EPO, plasmids were mixed 1:10 with a contrast solution of fast green (0.2%) in sterile PBS.

V.2.4. Electroporations

Electroporations (EPO) were performed in postnatal 2 days (P2) pups as described previously (Boutin et al., 2008; Fernandez et al., 2011). Briefly, pups were anesthetized in ice and placed on a custom-made support in a stereotaxic rig. Injections were performed at the midpoint of a virtual line traced between the eye and

the lambda. A 34G needle attached to a Hamilton syringe was inserted at a depth of 2.5 mm from the skull surface and 1.5µl of plasmid solution was injected into the lateral ventricle. The accuracy of the injection was verified by the filling of the ventricle with the contrast solution. Successfully injected mice were then subjected to 5 electrical pulses (95 V, 50 ms, separated by 950 ms intervals) using the Super Electroporator NEPA21 type II (Nepa Gene Co., Ltd, Ichikawa-City, Japan) and tweezer electrodes coated with conductive gel (SignaGel, Parker Laboratories, Fairfield, NJ, USA). Electrodes were positioned in order to target the lateral, the dorsal or the medial wall. After EPO, pups were warmed up until they fully recovered and returned to their mother.

V.2.5. BrdU treatments and tissue processing

For analysis of CalR(+) PG cells spatial and temporal origin, BrdU (Sigma-Aldrich, St. Louis, MO) was added in drinking water at a concentration of 1 mg/mL supplemented with sucrose at 10 mg/mL for 15 days (from P12 to P27), protected from light and changed every 2 days. Animals were sacrificed at 45 days post EPO. After deep anesthesia with intraperitoneal pentobarbital, mice were transcardially perfused with a Ringer solution and a 4% paraformaldehyde in 0.1M PB solution, brains were removed, post-fixed for 24h and cut with a vibratome (Leica VT1000S, Wetzlar, Germany). 50 µm coronal sections were collected from the olfactory bulb to the lateral ventricle in series of 6 and kept at -20° C in antifreeze solution (glucose 15%, sodium azide 0,02%, ethylene glycol 30%, PB 0,1M).

For birth dating of CalR(+) PG cells, CalR::EGFP transgenic mice (P30) received four intraperitoneal injections of 20 mg/mL BrdU (Sigma-Aldrich B5002) in sterile 0.9% NaCl solution (100 mg/kg), 2 hours apart. At days 15, 20, 30, 40, 50 and 60 after injection, mice were anesthetized by intraperitoneal injection of ketamine and xylazine mixture (90 and 100 mg/kg, respectively), and transcardially perfused with 4% paraformaldehyde diluted in PBS. The olfactory bulbs were removed and postfixed overnight at 4 ˚C. Horizontal sections (30 µm) were sliced on a vibratome (Leica VT1000S).

V.2.6. Immunostaining

For BrdU staining, free-floating sections were incubated for 1 hr in TritonX100 (0.2-0.4% in PBS), pretreated in 1N (10 min, 37˚C) and 2N (20 min, 37˚C) HCl, and

washed in 0.1 M borate buffer pH 8.4 (5-30 min). After rinsing three times with PBS (10 min), sections were incubated in blocking solution containing BSA (2%) and TritonX100 (0.3-0.4%), for 1 hour before incubation with the primary antibodies (see table 1).

For c-fos staining, antigen retrieval treatment was performed in 10 mM Citrate Buffer pH 6 (20 min, 80°C). After rinsing three times with TritonX100 (0.4% in PBS), sections were incubated in blocking solution for 2-4 hours at room temperature (BSA 0.25%, Casein, 0.05%, Top block 0.25% + TritonX100 0.4% in PBS) before incubation with the primary antibodies overnight at 4°C (table 1).

Following incubation with primary antibodies, sections were incubated 2h at room temperature with the corresponding secondary antibody (table 1). To amplify Tomato signal for Arborization reconstruction, sections were incubates with anti-RFP antibody. To amplify YFP signal, sections were incubated with anti-GFP primary antibody before any antigen retrieval treatment and were incubated with a biotinylated secondary antibody followed by streptavidin-DTAF for 45min. Finally, sections were counterstained with DAPI and mounted with Prolong Antifade (Thermosfisher, Waltham, MA, USA) or Fluoromount-G (SouthernBiotech) mounting medium.

Table 1:

1ary antibodies	**Specie**	**Concentration**	**Source (cat. number)**
Anti-BrdU	Rat	1:500	ABD Serotech (ABD0030)
Anti-BrdU	Rat	1:500	Abcam (Ab6326)
Anti-Calretinin	Rabbit	1:2000	SWANT (7697)
Anti-Calretinin	Mouse	1:2000	SWANT (6B3)
Anti-Calbindin	Mouse	1:2000	SWANT (D28K)
Anti-c-fos	Goat	1:50	Santa Cruz (Sc-52-G)
Anti-TH	Mouse	1:400	Millipore (MAB318)
Anti-GFP	Chicken	1:1000	JAVES (GFP(-)1020)
Anti-Doublecortin	Goat	1:500	Santa Cruz (Sc-8066)
Anti-RFP	Rabbit	1:1500	MBL (PM005)
Secondary Antibodies	**Specie**	**Concentration**	**Source (catalog number)**
Anti-rat AlexaFluor 555	Donkey	1:1000	TermoFisher (A-21434)
Anti-rat AlexaFluor 546	Goat	1:200	TermoFisher (A-11081)
Anti-mouse AlexaFluor 555	Donkey	1:1000	TermoFisher (A-31570)
Anti-mouse AlexaFluor 647	Donkey	1:1000	TermoFisher (A-31571)
Anti-rabbit AlexaFluor 555	Donkey	1:1000	TermoFisher (A-31572)
Anti-rabbit AlexaFluor 647	Donkey	1:1000	TermoFisher (A-31573)
Anti-rabbit AlexaFluor 633	Goat	1:200	TermoFisher (A-21070)
Anti-goat AlexaFluor 555	Donkey	1:1000	TermoFisher (A-21432)

Anti-chicken biotinylated	Donkey	1:1000	Jackson Lab (703-065-155)
Streptavidin-DTAF	-	1:250	Jackson Lab (016-010-084)

V.2.7. Quantifications

For the analysis of CalR(+) PG interneurons neurogenesis (Fig.1B) and spatial and temporal origin (Fig.1C-D), YFP(+) cells were counted in the glomerular layer on live image using an epifluorescent microscope (Leica DM5500, objective HCX PL APO 40x 1,25 oil).

For CalR::EGFP interneurons origin (Fig.2A), 3 animals were analyzed for dorsal and medial EPO, and the number of CalR(+) and EGFP(+) PG cells among the Td-Tomato-expressing population analyzed (>85 Td-tomato(+) cells per EPO).

For CalR(+)/EGFP(+) PG interneurons birth dating analysis (Fig.2F), series of 3 slices (3 pictures per slice) were analyzed with a confocal microscope (Leica SP5), and the number of BrdU-positive nuclei and EGFP-positive cells located in the glomerular layer counted (>120 BrdU-positive cells per animal).

For c-fos analysis (Fig.6E), images were taken with a confocal microscope (Leica SP5) using a 40x objective (HCX PL APO 40x 1.25 oil). c-fos-positive nuclei expressing CR, CB and TH in the glomerular layer were quantified (>120 c-fos-positive cell per animal; 3 animals per condition). Analysis was focused on cells bordering glomeruli where an intense c-fos staining was observed.

For arborization analysis of CalR(+) PG interneurons, 0.3 µm stack images were taken with a confocal microscope and 3D neurons reconstruction were performed and analyzed with the software Neurolucida 360 (43 EGFP(+) cells vs 12 EGFP(-), equally distributed between septal and dorsal EPO, i.e. 26 and 29 CalR(+) neurons, respectively; 3 mice per EPO).

Electrophysiological data were analyzed using Axograph X (Axograph Scientific). Current amplitudes were measured as the peak of an average response computed from multiple sweeps. Spike amplitudes were measured between the peak and the most negative voltage reached immediately after the spike. Individual spontaneous EPSCs or IPSCs with amplitude >5 pA were automatically detected by the Axograph X software using a sliding template function. For measuring the AMPA/NMDA ratio, neurons were first voltage-clamped at –75 mV and M/T cell to PG

cells excitatory inputs were evoked with an electrical stimulation in the EPL. Stimulation intensity was adjusted to obtain isolated responses. Neurons were then voltage-clamped at +50/60mV to release the Mg++ blockade of NMDA receptors. After a stabilization period of 5 to 15 min, the NMDA receptor antagonist D-2-amino-5-phosphonopentanoic acid (D-AP5, 50 µM, Abcam biochemicals, Cambridge, UK) was bath applied to isolate AMPA currents. Isolated AMPA currents were digitally subtracted offline from the total EPSCs to obtain the NMDA currents.

Results are expressed as mean ± SEM. Statistical significance was determined by unpaired Student's *t* test at the $p < 0.05$ level or a Mann-Whitney test when data did not assume a normal distribution.

V.3. Results

V.3.1. Spatio-temporal origin of CalR(+) periglomerular cells

The postnatal SVZ produces distinct subtypes of PG interneurons in a region dependent manner. We have shown that CalR(+) PG cells originate from the dorsal and medial most region of the SVZ at birth (Fernández et al., 2011). The temporal dynamic of their postnatal production, however, remains elusive. To address this question, we combined targeted electroporation of specific SVZ microdomains to a Cre-lox approach for permanent fate mapping of NSCs located in the lateral, dorsal and medial aspects of the postnatal SVZ (**Figure 1A**). We then analyzed their CalR(+) PG cell progeny on extended periods of time (up to 3 months). We first focused our analysis on recombined YFP(+) PG cells expressing the immature neuronal marker Dcx to determine the spatial origin of the most recently generated CalR(+) PG cells at P45 and P90 (**Figure 1B and C**). As previously described, quantifications revealed a bias for YFP(+) cells from the medial and to a lesser extend dorsal SVZ to specify in CalR(+) PG interneurons (87.33 ± 10.27% and 51 ± 7.78%, respectively at P45; n=2; >30 Dcx+ cells; **Figure 1D**), while this was rare for those originating from the lateral SVZ (not quantified). Those percentages remained stable at P90 (88.33 ± 2.91% and 44.67 ± 17.65% respectively; n=3 for dorsal and medial EPO, >30 Dcx+ cells), indicating that both microdomains remain active and keep producing CalR(+) PG interneurons. These observations further imply that no change in regional CalR(+) PG interneuron origin is observed over time.

We next assessed the temporal dynamic in neurogenic activity observed between these distinct SVZ microdomains. Thus, we administrated BrdU through drinking water during the second half of the first month of postnatal life, and sacrificed the animals at 1.5 months. BrdU and Dcx immunodetection allowed us to discriminate early (BrdU-/Dcx-), intermediate (BrdU+/Dcx-) and late born interneurons (BrdU-/Dcx+), among recombined YFP(+) cells in the GL (**Figures 1C**). Quantifications revealed a gradual decrease of neurogenesis for all three microdomains, which appeared more pronounced for the medial SVZ (32 YFP(+) cells; n=6 for lateral EPO; 164 YFP(+) cells; n=6 for dorsal EPO and 240 YFP(+) cells; n=3 for medial EPO, **Figure 1E, F**). Thus, while CalR(+) PG interneurons

present a dual medial and dorsal origin, the contribution of the medial SVZ declines faster than the contribution of the dorsal SVZ in their generation.

These observations prompted us to investigate possible morphological differences between CalR(+) PG interneurons produced by the medial and dorsal SVZ. Individual CalR(+) PG interneurons originating from both SVZ microdomains were reconstructed 21 days post-electroporation. All cells presented a polarized dendritic tree extending towards a single glomerulus (**Figure 1G**). Quantitative analysis of the total length, surface and number of primary dendrites however suggested a reduced maturation for CalR(+) PG cells originating from the dorsal SVZ (**Figure 1H**), which was confirmed by a Sholl analysis (**Figure 1I**). Thus, despite a dual origin, CalR(+) PG cells present an overall similar morphology with a tendency for a greater complexity for those generated from the medial wall.

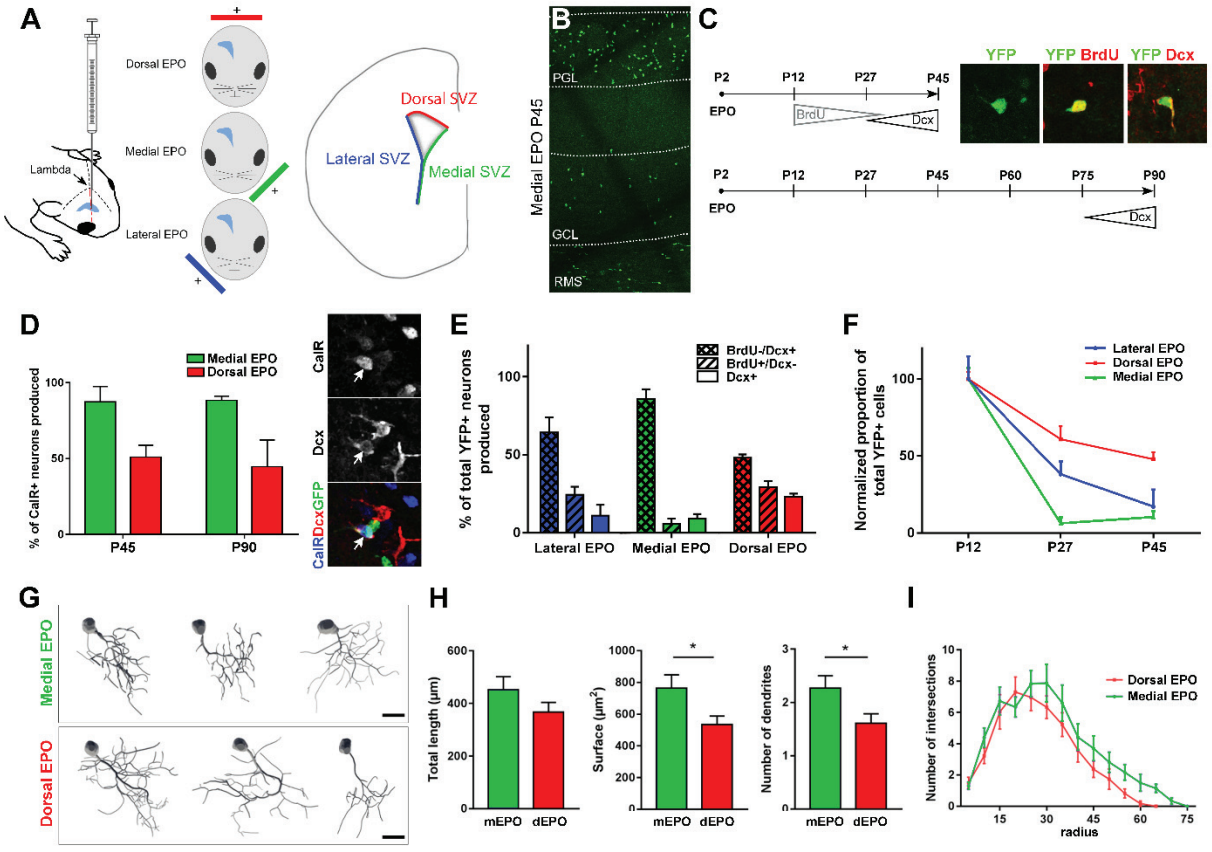

Figure 1: Postnatally generated CalR(+) PG interneurons present a dual spatial origin

(A-B) We modified a previously established targeted electroporation approach for permanent labeling and fate mapping of NSCs that reside in defined microdomains of the postnatal SVZ. A plasmid expressing the Cre recombinase was electroporated in lateral, dorsal and medial SVZ of RosaYFP Cre-reporter mice allowing the recombination and permanent expression of YFP in NSCs and their progeny. B) Overview illustrating the accumulation of YFP(+) cells in the OB at P45 following a medial EPO. (C) Long term fate mapping was combined with immunodetection of BrdU administered in drinking water (from P1 to P27) and of Dcx to discriminate between cohorts of neurons sequentially produced at distinct postnatal times. Animals were sacrificed at P45 or P90 for analysis. (D) Immunodetection of YFP(+)/CalR(+)/Dcx+ PG interneurons at P45 and P90 reveals their stable spatial origin over time. (E-F) Quantification of YFP(+) PG cells born at early (BrdU-/Dcx-), intermediate (BrdU+/Dcx-) and late time (BrdU-/Dcx+) during the first 45 days of postnatal life reveals the temporal dynamic of neurogenesis from the three SVZ microdomains. (G) Neurolucida reconstruction of YFP(+)/CalR(+) PG interneurons originating from the dorsal and medial SVZ at 21 dpe. (H) Quantification of dendritic arborization length, surface and number of primary dendrites in CalR(+) PG interneurons originating from the dorsal and medial SVZ. Scale bar: 10µm. (I) Sholl analysis representing the number and distribution of dendrite intersections with concentric circles of gradually increasing radius. Note the more compact morphology of CalR(+) PG interneurons originating from the dorsal SVZ. * $p<0.05$, unpaired t-test.

Abbreviations: dpe: days post electroporation; EPO: electroporation; Cre: Cre recombinase; SVZ: subventricular zone; CalR: Calretinin, PG: periglomerular; GL: glomerular layer; GCL: granule cell layer; RMS: rostral migratory stream.

V.3.2. CalR::EGFP transgenic mice recapitulate the complex spatio-temporal origin of CalR(+) PG cells

The CalR::EGFP transgenic mouse expressing EGFP under the control of the CalR promoter (Caputi et al., 2009) selectively labels CalR(+) PG cells and is therefore a useful tool to identify them in acute OB slices. However, EGFP labels ~80% of the CalR-expressing PG cells at 10 days and only ~50% in adult mice (Najac et al. 2015; **Figure 2A**) suggesting that this animal model may not recapitulate the complex spatio-temporal origin of CalR(+) PG interneurons but instead labels a subpopulation of PG cells with a specific origin. To address this concern, we first transiently electroporated NSCs in the medial or in the dorsal wall of the SVZ of CalR::EGFP newborn pups with a plasmid encoding tdTomato (see chapter 1 for further detail). Three weeks later, we quantified the fraction of tdTom+ PG cells that also expressed EGFP. We found that both the medial SVZ and dorsal SVZ produce EGFP(+)/CalR(+) PG cells (67 ± 10.3% and 29 ± 4.1% of the tdTom+/CalR(+) PG cells, respectively, n=3 mice; 69 and 43 CalR(+) cells respectively; **Figure 2B and C**). These observations underline that EGFP non-specifically labels CalR(+) PG neurons of both medial and dorsal origin in the CalR::EGFP transgenic mouse.

Second, we conducted a birthdating experiment to determine if the EGFP labeling also recapitulates the age diversity of CalR(+) PG cells or only transiently labels CalR(+) PG cells at a specific period of maturation. Thus, BrdU was administered to 30 days-old CalR::EGFP mice (n=20) that were sacrificed at different intervals (15-60 days) after the injection. We then analyzed the percentage of BrdU+/EGFP(+) PG cells among the BrdU+/CalR(+) PG cells. This fraction (around 50%) remained stable up to 60 days post-injection (**Figure 2D**). Thus, EGFP is stably expressed in a fraction of CalR(+) PG cells that can be from 15 days to, at least, 60 days old. Finally, we directly compared the morphology of EGFP(+) and EGFP(-) tdTom+/CalR(+) PG interneurons. Quantifications showed similar morphologies of the two cells populations (43 EGFP(+) cells and 12 EGFP(-) cells; n=3 mice) (**Figure 2E-F**). Consistent with this analysis, EGFP(+) PG cells filed with biocytin during patch-clamp recordings (n=10) apparently had no axon and small beaded dendrites projecting towards a single glomerulus. Together, these data indicate that EGFP stably labels a population of CalR(+) PG cells that includes neurons from different spatial origin and at different stages of maturation.

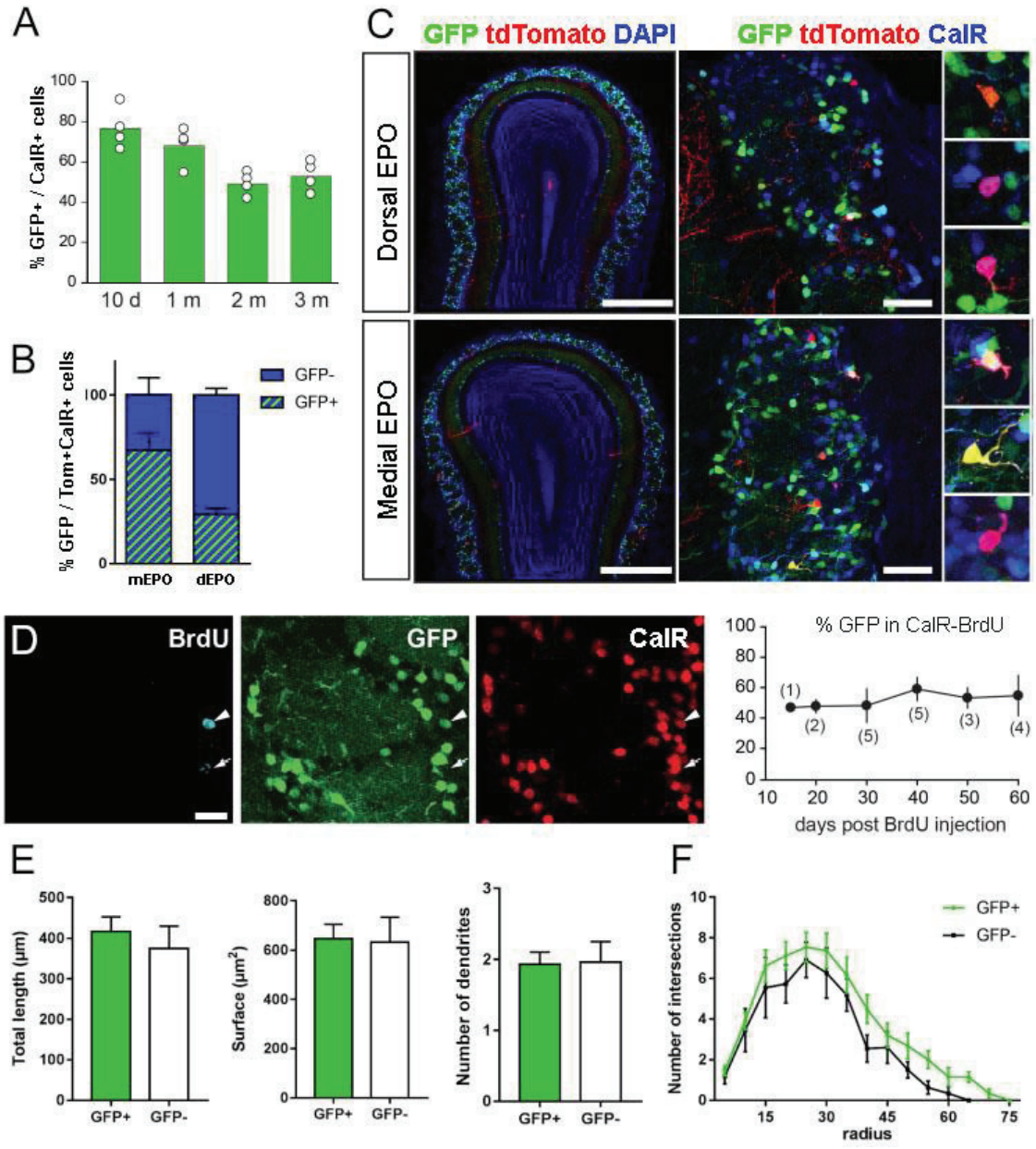

Figure 2. Labeling of a representative population of CalR(+) PG interneurons in the CalR::EGFP transgenic mice.

(A) Percentage of EGFP expression among the CalR(+) PG population at different postnatal ages. (B-C) Fate mapping of CalR(+) PG interneurons from dorsal and medial origin by electroporation of a tdTomato expressing plasmid in CalR::EGFP transgenic mice. Note that EGFP expression can be observed in both populations of CalR(+) PG interneurons. Scale bars: 500µm (left panel); 50µm (right panel) (D) Birth dating of CalR(+) PG interneuron demonstrates stable EGFP expression in CalR(+) PG interneurons up to 60 days. Scale bar: 10µm (E) Neurolucida reconstruction of EGFP(+) (n=43) and EGFP(-) tdTom+/CalR(+) PG interneurons reveals comparable dendritic arborization length, surface and number of primary dendrites. (F) Sholl analysis representing the number and distribution of dendrite intersections with concentric circles of gradually increasing radius.

V.3.3. CalR(+) interneurons are less active than other PG cells

Having established that EGFP expression faithfully reflects the spatio-temporal diversity of CalR(+) PG cells, we examined the functional properties of EGFP(+)/CalR(+) PG cells using patch-clamp recording in acute olfactory bulb horizontal slices from CalR::EGFP mice. In a first set of experiments, we used paired loose cell-attached recording to compare the spontaneous and OSN-evoked firing activity of EGFP(+)/CalR(+) PG cells with those of other subtypes of PG cells. OSN stimulations that reliably elicited the discharge of a randomly chosen EGFP(-) PG cells were first determined. Then, we simultaneously recorded from an EGFP(+) cell projecting into the same glomerulus (**Figure 3**, n=13 pairs). As illustrated in Figure 3, spontaneous and evoked action potential capacitive currents were large (133 ± 136 pA, range 36-532) and biphasic in EGFP(-) PG cells. The number of spikes elicited within the 200 ms following the stimulation of OSN (from 2 to >16 spikes, average 6.3 ± 4.6) as well as the duration of the burst varied across cells, consistent with the diversity of OSN-evoked activation profiles in PG cells (Najac et al., 2015). In sharp contrast, very little spontaneous or evoked activity was detected in the simultaneously recorded EGFP(+) PG cells. OSN stimulations produced no response at all (n=4) or small monophasic capacitive currents (15.7 ± 5.8 pA, n=9) in EGFP(+) PG cells. Increasing the intensity of stimulation did not evoke larger responses suggesting that the weak response of CalR(+) PG cells does not reflect a higher firing threshold. We cannot exclude, because the seal resistance used in these experiments was usually low (<25 MOhm), that some of the events detected in the EGFP(+) PG cells were extracellularly detected spikes fired by neighboring neurons. Regardless of this potential caveat, these data suggest that CalR(+) PG cells are remarkably silent compared with other PG cell subtypes.

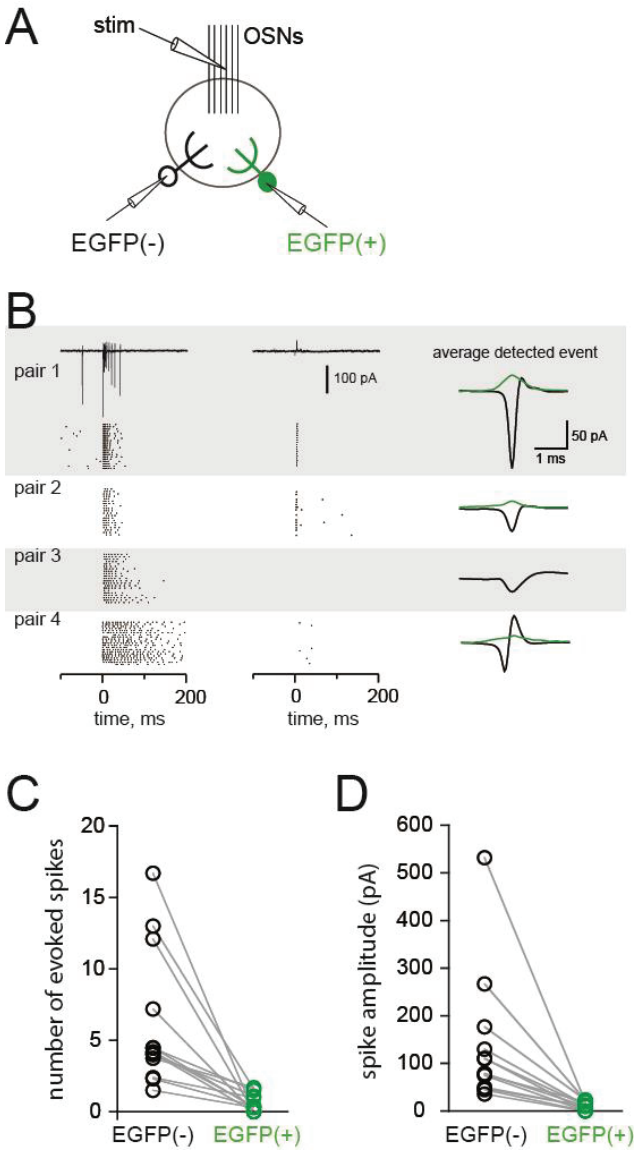

Figure 3: Comparison of OSN-evoked discharges in CalR-expressing PG cells and in other PG cells.

(A) Schematic of the experiment. Two PG cells projecting into the same glomerulus, one EGFP(+) and one EGFP(-), were recorded in the loose-cell attached configuration. Their firing was elicited by an electrical stimulation of the OSNs. (B) Raster plots from 4 out of 13 pairs are shown with 20 consecutive sweeps for each pair. A typical response is shown for pair 1. OSNs were stimulated at t=0, at an intensity of 30-200 µA. The average evoked capacitive action current is shown on the right for each pair (green trace: EGFP(+) cell; black trace: EGFP(-) cell). (C-D) summary plots of the results (n=13 pairs). (C) Average number of spikes evoked within the 200 ms following the stimulation. (D) Amplitude of the average capacitive current evoked by the stimulation. Dots from the same pair are connected.
Abbreviations: stim: stimulation; OSNs; olfactory sensory neurons

V.3.4. Intrinsic membrane properties of CalR(+) interneurons

Next, we examined the intrinsic membrane properties of EGFP(+) PG cells using whole cell recordings. EGFP(+) PG cells had a high membrane resistance of 2.5 ± 1 GOhm (n=25), a value that is most likely underestimated because of the current leak through the pipette seal, but nevertheless suggests the expression of few ionic channels. In the current-clamp mode, depolarizing current injections from a holding potential maintained around -70 mV induced at most a single action potential (**Figure 4A**). However, only half of the cells (n=18/40) were able to fire an overshooting spike (with an amplitude > ~40 mV) (**Figure 4B**). The other half did not fire at all or fired a single rudimentary action potential (amplitude < 40 mV, n=22), much like immature newborn neurons. Three typical examples of this diversity are illustrated in **Figure 4A**. PG cells firing a full size action potential had more complex voltage responses, consistent with a maturation of the membrane properties. Thus, their single action potential was sometime riding on the top of a long-lasting depolarization possibly mediated by a calcium spike, and hyperpolarizing steps evoked a sag in membrane potential suggesting the activation of an Ih current. In rare cases (n=5 over hundreds of cells tested), we recorded cells that spontaneously and regularly fired a single action potential at about 0.5-1 Hz (fig. sup). This cell to cell variability, that can be illustrated using the size of the spike as an indicator of cell maturation, was often seen within the same slice from animals at different developmental ages (P15-P38). Thus, consistent with their ongoing production, EGFP(+)/CalR(+) PG cells constitute a population of neurons with variable membrane properties that likely reflect different stages of maturation.

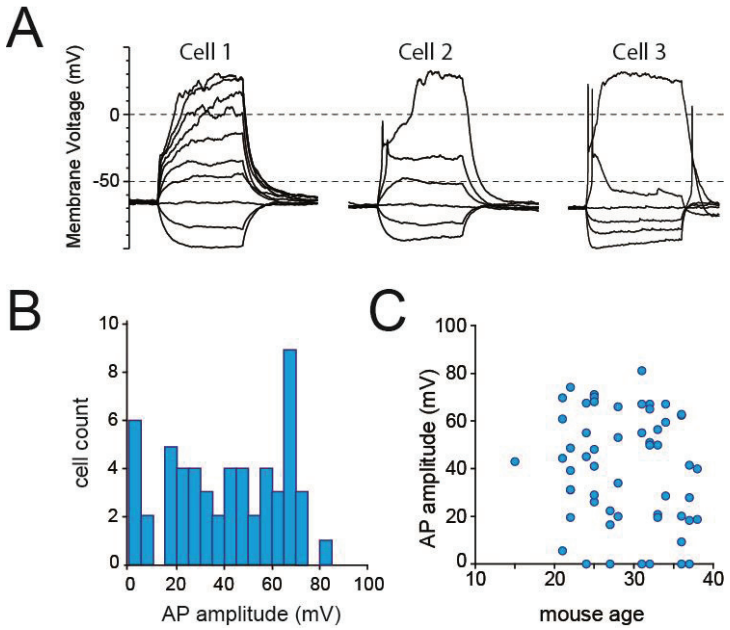

Figure 4: Diversity of intrinsic membrane properties across CalR(+)/EGFP(+) PG cells.

(A) Some cells did not fire at all (as cell 1) or fired a single rudimentary action potential (cell 2). Cells firing an overshooting action potential (as cell 3) had more complex membrane properties but also fired at most a single spike. (B) Distribution histogram of action potential amplitude in CalR(+)/EGFP(+) PG cells. (C) The ability to fire a full spike did not depend on the age of the mouse.
Abbreviation: PA: action potential

Voltage-clamp recordings were then done to examine the voltage-activated conductances underlying the membrane potential responses. Consistent with a recently published study (Fogli Iseppe et al., 2016), classical voltage-clamp protocols activated only few conductances. While inward Ih currents were induced in some cells by a 40 mV hyperpolarizing pre-pulse (from a holding potential Vh = -75 mV), depolarizing steps only evoked fast inward Na^+ currents followed by rapidly inactivating outward K^+ currents (**Figure 5A**). The K^+ currents were large and fast in every cells tested (average amplitude of 1 ± 0.4 nA at Vh = -10 mV, deactivation time constant: 12.4 ± 0.4 ms, n=19) and strongly reduced by a 20 mV depolarizing prepulse (88 ± 6 % decrease, n=9, not shown), consistent with A-type K^+ currents. Sodium currents were, in contrast, often small or even totally absent in some cells. Accordingly, in the presence of TEA, 4-AP and Cs that abolished the K^+ currents, Na^+ currents had variable maximal amplitudes but only a fraction of the cells expressed Na^+ currents comparable in size to those seen in other PG cell subtypes (**Figure 5B**

and 5C). No other inward currents were seen under these conditions suggesting that Ca^{2+} currents may be too small to be detected (Fogli Iseppe et al., 2016). The remarkable absence of any delayed K^+ currents is unusual in neurons and impedes CalR(+) PG cells to repolarize in response to long-lasting depolarizing inputs. This explains why, in our current-clamp recordings, supra-threshold current steps induced slowly developing long-lasting depolarization (**Figure 4A**). Although the physiological significance of this passive depolarization is unclear, it was seen in every cell tested and was therefore a robust functional marker of CalR(+) PG cells. Together, our data indicate that EGFP(+)/CalR(+) PG cells, regardless of their degree of maturation, express a surprisingly poor repertoire of voltage-activated conductances.

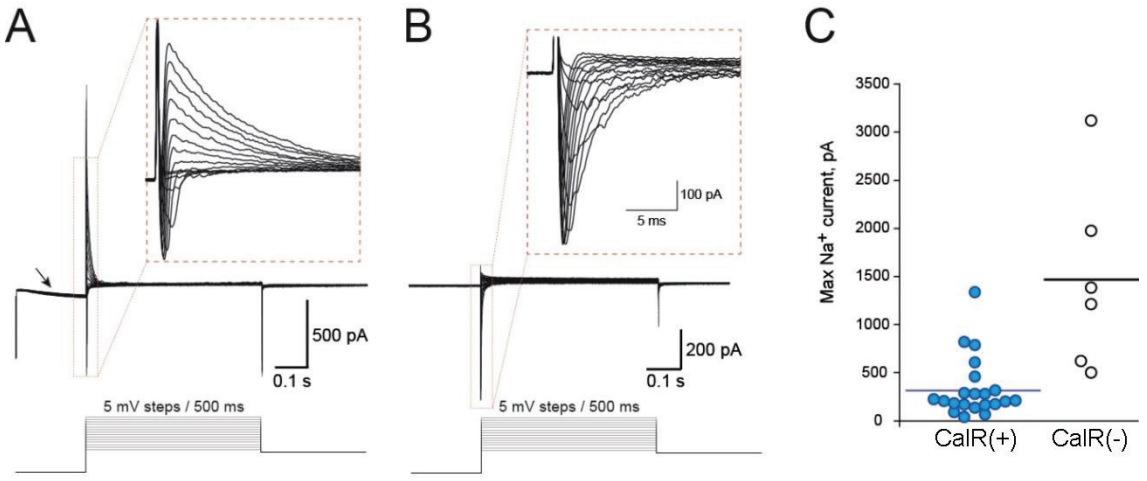

Figure 5: Voltage-activated conductances in CalR(+)/EGFP(+) PG cells

(A) Currents induced by consecutive voltage steps following a hyperpolarizing prepulse (-40 mV from Vh=-75 mV). Three voltage-activated conductances were detected, an Ih current (arrow), fast inward Na^+ currents and fast outward K^+ currents (shown at a higher magnification in the inset). (B) Same protocol in the presence of K+ channel blockers (Cs, TEA and 4-AP) in the intra- and extracellular solutions. Only Na+ currents remained. (C) Maximal Na^+ current amplitudes recorded in CalR(+)/EGFP(+) PG cells compared with those recorded in CalR(-) PG cells. Recording were done as in B.

V.3.5. CalR(+) interneurons are poorly connected to the glomerular network

The membrane properties of EGFP(+)/CalR(+) PG cells explain, at least partially, their low firing activity. In addition, we have already shown that EGFP(+) PG cells are weakly connected to mitral and tufted cells compared to other PG cells. Thus, EGFP(+) cells receive less spontaneous excitatory inputs than other type 2 PG cells and respond to a stimulation of the olfactory nerve with a smaller composite EPSC (Najac et al., 2015). This is here illustrated with a paired recording of two PG cells (one EGFP(+) and one EGFP(-)) projecting into the same glomerulus (**Figure 6A**). To complement our previous analysis, we recorded cells from animals at different ages (n=52) and also examined their inhibitory inputs (n=42). The majority of the cells tested received a low frequency of spontaneous EPSCs (90% received less than 5 sEPSC/s and 75% less than 2 sEPSC/sec) (**Figure 6B**). This is a much lower sEPSC frequency than in other type 2 PG cells embedded in the same network. For instance, PG cells labeled in the Kv3.1-EYFP reporter mouse, which likely represent CalB(+) PG cells, receive on average 17 sEPSCs/s (Najac et al., 2015). Similarly, most EGFP(+) cells tested received few spontaneous IPSCs (90% less than 5 sIPSC/s and nearly 70% less than 2 sIPSC/sec). There was no obvious relationship between the frequencies of sEPSCs and sIPSCs in cells in which these two synaptic inputs were recorded (not shown), consistent with our results demonstrating that IPSCs do not originate from the glomerular network. There was also no obvious relationship between the age of the animal and the frequencies of the spontaneous synaptic inputs recorded in EGFP(+) PG cells. Remarkably, cells receiving no synaptic inputs were observed at any ages.

Consistent with the low frequency of spontaneous EPSCs which suggests a small number of connections with mitral and tufted cells, OSN stimulation evoked a barrage of few fast EPSCs in voltage-clamp (average current 12 ± 3 pA at Vh = -75 mV, n=5). Yet, these small inputs produced a significant (6 ± 1 mV, n=5) depolarization in the current-clamp mode (**Figure 6C**). Interestingly, the slow time course of the OSN-evoked EPSP was similar as the time course of the OSN-evoked EPSC recorded in voltage-clamp at positive holding potential suggesting a strong contribution of NMDA receptors. This could not be tested directly with a bath application of an NMDA receptor antagonist that would also shorten mitral and tufted cell responses and

therefore reduce the release of glutamate onto PG cells. Thus, we quantified the AMPA/NMDA ratio of individual EPSC to determine the contribution of NMDA receptors at mitral/tufted to EGFP(+)/CalR(+) PG cells synapses (**Figure 6D**). EPSCs recorded at a positive potential (Vh = +50/60 mV) were evoked with a stimulation in the EPL first in control conditions and then in the presence of the NMDA receptor antagonist D-AP5 (50 µM) to isolate the AMPA component. Averaged EPSCs were collected from CalR(+) PG cells that were all capable of firing an overshooting spike (n=5, spike amplitude range 55-67 mV). Under these conditions, the AMPA/NMDA ratio of these cells was close to 1. This value, which reflects a relatively high density of NMDA receptors, was several folds lower than in PG cells labeled in the Kv3.1-EYFP reporter mouse (**Figure 6D**). This confirms the predominance of NMDA receptors at excitatory synapses on CalR(+) PG cells and suggests that these synapses are still immature.

Finally, we investigated the *in-vivo* correlates of this low connectivity by assessing c-fos expression in PG interneuron subtypes (n=1104 c-fos+ cells in 3 mice) (**Figure 6E**). Interestingly, the majority of CalB(+) PG interneurons were positive for c-fos (72.3 ± 2%), in line with their pronounced activity in vitro (**Figure 6F**). In comparison, a smaller percentage of TH(+) PG interneurons were positive for this immediate early gene (28.1 ± 7%), while only rare CalR(+)/c-fos+ cells were observed (11.5 ± 1%), thereby correlating with the in vitro evidences for a poor connectivity of this subtype of interneurons.

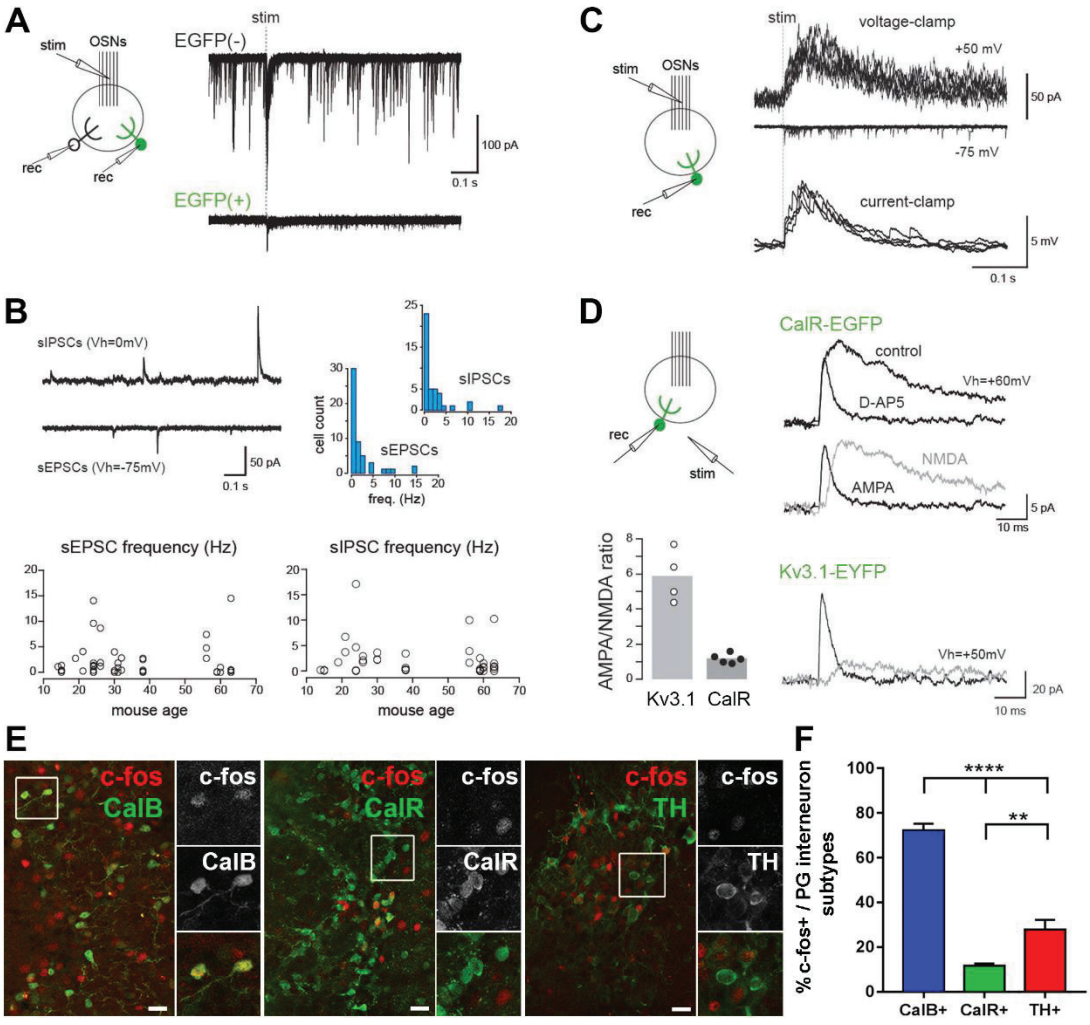

Figure 6: Synaptic inputs of CalR(+)/EGFP(+) PG cells

(A) Paired recording between an EGFP(+)/CalR(+) PG cell and a non-labeled PG cell projecting into the same glomerulus. 15 traces are superimposed for each cell. The dashed line indicates OSN stimulation. (B) Spontaneous IPSCs (recorded at Vh=0 mV, top trace) and EPSCs (recorded at Vh=-75 mV, lower trace) in a representative EGFP(+)/CalR(+) PG cell. Right, distribution histograms (bin of 1 Hz) of synaptic input frequencies showing the predominance of cells receiving few inputs. Bottom, summary graphs of excitatory and inhibitory input frequencies in cells from mice at different developmental ages. Each dot represents a cell. (C) Responses of an EGFP(+)/CalR(+) PG cell evoked by the stimulation of the OSNs. In voltage-clamp, the cell responded with a barrage of small and fast EPSCs at negative potential (middle traces) that converted into a large and slow EPSC at a positive holding potential (top). 7 traces superimposed in each case. The corresponding slow depolarization recorded in current-clamp (bottom trace) resulted from the temporal summation of slow EPSPs. Stimulation 150 µA. (D) Comparison of AMPA/NMDA ratios at excitatory synapses in CalR(+)-EGFP(+) PG cells (top traces) and in Kv3.1-EYFP(+) PG cells (bottom traces). EPSCs elicited by an electrical stimulation close to the cell in the EPL were recorded at a positive holding potential in control conditions and in the presence of D-AP5 (50 µM) to isolate the AMPA EPSC. The NMDA EPSC (grey trace) was obtained by

subtracting the D-AP5 trace from the control trace. Summary bars show the average AMPA/NMDA ratio in CalR(+)-EGFP(+) PG cells and in Kv3.1-EYFP(+) PG cells. Each dot represents a cell. (E-F) Immunostaining of c-fos reactive PG cells in TH(+), CalR(+) and CalB interneurons at 21 dpe. The proportion of each subtypes of PG interneurons expressing c-fos have been quantified. Animals were not stimulated with any specific odor.
Abbreviations: CalB: calbindin; CalR: calretinin; OSNs: olfactory sensory neurons; PG: periglomerular; rec: record; stim: stimulation; TH: tyrosine hydroxylase

V.3.6. Synaptic integration of CalR(+) PG cells do not progress over time

The diversity of membrane properties observed in our random sampling of EGFP(+) PG cells (**Figures 4 and 5**) is consistent with a developmental maturation of the intrinsic membrane properties. How synaptic integration progresses with time is less clear. To clarify this question, we examined the properties of age-matched EGFP(+) PG cells co-labeled, using targeted electroporation of the medial SVZ, with tdTomato (**Figures 7A-B**). TdTom(+)/EGFP(+) PG cells were recorded at different intervals after electroporation (n=50, 15-65 dpe). As expected, these cells had overall similar properties as those described above, i.e. they fired at most a single spike and received little spontaneous synaptic inputs. However, most of the cells tested (n=22/25) fired an overshooting action potential. This confirms that the size of the spike is a good indicator of maturation and that cells that did not fire or fired a rudimentary action potential in our random sampling of EGFP(+) PG cells were likely the most recently generated neurons. In contrast, the frequency of their spontaneous synaptic inputs was not correlated with the age of the cell (**Figure 7C**). Similar to randomly chosen EGFP(+) PG cells, tdTom(+)/EGFP(+) PG cells received between 0 and 10 EPSCs per second (mean 2.3 ± 2.7, n=47) and for the majority of them less than 3 IPSCs/s (mean 1.0 ± 1.7, n=41) whether they were young (15-23 dpe) or older (54-63 dpe). Thus, the mean frequency of sEPSC was not different in young cells (2.2 ± 0.5 EPSCs/sec, n=25) and in old cells (2.4 ± 0.8 EPSCs/sec, n=12, P=0.88). The mean sIPSC frequency was also not different in young cells (0.7 ± 0.2 IPSC/sec, n=21) and in old cells (1.2 ± 0.3 IPSCs/sec, n=11, P=0.17). Of note, cells without any detectable synaptic inputs were recorded at all ages indicating that synaptic integration does not change over time.

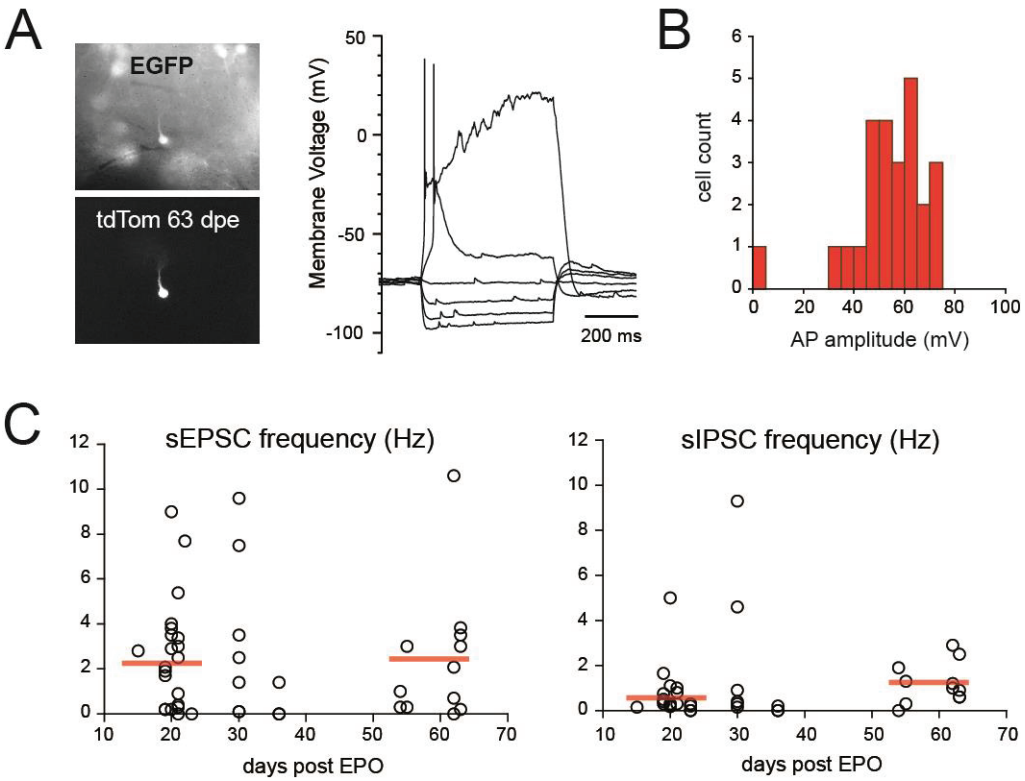

Figure 7: Synaptic integration of CalR(+)/EGFP(+) PG cells does not change over time

(A) Current-voltage relationship of an EGFP(+) PG cell (top) co-labeled with tdTomato (tdTom, bottom), 63 days after electroporation of a tdTomato expressing plasmid in a CalR::EGFP transgenic mouse. (B) Distribution of action potential amplitudes in all the EGFP(+)/tdTom+ cells recorded 15-65 days post-electroporation. (C) Excitatory (left) and inhibitory (right) input frequencies in EGFP(+)/tdTom+ PG cells recorded at different intervals after electroporation. Each dot represents a cell. Horizontal bars show average frequencies for cells recorded at 15-23 days or 54-63 days post electroporation.

Abbreviations: AP: action potential; dpe: days post electroporation; EPO: electroporation

V.4. Discussion

Here, we present evidences that the population of CalR(+) PG interneurons have a complex spatial origin that spreads well into adulthood. CalR(+) PG interneurons however present homogeneous morphologies, and share peculiar and persistent functional properties resembling those of immature neurons. Thus, despite of their abundance, CalR-expressing cells present properties distinct from other PG interneuron subtypes, which question their role in olfactory processing.

V.4.1. The high diversity of PG interneurons subtypes suggests that they play distinct roles in olfactory processing

Neurogenesis persists throughout life in the OB. Shortly after migrating to the glomerular layer newborn PG interneurons are immature, disconnected from the preexisting network and incapable of firing action potentials. They then progressively receive synaptic contacts while their morphology and membrane properties become more complex. Their output become functional toward the end of this activity-dependent maturation process that takes about 4 weeks in the adult OB (Belluzzi et al., 2003; Carleton et al., 2003; Whitman and Greer, 2007; Bardy et al., 2010; Lepousez et al., 2013; Livneh et al., 2014).

PG interneurons represent a highly heterogeneous populations of cells based on the expression of different markers but also on their connectivity pattern. CalR(+) PG interneurons have been described as type II PG interneurons (Kosaka and Kosaka, 2007). In contrast to type I PG interneurons, directly activated by OSNs inputs, type II PG interneurons do not receive direct synaptic inputs from the OSN terminals. They are however believed to be indirectly activated by mitral/tufted cells to reciprocally shape the olfactory signal transmitted by these projection neurons to cortical areas. Our results however demonstrate that CalR(+) interneurons receive only few inputs from mitral and tufted cells and have a weak activity. These observations suggest that CalR(+) interneurons minimally influence OB network activity. Their function in olfactory information processing remains to be fully investigated.

V.4.2. The limited connectivity of CalR(+) PG interneurons persists for extended periods of time

The immature functional properties of CalR(+) interneurons may reflect an early and transient CalR expression in newborn PG interneurons. Such transient CalR expression could explain the temporal decrease in the number of EGFP(+) expressing cells observed in the CalR::GFP mice. Consistent with this idea, previous studies have described such transient CalR expression in newborn granule cells in the hippocampus (Brandt et al., 2003). This would however imply that the proportion of CalR(+) interneurons in the GL would decrease over time in favor of TH(+) and CalB(+) interneurons. Previous studies however evidenced that the relative proportion of each PG subtype in the GL do not vary in time until P30 in adult animals (Kohwi et al., 2007). This is further supported by our BrdU experiments that reveal that the proportion of CalR(+)/EGFP(+) cells remains stable for at least two months, indicating that the expression of CalR is not lost into adulthood. Finally, our electrophysiological results indicate that the immature electrophysiological properties of CalR(+) interneurons, do not change with age. Altogether, our results indicate that CalR(+) PG interneurons present unique functional properties that persist for extended periods of time. It is noteworthy that these properties are also observed in other brain regions, e.g. in cortical CalR(+) interneurons (Inta et al., 2008). This suggests that CalR(+) interneurons are unlikely to play significant role in modulating neuronal circuits activity via classical synaptic means, and suggest that they may serve other functions that remain to be discovered.

V.4.3. CalR(+) interneurons have different spatial and temporal origins

Our fate mapping experiments demonstrate that the germinal activity of all SVZ walls drops massively during the first few weeks after birth. The time-course of this decrease was comparable in all walls of the SVZ, including the lateral wall, which contribution to OB neurogenesis has been the most studied so far. These observations are in line with previous studies. It was indeed estimated that 41% of granule cells in the main OB are generated during the first postnatal week, 23% during the second postnatal week and only 14% thereafter (Hinds, 1968; Bayer, 1983). Remarkably however, our results demonstrate that germinal activity persists in

all SVZ walls up to at least three months after birth, thereby challenging the general belief of a gradual restriction of germinal activity to the lateral SVZ only.

Long term fate mapping of NSCs located in defined SVZ walls, also confirms the dual origin of CalR(+) interneurons from the dorsal and the medial SVZ throughout postnatal life (Fernández et al., 2011). Consistent with our results, a fraction of CalR(+) PG cells was shown to derive from the pallium (Emx1 lineage), which give rise to the dorsal part of the postnatal SVZ (Kohwi et al., 2007). The origin of the remaining CalR interneurons however remained largely elusive. Thus, while a small subpopulation of CalR(+) neurons (18%) was proposed to derive from the embryonic LGE (Dlx5/6 lineage) (Kohwi et al., 2007), our results demonstrate that a large fraction originate from the medial most regions of the postnatal SVZ. While the medial wall of the SVZ generate the majority of CalR(+) PG interneurons at birth, its germinal activity decreases drastically during the first 15 days of postnatal life. Thus, CalR(+) interneurons more likely originate from the dorsal SVZ into adulthood. Consistent with an increase in the contribution of the dorsal SVZ to CalR(+) neurons generation in the adult brain, the proportion of CalR(+) interneurons originating from the Emx1 lineage represent 42% of the CalR(+) neurons produced in the adult OB versus only 24% at birth (Kohwi et al., 2007). Our analysis however indicates that this complex spatial and temporal origin does not translate into morphological and electrophysiological differences.

V.4.4. CalR(+) PG interneurons may have unconventional functions in the treatment of olfactory information

A recent study suggested that CalR(+) PG interneurons, because of their peculiar electrophysiological properties, may improve the signal-to-noise ratio of olfactory signals (Fogli Iseppe et al., 2016). For instance, CalR(+) interneurons could be activated by weak excitatory inputs such as random excitatory inputs (noise) and inhibit projection neurons to reduce their basal activity. In contrast, other PG cells interneurons appear to be activated by high excitatory inputs, such as those induced by an odorant (signal). Our c-fos analysis supports such hypothesis. Indeed, the quantifications were done in regions of the GL showing high number of c-fos+ cells. In these activated glomeruli, a large proportion of CalB(+) interneurons were c-fos+

while only few CalR(+) cells expressed this marker of activity. It would be interesting to test if this balance of activation is affected in non-activated glomeruli.

Alternatively, CalR(+) interneurons because of their poor connectivity, may serve other purposes in olfactory information. It is tempting to speculate that this “dormant” pool of interneurons may be recruited in specific situation, to code for life threatening olfactory information (e.g. predator smell). Optogenetic approaches as well as exposition to strong odorants will be necessary to fully understand the significance of this peculiar interneuron population in olfactory processing.

Bardy C, Alonso M, Bouthour W, Lledo P-M (2010) How, When, and Where New Inhibitory Neurons Release Neurotransmitters in the Adult Olfactory Bulb. J Neurosci 30:17023–17034

Batista-Brito R, Close J, Machold R, Fishell G (2008) The distinct temporal origins of olfactory bulb interneuron subtypes. J Neurosci 28:3966–3975.

Bayer SA (1983) 3H-Thymidine-radiographic Studies of Neurogenesis in the Rat Olfactory Bulb. Exp Brain Res 50:329–340.

Belluzzi O, Benedusi M, Ackman J, LoTurco JJ (2003) Electrophysiological differentiation of new neurons in the olfactory bulb. J Neurosci 23:10411–10418.

Brandt MD, Jessberger S, Steiner B, Kronenberg G, Reuter K, Bick-Sander A, Von Der Behrens W, Kempermann G (2003) Transient calretinin expression defines early postmitotic step of neuronal differentiation in adult hippocampal neurogenesis of mice. Mol Cell Neurosci 24:603–613.

Caputi A, Rozov A, Blatow M, Monyer H (2009) Two calretinin-positive gabaergic cell types in layer 2/3 of the mouse neocortex provide different forms of inhibition. Cereb Cortex 19:1345–1359.

Carleton A, Petreanu LT, Lansford R, Alvarez-Buylla A, Lledo P-M (2003) Becoming a new neuron in the adult olfactory bulb. Nat Neurosci 6:507–518.

Fernández ME, Croce S, Boutin C, Cremer H, Raineteau O (2011) Targeted electroporation of defined lateral ventricular walls: a novel and rapid method to study fate specification during postnatal forebrain neurogenesis. Neural Dev 6:13.

Fogli Iseppe A, Pignatelli A, Belluzzi O (2016) Calretinin-Periglomerular Interneurons in Mice Olfactory Bulb: Cells of Few Words. Front Cell Neurosci 10:1–13.

Fukunaga I, Berning M, Kollo M, Schmaltz A, Schaefer AT (2012) Two Distinct Channels of Olfactory Bulb Output. Neuron 75:320–329.

Fukunaga I, Herb J, Kollo M, Boyden ES, Andreas T (2014) Independent control of gamma and theta activity by distinct interneuron networks in the olfactory bulb Nat Neurosci 17:1208–1216.

Geramita M, Urban NN (2017) Differences in Glomerular-Layer-Mediated Feedforward Inhibition onto Mitral and Tufted Cells Lead to Distinct Modes of Intensity Coding. J Neurosci 37:1428–1438.

Gire DH, Schoppa NE (2009) Control of on/off glomerular signaling by a local GABAergic microcircuit in the olfactory bulb. J Neurosci 9:19–22.

Hinds JW (1968) Autoradiographic Study of Histogenesis in the Mouse Olfactory Bulb. I. Time of origin of neurons and neuroglia. J Comp Neurol 134:287–304.

Inta D, Alfonso J, von Engelhardt J, Kreuzberg MM, Meyer AH, van Hooft JA, Monyer H (2008) Neurogenesis and widespread forebrain migration of distinct GABAergic neurons from the postnatal subventricular zone. Proc Natl Acad Sci 105:20994–20999.

Kohwi M, Petryniak MA, Long JE, Ekker M, Obata K, Yanagawa Y, Rubenstein JL, Alvarez-Buylla A (2007) A subpopulation of olfactory bulb GABAergic interneurons is derived from Emx1- and Dlx5/6-expressing progenitors. J Neurosci 27:6878–6891.

Kosaka K, Kosaka T (2007) Chemical properties of type 1 and type 2 periglomerular cells in the mouse olfactory bulb are different from those in the rat olfactory bulb. Brain Res 1167:42–55.

Lepousez G, Lledo PM (2013) Odor Discrimination Requires Proper Olfactory Fast Oscillations in Awake Mice. Neuron 80:1010–1024

Livneh Y, Adam Y, Mizrahi A (2014) Odor Processing by Adult-Born Neurons. Neuron 81:1097–1110

Metzger F, Repunte-Canonigo V, Matsushita S, Akemann W, Diez-Garcia J, Ho CS, Iwasato T, Grandes P, Itohara S, Joho RH, Knöpfel T (2002) Transgenic mice expressing a pH and Cl- sensing yellow-fluorescent protein under the control of a potassium channel promoter. Eur J Neurosci 15:40–50.

Najac M, De Saint Jan D, Reguero L, Grandes P, Charpak S (2011) Monosynaptic and Polysynaptic Feed-Forward Inputs to Mitral Cells from Olfactory Sensory Neurons. J Neurosci 31:8722–8729.

Najac M, Sanz Diez A, Kumar A, Benito N, Charpak S, De Saint Jan D (2015) Intraglomerular lateral inhibition promotes spike timing variability in principal neurons of the olfactory bulb. J Neurosci 35:4319–4331.

Panzanelli P., Fritschy JM, Yanagawa Y, Obata K, M.Sassoè-Pogneto (2007) GABAergic Phenotype of Periglomerular Cells in the Rodent Olfactory Bulb. J Comp Neurol 502:990–1002.

Parrish-Aungst S, Shipley MT, Erdelyi F, Szabo G, Puche AC (2007) Quantitative Analysis of Neuronal Diversity in the Mouse Olfactory Bulb. J Comp Neurol 501:825–836.

Shao Z, Puche a. C, Liu S, Shipley MT (2012) Intraglomerular inhibition shapes the strength and temporal structure of glomerular output. J Neurophysiol 108:782–793.

Shao Z, Puche AC, Kiyokage E, Szabo G, Shipley MT (2009) Two GABAergic Intraglomerular Circuits Differentially Regulate Tonic and Phasic Presynaptic Inhibition of Olfactory Nerve Terminals. J Neurophysiol 101:1988–2001.

Shao Z, Puche AC, Shipley MT (2013) Intraglomerular inhibition maintains mitral cell response contrast across input frequencies. J Neurophysiol 110:2185–2191.

Srinivas S, Watanabe T, Lin CS, William CM, Tanabe Y, Jessell TM, Costantini F (2001) Cre reporter strains produced by targeted insertion of EYFP and ECFP into the ROSA26 locus. BMC Dev Biol 1:4.

Whitman MC, Greer CA (2007a) Adult-Generated Neurons Exhibit Diverse Developmental Fates. Dev Neurobiol 67:1079–1093.

Whitman MC, Greer CA (2007b) Synaptic Integration of Adult-Generated Olfactory Bulb Granule Cells: Basal Axodendritic Centrifugal Input Precedes Apical Dendrodendritic Local Circuits. J Neurosci 27:9951–9961.

VI. CHAPTER 3:

A DUAL ROLE FOR THE TRANSCRIPTION FACTOR SP8 IN POSTNATAL OB NEUROGENESIS

In this chapter, I performed all experiments in the $Sp8^{fl/fl}$ model and delayed deletions with the grateful help of Amel Amara and Yacine Tensaouti during their L3 and M1 internship respectively. Transient manipulation experiments were performed by Anahi Hurtado and Maria Fernandez.

A dual role for the transcription factor Sp8 in postnatal neurogenesis

Elodie Gaborieau[1], Anahi Hurtado-Chong[2], Maria Fernández[2], Kasum Azim[2], and Olivier Raineteau[1,2]

[1]*Univ Lyon, Université Claude Bernard Lyon 1, Inserm, Stem Cell and Brain Research Institute U1208, 69500 Bron, France*

[2]*Brain Research Institute, University of Zürich, Zürich, Switzerland*

ABSTRACT

Neural stem cells (NSCs) of the postnatal subventricular zone (SVZ) continue producing distinct subtypes of olfactory bulb interneurons throughout life, in a complex spatial and temporal manner. Understanding the transcriptional coding of this diversity remains a great challenge of modern neurosciences. Interneurons expressing calretinin represent the main interneuron subtype produced in the glomerular layer (GL) after birth. Previous studies have suggested that their specification relies on expression of the transcription factor Sp8 by SVZ NSCs. In this study, we combined transcriptional datasets of NSCs isolated from distinct SVZ microdomains and fate mapping of NSCs that generate CalR+ or non-CalR+ interneurons, in order to re-assess the pattern of Sp8 expression during postnatal neurogenesis. We highlight a complex pattern of Sp8 expression, which appears to be expressed in all interneurons lineages, before getting gradually restricted to maturing CalR+ interneurons in the OB. To decipher the early and late functions of Sp8 in postnatal OB neurogenesis, we combined transient, permanent and conditional genetic approaches to manipulate Sp8 at different neurogenic stages. Our results highlight a dual role for Sp8 during postnatal neurogenesis. While Sp8 plays an early role in controlling proliferation in neuroblasts of all lineages, our results demonstrate that it is not involved in the early specification of CalR+ PG interneurons, but plays a crucial role in maintaining their integrity.

VI.1. Introduction

The subventricular zone (SVZ) is a brain region that shows intense germinal activity throughout postnatal life, producing new neurons that migrate and integrate in the olfactory bulb (OB). Its accessibility and regional organization in three microdomains (i.e. lateral, dorsal and medial) that generate distinct interneuron subtypes (Fiorelli et al., 2015) makes it an attractive model to study and understand the transcriptional coding of interneuron diversity.

Neuronal specification occurs early in the SVZ, by the expression of specific transcription factors (TFs) in neural stem cells (NSCs) and their immediate progeny. Newly specified neuroblasts then migrate in the rostral migratory stream (RMS) to the OB where they integrate in the glomerular or granular cell layers. Once integrated, it is generally accepted that the transcriptional activity of mature neurons decreases and relocalizes mainly at synapses in order to modify their efficiency. However, recent studies (reviewed in Deneris and Hobert 2015) have shown that the identity (i.e. neurotransmitter phenotype and connectivity) and the integrity of post-mitotic neurons is actively maintained. Thus, TFs, such as those acting in specification, continue to be expressed across the life span of a neuron.

Calretinin-expressing (CalR+) interneurons are the largest population of OB periglomerular (PG) interneurons produced after birth. They represent 40 to 50% of the whole population of PG interneurons, although their function in olfactory information processing remains to be explored (Kohwi et al., 2007; Panzanelli P. et al., 2007). Electroporation approaches have revealed a restricted spatial origin of CalR+ PG interneurons (Fernández et al., 2011). Thus, while CalB+ and TH+ interneurons originate from the lateral and dorsal SVZ respectively, CalR+ interneurons are produced by NSCs from the medial and the dorsal SVZ. Surprisingly, in contrast to CalB+ and TH+ interneurons, limited information exists regarding the TFs that guide CalR+ neurons specification. The TF Sp8 is to date, the only TF that has been suggested to act in their specification (Waclaw et al., 2006). Its conditional deletion in LGE progenitors, which gives the major part of the postnatal SVZ, leads to an impaired OB neurogenesis with a larger impact on CalR+ PG interneurons (Waclaw et al., 2006).

In this study, we combined transcriptional datasets of NSCs isolated from distinct SVZ microdomains (Azim et al., 2015) and fate mapping of NSCs that generate CalR+ or non-CalR+ interneurons, in order to re-assess the pattern of Sp8 expression during postnatal neurogenesis. We highlight a complex pattern of Sp8 expression, which appears to be expressed in all interneurons lineages, before getting gradually restricted to maturing CalR+ interneurons in the OB. To decipher the early and late functions of Sp8 in postnatal OB neurogenesis, we combined transient, permanent and conditional genetic approaches to manipulate Sp8 at different neurogenic stages. Our results highlight a dual role for Sp8 during postnatal neurogenesis: **i)** an early role in proliferation in neuroblasts of all lineages, **ii)** a role as terminal selector gene that is restricted to mature CalR+ PG interneurons.

VI.2. Material and Methods

VI.2.1. Animals

Transient genetic manipulations were performed in CD1 mice. Permanent deletion of Sp8 were assessed in $Sp8^{tm2Smb}$ (Jackson Laboratory) or RosaYFP-Sp8 mice kindly donated by D^r Ugo Borello. All procedures were performed in accordance with European requirements 2010/63/UE and have been approved by the Animal Care and Use Committee CELYNE (APAFIS#187 & 188). Animal procedures were executed in accordance with UK/Swiss/French law, with strict consideration given to the care and use of animals

VI.2.2. Plasmids

VI.2.2.1. Subcloning of Sp8

The mouse *Sp8* gene was amplified from a pXY-Asc plasmid (Open Biosystems, clone ID 30653287) by PCR using specific primers designed to add Xho I and Sac I restriction sites (sense primer (Xho5') 5' agt cct cga gat ggc aac ttc act tct ag 3'; antisense primer Sac 3' gat cga gct ctc act cca ggc cgt tgc g). The PCR product was purified from an agarose gel using a Qiagen kit following manufacturer's instructions and digested with the corresponding restriction enzymes (XhoI (C^TCGAG) #R0146S; SacI (GAGCT^C) #R0156S; New England Biolabs) before subcloning it into a pCAAG-IRES-nlsGFP plasmid. The correct integration of the gene was verified by sequencing. To check the efficient expression of the generated plasmid, about 100.000 HEK cells were transfected with 2µg of DNA (Sp8-IRES_GFP plasmid alone or pCAAG + pCX-GFP plasmid used as a positive control) using Lipofectamine (prepared in Optimem, Invitrogen). 72 h post transfection, cells were fixed and immunostained against Sp8 (**Figure S2**).

VI.2.2.2. shRNA testing efficiency

Five different shRNAs against Sp8 were purchased from Open Biosystems (TRCN0000085558, TRCN0000085559, TRCN0000085560, TRCN0000085561, TRCN000008555862). Their interfering efficiency was first tested *in-vitro*. HEK cells were co-transfected with shRNA + pCAAG-Sp8-IRES-nlsGFP plasmids using the lipofectamine method following manufacturer's instructions (Invitrogen). 72 h post

transfection, cells were harvested and lysed to extract RNA (Qiagen RNAeasy extraction kit), which was then retro-transcripted into cDNA to be analyzed by qPCR using a 1:100 dilution. The standard curve was prepared from a Sp8 overexpressing sample that was diluted at different concentrations. *HPGRT* was used as housekeeping gene. The shRNA 9 showing the best inhibition was chosen for further experiments (**Figure S2**).

VI.2.3. Cell culture

In vitro experiments to test the plasmids were performed using the NS-5 cell line. Cells were cultured as previously described (Conti *et al.*, 2005) and nucleofected using the Amaxa Nucleofector (Lonza), SG solution, program EN150 and 0.5 µg of DNA/million cells. Following nucleofection, cells were either plated in NS cell basal medium for 48 hours into plastic plates or induced to differentiate into neurons by plating them into poly-ornithine and laminin coated glass coverslips in D1 medium (NS cell basal medium supplemented with 1 % B27, 0.5% N2, 5 ng/mL FGF2) for 8 days. Cells were then fixed and immunostained for further analysis.

VI.2.4. Electroporations

CD1, $Sp8^{fl/fl}$ or RosaYFP-$Sp8^{fl/fl}$ pups were electroporated at 2 postnatal days (P2) as described previously (Boutin *et al.*, 2008; Fernandez *et al.*, 2011). Briefly, pups were anesthetized in ice and placed on a custom made support in a stereotaxic rig. Injections were performed at the midpoint of a virtual line traced between the eye and lambda. A 34G needle attached to a Hamilton syringe was inserted at a depth of 2 mm from the skull surface and 1.5µl of plasmid solution was injected into the lateral ventricle.

For fate mapping experiments, a solution of pCX-GFP [5 µg/µl] plasmid + fast green (0.2%) in sterile PBS was used in CD1 mice. For gain and loss of function experiments, Sp8 or shRNA vs Sp8 plasmids were combined with pCX-GFP plasmid at a 3:1 ratio [5 µg/µl] + fast green (0.2%) in CD1 mice. For early and late conditional deletion experiments, pCAG-CRE or pCAG-ERT2-CRE-ERT2 plasmids was combined to pCX-GFP plasmid at a 2:1 ratio [5 µg/µL] + fast green (0.2%) in $Sp8^{fl/fl}$ mice. Co-expression of both plasmids has an efficiency higher than 80% (Boutin *et al.*, 2008) and therefore, this strategy allows precise tracking of the electroporated cells due to the strong and sustained expression of the pCX-GFP plasmid. For late

conditional deletion, ERT2-CRE-ERT2 plasmid was used in RosaYFP x Sp8 mice. Empty or scrambled plasmids +/- pCX-GFP were used accordingly as controls in littermates.

The accuracy of the injection was verified by the filling of the ventricle with the dark solution. Successfully injected mice were then subjected to 5 electrical pulses (95 V, 50 ms, separated by 950 ms intervals) using the Super Electroporator NEPA21 type II (Nepa Gene Co., Ltd) and tweezer electrodes coated with conductive gel (Signa gel, Parker Laboratories, Fairfield, New Jersey, USA), positioning electrodes to target either the lateral or the medial wall (Fernandez *et al.*, 2011). After electroporation pups were warmed up until fully recovered and returned to their mother.

VI.2.5. Tissue process

Mice were sacrificed at 4 days post electroporation (dpe), 10 or 21 dpe to assess the effect on radial glia or mature neurons respectively. After deep anesthesia with intraperitoneal pentobarbital, mice were transcardially perfused and brains removed, post-fixed for two days and cut in a vibratome (Leica VT1000 S). 50um sections were collected from the OB to the lateral ventricle in series of 6 and kept at -20° C in antifreeze solution (glucose 15%, sodium azide 0,02%, ethylene glycol 30%, PB 0,1M).

VI.2.5.1. Immunohistochemistry

Free floating sections or cells grown on coverslips are blocked in TNB-Tx buffer (BSA 0.25%, Casein, 0.05%, Top block 0.25% + triton X100 0.4%) Triton 100X. When antigen retrieval was needed, sections were incubated at 80°C in Citrate Buffer (10 mM, pH 6) for 20 minutes. For BrdU staining, section were subjected to an antigen retrieval and incubated at 37°C° in HCl 2N for 30 minutes followed by 30 minutes in Borate Buffer 0.1M at room temperature. Sections are then incubated with the primary antibody overnight (see table 1). Next, sections were incubated with the corresponding secondary antibody (see table 1). To amplify the signal in YFP animals, sections were incubated with a biotinylated secondary antibody and incubated in streptavidin-DTAF (1:250) for 30 min. Finally, sections were counterstained with DAPI and mounted with Fluoromount mounting medium.

Table 1:

Primary antibodies	Specie	Concentration	Source (catalog number)
anti-Sp8	Rabbit	1:2000	Millipore (ab15260)
Anti-Calretinin	Rabbit	1:2000	SWANT (7697)
Anti-Calretinin	Mouse	1:2000	SWANT (6B3)
Anti-Calbindin	Mouse	1:2000	SWANT (D28K)
Anti-TH+	Mouse	1:400	Millipore (MAB318)
Anti-GFP	Chicken	1:1000	AVES Lab (GFP-1020)
Anti-Ki67	Mouse	1:400	Abcam (ab6526)
Anti-Ki67	Rabbit	1:500	Thermoscientific (RM9106-S1)
Anti-NeuN	Mouse	1:400	Millipore (MAB377)
Anti-Doublecortin	Goat	1:500	Santa Cruz (Sc-8066)
Anti-Caspase	Rabbit	1:1000	Millipore (ab3623)
Secondary antibodies	**Specie**	**Concentration**	**Source (catalog number)**
Anti-mouse AlexaFluor 555	Donkey	1:1000	TermoFisher (A-31570)
Anti-mouse AlexaFluor 647	Donkey	1:1000	ThermoFisher (A-31571)
Anti-rabbit Alexa Fluor 555	Donkey	1:1000	ThermoFisher (A-31572)
Anti-rabbit AlexaFluor 647	Donkey	1:1000	ThermoFisher (A-31573)
Anti-goat Alexa Fluor 647	Donkey	1:1000	ThermoFisher (A21447)
Anti-chicken biotinylated	Donkey	1:1000	Jackson Lab (703-065-155)
Streptavidin-DTAF	-	1:250	Jackson Lab (016-010-084)

VI.2.6. Quantifications

Quantifications were done on live image using an epifluorescent microscope (Leica DM5500, objective HCX PL APO 40x 1,25 oil) or on pictures taken with a confocal microscope (MCBL, Leica SP5, objective HCX PL APO 40x 1.25 oil) and processed with Image J and Photoshop CS4. For 3D neurons reconstruction, 0.3µm stack images were taken with a confocal microscope and 3D reconstruction were performed and analyzed with the software Neurolucida 360 (MBF Bioscience, Vermont, USA). Statistical significance was determined by unpaired *t* test at the $p < 0.05$ level or a Mann-Whitney test when data did not assume a normal distribution (Prism 7, GraphPad Software, California, USA).

VI.3. Results

VI.3.1. Sp8 is expressed in neuroblasts of all periglomerular interneuron lineages but gradually become restricted to CalR+ interneurons

Sp8 is expressed in the forebrain early during embryonic development. Its expression persists after birth in restricted regions, including the SVZ, RMS and OB. While Sp8 mRNA is detected in NSCs and TAPs of the postnatal SVZ (supplementary **Figure S1**), nuclear expression of Sp8 is only observed in Dcx+ neuroblasts in the SVZ of early postnatal mice (P6) (**Figure 1A**). As a consequence, most of the Dcx+ neuroblasts of the RMS express Sp8 (**Figure 1C**). In the OB at P23, most Sp8+ cells are observed in the glomerular cell layer (GL), while some cells are also present in the granular cell layer (GCL) (**Figure 1B**).

In order to investigate the pattern of Sp8 expression in PG interneuron lineages originating from distinct SVZ microdomains, we electroporated a GFP expression plasmid in lateral, dorsal and medial SVZ NSCs. Immunodetection of Sp8 in GFP+ cells in the RMS 2 days post-electroporation (2 dpe) revealed that most migrating neuroblasts express Sp8 independently of their origin (lateral EPO: 82.1% ± 3.9; n=3 animals; dorsal EPO: 69.9% ± 3.4; n=4 animals; medial EPO: 75.4% ± 0.7; n=3 animals; **Figure 1D**). This homogeneous expression becomes gradually restricted in subpopulations of mature neurons within the glomerular and granular cell layers. Thus, Sp8 expression is largely downregulated at 21 dpe in interneurons originating from the lateral SVZ (12.8% ± 5.8; n=4 animals), and to a lesser extend in those originating from the dorsal SVZ (42.1% ± 5.1; n=4 animals). In striking contrast, it is largely maintained in interneurons originating in the medial SVZ (69.6% ± 3.2; n=4 animals) (**Figure 1E-F**).

Owing to the different spatial origin of OB interneuron subtypes, these observations suggest that Sp8 expression is only maintained in specific OB lineages. We identified the three main subtypes of periglomerular GABAergic interneurons by immunodetection of CalB, CalR and TH (**Figure 1G-I**). In agreement with their respective origin (Fernández et al., 2011), the vast majority of CalR+ periglomerular interneurons expressed Sp8 (74.3% ± 2.2; n=4 animals), while only 10.3% ± 1.7 and 18.5% ± 2.5 of CalB+ and TH+ neurons, respectively, kept expressing Sp8 (n=4 animals mice each) (**Figure 1J**).

Altogether, our results highlight a complex spatial and temporal pattern of Sp8 expression. While it is expressed in migrating neuroblasts of all lineages, its expression becomes gradually restricted to CalR+ PG interneurons, suggesting a dual role in OB neurogenesis.

Figure 1: Sp8 expression is observed in all neuroblasts originating from all SVZ microdomains but becomes gradually restricted to mature CalR+ PG interneurons

(**A**) Representative immunostaining revealing Sp8 expression in the postnatal SVZ. Scale bar: 50µm. The right panel shows high magnifications of nuclear expression in young Dcx+ neuroblasts in the RMS (**a**) and the absence of Sp8 expression in Dlx2+ TAPs (**b**) Scale bars:10µm and 20µm. (**B**) Representative immunostaining of Sp8 in the OB of P23 animals. Scale bar: 200µm. The two panels below show the specific expression in subpopulations of periglomerular (**a**) and granular neurons. (**b**). Scale bars: 50µm and 100µM. (**C-F**) Electroporation of the 3 microdomains of the SVZ (i.e. lateral, dorsal and medial) to label newborn neurons at P2. (**C**) Representative immunostaining of GFP+ labeled migrating neuroblasts in the RMS 4 days after EPO of the medial SVZ. High magnifications show the expression of Sp8 in GFP+ newborn neurons. Scale bar: 20µm. (**D-F**) Quantifications of the proportion of GFP+ migrating neuroblasts in the RMS at 4 dpe (**D**) and GFP+ neurons in the OB at 21 dpe in the GL (**E**). The restriction of the expression pattern of Sp8 from neuroblasts to mature OB neurons originating from the medial SVZ is summarized in graph (**F**). (**G-I**) Representative immunostainings reveal Sp8 expression in the 3 main subpopulations of PG interneurons (CalR, CalB and TH) at 21 dpe. Scale bar: 20µm (**J**) Quantification of the proportion of PG interneurons expressing Sp8. Error bars represent the standard error of the mean; *p≤0.05; **p≤0.01; ***p≤0.001; ****p ≤0.0001 determined by unpaired t-test
Abbreviations: dpe: days post-electroporation; RMS: Rostral Migratory Stream; PGL: Periglomerular layer

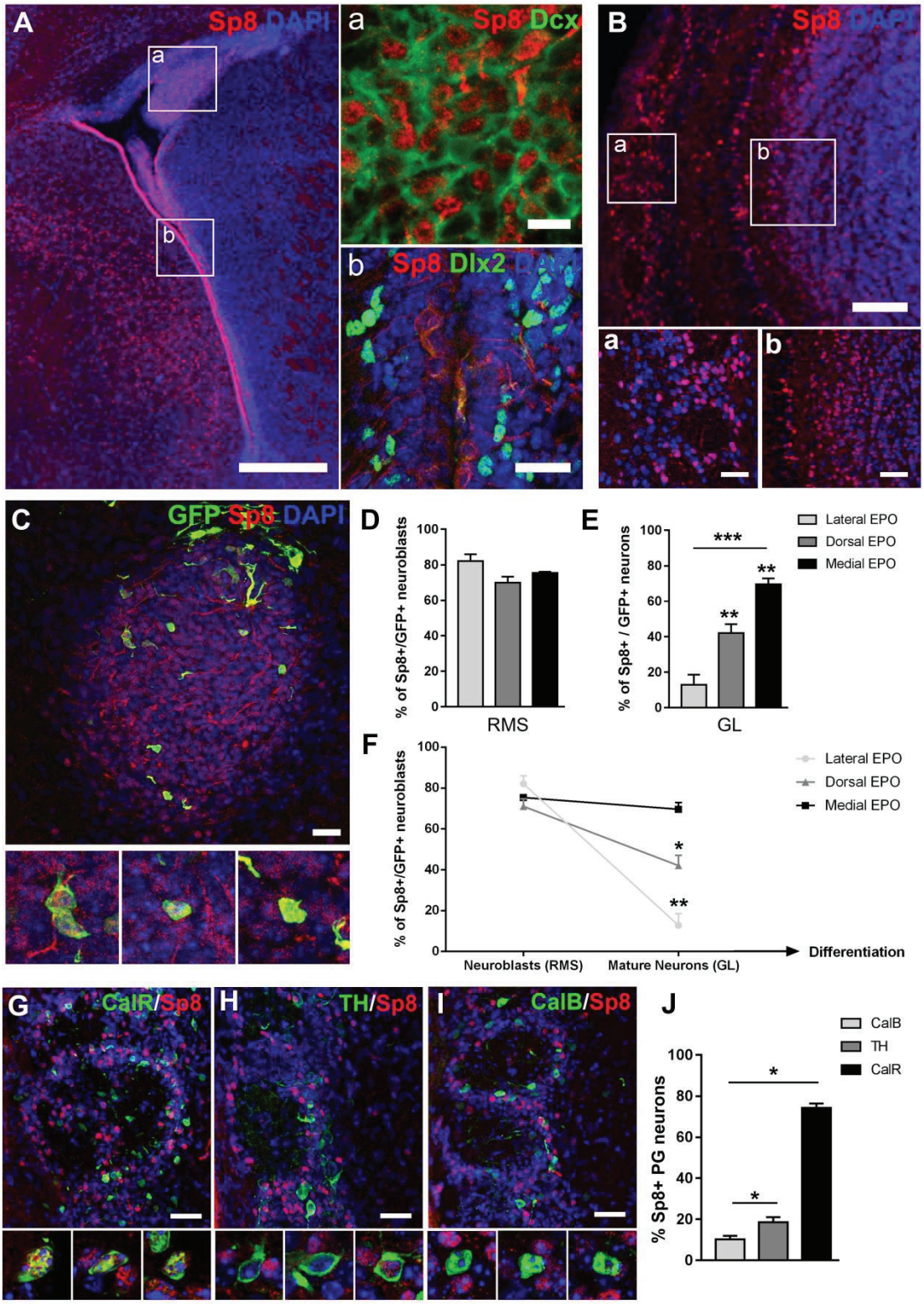
A
Sp8 DAPI
a
b
a
Sp8 Dcx
b
Sp8 Dlx2
B
Sp8 DAPI
a
b
a
b
C
GFP Sp8 DAPI
D
% of Sp8+/GFP+ neuroblasts
100
80
60
40
20
0
RMS
E
% of Sp8+ / GFP+ neurons
***
**
**
GL
Lateral EPO
Dorsal EPO
Medial EPO
F
% of Sp8+/GFP+ neuroblasts
*
**
Neuroblasts (RMS)
Mature Neurons (GL)
Differentiation
Lateral EPO
Dorsal EPO
Medial EPO
G
CalR/Sp8
H
TH/Sp8
I
CalB/Sp8
J
% Sp8+ PG neurons
*
*
CalB
TH
CalR

VI.3.2. Sp8 influences proliferation and cell cycle exit in the postnatal SVZ

To investigate the early role of Sp8 in SVZ neural stem cells and their immediate progeny, we used an electroporation approach to transiently manipulate its expression. Gain and loss of function were performed with non-integrative plasmids coding for the Sp8 protein or a shRNA against Sp8, respectively.

The correct cloning of the Sp8 insert in the pCAAG-IRES-nlsGFP vector was verified after digestion with the corresponding restriction enzymes (**Figure S2A**). Efficiency of the Sp8 expressing plasmid was verified on HEK cells transfected with the pCAAG-Sp8-IRES-nlsGFP plasmid. Immunochemistry with Sp8 antibody was performed 48 hours post-transfection. Transfected cells expressing GFP reporter highly co-express Sp8. Non-transfected cells do not express nether GFP nether Sp8 (**Figure S2B**). The efficiency of five different shRNA (shRNA 8 to 12) was tested on HEK cells co-transfected with the Sp8 expressing plasmid. Sp8 mRNA expression was measured by real time PCR 48 hours post-transfection. The shRNA 9 was the most efficient with 63% (4 individual experiments) of interference rate compared to Sp8 control (**Figure S2C**). Therefore, the shRNA 9 was further tested by immunocytochemistry to investigate its interference efficiency at the protein level. Optical densitometry analysis was performed on transfected cells following Sp8 immunostaining. Again, the shRNA 9 significantly knock-down Sp8 expression (77.86 ± 0.312%, n=20 cells, **Figure S2D**). The weaker interference efficiency revealed by immunostaining compared to qPCR results could be due to the short half-life of the protein, and/or to underestimation of the results resulting from unspecific staining (not subtracted in these experiments). Nevertheless, these results confirm the efficient knock-down of Sp8 by shRNA9, which was therefore chosen for all *in-vivo* experiments.

Following overexpression of Sp8 in NSCs, we observed a reduction in the proportion of radial glial cells (RGCs) within the population of GFP+ electroporated cells in the SVZ at 4 dpe (Control: 34.8% ± 4.7; n=12; Sp8: 21.9% ± 3.8; n=14; **Figure 2C**). In agreement with the absence of Sp8 expression in most RGCs and progenitors (see above), Sp8 knockdown showed no effects onto RGCs (Control:

36.1% ± 6; n=12; shRNA Sp8: 32.1% ± 5.1; n=15; **Figure 2D**). These data suggests that the ectopic expression of Sp8 in RGCs promotes their premature differentiation.

We next investigated the potential role of Sp8 in controlling proliferation and cell cycle exit. We analyzed the proliferative capacities of GFP+ electroporated cells (RGCs and TAPs) following transient overexpression and knockdown of Sp8. Sp8 overexpression led to a significant decrease in the proportion of proliferative cells in the SVZ at 4 dpe (Control: 26.95% ± 3.0; n=8; Sp8: 19.33% ± 2.8, n=8; **Figure 2E**). In contrast, Sp8 knockdown resulted in an increased proliferation, suggesting a reduced cell cycle exit of late progenitors (Control: 37.87% ± 3.0; n=8; shRNA Sp8: 53.03% ± 2.9, n=10; **Figure 2F**). Indeed, analysis of the cell cycle exit by injection of EdU 24h before analysis and co-localization with the proliferation marker Ki67 progenitors, revealed a reduced number of EdU+/Ki67- electroporated cells within the SVZ (Control: 45.75% ± 1.6; n=8; shRNA Sp8: 37.96% ± 2.7, n=10; **Figure 2H**). Altogether, these results suggest that Sp8 induces cell cycle exit and thus the differentiation of postnatal progenitors.

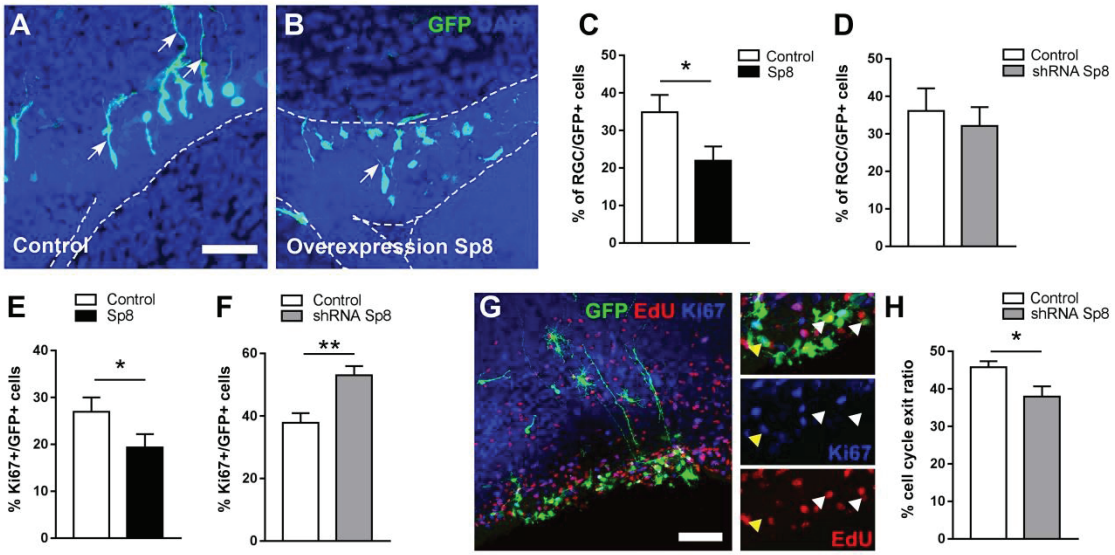

Figure 2: Transient manipulation of Sp8 expression in NSCs influence the proliferative behavior of progenitors independently of their origin

(A-B) Confocal pictures revealing the morphology of labelled progenitors in the dorsal SVZ 4 days after overexpression of Sp8. Scale bar: 40µm. (C-D) Quantification of the proportion of RGCs after transient Sp8 overexpression (C) and deletion (D) in the dorsal and lateral SVZ. (E-F) Quantification of the percentage of proliferative cells (Ki67+) following Sp8 overexpression (E) and deletion (F) in the dorsal and lateral SVZ. (G) Representative immunostaining of proliferative labelled progenitors (GFP+Ki67+) at 4 dpe in the dorsal SVZ. Animals were injected with a single dose of EdU 24h before sacrifice, to identify the population that exit the cell cycle between 3 and 4 dpe (i.e. EdU+/Ki67-, white arrowheads). High magnification on Ki67+ and EdU+ progenitors are shown on the right panels. Scale bar: 50 µm. (H) The percentage of progenitors that exit the cell cycle between 3 and 4 dpe is determined by the quantification of EdU+Ki67-/EdU+ cells in dorsal and lateral SVZ. Error bars represent the standard error of the mean; *p≤0.05; **p≤0.01 determined by Mann Whitney test (D; E; H) or unpaired t-test (C; F)

Abbreviations: RGCs: Radial Glial Cells

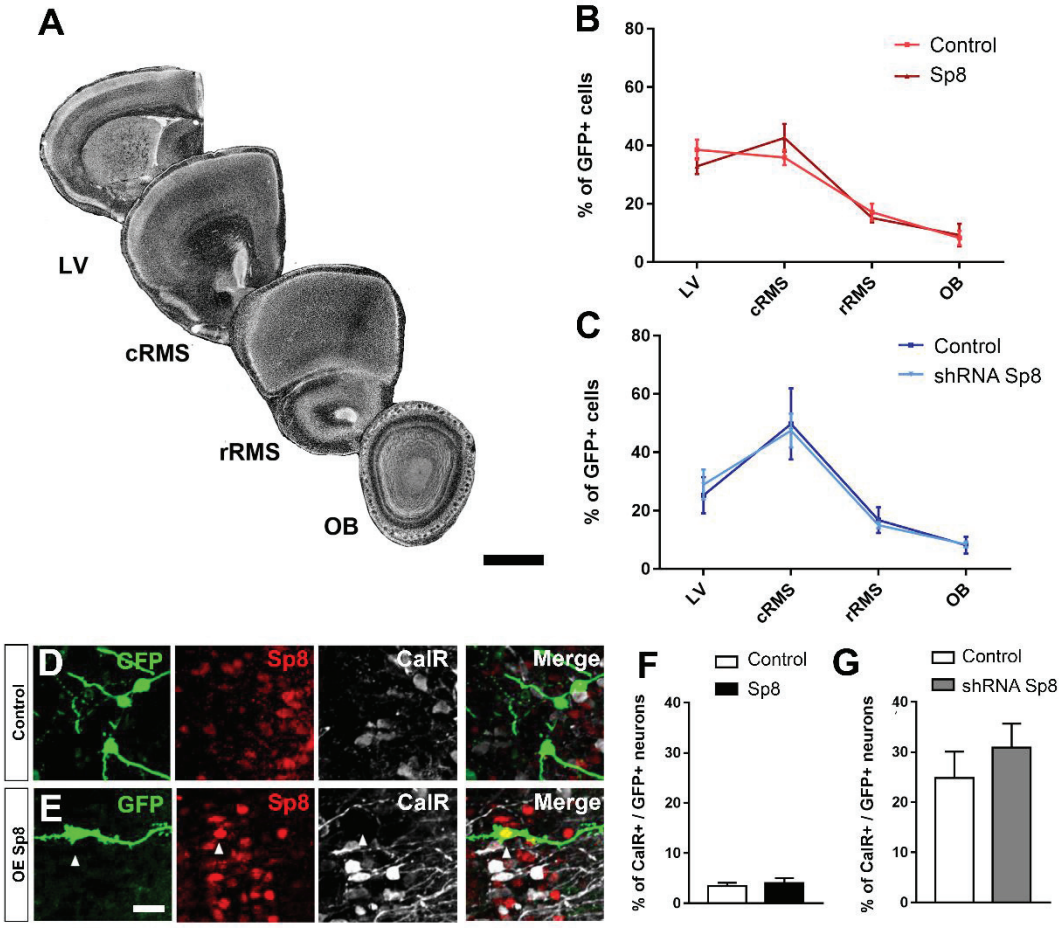

Figure 3: Transient manipulation of Sp8 expression in NSCs does not influence the migration of neuroblasts nor the specification of CalR+ PG interneurons

(A) Illustration of serial coronal sections stained with DAPI of 4 dpe brains, along the rostro-caudal axis from the lateral ventricle to the OB. Scale bar: 500µm. (B-C) Quantification of the percentage of GFP+ cells distributed in the lateral ventricle, in the caudal and rostral RMS and in the OB. (D-E) Representative immunostainings of GFP+ newborn neurons expressing CalR at 21 dpe in control brain (D) and after Sp8 overexpression (E). Scale bar: 10µm. (F-G) Quantification of the proportion of CalR+ interneurons in the granular and glomerular layers 21 days after overexpression (F) or deletion (G) of Sp8 in NSCs of the lateral or medial SVZ, respectively.

LV: lateral ventricle; cRMS: caudal part of the rostral migratory stream; rRMS: rostral part of the rostral migratory stream; OB: olfactory bulb

VI.3.3. Sp8 is not involved in neuroblasts migration nor CalR+ interneuron specification

The nuclear expression of Sp8 appearing only in young neuroblasts questions its role in neuroblasts migration. We quantified the number of electroporated cells in the SVZ as well as at different rostro-caudal coordinates of the rostral-migratory stream (RMS), following overexpression or knockdown of Sp8. At 4 dpe, most of the electroporated cells were observed invading the RMS caudal more regions, with only few having reached its rostral most compartments, corresponding to the OB peduncle (**Figure 3A-C**). Manipulation of Sp8 expression had no effect on this distribution, indicating that Sp8 is not involved in the control of neuroblasts migration.

We next investigated the role of Sp8 in the specification of CalR+ interneurons, in agreement with earlier studies (Waclaw et al., 2006). We took advantage of the regional generation of CalR+ PG interneurons in the postnatal SVZ. An instructive role of Sp8 in CalR+ interneurons specification was investigated by overexpressing it in the lateral SVZ, which only produces rare CalR+ interneurons (Fernández et al., 2011). Among all interneurons produced by this microdomain, only 3.4% ± 0.7 (n=5) located in the granular layer expressed CalR+ (**Figure 3F**). This percentage was not changed 21 days following Sp8 overexpression (4% ± 1; n=5), despite persistent immunodetection of Sp8 in electroporated cells (**Figure 3E**). We next investigated the consequences of Sp8 knockdown in CalR+ interneurons specification by electroporating a shRNA construct in the medial SVZ. As many as 24.86% ± 5.2 of the electroporated GFP+ cells originating from this wall and migrating in the glomerular and granular cell layers acquire expression of CalR at 21 dpe, a percentage that remained unchanged by Sp8 knockdown (30.91% ± 4.8; n=4; **Figure 3G**). Together, these results suggest that Sp8 is neither necessary nor sufficient to specify CalR+ interneurons in the postnatal OB.

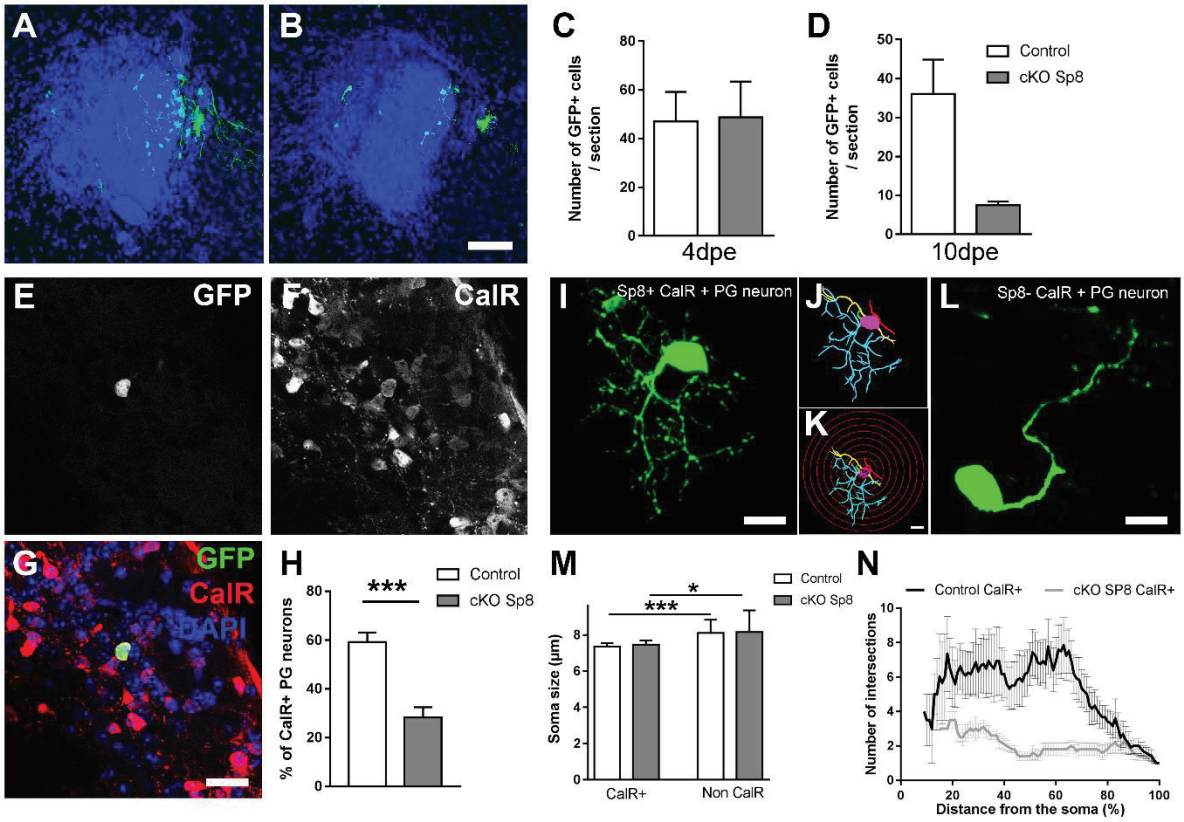

Figure 4: Deletion of Sp8 in NSCs of the medial SVZ affects the maturation and survival of CalR+ PG interneurons

(A-B) Representative example of GFP+ migrating neuroblasts in the RMS in control and cKO Sp8 brains at 10 days post medial EPO. Scale bar: 200µm. (C-D) Quantification of GFP+ neuroblasts in the RMS at 4 dpe (C) and 10 dpe (D) after permanent Sp8 deletion in medial NSCs. (E-G) Immunostaining for GFP+ labeled neurons expressing CalR in the GL. Scale bar: 20µm. (H) Quantification of the proportion of GFP+/CalR+ in control and following conditional Sp8 deletion. (I-L) Representative confocal picture of CalR+/Sp8+ (I) and CalR+/Sp8- PG interneurons (L). Scale bars: 10µm. 3D reconstruction of the Sp8+/CalR+ interneuron with the software Neurolucida 360 (J) Representative illustration of concentric circles separated from each other by 5µm (radius, K) to perform the sholl analysis presented in N. (M) Measurement of the size of the soma of CalR+ and non-CalR+ PG interneurons in control and after permanent deletion of Sp8. (N) Sholl analysis determines the number of intersections between the dendritic arborization and each circle in function of the distance from the soma. Error bars represent the standard error of the mean; *p≤0.05; **p≤0.01; ***p≤0.001

VI.3.4. Early Sp8 ablation affects newborn neuron survival and maturation

In order to perform a conditional and permanent deletion of Sp8, we used floxed Sp8 ($Sp8^{fl/fl}$) transgenic mice crossed with Cre reporter mice (RosaYFP). We first induced an early and permanent deletion of Sp8 in NSCs and their progeny by electroporating a plasmid coding for the CRE-recombinase in select SVZ walls. The permanent deletion of Sp8 was confirmed at 21 dpe in PG neurons originating from the medial SVZ as revealed by the complete absence of Sp8 expression in electroporated cells (**supplementary figure S3B-C**). Electroporation of NSCs of the medial wall revealed a delayed loss of labeled neuroblasts, which was not visible at 4 dpe but became prominent at 10 dpe (**Figure 4**). In order to investigate if these effects were specific of the CalR+ lineage, we quantified the proportion of labeled PG interneurons expressing CalR at 21 dpe. As expected, CalR+ interneurons that represent 59.2% ± 3.9 (n=4) of labeled PG interneurons, only represented 28.2% ± 4.2 (n=4) of the remaining cells following Sp8 ablation (**Figure 4H**). Among these few CalR+ surviving neurons, the majority showed an atrophied dendritic arborization compared to Sp8 expressing neurons (**Figure 4I-L**), although soma sized remained normal (**Figure 4M**). Indeed, the complexity of the arborization, revealed by a sholl analysis, was consistently reduced when compared to Sp8-expressing CalR+ PG interneurons (**Figure 4N**). The other PG interneurons subtypes (i.e. CalB+ and TH+ interneurons) were also affected although to a lesser extent following permanent deletion of Sp8 in dorsolateral NSCs (data not shown). Altogether, these results support a role of Sp8 as a terminal selector gene that insure the correct integration and survival of maturing CalR+ interneurons.

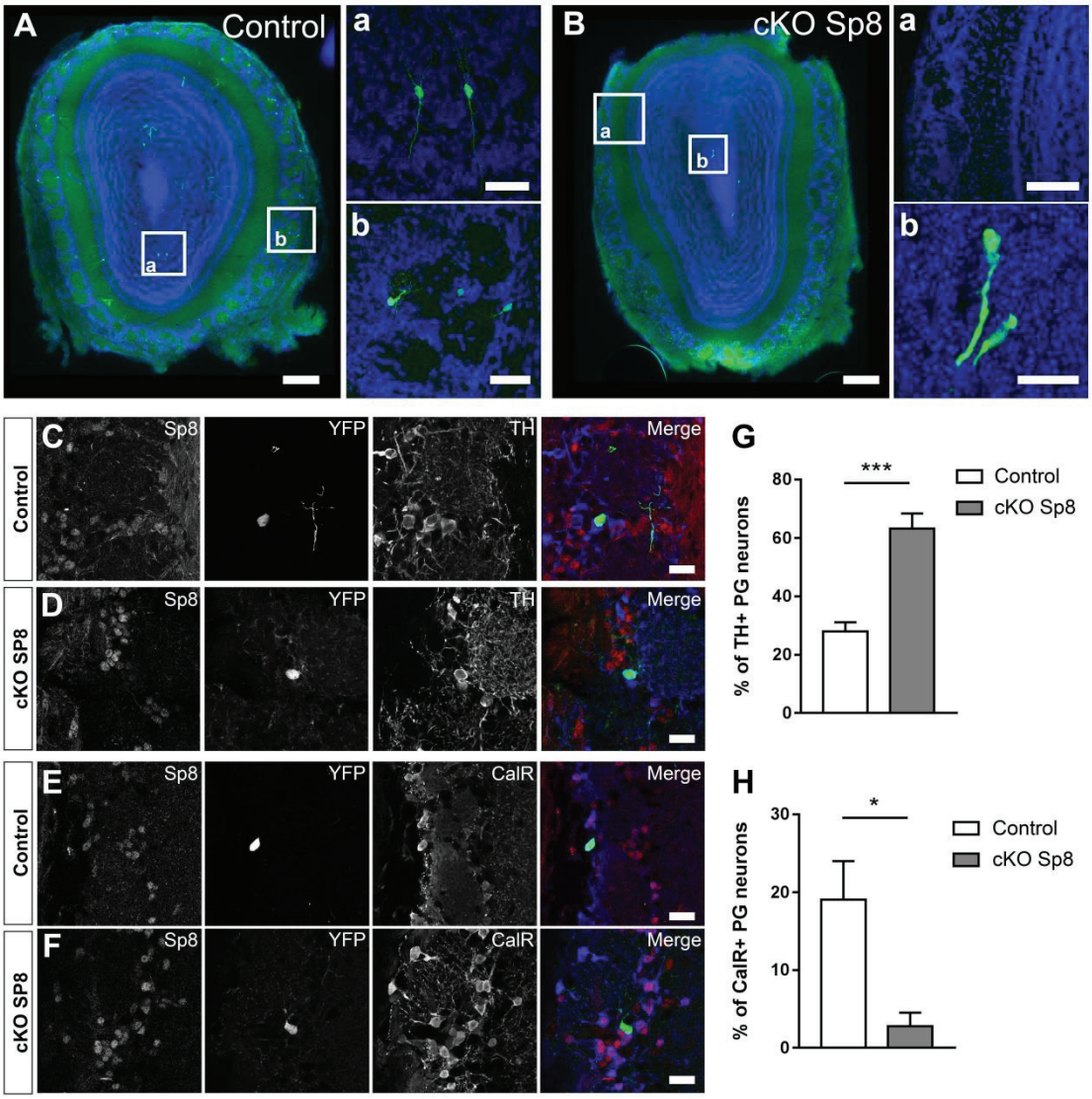

Figure 5: Delayed conditional deletion of Sp8 in maturing neurons leads to a severe phenotype on CalR+ PG interneurons survival but does not affect TH+ interneurons

(A-B) Illustration of labeled neurons in the RMS, GL and GCL of the OB at 21 dpe after medial EPO in control mice (A) or following deletion of Sp8 at 11 dpe (B). Scale bars: 200µm, 20µm(Aa), 40µm(Ab), 50µm(Ba), 20µm(Bb). (C-F) Representative immunostainings reveal TH and CalR expression in labeled neurons following dorso-lateral EPO in control brains or after deletion of Sp8. Scale bars: 20µm (G-H) Quantification of the proportion of CalR+ and TH+ PG interneurons in controls and after Sp8 deletion. Error bars represent the standard error of the mean; *p≤0.05; ***p≤0.001 determined by Mann Whitney test (CalR+) or unpaired t-test (TH+)

VI.3.5. Late Sp8 ablation supports a specific role in CalR+ interneurons survival

In order to confirm the importance of Sp8 expression in the maintenance of mature CalR+ interneurons, we induced Sp8 ablation at later stages of newborn neurons differentiation. An inducible Cre recombinase (i.e. ERT2-CRE-ERT2) was electroporated in the medial SVZ of $Sp8^{fl/fl}$ transgenic mice and Sp8 deletion was induced by tamoxifen injection at 11 dpe, when most electroporated neurons have reached their destination. Interestingly, the effect of delayed Sp8 ablation on CalR+ neurons survival was similar but more drastic than following early Sp8 deletion. Indeed, no labeled newborn neurons were detected in the GL following Sp8 deletion (**Figure 5A-B**). However, some migrating neuroblasts were still observed in the OB which confirmed the efficiency of the electroporation and further supported that early stages of neuronal differentiation, including migration were not affected.

In order to confirm that these pro-survival effects were specific to CalR+ neurons, owing to the gradual restriction of Sp8 to this subpopulation of interneurons, we performed a targeted ablation in the dorso-lateral SVZ. As expected, the population of CalR+ PG interneurons was lost following Sp8 deletion (19.1% ±5.0 vs 2.8% ± 1.8. **Figure 5H**). Simultaneously, the proportion of TH+ neurons, the main interneuron subtype produced by the dorso-lateral SVZ increased proportionally (28.0% ± 3.1 vs 63.2% ± 5.1; **Figure 5G**). Thus, interneuron populations that downregulate Sp8 in the OB are not affected by delayed Sp8 deletion.

VI.4. Discussion

Through this study, we demonstrate that Sp8 is not involved in the early specification of CalR+ PG interneurons of the OB but plays a crucial role in maintaining their integrity.

Our observations emphasize a complex expression pattern of Sp8 during postnatal OB neurogenesis, which suggests distinct functions during defined stages of the neuronal differentiation process. Previous studies have demonstrated a strict spatial origin of OB interneurons subtypes, which is particularly apparent for PG interneurons subtypes (reviewed in Fiorelli et al. 2015). Thus, CalR+ interneurons originate from both the medial and dorsal walls of the SVZ, while TH+ and CalB+ arise from the dorsal and lateral walls respectively. This spatial origin of defined neuronal lineages can be appreciated by targeted electroporation of distinct SVZ walls (Fernández et al., 2011). Fate mapping of these distinct lineages reveals that Sp8 expression is initially common to all migrating neuroblasts in the postnatal SVZ and RMS. Interestingly, Sp8 transcripts can be detected in NSCs and TAPs but expression of the protein only appears in Dcx+ neuroblasts of the SVZ and in the RMS. This early priming has been previously reported for adult NSCs, particularly for neurogenic TFs (see for example Beckervordersandforth et al. 2010; Azim et al. 2015).

Gain and loss of function experiments suggest an early role for Sp8 in controlling cell cycle exit and initiation of neuronal differentiation. Thus, ectopic Sp8 expression in NSCs promotes the premature differentiation of progenitors into neuroblasts and depletes the pool of RGCs. In contrast, Sp8 knock down does not affect NSCs proliferation, in accordance with the lack of protein expression in these cells, but decreases cell cycle exit of postnatal progenitors. These results are in line with the previously described role of Sp8 in regulating proliferation and differentiation processes during embryogenesis (Zembrzycki et al., 2007; Borello et al., 2014). The molecular mechanisms underlying these effects need to be further investigated. Sp8 is known to tightly control proliferation and differentiation during embryonic brain development (Treichel et al., 2003; Griesel et al., 2006; Borello et al., 2014), possibly by activating and sustaining Fgf8 signaling in the rostral most forebrain regions (Griesel et al., 2006; Zembrzycki et al., 2007). A recent study published by Li et al.

confirmed the pro-neurogenic effect of Sp8 in the adult SVZ coordinately with Sp9 (Li et al., 2017). They identified Prokr2, a G protein-coupled receptor of chemokines Prok2 and Tshz1 (Teashirt Zinc Finger Homeobox 1), as a downstream target of Sp8/9. This receptor is expressed in newly born neuroblasts and is required for neuronal differentiation. Thus, Sp8 appears as a key factor influencing major signaling pathways to regulate neuronal differentiation in the postnatal brain. As neurons mature, our results show that Sp8 expression becomes restricted to CalR+ PG interneurons, in line with previous findings (Waclaw et al., 2006; Kosaka and Kosaka, 2012). Interestingly, Sp8 deletion affects CalR+ PG interneurons numbers, while other interneurons subtypes are only minimally affected. This observation may be explained by a role of Sp8 in CalR+ PG interneurons specification, and/or survival. A role of Sp8 in specifying CalR+ PG interneurons is not supported by our results. Indeed, overexpression of Sp8+ in NSCs of the lateral SVZ was not sufficient to generate CalR+ PG interneurons. Inversely, Sp8 knockdown in NSCs of the medial SVZ does not impact the generation of CalR+ PG interneurons, further supporting that this transcription factor is not required for the specification of this interneuron population. In contrast, our results support a role of Sp8 in maintaining CalR+ PG interneurons integrity and survival. Interestingly, the apoptotic phenotype in CalR+ neurons appears to be stronger after delayed Sp8 deletion while TH+ interneurons were not affected, as evidenced by the increase of their relative proportion. A similar survival effect was recently reported in Sp8/Sp9 cKO mice (Li et al., 2017). However, the observed cell death also encompass TH+ neurons suggesting a broad and non-overlapping expression of Sp8 and Sp9 in mature PG interneurons subtypes. The mechanisms involved in the survival of mature CalR+ interneurons remain to be elucidated. This apoptosis is likely to not occur abruptly. Indeed, activated caspase 3 immunodetection did not reveal any peak of synchronized apoptosis at 4 or 10 days following Sp8 depletion. As previously observed in other contexts, apoptosis is likely to occur over extended periods of time and may therefore be difficult to detect at a single time point (Platel et al., 2011). This goes in line with the detection of surviving cells with atrophied morphologies in our experiments. The few CalR+ interneurons that persist after Sp8 ablation exhibit an atrophied arborization, which supports a default in maturation and integration of these PG interneurons.

Our observations all converge in defining Sp8 as a terminal selector gene (TSG). TSGs are TFs that specify and maintain the identity of mature neuron subtypes and insure their survival, maturation and integration. They maintain individual neuronal identities by directly controlling the expression of downstream, terminal differentiation genes. For instance, TSGs maintain the neuronal identity by activating neurotransmitter-type gene batteries encoding the capacity for their synthesis, reuptake, and plasma or vesicular membrane transport (Saucedo-Cardenas et al., 1998; Pattyn et al., 1999; Ding et al., 2003). Other studies also provide intriguing examples of their requirement for maintenance of neuronal connectivity, such as for Nurr1 in dopaminergic neurons (Kadkhodaei et al., 2009). In addition, TSGs are continuously required for survival of post-mitotic neurons through transcriptional maintenance of proper levels of expression of several anti-apoptotic and pro-apoptotic genes (Tsarovina et al., 2010). Although the exact mechanisms by which Sp8 acts remain to be explore, other studies have identified terminal selector genes in the OB as well as in other brain regions, which are likely to act in similar ways. For instance, the TF Pax6 have been suggested to play a role both in the early specification of TH+ interneurons but also in their survival once mature in the OB (Ninkovic et al., 2015). Pax6 modulates apoptotic signaling pathway by regulating the expression of the crystallin αA which prevents caspase 3A activation. Experiments aimed at measuring and possibly rescuing crystallin αA level of expression following Sp8 deletion will be necessary to investigate if similar mechanisms are in play to mediate CalR+ PG interneurons survival.

Our observation of a tight control of CalR+ PG interneurons survival suggests the existence of multiple mechanisms, acting at distinct stages of the neurogenesis process as well as onto different lineages, to control the number of newborn neurons incorporating in the OB circuitry. Such a fine control of the production and maintenance would be necessary if define subtypes of PG interneurons would control different aspects in the treatment of olfactory signal integration. Indeed, the specific properties and distinct connectivity of PG interneurons subtypes (Kosaka and Kosaka, 2005, see also chapter 2) suggest different roles in the treatment of olfactory information (Kosaka and Kosaka, 2005; Panzanelli P. et al., 2007; Parrish-Aungst et al., 2007; Gire and Schoppa, 2009). A tight control of PG interneurons numbers might be key in processing olfaction signal, which remains to be functionally explored. In

this context, transcription factors such as Sp8, acting as terminal selection genes, would therefore allow the number of interneurons of each subtype to be dynamically and finely controlled in order to maintain a functional network. In this context, an olfactory behavioral study following deletion of Sp8 in all mature CalR+ neurons would be a first step in studying such mechanism and its functional impact.

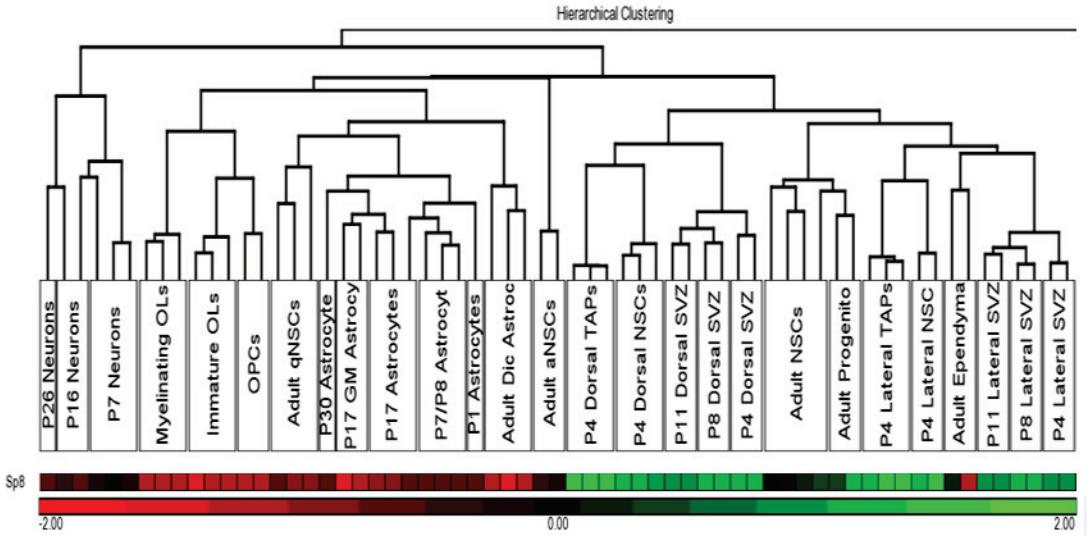

Figure S1: Detection of Sp8 mRNA in neural lineages by microarray

For further examining Sp8 expression within the dorsal and lateral regions of the lateral ventricle, as well as in the cells and lineages they contain and produce, we made use of previously published datasets to perform a meta-analysis (Azim et al., 2015, GSE60905; Cahoy et al., 2008, GSE9566 and Beckervordersandforth et al.; 2010, GSE18765). Sp8 mRNA is detected in all NSCs and TAPs of both the dorsal and lateral SVZ at P4, P8 and P11 and in lesser extent in adult NSCs. This expression is not visible in ependymal cells and glial cells, and is low in cells of the neuronal lineage. The low level of mRNA expression in mature neurons compared to NSCs and TAPs is likely due to the presence of a large variety of neuronal subtypes in the samples analyzed here.

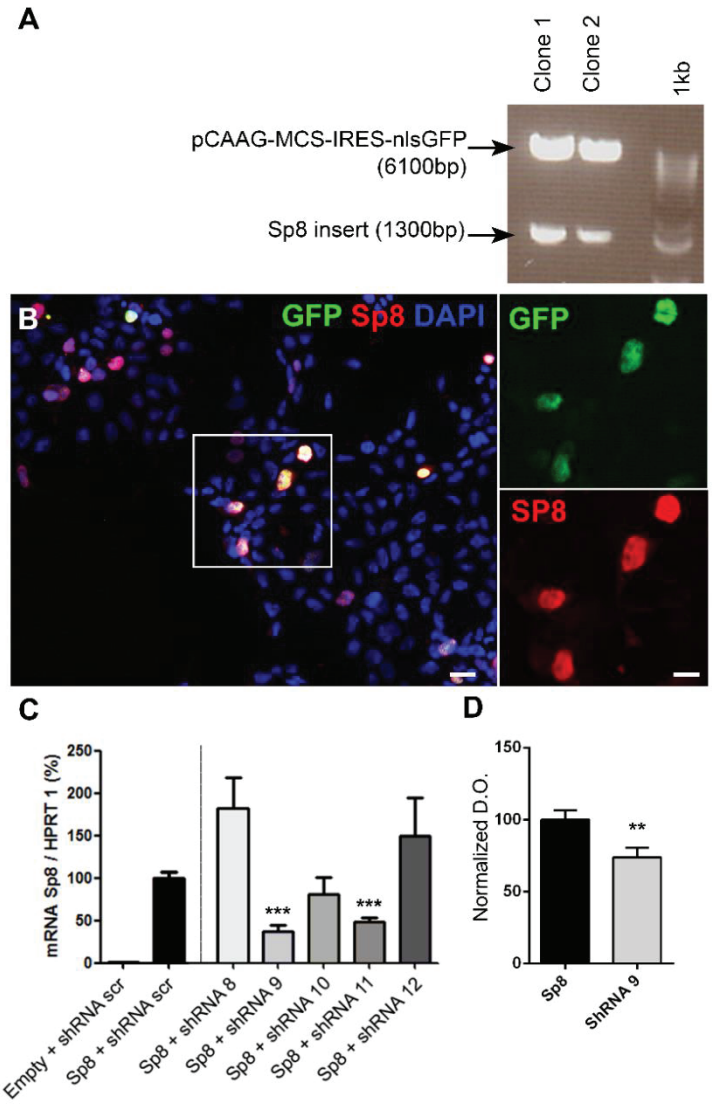

Figure S2: Efficiency of Sp8 knock-down by select shRNA *in-vitro*

(A) PCR products of two Sp8 clones digested with 5'Xho1 & 3' Sac1 restriction enzymes. The presence of two bands indicates successful cloning of Sp8 gene into the pCAAG vector. The upper band indicates the vector (6100bp) and the lower band indicates the desired Sp8 gene (1300bp). (B) Efficient Sp8 expression in HEK cells transfected with Sp8-IRES-GFP plasmid. Transfected cells are identified thanks to GFP signal from the IRES-GFP sequence. Sp8 expression is tested by immunocytochemistry 48 hours after transfection. Non-transfected cells (counterstained with DAPI) do not express basal levels of Sp8, whereas intense staining for Sp8 is observed in GFP+ transfected cells. The nuclear localization of the staining supports the specificity Sp8 expression and Sp8 antibody. (C) Efficiency of five different shRNA (8 to 12) co-transfected with Sp8 transgene in HEK cells. Sp8 mRNA expression was measured by real time PCR. These interfering experiments reveal a better efficiency of shRNA 9, which was therefore selected for all knock-down experiments. Controls correspond to transfection with an Empty plasmid + shRNA scramble. (D) Optical densitometric analysis of Sp8 protein level in HEK cells following interference with shRNA 9, confirming the efficiency of Sp8 knock-down at the protein level. Error bars represent the standard error of the mean; **p<0.01 determined by Unpaired t-test

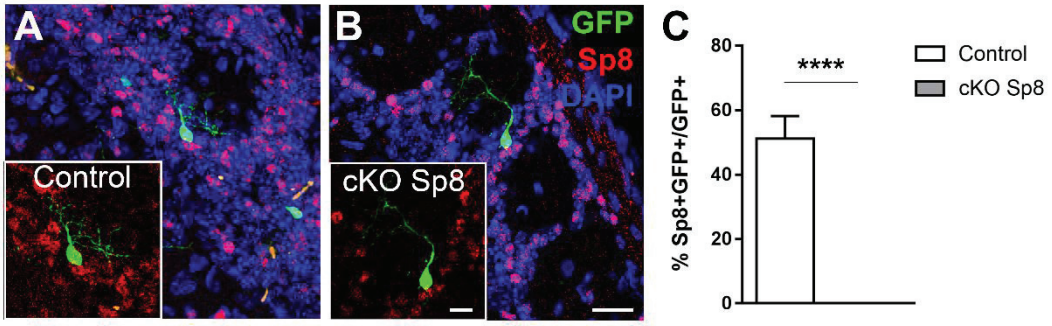

Figure S3: Efficiency of Permanent Sp8 deletion in NSCs and their progeny.

(A-B) Representative immunodetection of Sp8 in PG GFP+ electroporated cells at 21dpe in control (A) and cKO Sp8 animal (B). Scale bars: 10µm and 20µm. (C) Proportion of electroporated PG neurons expressing Sp8 at 21 dpe in control and cKO animals. Error bars represent the standard error of the mean; ****p≤0.0001 determined unpaired t-test

Azim K, Hurtado-Chong A, Fischer B, Kumar N, Zweifel S, Taylor V, Raineteau O (2015) Transcriptional Hallmarks of Heterogeneous Neural Stem Cell Niches of the Subventricular Zone. Stem Cells 33:2232–2242.

Beckervordersandforth R, Tripathi P, Ninkovic J, Bayam E, Lepier A, Stempfhuber B, Kirchhoff F, Hirrlinger J, Haslinger A, Lie DC, Beckers J, Yoder B, Irmler M, Götz M (2010) In vivo fate mapping and expression analysis reveals molecular hallmarks of prospectively isolated adult neural stem cells. Cell Stem Cell 7:744–758.

Borello U, Madhavan M, Vilinsky I, Faedo A, Pierani A, Rubenstein J, Campbell K (2014) Sp8 and COUP-TF1 reciprocally regulate patterning and fgf signaling in cortical progenitors. Cereb Cortex 24:1409–1421.

Boutin C, Diestel S, Desoeuvre A, Tiveron MC, Cremer H (2008) Efficient in vivo electroporation of the postnatal rodent forebrain. PLoS One 3:e1883

Cahoy JD, Emery B, Kaushal A, Foo LC, Zamanian JL, Christopherson KS, Xing Y, Lubischer JL, Krieg PA, Krupenko SA, Thompson WJ, Barres BA (2008) A transcriptome database for astrocytes, neurons, and oligodendrocytes: a new resource for understanding brain development and function. J Neuroscience 28:264-278

Deneris ES, Hobert O (2015) Maintenance of postmitotic neuronal cell identity Evan. Nat Neurosci 17:899–907.

Ding Y-Q, Marklund U, Yuan W, Yin J, Wegman L, Ericson J, Deneris E, Johnson RL, Chen Z-F (2003) Lmx1b is essential for the development of serotonergic neurons. Nat Neurosci 6:933–938

Fernández ME, Croce S, Boutin C, Cremer H, Raineteau O (2011) Targeted electroporation of defined lateral ventricular walls: a novel and rapid method to study fate specification during postnatal forebrain neurogenesis. Neural Dev 6:13.

Fiorelli R, Azim K, Fischer B, Raineteau O (2015) Adding a spatial dimension to postnatal ventricular-subventricular zone neurogenesis. Development 142:2109–2120.

Gire DH, Schoppa NE (2009) Control of on/off glomerular signaling by a local GABAergic microcircuit in the olfactory bulb. J Neurosci 9:19–22.

Griesel G, Treichel D, Collombat P, Krull J, Zembrzycki A, van den Akker WMR, Gruss P, Simeone A, Mansouri A (2006) Sp8 controls the anteroposterior patterning at the midbrain-hindbrain border. Development 133:1779–1787.

Kadkhodaei B, Ito T, Joodmardi E, Mattsson B, Rouillard C, Carta M, Muramatsu S-I, Sumi-Ichinose C, Nomura T, Metzger D, Chambon P, Lindqvist E, Larsson N-G, Olson L, Bjorklund A, Ichinose H, Perlmann T (2009) Nurr1 Is Required for Maintenance of Maturing and Adult Midbrain Dopamine Neurons. J Neurosci 29:15923–15932

Kohwi M, Petryniak MA, Long JE, Ekker M, Obata K, Yanagawa Y, Rubenstein JL, Alvarez-Buylla A (2007) A subpopulation of olfactory bulb GABAergic interneurons is derived from Emx1- and Dlx5/6-expressing progenitors. J Neurosci 27:6878–6891.

Kosaka K, Kosaka T (2005) Synaptic organization of the glomerulus in the main olfactory bulb: Compartments of the glomerulus and heterogeneity of the periglomerular cells. Anat Sci Int 80:80–90

Kosaka T, Kosaka K (2012) Further characterization of the juxtaglomerular neurons in the mouse main olfactory bulb by transcription factors, Sp8 and Tbx21. Neurosci Res 73:24–31.

Li J et al. (2017) Transcription Factors Sp8 and Sp9 Coordinately Regulate Olfactory Bulb Interneuron Development. Cereb Cortex:1–17

Ninkovic J, Pinto L, Petricca S, Lepier A, Sun J, Rieger M a, Schroeder T, Cvekl A, Favor J, Sciences V (2015) The transcription factor Pax6 regulates survival of dopaminergic olfactory bulb neurons via crystallin αA. Neuron 68:682–694.

Panzanelli P., Fritschy JM, Yanagawa Y, Obata K, M.Sassoè-Pogneto (2007) GABAergic Phenotype of Periglomerular Cells in the Rodent Olfactory Bulb. J Comp Neurol 502:990–1002.

Parrish-Aungst S, Shipley MT, Erdelyi F, Szabo G, Puche AC (2007) Quantitative Analysis of Neuronal Diversity in the Mouse Olfactory Bulb. J Comp Neurol 501:825–836.

Pattyn A, Morin X, Cremer H, Goridis C, Brunet JF (1999) The homeobox gene Phox2b is essential for the development of autonomic neural crest derivatives. Nature 399:366–370

Platel J, Dave KA, Gordon V, Lacar B, Maria E, Bordey A (2011) NMDA receptors activated by subventricular zone astrocytic glutamate are critical for neuroblast survival prior to entering a synaptic network. Neuron 65:859–872.

Saucedo-Cardenas O, Quintana-Hau JD, Le WD, Smidt MP, Cox JJ, De Mayo F, Burbach JP, Conneely OM (1998) Nurr1 is essential for the induction of the dopaminergic phenotype and the survival of ventral mesencephalic late dopaminergic precursor neurons. Proc Natl Acad Sci U S A 95:4013–4018

Treichel D, Schöck F, Jäckle H, Gruss P, Mansouri A (2003) mBtd is required to maintain signaling during murine limb development. Genes Dev 17:2630–2635.

Tsarovina K, Reiff T, Stubbusch J, Kurek D, Grosveld FG, Parlato R, Schütz G, Rohrer H (2010) The Gata3 transcription factor is required for the survival of embryonic and adult sympathetic neurons. J Neurosci 30:10833–10843.

Waclaw RR, Allen ZJ, Bell SM, Erdélyi F, Szabó G, Potter SS, Campbell K (2006) The zinc finger transcription factor Sp8 regulates the generation and diversity of olfactory bulb interneurons. Neuron 49:503–516.

Zembrzycki A, Griesel G, Stoykova A, Mansouri A (2007) Genetic interplay between the transcription factors Sp8 and Emx2 in the patterning of the forebrain. Neural Dev 2:8

VII. GENERAL DISCUSSION AND PERSPECTIVES

VII.1. Origin and coding of CalR+ interneurons over space and time

CalR+ interneurons are the predominant cell type produced in the glomerular cell layer during postnatal life. Because of their restricted spatial origin, it suggests that germinal activity of some SVZ microdomains gradually become dominant in producing PG interneurons over postnatal life (Merkle et al., 2007; Batista-Brito et al., 2008). Thus, specific progenitor domains might become prevalent in the production of specific OB interneurons subtypes during specific time windows. First evidences for such dynamic temporal changes are given by our permanent labeling and fate mapping analysis of NSCs residing in specific SVZ microdomains. Our results describe a massive decrease in the generation of OB interneurons by all SVZ walls in the first few weeks after birth. The dynamic of this drop however differs between walls, with a faster drop in the medial SVZ compared to the dorsal and lateral ones. Because of the dual origin of CalR+ PG interneurons (i.e. from the medial and dorsal walls), it is likely that dorsal SVZ progenitors relay medial progenitors in the production of this interneurons subtype. Alternatively, other more rostral regions, which are not labeled by the electroporation approach, may become dominant in producing PG interneurons as previously suggested (Hack et al., 2005). The temporal dynamics of this regional germinal activity, its impact on the production of specific OB interneuron subtypes and its functional significance remain to be fully explored. It is indeed tempting to speculate that production of specific OB interneuron subtypes is critical in shaping aspects of olfaction that become critical at defined postnatal time or under specific environmental constrains. In line with this hypothesis is the recent demonstration of a regulation of regionally distinct adult neural stem cells and neurogenesis by hypothalamic inputs (Paul et al., 2017). In this study, hunger and satiety regulate adult neurogenesis by modulating the activity of this regional hypothalamic-SVZ connection to recruit distinct NSC pools, allowing on-demand neurogenesis in response to physiology and environmental signals.

The restricted spatial origin and immature properties of CalR+ PG interneurons represent a unique opportunity for exploring the transcriptional mechanisms controlling their specification and delayed maturation. Our transgenic manipulations of Sp8 expression revealed that Sp8 is not involved in CalR+ PG interneurons specification. Thus, the TFs involved in CalR neurons specification remain to be identified. The medial SVZ originates from the embryonic septum.

Several TFs are expressed in the septum and persist in the postnatal SVZ such as Nkx6.2 and Zic proteins, that are likely be involved in CalR+ interneurons specification (Merkle et al., 2014). Zic proteins are highly expressed in the medial and dorsal SVZ, but are consistently absent from the lateral SVZ. For instance, a whole genome comparative transcriptome analysis revealed enrichment of Zic2 and Zic3 in the dorsal SVZ, a region that give rise to CalR+ interneurons (Azim et al., 2015). While Zic3 expression is restricted to NSCs, Zic2 persists in their immediate progeny. Furthermore, 40% of PG cells produced by NSCs labeled in the medial wall of the anterior ventral SVZ express Zic 1/3 (Merkle et al., 2014). As a consequence, the role of Zic proteins in CalR+ PG interneurons specification has recently been studied. Manipulation of Zic1/2 in the dorsal SVZ induces the generation of CalR+ neurons while suppressing dopaminergic fate by competing with Pax6 (Tiveron et al., 2017). Because of the dual origin of CalR+ PG interneurons, it would be of particular interest to investigate in more details the pattern of expression and function of Zic proteins in the medial and dorsal SVZ. Additional TFs could also be involved in CalR+ PG interneuron specification. Indeed, fate mapping studies indicate that Zic3-expressing progenitors only give rise to a fraction (~20%) of CalR+ PG interneurons (Qin et al., 2015). In addition, a conditional inactivation of Gsh2 in the septum, results in impaired generation of Sp8-positive neuroblasts as well as reduced cell proliferation within the medial SVZ. It remains to be investigated if these effects are dependent on Zic proteins expression. The isolation of CalR+ PG interneurons in the CalR::EGFP mice model would allow the characterization of their transcriptional profile, as previously performed for SVZ progenitors (Azim et al., 2015) and the identification of new TFs associated with the CalR lineage.

VII.2. Role of CalR+ PG interneurons in the glomerular network

The OB is a highly plastic region where sensory-driven experience modulates odor responsiveness, discrimination and memory. At the cellular level, olfactory enrichment promotes the survival of newborn granule and PG cells (Rochefort and Lledo, 2005; Bovetti et al., 2009; Moreno et al., 2009), refines newborn PG cells synaptic connectivity (Livneh et al., 2014) and decreases principal neurons responsiveness (Buonviso and Chaput, 1999). Altogether, these evidences suggest that inhibition mediated by newborn neurons provide a major source of functional plasticity to the OB network. In this context, the role of CalR+ PG interneurons, which

remain weakly connected and active, is particularly puzzling. We can hypothesize that these “dormant” CalR+ PG interneurons represent a “reserve pool” of interneurons whose maturation and integration in the pre-existing glomerular network await to be triggered or accelerated by sensory driven experience. CalR+ PG interneurons production reaches a pick during the first weeks of postnatal life (Batista-Brito et al., 2008), a critical period when newborn animals need to integrate and interpret new odors. It is therefore tempting to imagine that CalR+ PG interneurons would be recruited by odor enrichment or sensory experience. In contrast, our laboratory animals are raised in closed cages and are therefore not exposed to such variety of odors. The enrichment of their environment with a mixture of odorants would induce a broad activation of OB circuits (Rochefort et al., 2002; Woo et al., 2008). This would allow studying the consequence of olfactory enrichment on CalR+ PG interneurons maturation by electrophysiological and histological means. This could be complemented by analysis of GAD67 expression by CalR+ PG interneurons. Indeed, TH+ and CalB+ PG interneurons express the GABAergic synthesizing enzyme GAD (80% of TH+ and 65% of CalB+ cells express GAD), the majority of which express the GAD67 isoform. In contrast, CalR+ PG interneurons are not all positive for GAD, and almost exclusively express GAD65 (Parrish-Aungst et al., 2007). In many brain regions GAD67 expression is dependent on neural activity (Gomez-Lira, 2005), while GAD65 expression is generally activity-independent. Whether the two GAD isoforms are differentially regulated by neural activity in CalR+ PG interneurons would be of interest to investigate.

It should however be noted that in accordance with the very restricted map of individual odorants in the GL, the recruitment of CalR+ PG interneurons by odor enrichment may be restricted to only few glomeruli, and may therefore be difficult to demonstrate. An optogenetic approach may allow circumventing this problem by allowing a more global stimulation of OB glomeruli. CalR+ PG interneurons are type II PG cells which should be recruited by principal projection neurons (i.e. mitral and tufted cells) (Kosaka and Kosaka, 2007). External tufted cells are specific glutamatergic neurons located in the superficial region of the EPL and which drive the activity of olfactory glomeruli (De Saint Jan et al., 2009). Therefore, the expression of ChR2 in external tufted or in olfactory sensory neurons would allow investigating the recruitment of CalR+ interneurons by neuronal activity.

VII.3. Molecular mechanisms of neuronal maturation and integration

CalR+ PG interneurons remain an enigmatic population of cells, which keep some secrets. About 50% of newly generated neurons in the postnatal brain are eliminated in the first days after their arrival in the OB, in an activity dependent manner (Petreanu and Alvarez-Buylla, 2002). The mechanisms implicated in the long-term survival of CalR+ PG interneurons, despite of their weak synaptic integration, remain to be fully explored. Indeed, it is generally accepted that synaptic integration is necessary for trophic support and long-term survival of newborn neurons during both embryonic development and postnatal life (see fo example Naruse and Keino, 1995). Our results show that the TF Sp8 is expressed specifically in CalR+ interneurons, while it is downregulated in TH+ and CalB+ interneurons. This suggests that Sp8 may be essential for the survival of immature, largely non-synaptically integrated, interneurons. Sp8-expressing interneurons are also observed in other brain region in physiological conditions as well as following stroke or ischemic injuries (Liu et al., 2009; Wei et al., 2011). It would be particularly interesting to study if these neurons share the same immature properties than CalR+ PG interneurons. In addition, conditional manipulation of Sp8 expression in select populations of neurons, may allow studying its role in maturation and survival. Finally, a transcriptional analysis of CalR+ PG interneurons pre and post Sp8 deletion would allow exploring the downstream targets of this TF and to decipher the molecular mechanisms by which it affects neuronal maturation and integration.

VIII. BIBLIOGRAPHY

BIBLIOGRAPHY

Allen ZJ, Waclaw RR, Colbert MC, Campbell K (2007) Molecular identity of olfactory bulb interneurons: Transcriptional codes of periglomerular neuron subtypes. J Mol Histol 38:517–525.

Alonso M, Viollet C, Gabellec M-M, Meas-Yedid V, Olivo-Marin J-C, Lledo P-M (2006) Olfactory Discrimination Learning Increases the Survival of Adult-Born Neurons in the Olfactory Bulb. J Neurosci 26:10508–10513.

Alvarez-Buylla A, García-Verdugo JM, Tramontin AD (2001) A unified hypothesis on the lineage of neural stem cells. Nat Rev Neurosci 2:287–293.

Alves JAJ, Barone P, Engelender S, Fróes MM, Menezes JRL (2002) Initial stages of radial glia astrocytic transformation in the early postnatal anterior subventricular zone. J Neurobiol 52:251–265.

Anderson SA, Eisenstat DD, Shi L, Rubenstein JLR (1997) Interneuron Migration from Basal Forebrain to Neocortex: Dependence on Dlx Genes. Science (80-) 278:474–476.

Anthony TE, Klein C, Fishell G, Heintz N (2004) Radial glia serve as neuronal progenitors in all regions of the central nervous system. Neuron 41:881–890.

Arevian AC, Kapoor V, Urban NN (2008) Activity-dependent gating of lateral inhibition in the mouse olfactory bulb. Nat Neurosci 11:80–87.

Azim K, Hurtado-Chong A, Fischer B, Kumar N, Zweifel S, Taylor V, Raineteau O (2015) Transcriptional Hallmarks of Heterogeneous Neural Stem Cell Niches of the Subventricular Zone. Stem Cells 33:2232–2242.

Bailey MS, Puche AC, Shipley MT (1999) Development of the olfactory bulb: Evidence for glia-neuron interactions in glomerular formation. J Comp Neurol 415:423–448.

Balu R, Pressler RT, Strowbridge BW (2007) Multiple Modes of Synaptic Excitation of Olfactory Bulb Granule Cells. J Neurosci 27:5621–5632.

Batista-Brito R, Close J, Machold R, Fishell G (2008) The distinct temporal origins of olfactory bulb interneuron subtypes. J Neurosci 28:3966–3975.

Bayer SA (1983) 3H-Thymidine-radiographic Studies of Neurogenesis in the Rat Olfactory Bulb. Exp Brain Res 50:329–340.

Bell SM, Schreiner CM, Waclaw RR, Campbell K, Potter SS, Scott WJ (2003) Sp8 is crucial for limb outgrowth and neuropore closure. Proc Natl Acad Sci U S A 100:12195–12200

Belluscio L, Lodovichi C, Feinstein P, Mombaerts P, Katz LC (2002) Odorant receptors instruct functional circuitry in the mouse olfactory bulb. Nature 419:296–300.

Biebl M, Cooper CM, Winkler J, Kuhn HG (2000) Analysis of neurogenesis and programmed cell death reveals a self-renewing capacity in the adult rat brain. Neurosci Lett 291:17–20.

Blanchart A, De Carlos JA, Lopez-Mascaraque L (2006) Time Frame of Mitral Cell Development in the Mice Olfactory Bulb. J Comp Neurol 496:529–543.

Bolteus AJ, Bordey A (2004) GABA Release and Uptake Regulate Neuronal Precursor Migration in the Postnatal Subventricular Zone. J Neurosci 24:7623–7631.

Boutin C, Hardt O, de Chevigny A, Coré N, Goebbels S, Seidenfaden R, Bosio A, Cremer H (2010) NeuroD1 induces terminal neuronal differentiation in olfactory neurogenesis. Proc Natl Acad Sci U S A 107:1201–1206.

Bouwman P, Philipsen S (2002) Regulation of the activity of Sp1-related transcription factors. Mol Cell Endocrinol 195:27–38.

Bovetti S, Veyrac A, Peretto P, Fasolo A, de Marchis S (2009) Olfactory enrichment influences adult neurogenesis modulating GAD67 and plasticity-related molecules expression in newborn cells of the olfactory bulb. PLoS One 4:e6359

Breton-Provencher V, Bakhshetyan K, Hardy D, Bammann RR, Cavarretta F, Snapyan M, Côté D, Migliore M, Saghatelyan A (2016) Principal cell activity induces spine relocation of adult-born interneurons in the olfactory bulb. Nat Commun 7:12659.

Breton-Provencher V, Saghatelyan A (2012) Newborn neurons in the adult olfactory bulb: Unique properties for specific odor behavior. Behav Brain Res 227:480–489.

Bribian A, Figueres-Onate M, Martin-Lopez E, Lopez-Mascaraque L (2016) Decoding astrocyte heterogeneity: New tools for clonal analysis. Neuroscience 323:10–19.

Brill MS et al. (2009) Adult generation of glutamatergic olfactory bulb interneurons. Nat Neurosci 12:1524–1533.

Brill MS, Snapyan M, Wohlfrom H, Ninkovic J, Jawerka M, Mastick GS, Ashery-Padan R, Saghatelyan A, Berninger B, Götz M (2008) A dlx2- and pax6-dependent transcriptional code for periglomerular neuron specification in the adult olfactory bulb. J Neurosci 28:6439–6452

Britz O, Mattar P, Nguyen L, Langevin LM, Zimmer C, Alam S, Guillemot F, Schuurmans C (2006) A role for proneural genes in the maturation of cortical progenitor cells. Cereb Cortex 16.

Buck L, Axel R (1991) A novel multigene family may encode odorant receptors: A molecular basis for odor recognition. Cell 65:175–187.

Bultje RS, Castaneda-castellanos DR, Jan LY, Jan Y, Kriegstein AR, Shi S (2009) Mammalian Par3 regulates progenitor cell asymmetric division via Notch signaling in the developing neocortex. Neuron 63:189–202.

Buonviso N, Chaput M (1999) Olfactory experience decreases responsiveness of the olfactory bulb in the adult rat. Neuroscience 95:325–332.

Calzolari F, Michel J, Baumgart EV, Theis F, Götz M, Ninkovic J (2015) Fast clonal expansion and limited neural stem cell self-renewal in the adult subependymal zone. Nat Neurosci 18:90-92

Campbell K, Götz M (2002) Radial glia : for vertebrate brain development. Trends Neurosci 25:235–238.

Carleton A, Petreanu LT, Lansford R, Alvarez-Buylla A, Lledo P-M (2003) Becoming a new neuron in the adult olfactory bulb. Nat Neurosci 6:507–518.

Casper KB, McCarthy KD (2006) GFAP-positive progenitor cells produce neurons and oligodendrocytes throughout the CNS. Mol Cell Neurosci 31:676–684.

Cheng L-C, Pastrana E, Tavazoie M, Doetsch F (2009) miR-124 regulates adult neurogenesis in the SVZ stem cell niche. Nat Neurosci 12:399–408.

Chiu K, Greer CA (1996) Immunocytochemical analyses of astrocyte development in the olfactory bulb. Dev Brain Res 95:28–37.

Codega P, Silva-Vargas V, Paul A, Maldonado-Soto AR, DeLeo AM, Pastrana E, Doetsch F (2015) Prospective identification and purification of quiescent adult neural stem cells from their in vivo niche. Neuron 82:545–559.

Conover JC, Doetsch F, Garcia-Verdugo JM, Gale NW, Yancopoulos GD, Alvarez-Buylla A (2000) Disruption of Eph/ephrin signaling affects migration and proliferation in the adult subventricular zone. Nat Neurosci 3:1091–1097.

Corbin JG, Gaiano N, Machold RP, Langston A, Fishell G (2000) The Gsh2 homeodomain gene controls multiple aspects of telencephalic development. Development 127:5007–5020

Costa MR, Wen G, Lepier A, Schroeder T, Gotz M (2007) Par-complex proteins promote proliferative progenitor divisions in the developing mouse cerebral cortex. Development 135:11–22

Couper Leo JM, Devine AH, Brunjes PC (2000) Focal denervation alters cellular phenotypes and survival in the developing rat olfactory bulb: a developmental analysis. J Comp Neurol 425:409–421.

Curto GG, Nieto-Estévez V, Hurtado-Chong A, Valero J, Gómez C, Alonso JR, Weruaga E, Vicario-Abejón C (2014) Pax6 Is Essential for the Maintenance and Multi-Lineage Differentiation of Neural Stem Cells, and for Neuronal Incorporation into the Adult Olfactory Bulb. Stem Cells Dev 23:1–61

Davis BJ, Macrides F (1981) The organization of centrifugal projections from the anterior olfactory nucleus, ventral hippocampal rudiment, and piriform cortex to the main olfactory bulb in the hamster: An autoradiographic study. J Comp Neurol 203:475–493.

de Chevigny A, Core N, Follert P, Wild S, Bosio A, Yoshikawa K, Cremer H, Beclin C (2012) Dynamic expression of the pro-dopaminergic transcription factors Pax6 and Dlx2 during postnatal olfactory bulb neurogenesis. Front Cell Neurosci 6:1–8.

De Saint Jan D, Hirnet D, Westbrook GL, Charpak S (2009) External Tufted Cells Drive the Output of Olfactory Bulb Glomeruli. J Neurosci 29:2043–2052

Dellovade TL, Pfaff DW, Schwanzel-Fukuda M (1998) Olfactory bulb development is altered in small-eye (Sey) mice. J Comp Neurol 402:402–418.

Deneris ES, Hobert O (2015) Maintenance of postmitotic neuronal cell identity Evan. Nat Neurosci 17:899–907.

Dimou L, Simon C, Kirchhoff F, Takebayashi H, Gotz M (2008) Progeny of Olig2-Expressing Progenitors in the Gray and White Matter of the Adult Mouse Cerebral Cortex. J Neurosci 28:10434–10442

Doetsch F (2003) The glial identity of neural stem cells. Nat Neurosci 6:1127–1134.

Doetsch F, Caille I, Lim DA, García-Verdugo JM, Alvarez-Buylla A (1999) Subventricular zone astrocytes are neural stem cells in the adult mammalian brain. Cell 97:703–716.

Doetsch F, García-Verdugo JM, Alvarez-Buylla a, García-Verdugo A, Alvarez-Buylla J (1997) Cellular Composition and Three-Dimensional Organization of the Subventricular Germinal Zone in the Adult Mammalian Brain. J Neurosci 17(13):5046–5061

Dong H-W, Hayar A, Ennis M (2007) Activation of group I metabotropic glutamate receptors on main olfactory bulb granule cells and periglomerular cells enhances synaptic inhibition of mitral cells. J Neurosci 27:5654–5663

Dubacq C, Fouquet C, Trembleau A (2014) Making scent of the presence and local translation of odorant receptor mRNAs in olfactory axons. Dev Neurobiol 74:259–268.

Eisenstat DD, Liu J, Mione M, Zhong W, Yu G, Anderson SA, Ghattas I, Puelles L, Rubenstein JLR (1999) Define Distinct Stages of Basal Forebrain Differentiation. J Comp Neurol 414:217–237.

Eroglu C, Barres BA (2010) Regulation of synaptic connectivity by glia. Nature 468:223–231.

Farkas LM, Huttner WB (2008) The cell biology of neural stem and progenitor cells and its significance for their proliferation versus differentiation during mammalian brain development. Curr Opin Cell Biol 20:707–715

Fernández ME, Croce S, Boutin C, Cremer H, Raineteau O (2011) Targeted electroporation of defined lateral ventricular walls: a novel and rapid method to study fate specification during postnatal forebrain neurogenesis. Neural Dev 6:13.

Fiorelli R, Azim K, Fischer B, Raineteau O (2015) Adding a spatial dimension to postnatal ventricular-subventricular zone neurogenesis. Development 142:2109–2120.

Firestein S (2001) How the olfactory system makes sense of scents. Nature 413:211–218.

Fode C, Ma Q, Casarosa S, Ang SL, Anderson DJ, Guillemot F (2000) A role for neural determination genes in specifying the dorsoventral identity of telencephalic neurons. Genes Dev 14:67–80.

Fuentealba LCC, Rompani SBB, Parraguez JII, Obernier K, Romero R, Cepko CLL, Alvarez-Buylla A (2015) Embryonic Origin of Postnatal Neural Stem Cells. Cell 161:1644–1655

Fukunaga I, Berning M, Kollo M, Schmaltz A, Schaefer AT (2012) Two Distinct Channels of Olfactory Bulb Output. Neuron 75:320–329.

Fukunaga I, Herb J, Kollo M, Boyden ES, Andreas T (2014) Independent control of gamma and theta activity by distinct interneuron networks in the olfactory bulb Nat Neurosci 17:1208–1216.

Furutachi S, Miya H, Watanabe T, Kawai H, Yamasaki N, Harada Y, Imayoshi I, Nelson M, Nakayama KI, Hirabayashi Y, Gotoh Y (2015) Slowly dividing neural progenitors are an embryonic origin of adult neural stem cells. Nat Neurosci 18:657–665

Gaiano N, Nye JS, Fishell G (2000) Radial Glial Identity Is Promoted by Notch1 Signaling in the Murine Forebrain. Neuron 26:395–404

García-Marqués J, López-Mascaraque L (2013) Clonal identity determines astrocyte cortical heterogeneity. Cereb Cortex 23:1463–1472.

García-Marqués J, López-Mascaraque L (2016) Clonal Mapping of Astrocytes in the Olfactory Bulb and Rostral Migratory Stream. Cereb cortex 27:2195–2209.

Geramita MA, Burton SD, Urban NN (2016) Distinct lateral inhibitory circuits drive parallel processing of sensory information in the mammalian olfactory bulb. Elife 5:1–22.

Giachino C, Basak O, Lugert S, Knuckles P, Obernier K, Fiorelli R, Frank S, Raineteau O, Alvarez–Buylla A, Taylor V (2014) Molecular Diversity Subdivides the Adult Forebrain Neural Stem Cell Population. Stem Cells 32:70–84.

Giorgi-gerevini V Di, Melchiorri D, Battaglia G (2005) Endogenous activation of metabotropic glutamate receptors supports the proliferation and survival of neural progenitor cells. Cell death and differentiation 12:1124–1133.

Gomez-Lira G (2005) Programmed and Induced Phenotype of the Hippocampal Granule Cells. J Neurosci 25:6939–6946

Gong Q, Shipley MT (1995) Evidence that pioneer olfactory axons regulate telencephalon cell cycle kinetics to induce the formation of the olfactory bulb. Neuron 14:91–101.

Gonzalez-Perez O, Alvarez-buylla A (2011) Oligodendrogenesis in the subventricular zone and the role of epidermal growth factor. Brain Res Rev 67:147–156.

Gritti A, Bonfanti L, Doetsch F, Caille I, Alvarez-Buylla A, Lim DA, Galli R, Verdugo JM, Herrera DG, Vescovi AL (2002) Multipotent neural stem cells reside into the rostral extension and olfactory bulb of adult rodents. J Neurosci 22:437–445

Haberly LB, Price JL (1978) Association and commissural fiber systems of the olfactory cortex of the rat. I. Systems originating in the piriform cortex and adjacent areas. J Comp Neurol 178:711–740.

Hack I, Bancila M, Loulier K, Carroll P, Cremer H (2002) Reelin is a detachment signal in tangential chain-migration during postnatal neurogenesis. Nat Neurosci 5:939–945

Hack MA, Saghatelyan A, de Chevigny A, Pfeifer A, Ashery-Padan R, Lledo P-M, Götz M (2005) Neuronal fate determinants of adult olfactory bulb neurogenesis. Nat Neurosci 8:865–872.

Harrison SM, Houzelstein D, Dunwoodie SL, Beddington RSP (2000) Sp5 , a New Member of the Sp1 Family, Is Dynamically Expressed during Development and Genetically Interacts with Brachyury. Developmental Biology 372:358–372.

Hebert JM (2003) FGF signaling through FGFR1 is required for olfactory bulb morphogenesis. Development 130:1101–1111

Herculano-Houzel S (2014) The glia/neuron ratio: How it varies uniformly across brain structures and species and what that means for brain physiology and evolution. Glia 62:1377–1391.

Hevner RF, Hodge RD, Daza RAM, Englund C (2006) Transcription factors in glutamatergic neurogenesis: Conserved programs in neocortex, cerebellum, and adult hippocampus. Neurosci Res 55:223–233.

Hildebrand JG, Shepherd GM (1997) Mechanisms of olfactory discrimination : Converging Evidence for Common Principles Across Phyla. :595–631.

Hinds JW (1968a) Autoradiographic Study of Histogenesis in the Mouse Olfactory Bulb. I. Time of origin of neurons and neuroglia. J Comp Neurol 134:287–304.

Hinds JW (1968b) Autoradiographic study of histogenesis in the mouse olfactory bulb. II. Cell proliferation and migration. J Comp Neurol 134:305–322.

Hoch R V., Rubenstein JLR, Pleasure S (2009) Genes and signaling events that establish regional patterning of the mammalian forebrain. Semin Cell Dev Biol 20:378–386.

Houades V, Rouach N, Ezan P, Kirchhoff F, Koulakoff A, Giaume C (2006) Shapes of astrocyte network in the juvenile brain. Neuron Glia Biology 2:3-14

Hurtado-Chong A, Yusta-Boyo MJ, Vergaño-Vera E, Bulfone A, De Pablo F, Vicario-Abejón C (2009) IGF-I promotes neuronal migration and positioning in the olfactory bulb and the exit of neuroblasts from the subventricular zone. Eur J Neurosci 30:742–755.

Igarashi KM, Ieki N, An M, Yamaguchi Y, Nagayama S, Kobayakawa K, Kobayakawa R, Tanifuji M, Sakano H, Chen WR, Mori K (2012) Parallel mitral and tufted cell pathways route distinct odor information to different targets in the olfactory cortex. J Neurosci 32:7970–7985.

Imai T (2014) Construction of functional neuronal circuitry in the olfactory bulb. Semin Cell Dev Biol 35:180–188

Imamura F, Ayoub AE, Rakic P, Greer CA (2011) Timing of neurogenesis is a determinant of olfactory circuitry. Nat Neurosci 14:331–337.

Imayoshi I, Sakamoto M, Ohtsuka T, Takao K, Miyakawa T, Yamaguchi M, Mori K, Ikeda T, Itohara S, Kageyama R (2008) Roles of continuous neurogenesis in the structural and functional integrity of the adult forebrain. Nat Neurosci 11:1153–1161

Inaki K, Nishimura S, Nakashiba T, Itohara S, Yoshihara Y (2004) Laminar organization of the developing lateral olfactory tract revealed by differential expression of cell recognition molecules. J Comp Neurol 479:243–256.

Jiang X, Zhang M, You Y, Liu F (2013) The production of somatostatin interneurons in the olfactory bulb is regulated by the transcription factor sp8. PLoS One 8:e70049

Jiménez D, García C, De Castro F, Chédotal A, Sotelo C, De Carlos JA, Valverde F, López-Mascaraque L (2000) Evidence for intrinsic development of olfactory structures in Pax-6 mutant mice. J Comp Neurol 428:511–526.

Kadkhodaei B, Alvarsson A, Schintu N, Ramskold D, Volakakis N, Joodmardi E, Yoshitake T, Kehr J, Decressac M, Bjorklund A, Sandberg R, Svenningsson P, Perlmann T (2013) Transcription factor Nurr1 maintains fiber integrity and nuclear-encoded mitochondrial gene expression in dopamine neurons. Proc Natl Acad Sci 110:2360–2365

Kadkhodaei B, Ito T, Joodmardi E, Mattsson B, Rouillard C, Carta M, Muramatsu S-I, Sumi-Ichinose C, Nomura T, Metzger D, Chambon P, Lindqvist E, Larsson N-G,

Olson L, Bjorklund A, Ichinose H, Perlmann T (2009) Nurr1 Is Required for Maintenance of Maturing and Adult Midbrain Dopamine Neurons. J Neurosci 29:15923–15932

Kaplan MS (1985) Formation and Turnover of Neurons in Young and Senescent Animals: An Electronmicroscopic and Morphometric Analysis. Ann N Y Acad Sci 457:173–192.

Kasberg AD, Brunskill EW, Potter SS (2013) SP8 regulates signaling centers during craniofacial development. Dev Biol.

Kawakami Y (2004) Sp8 and Sp9, two closely related buttonhead-like transcription factors, regulate Fgf8 expression and limb outgrowth in vertebrate embryos. Development 131:4763–4774

Ke M-T, Fujimoto S, Imai T (2013) SeeDB: a simple and morphology-preserving optical clearing agent for neuronal circuit reconstruction. Nat Neurosci 16:1154–1161

Kelsch W, Lin C, Lois C (2008) Sequential development of synapses in dendritic domains during adult neurogenesis. PNAS 105:16803–16808.

Kelsch W, Mosley CP, Lin C-W, Lois C (2007) Distinct mammalian precursors are committed to generate neurons with defined dendritic projection patterns. PLoS Biol 5:e300

Khakh BS, Sofroniew M V, Angeles L, Angeles L (2015) Diversity of astrocyte functions and phenotypes in neural circuits. Nat Neurosci 18:942–952.

Kobayakawa K, Kobayakawa R, Matsumoto H, Oka Y, Imai T, Ikawa M, Okabe M, Ikeda T, Itohara S, Kikusui T, Mori K, Sakano H (2007) Innate versus learned odour processing in the mouse olfactory bulb. 450.

Kohwi M, Doe CQ (2013) Temporal fate specification and neural progenitor competence during development. Nat Rev Neurosci 14:823–838

Kohwi M, Osumi N, Rubenstein JLR, Alvarez-Buylla A (2005) Pax6 is required for making specific subpopulations of granule and periglomerular neurons in the olfactory bulb. J Neurosci 25:6997–7003.

Kohwi M, Petryniak MA, Long JE, Ekker M, Obata K, Yanagawa Y, Rubenstein JL, Alvarez-Buylla A (2007) A subpopulation of olfactory bulb GABAergic interneurons is derived from Emx1- and Dlx5/6-expressing progenitors. J Neurosci 27:6878–6891.

Kosaka K, Kosaka T (2005) Synaptic organization of the glomerulus in the main olfactory bulb: Compartments of the glomerulus and heterogeneity of the periglomerular cells. Anat Sci Int 80:80–90

Kosaka K, Kosaka T (2007) Chemical properties of type 1 and type 2 periglomerular cells in the mouse olfactory bulb are different from those in the rat olfactory bulb. Brain Res 1167:42–55.

Kosaka T, Kosaka K (2012) Further characterization of the juxtaglomerular neurons in the mouse main olfactory bulb by transcription factors, Sp8 and Tbx21. Neurosci Res 73:24–31.

Kovalchuk Y, Homma R, Liang Y, Maslyukov A, Hermes M, Thestrup T, Griesbeck O, Ninkovic J, Cohen LB, Garaschuk O (2015) In vivo odourant response properties of migrating adult-born neurons in the mouse olfactory bulb. Nat Commun 6:6349

Kriegstein A, Alvarez-buylla A (2009) The Glial Nature of Embryonic and Adult Neural Stem Cells. Annu Rev Neurosci 32:149–184.

Kriegstein AR, Götz M (2003) Radial glia diversity: A matter of cell fate. Glia 43:37–43

Lagace DC, Whitman MC, Noonan MA, Ables JL, DeCarolis NA, Arguello AA, Donovan MH, Fischer SJ, Farnbauch LA, Beech RD, DiLeone RJ, Greer CA, Mandyam CD, Eisch AJ (2007) Dynamic contribution of nestin-expressing stem cells to adult neurogenesis. J Neurosci 27:12623–12629

Lee HO, Norden C (2013) Mechanisms controlling arrangements and movements of nuclei in pseudostratified epithelia. Trends Cell Biol 23:141–150.

Lemasson M (2005) Neonatal and Adult Neurogenesis Provide Two Distinct Populations of Newborn Neurons to the Mouse Olfactory Bulb. J Neurosci 25:6816–6825

Levi G, Puche AC, Mantero S, Barbieri O, Trombino S, Paleari L, Egeo A, Merlo GR (2003) The Dlx5 homeodomain gene is essential for olfactory development and connectivity in the mouse. Mol Cell Neurosci 22:530–543.

Levison SW, Goldman JE (1993) Both oligodendrocytes and astrocytes develop from progenitors in the subventricular zone of postnatal rat forebrain. Neuron 10:201–212.

Li X, Sun C, Lin C, Ma T, Madhavan MC, Campbell K, Yang Z (2011) The transcription factor Sp8 is required for the production of parvalbumin-expressing interneurons in the olfactory bulb. J Neurosci 31:8450–8455.

Liang H, Xiao G, Yin H, Hippenmeyer S, Horowitz JM, Ghashghaei HT (2013) Neural development is dependent on the function of specificity protein 2 in cell cycle progression. Development 140:552–561

Liu F, You Y, Li X, Ma T, Nie Y, Wei B, Li T, Lin H, Yang Z (2009) Brain injury does not alter the intrinsic differentiation potential of adult neuroblasts. J Neurosci 29:5075–5087

Livneh Y, Adam Y, Mizrahi A (2014) Odor Processing by Adult-Born Neurons. Neuron 81:1097–1110

Livneh Y, Mizrahi A (2011) Experience-dependent plasticity of mature adult-born neurons. Nat Neurosci 15:26–28

Lledo PM, Merkle FT, Alvarez-Buylla A (2008) Origin and function of olfactory bulb interneuron diversity. Trends Neurosci 31:392–400.

Llorens-Bobadilla E, Zhao S, Baser A, Saiz-Castro G, Zwadlo K, Martin-Villalba A (2015) Single-Cell Transcriptomics Reveals a Population of Dormant Neural Stem Cells that Become Activated upon Brain Injury. Cell Stem Cell 17:329–340

Lois C, Alvarez-Buylla A (1994) Long-distance neuronal migration in the adult mammalian brain. Science 264:1145–1148.

Lois C, Garcia-Verdugo JM, Alvarez-Buylla A (1996) Chain migration of neuronal precursors. Science 271:978–981.

Long JE, Garel S, Alvarez-Dolado M, Yoshikawa K, Osumi N, Alvarez-Buylla A, Rubenstein JLR (2007) Dlx-Dependent and -Independent Regulation of Olfactory Bulb Interneuron Differentiation. J Neurosci 27:3230–3243.

Long JE, Garel S, Depew MJ, Tobet S, Rubenstein JLR (2003) DLX5 regulates development of peripheral and central components of the olfactory system. J Neurosci 23:568–578

López-Mascaraque L, De Carlos J a, Valverde F (1996) Early onset of the rat olfactory bulb projections. Neuroscience 70:255–266.

Luskin MB (1993) Restricted proliferation and migration of postnatally generated neurons derived from the forebrain subventricular zone. Neuron 11:173–189.

Malatesta P, Hack MA, Hartfuss E, Kettenmann H, Klinkert W, Kirchhoff F, Götz M (2003) Neuronal or glial progeny: Regional differences in radial glia fate. Neuron 37:751–764.

Mallamaci A (2013) Developmental control of cortico-cerebral astrogenesis. Int J Dev Biol 57:689–706.

Malnic B, Hirono J, Sato T, Buck LB (1999) Combinatorial receptor codes for odors. Cell 96:713–723

Mandairon N, Sacquet J, Garcia S, Ravel N, Jourdan F, Didier A (2006) Neurogenic correlates of an olfactory discrimination task in the adult olfactory bulb. Eur J Neurosci 24:3578–3588.

Marín O, Rubenstein JLR (2001) A long, remarkable journey: Tangential migration in the telencephalon. Nat Rev Neurosci 2:780–790

Martynoga B, Drechsel D, Guillemot F, Ochoa-espinosa A, Affolter M, Fedoriw A, Mugford J (2012) Molecular Control of Neurogenesis : A View from the Mammalian Cerebral Cortex. Cold Spring Harb Perspect Biol 4:1–14.

Mazo C, Lepousez G, Nissant A, Valley MT, Lledo P-M (2016) GABAB Receptors Tune Cortical Feedback to the Olfactory Bulb. J Neurosci 36:8289–8304

McCarthy M, Turnbull DH, Walsh C a, Fishell G (2001) Telencephalic neural progenitors appear to be restricted to regional and glial fates before the onset of neurogenesis. J Neurosci 21:6772–6781.

Menezes JR, Smith CM, Nelson KC, Luskin MB (1995) The division of neuronal progenitor cells during migration in the neonatal mammalian forebrain. Mol Cell Neurosci 6:496–508

Menn B, Garcia-Verdugo JM, Yaschine C, Gonzalez-Perez O, Rowitch D, Alvarez-Buylla A (2006) Origin of Oligodendrocytes in the Subventricular Zone of the Adult Brain. J Neurosci 26:7907–7918

Merkle FT, Fuentealba, Luis C.Kessaris N, Alvarez-buylla A (2014) Adult neural stem cells in distinct microdomains generate previously unknown interneuron types Florian. Nat Neurosci 17:207–214.

Merkle FT, Mirzadeh Z, Alvarez-buylla A (2007) Mosaic organization of neural stem cells in the adult brain. Science 317:381–384

Merkle FT, Tramontin AD, García-Verdugo JM, Alvarez-Buylla A (2004) Radial glia give rise to adult neural stem cells in the subventricular zone. Proc Natl Acad Sci 101:17528–17532.

Mihalas AB, Hevner RF (2017) Control of Neuronal Development by T-Box Genes in the Brain, 1st ed. Elsevier Inc.

Miller M, Nowakoski R (1988) Use of bromodeoxyuridine immunohistochemistry to examine the proliferation, migration and time of origen of cells in the central nervous system. Brain Res 457:44–52.

Ming G, Song H (2005) Adult Neurogenesis in the Mammalian Central Nervous System. Annu Rev Neurosci 28:223–250

Mirzadeh Z, Merkle FT, Soriano-Navarro M, García-Verdugo JM, Alvarez-Buylla A (2008) Neural stem cells confer unique pinwheel architecture to the ventricular surface in neurogenic regions of the adult brain. Cell Stem Cell 11:265–278.

Miyata T (2008) Development of three-dimensional architecture of the neuroepithelium: Role of pseudostratification and cellular “community.” Dev Growth Differ 50:105–112.

Mizrahi A (2007) Dendritic development and plasticity of adult-born neurons in the mouse olfactory bulb. Nat Neurosci 10:444–452.

Mombaerts P (1996) Targeting olfaction. Curr Opin Neurobiol 6:481–486.

Mombaerts P (2006) Axonal wiring in the mouse olfactory system. Annu Rev Cell Dev Biol 22:713–737.

Mombaerts P, Wang F, Dulac C, Chao SK, Nemes A, Mendelsohn M, Edmondson J, Axel R (1996) Visualizing an olfactory sensory map. Cell 87:675–686.

Moreno MM, Linster C, Escanilla O, Sacquet J, Didier A, Mandairon N (2009) Olfactory perceptual learning requires adult neurogenesis. Proc Natl Acad Sci 106:17980–17985

Mori K (1999) The Olfactory Bulb: Coding and Processing of Odor Molecule Information. Science (80-) 286:711–715

Mori K, Sakano H (2011) How Is the Olfactory Map Formed and Interpreted in the Mammalian Brain? Annu Rev Neurosci 34:467–499

Murase S ichi, Horwitz AF (2004) Directions in Cell Migration Along the Rostral Migratory Stream: The Pathway for Migration in the Brain. Curr Top Dev Biol 61:135–152.

Nagayama S, Enerva A, Fletcher ML, Masurkar A V., Igarashi KM, Mori K, Chen WR (2010) Differential Axonal Projection of Mitral and Tufted Cells in the Mouse Main Olfactory System. Front Neural Circuits 4:1–8

Nagayama S, Homma R, Imamura F (2014) Neuronal organization of olfactory bulb circuits. Front Neural Circuits 8:1–19

Naruse I, Keino H (1995) Apoptosis in the developing CNS. Prog Neurobiol 47:135-155

Naruse M, Ishizaki Y, Ikenaka K, Tanaka A, Hitoshi S (2017) Origin of oligodendrocytes in mammalian forebrains: a revised perspective. J Physiol Sci 67:1–8.

Nave K-A (2010) Myelination and support of axonal integrity by glia. Nature 468:244–252

Nguyen-Ba-Charvet KT (2004) Multiple Roles for Slits in the Control of Cell Migration in the Rostral Migratory Stream. J Neurosci 24:1497–1506

Ninkovic J, Mori T, Gotz M (2007) Distinct modes of neuron addition in adult mouse neurogenesis. J Neurosci 27:10906–10911

Ninkovic J, Pinto L, Petricca S, Lepier A, Sun J, Rieger M a, Schroeder T, Cvekl A, Favor J, Sciences V (2015) The transcription factor Pax6 regulates survival of dopaminergic olfactory bulb neurons via crystallin αA. Neuron 685:682–694.

Nishiyama A (2007) Polydendrocytes: NG2 Cells with Many Roles in Development and Repair of the CNS. Neurosci 13:62–76

Nishizumi H, Sakano H (2015) Developmental regulation of neural map formation in the mouse olfactory system. Dev Neurobiol 75:594–607.

Noctor SC, Flint AC, Weissman TA, Dammerman RS, Kriegstein AR (2001) Neurons derived from radial glial cells establish radial units in neocortex. Nature 409:714–720

Noctor SC, Martínez-cerdeño V, Arnold R (2008) Distinct Behaviors of Neural Stem and Progenitor Cells Underlie Cortical Neurogenesis. J Comp Neurol 508:28–44.

Noctor SC, Martinez-Cerdeno V, Ivic L, Kriegstein AR, Martínez-Cerdeño V, Ivic L, Kriegstein AR, Martinez-Cerdeno V, Ivic L, Kriegstein AR (2004) Cortical neurons arise in symmetric and asymmetric division zones and migrate through specific phases. Nat Neurosci 7:136–144

Nomura T, Haba H, Osumi N (2007) Role of a transcription factor Pax6 in the developing vertebrate olfactory system. Dev Growth Differ 49:683–690.

Paina S, Garzotto D, DeMarchis S, Marino M, Moiana A, Conti L, Cattaneo E, Perera M, Corte G, Calautti E, Merlo GR (2011) Wnt5a Is a Transcriptional Target of Dlx Homeogenes and Promotes Differentiation of Interneuron Progenitors In Vitro and In Vivo. J Neurosci 31:2675–2687

Panzanelli P, Bardy C, Nissant A, Pallotto M, Sassoe M, Lledo P, Fritschy J (2009) Early Synapse Formation in Developing Interneurons of the Adult Olfactory Bulb. 29:15039–15052.

Panzanelli P., Fritschy JM, Yanagawa Y, Obata K, M.Sassoè-Pogneto (2007) GABAergic Phenotype of Periglomerular Cells in the Rodent Olfactory Bulb. J Comp Neurol 502:990–1002.

Parrish-Aungst S, Shipley MT, Erdelyi F, Szabo G, Puche AC (2007) Quantitative Analysis of Neuronal Diversity in the Mouse Olfactory Bulb. J Comp Neurol 501:825–836.

Pastrana E, Cheng L-CC, Doetsch F (2009) Simultaneous prospective purification of adult subventricular zone neural stem cells and their progeny. Proc Natl Acad Sci U S A 106:6387–6392

Paul A, Chaker Z, Doetsch F (2017) Hypothalamic regulation of regionally distinct adult neural stem cells and neurogenesis. Science (80-) 356:1383–1386

Peretto P, Giachino C, Aimar P, Fasolo A, Bonfanti L (2005) Chain formation and glial tube assembly in the shift from neonatal to adult subventricular zone of the rodent forebrain. J Comp Neurol 487:407–427.

Peretto P, Merighi A, Fasolo A, Bonfanti L (1999) The subependymal layer in rodents: A site of structural plasticity and cell migration in the adult mammalian brain. Brain Res Bull 49:221–243.

Petreanu L, Alvarez-Buylla A (2002) Maturation and death of adult-born olfactory bulb granule neurons: role of olfaction. J Neurosci 22:6106–6113.

Pinching a J, Powell TP (1971a) The neuron types of the glomerular layer of the olfactory bulb. J Cell Sci 9:305–345.

Pinching a J, Powell TP (1971b) Ultrastructural features of transneuronal cell degeneration in the olfactory system. J Cell Sci 8:253–287

Platel J-C, Lacar B, Bordey A (2008a) GABA and glutmatate signaling: homeostatic control of adult forebrain neurogenesis. J Mol Histol 38:303–311.

Platel J, Dave KA, Gordon V, Lacar B, Maria E, Bordey A (2011) NMDA receptors activated by subventricular zone astrocytic glutamate are critical for neuroblast survival prior to entering a synaptic network. Neuron 65:859–872.

Platel J, Heintz T, Young S, Gordon V, Bordey A (2008b) Tonic activation of GLU K5 kainate receptors decreases neuroblast migration in whole-mounts of the subventricular zone. J Physiol 16:3783–3793.

Puche a C, Shipley MT (2001) Radial glia development in the mouse olfactory bulb. J Comp Neurol 434:1–12

Qin S, Chapman H, Ware SM, Waclaw RR, Campbell K (2015) Assessing the medial contribution to olfactory bulb interneuron diversity and the role of Gsx2 in medial progenitors, in Annual meeting of SfN, Chicago

Ravasi T, Huber T, Zavolan M, Forrest A, Gaasterland T, Grimmond S (2003) Systematic Characterization of the Zinc-Finger-Containing Proteins in the Mouse Transcriptome. Genome Res 13:1430–1442

Richardson WD, Young KM, Tripathi RB, McKenzie I (2011) NG2-glia as multipotent neural stem cells-fact or fantasy? Neuron 70:661–673.

Rochefort C, Gheusi G, Vincent J-D, Lledo P-M (2002) Enriched odor exposure increases the number of newborn neurons in the adult olfactory bulb and improves odor memory. J Neurosci 22:2679–2689.

Rochefort C, Lledo PM (2005) Short-term survival of newborn neurons in the adult olfactory bulb after exposure to a complex odor environment. Eur J Neurosci 22:2863–2870.

Roux L, Benchenane K, Rothstein JD, Bonvento G, Giaume C (2011) Plasticity of astroglial networks in olfactory glomeruli. Proc Natl Acad Sci 108:18442–18446

Rowitch DH, Kriegstein AR (2010) Developmental genetics of vertebrate glial–cell specification. Nature 468:214–222.

Rubenstein JLR, Martinez S, Shimamura K, Puelles L (1994) The Embryonic Vertebrate Forebrain: The Prosomeric Model. Science (80-) 266:578–580.

Saghatelyan A, de Chevigny A, Schachner M, Lledo P-M (2004) Tenascin-R mediates activity-dependent recruitment of neuroblasts in the adult mouse forebrain. Nat Neurosci 7:347–356

Saghatelyan A, Roux P, Migliore M, Rochefort C, Desmaisons D, Charneau P, Shepherd GM, Lledo PM (2005) Activity-dependent adjustments of the inhibitory

network in the olfactory bulb following early postnatal deprivation. Neuron 46:103–116.

Sahara S, Kawakami Y, Izpisua Belmonte JC, O'Leary DDM (2007) Sp8 exhibits reciprocal induction with Fgf8 but has an opposing effect on anterior-posterior cortical area patterning. Neural Dev 2:10.

Schoppa NE (2006) Synchronization of olfactory bulb mitral cells by precisely timed inhibitory inputs. Neuron 49:271–283.

Schoppa NE, Westbrook GL (2001) Glomerulus-specific synchronization of mitral cells in the olfactory bulb. Neuron 31:639–651.

Sequerra EB (2014) Subventricular zone progenitors in time and space: generating neuronal diversity. Front Cell Neurosci 8:434 Available at: http://journal.frontiersin.org/Journal/10.3389/fncel.2014.00434/abstract.

Shepherd GM, Greer CA, Mazzarello P, Sassoè-Pognetto M (2011) The first images of nerve cells: Golgi on the olfactory bulb 1875. Brain Res Rev 66:92–105.

Siegenthaler J a, Ashique AM, Zarbalis K, Patterson KP, Hecht JH, Kane M a, Folias AE, Choe Y, Scott R, Kume T, Napoli JL, Peterson AS, Samuel J (2010) Retinoic acid from the meninges regulates cortical neuron generation. Cell 139:597–609.

Snapyan M, Lemasson M, Brill MS, Blais M, Massouh M, Ninkovic J, Gravel C, Berthod F, Gotz M, Barker PA, Parent A, Saghatelyan A (2009) Vasculature Guides Migrating Neuronal Precursors in the Adult Mammalian Forebrain via Brain-Derived Neurotrophic Factor Signaling. J Neurosci 29:4172–4188

Sosulski DL, Lissitsyna Bloom M, Cutforth T, Axel R, Datta SR (2011) Distinct representations of olfactory information in different cortical centres. Nature 472:213–216

Spassky N, Merkle FT, Flames N, Tramontin AD, Garcıa-Verdugo J-M, Alvarez-Buylla A (2005) Adult Ependymal Cells Are Postmitotic and Are Derived from Radial Glial Cells during Embryogenesis. J Neurosci 25:10–18.

Stenman J, Toresson H, Campbell K (2003) Identification of two distinct progenitor populations in the lateral ganglionic eminence: implications for striatal and olfactory bulb neurogenesis. J Neurosci 23:167–174

Sultan S, Mandairon N, Kermen F, Garcia S, Sacquet J, Didier A (2010) Learning-dependent neurogenesis in the olfactory bulb determines long-term olfactory memory. FASEB J 24:2355–2363

Supp DM, Witte DP, Branford WW, Smith EP, Potter SS (1996) Sp4 , a Member of the Sp1-Family of Zinc Finger Transcription Factors , Is Required for Normal Murine Growth , Viability , and Male Fertility. 299:284–299.

Tekki-Kessaris N, Woodruff R, Hall a C, Gaffield W, Kimura S, Stiles CD, Rowitch DH, Richardson WD (2001) Hedgehog-dependent oligodendrocyte lineage specification in the telencephalon. Development 128:2545–2554.

Telley L, Govindan S, Prados J, Stevant I, Nef S, Dermitzakis E, Dayer A, Jabaudon D (2016) Sequential transcriptional waves direct the differentiation of newborn neurons in the mouse neocortex. Science 351:1443–1446.

Tiveron M-C, Beclin C, Murgan S, Wild S, Angelova A, Marc J, Coré N, de Chevigny A, Herrera E, Bosio A, Bertrand V, Cremer H (2017) Zic-proteins are repressors of dopaminergic forebrain fate in mice and *C. elegans*. J Neurosci:3888–16

Toida K, Kosaka K, Heizmann CW, Kosaka T (1998) Chemically defined neuron groups and their subpopulations in the glomerular layer of the rat main olfactory bulb: III. Structural features of calbindin D28K-immunoreactive neurons. J Comp Neurol 392:179–198.

Toresson H, Campbell K (2001) A role for Gsh1 in the developing striatum and olfactory bulb of Gsh2 mutant mice. Development 128:4769–4780.

Toresson H, Potter SS, Campbell K (2000) Genetic control of dorsal-ventral identity in the telencephalon: opposing roles for Pax6 and Gsh2. Development 127:4361–4371.

Tramontin AD, García-Verdugo JM, Lim DA, Alvarez-Buylla A (2003) Postnatal development of radial glia and the ventricular zone (VZ): A continuum of the neural stem cell compartment. Cereb Cortex 13:580–587.

Treichel D, Becker M, Gruss P (2001) The novel transcription factor gene Sp5 exhibits a dynamic and highly restricted expression pattern during mouse embryogenesis. 101:175–179.

Treichel D, Sch??ck F, J??ckle H, Gruss P, Mansouri A (2003) mBtd is required to maintain signaling during murine limb development. Genes Dev 17:2630–2635.

Treloar HB, Purcell a L, Greer C a (1999) Glomerular formation in the developing rat olfactory bulb. J Comp Neurol 413:289–304.

Tsai H, Li H, Fuentealba LC, Molofsky A V, Zhuang H, Tenney A, Murnen AT, Stephen PJ, Merkle F, Kessaris N, Alvarez-buylla A, William D, Rowitch DH (2012) Regional Astrocyte Allocation Regulates CNS Synaptogenesis and Repair. Science (80-) 337:358–362.

Tucker ES, Polleux F, LaMantia AS (2006) Position and time specify the migration of a pioneering population of olfactory bulb interneurons. Dev Biol 297:387–401.

Valverde F, Santacana M, Heredia M (1992) Formation of an olfactory glomerulus: Morphological aspects of development and organization. Neuroscience 49:255–275.

Vassar R, Chao SK, Sitcheran R, Nuiiez M, Vosshall LB, Axel R (1994) Topographic O rganization of Sensory Projection to the O lfactory Bulb. Cell 79:981–991.

Vergaño-Vera E, Yusta-boyo MJ, Castro F De, Bernad A, Pablo F De, Vicario-abejón C, de Castro F, de Pablo F (2006) Generation of GABAergic and dopaminergic interneurons from endogenous embryonic olfactory bulb precursor cells. Development 133:4367–4379

Volakakis N, Kadkhodaei B, Joodmardi E, Wallis K, Panman L, Silvaggi J, Spiegelman BM, Perlmann T (2010) NR4A orphan nuclear receptors as mediators of CREB-dependent neuroprotection. Proc Natl Acad Sci 107:12317–12322

Wachowiak M, Shipley MT (2006) Coding and synaptic processing of sensory information in the glomerular layer of the olfactory bulb. Semin Cell Dev Biol 17:411–423.

Waclaw RR, Allen ZJ, Bell SM, Erdélyi F, Szabó G, Potter SS, Campbell K (2006) The zinc finger transcription factor Sp8 regulates the generation and diversity of olfactory bulb interneurons. Neuron 49:503–516.

Waclaw RR, Wang B, Pei Z, Ehrman LA, Campbell K (2009) Distinct Temporal Requirements for the Homeobox Gene Gsx2 in Specifying Striatal and Olfactory Bulb Neuronal Fates. Neuron 63:451–465

Wallace JL, Wienisch M, Murthy VN (2017) Development and Refinement of Functional Properties of Adult-Born Neurons. Neuron:1–14

Walz A, Omura M, Mombaerts P (2006) Development and Topography of the Lateral Olfactory Tract in the Mouse: Imaging by Genetically Encoded and Injected Fluorescent Markers. J Neurobiol 66:835–846.

Wang B, Wang B, Waclaw RR, Ii ZJA, Guillemot F, Campbell K (2009) Ascl1 is a required downstream effector of Gsx gene function in the embryonic mouse telencephalon embryonic mouse telencephalon.

Wei B, Nie Y, Li X, Wang C, Ma T, Huang Z, Tian M, Sun C, Cai Y, You Y, Liu F, Yang Z (2011) Emx1-expressing neural stem cells in the subventricular zone give rise to new interneurons in the ischemic injured striatum. Eur J Neurosci 33:819–830

Weinandy F, Ninkovic J, Götz M (2011) Restrictions in time and space - new insights into generation of specific neuronal subtypes in the adult mammalian brain. Eur J Neurosci 33:1045–1054.

Whitman MC, Greer CA (2007a) Adult-Generated Neurons Exhibit Diverse Developmental Fates. Dev Neurobiol 67:1079–1093.

Whitman MC, Greer CA (2007b) Synaptic Integration of Adult-Generated Olfactory Bulb Granule Cells: Basal Axodendritic Centrifugal Input Precedes Apical Dendrodendritic Local Circuits. J Neurosci 27:9951–9961.

Wichterle H, Garcia-Verdugo JM, Herrera DG, Alvarez-Buylla A (1999) Young neurons from medial ganglionic eminence disperse in adult and embryonic brain. Nat Neurosci 2:461–466.

Wichterle H, Turnbull DH, Nery S, Fishell G, Alvarez-Buylla A (2001) In utero fate mapping reveals distinct migratory pathways and fates of neurons born in the mammalian basal forebrain. Development 128:3759–3771.

Willaime-Morawek S, Seaberg RM, Batista C, Labbé E, Attisano L, Gorski JA, Jones KR, Kam A, Morshead CM, Van Der Kooy D (2006) Embryonic cortical neural stem cells migrate ventrally and persist as postnatal striatal stem cells. J Cell Biol 175:159–168.

Wilson RI, Mainen ZF (2006) Early Events in Olfactory Processing. Annu Rev Neurosci 29:163–201

Winner B, Cooper-Kuhn CM, Aigner R, Winkler J, Kuhn HG (2002) Long-term survival and cell death of newly generated neurons in the adult rat olfactory bulb. Eur J Neurosci 16:1681–1689.

Winpenny E, Lebel-Potter M, Fernandez ME, Brill MS, Götz M, Guillemot F, Raineteau O (2011) Sequential generation of olfactory bulb glutamatergic neurons by Neurog2-expressing precursor cells. Neural Dev 6:12.

Woo CC, Hingco EE, Johnson BA, Leon M (2008) Broad Activation of the Glomerular Layer Enhances Subsequent Olfactory Responses Cynthia. 32:51–55.

Yamaguchi M, Mori K (2005) Critical period for sensory experience-dependent survival of newly generated granule cells in the adult mouse olfactory bulb. Proc Natl Acad Sci U S A 102:9697–9702

Yokoi M, Mori K, Nakanishi S (1995) Refinement of odor molecule tuning by dendrodendritic synaptic inhibition in the olfactory bulb. Proc Natl Acad Sci U S A 92:3371–3375.

Young KM, Fogarty M, Kessaris N, Richardson WD (2007) Subventricular Zone Stem Cells Are Heterogeneous with Respect to Their Embryonic Origins and Neurogenic Fates in the Adult Olfactory Bulb. J Neurosci 27:8286–8296

Yun K, Garel S, Fischman S, Rubenstein JLR (2003) Patterning of the lateral ganglionic eminence by the Gsh1 and Gsh2 homeobox genes regulates striatal and olfactory bulb histogenesis and the growth of axons through the basal ganglia. J Comp Neurol 461:151–165.

Yun K, Potter S, Rubenstein JL (2001) Gsh2 and Pax6 play complementary roles in dorsoventral patterning of the mammalian telencephalon. Development 128:193–205.

Zembrzycki A, Griesel G, Stoykova A, Mansouri A (2007) Genetic interplay between the transcription factors Sp8 and Emx2 in the patterning of the forebrain. Neural Dev 2:8

Origin, diversity and transcriptional coding of periglomerular calretinin interneurons

The subventricular zone (SVZ) is a brain region that shows intense germinal activity throughout postnatal life. The postnatal SVZ is subdivided in microdomains containing neural stem cells (NSCs) that express defined transcription factors and generate distinct neuronal subtypes in the olfactory bulb (OB). Calretinin-expressing (CalR+) interneurons represent the largest population of OB periglomerular interneurons produced after birth. Yet, in contrast to others, limited information exists regarding their origin, diversity and function in the OB, as well as the transcription factors that guide their generation. Previous studies highlighted that CalR+ PG interneurons are generated by both the medial and dorsal SVZ microdomains, and suggested that the transcription factor Sp8 is involved in their generation.

This work aimed at 1) refining current approaches for manipulating gene expression in postnatal SVZ NSCs in a temporally controlled manner, 2) exploring the origin and the function of CalR+ periglomerular neurons, 3) investigating the role of Sp8 in the transcriptional coding of CalR+ periglomerular interneurons specification and maturation.

Refinement of the classical electroporation approach allowed the long-term fate mapping and timely-controlled genetic manipulation of NSCs of the SVZ. Using this refined approach allowed identifying two subpopulations of CalR+ interneurons that show different spatial and temporal origins after birth, as well as to explore the functional and morphological correlates of this diversity. A large and previously non-described fraction of CalR+ periglomerular interneurons exhibits properties of immature neurons (i.e. little synaptic inputs and weak excitability), questioning their role in olfactory processing. Finally, genetic manipulations of the transcription factor Sp8 at different stages during CalR+ interneuron differentiation highlighted its role in the long-term survival of mature CalR+ periglomerular interneurons, while excluding a role in their early specification. Altogether these results shed new lights on the origin, diversity and transcriptional coding of CalR+ periglomerular interneurons and call for a characterization of their role in olfactory processing.

Key words : postnatal germinal activity, neural stem cells, olfactory bulb, calretinin interneurons, transcription factor Sp8